

# **Lightweight structured steel members - properties and application**

Von der Fakultät Architektur, Bauingenieurwesen und Stadtplanung  
der Brandenburgischen Technischen Universität Cottbus-Senftenberg  
zur Erlangung des akademischen Grades

eines Doktor der Ingenieurwissenschaften (Dr.-Ing.)  
genehmigte Dissertation

vorgelegt von

M. Sc. Darita Shlychkova  
aus Sankt-Petersburg, Russland

Gutachter: Prof. Dr.-Ing. habil. Hartmut Pasternak  
Gutachter: Prof. Dr.-Ing. Biljana Scepanovic  
Gutachter: Prof. Dr. techn. Jörgen Robra  
Tag der Disputation: 28.04.2023

Schriftenreihe Stahlbau 2023, Heft 21, ISSN: 1611-5023

DOI: <https://doi.org/10.26127/BTUOpen-6531>

## **Acknowledgement**

The present thesis was created as part of the research project 'DESTRUKT/S' during my work as a doctoral student at the Chair of Steel and Timber Construction of the Brandenburg Technical University of Cottbus-Senftenberg.

Special thanks to my scientific supervisor Prof. Dr.-Ing. habil. Hartmut Pasternak for the support. He helped me in difficult periods and motivated me with professional advice.

I would like to thank Frau Professor Dr.-Ing. Biljana Scepanovic and Herr Professor Dr. techn. Jürgen Robra for the interest in this work and for taking on the further review.

I thank my colleagues at the Chair of Steel and Timber Construction and FMPA workers for their support and advice in carrying out the experiments.

I am very grateful to the team at the Chair of Joining and Welding Technology headed by Prof. Dr.-Ing. habil Vesselin Mikhailov for the good cooperation within the graduate class and for helping in manufacturing of experimental specimens.

Finally, I would like to express my gratitude to my family for their extraordinary support during the preparation of this work. Special thanks to my son, who literally kicked me to complete this work.

Darita Shlychkova

Cottbus, 04.08.2022

## **Abstract (EN)**

This thesis is dedicated to the structured sheet metals topic. Structured sheet metals are semi-finished products with the honeycomb (cell) shape, made by cold forming of the flat sheets. They represent an innovative technology in the field of lightweight construction. In recent years, this technology has undergone dynamic development what gives to researchers possibilities to improve the level of knowledge about structured sheets metals properties and explore new application fields for them.

The structuring improves basic properties, such as stiffness, compared to the flat sheet material. Due to these advantages, the use of structured sheet metals offers enormous innovation potential for efficient lightweight construction in many industrial sectors such as aerospace, rail transport technology, architectural products. Structured sheets have already been implementing in lighting technology, in the manufacture of household appliances and even in automotive industry. So that, the question arises if it possible to apply this kind of material successfully in other areas such as building industry.

This work contains an overview of the lightweight constructions historical development and stiffening elements in the steel industry, also the creation process of structured sheet metals, manufacturing investigated specimens, further bending tests, numerical simulations, analysis and comparison of resulting data and possible further use of lightweight beams with structured sheet elements as a building construction.

In this work beams compound of structured and flat plates are investigated. Steps of structured plates manufacturing process are described: hydroforming, point- and laser welding and bending. As a result, lightweight beams of two main shapes are manufactured: C- and square sectioned. There are four types of beams for each of the shapes are investigated. Every type has same geometrical dimensions, but thicknesses vary.

The series of laboratory tests with created beams under load is made. Three- and four-points bending tests are chosen for that.

This work also presents numerical analysis based on conducted experiments: buckling and global non-linear behavior of specimens by use of the software package ABAQUS/CAE are obtained. The behavior of the beams with structured and flat sheets under load is analyzed and the comparison of parameters such as load bearing capacity and stiffnesses is made.

Finally, in addition to laboratory and simulations, parametric modelling is done. Also, based on parametric calculations, the proposal for calculation the beams stiffness for with higher thicknesses is given. It allows to predict the behavior of beams with structured sheets with different thicknesses without manufacturing and conducting the expensive and time-taking laboratory experiments.

In conclusion, the recommendations for the simplifying of manufacturing process and for the improving of the beams stiffnesses are given.

## Abstract (EN)

Key words: lightweight constructions, sandwich members, structured sheet metals, lightweight steel beams, simply supported beams, hexagonal cells, FEM modelling, ABAQUS/CAE software.

## **Kurzfassung (DE)**

Diese Dissertation widmet sich dem Thema strukturierte Bleche. Strukturbleche sind Halbzeuge und haben eine Wabenform, die durch Kaltverformung der Flachbleche hergestellt werden. Sie stellen eine innovative Technologie im Bereich Leichtbau dar. In den letzten Jahren hat diese Technologie eine dynamische Entwicklung erfahren, was den Forschern Möglichkeiten gibt, den Wissensstand über die Eigenschaften von strukturierten Blechen zu verbessern und neue Anwendungsfelder für sie zu erforschen.

Die Strukturierung verbessert grundlegenden Eigenschaften, wie beispielsweise die Steifigkeit, im Vergleich zum Flachmaterial. Aufgrund dieser Vorteile bietet der Einsatz den strukturierten Blechen in vielen Industriebereichen wie Luft- und Raumfahrt, Schienenverkehrstechnik, Architekturprodukte ein enormes Innovationspotenzial für eine effiziente Leichtbau. Strukturierte Bleche finden bereits Anwendung in der Beleuchtungstechnik, bei der Herstellung von Haushaltsgeräten und sogar in der Automobilindustrie. Daher stellt sich die Frage, ob es möglich wäre, diese Art von Material erfolgreich in anderen Bereichen, wie zum Beispiel in der Bauindustrie, einzusetzen.

Diese Arbeit verschafft einen Überblick über die historische Entwicklung des Leichtbaus und der Versteifungselemente in der Stahlindustrie, der Entstehungsprozess strukturierter Bleche, die Herstellung der untersuchten Probekörpern, weiterführende Biegeversuche, numerische Simulationen, Analyse und Vergleich der resultierenden Daten, wie auch mögliche Weiterverwendung des Leichtbauträgers mit strukturierten Blechelementen im Hochbau.

In dieser Arbeit werden Träger aus strukturierten und ebenen Blechen untersucht. Die Stufen des Herstellprozesses von strukturierten Blechen können wie folgt beschrieben werden: Hydroforming, Punkt- und Laserschweißen und Biegen. Jede untersuchte Form wurde in vier unterschiedlichen Varianten vorgefertigt. Jede Variante verfügt über die gleiche Geometrie und unterscheiden sich durch ihre Dicke.

Biegeversuche werden an den erstellten Trägern unter Belastung durchgeführt. Die hierfür ausgewählten Methoden sind die Drei- und Vierpunkt-Biegeversuche.

Diese Arbeit präsentiert auch die numerischen Analysen, die sich auf durchgeführten Untersuchungen basieren. Knicken und das nichtlineare Verhalten von Proben werden durch die Anwendung des Softwarepakets ABAQUS/CAE abgebildet. Das Verhalten der Träger mit strukturierten und ebenen Blechen wird unter Belastung analysiert. Anschließend wird der Vergleich von solchen Parametern wie Tragfähigkeit und Steifigkeiten gezogen.

Zusätzlich zu den Versuchen und Simulationen wurde eine parametrische Modellierung vorgenommen. Außerdem auf der Grundlage den parametrischen Berechnungen wird der Vorschlag zur Berechnung für die Träger mit größeren Dicken gegeben. Es ermöglicht die Vorhersage des Verhaltens von Trägern aus strukturierten Blechen, die über den

## Kurzfassung (DE)

unterschiedlichen Dicken verfügen, ohne die Herstellung und Durchführung von kostenintensiven und zeitaufwändigen Laboruntersuchungen.

Abschließend werden Empfehlungen zur Vereinfachung des Herstellungsprozesses und zur Verbesserung der Trägersteifigkeit gegeben.

Schlagwörter: Leichtbau, Sandwichelemente, strukturierte Bleche, leichte Stahlträger, Waben, FEM Simulation, ABAQUS/CAE-Software.

**Contents**

Acknowledgement .....	I
Abstract (EN).....	II
Kurzfassung (DE) .....	IV
Contents .....	VI
List of figures.....	X
List of tables.....	XX
Nomenclature.....	XXIV
Formula symbols.....	XXIV
Abbreviations.....	XXVI
1 Introduction.....	1
1.1 Motivation and relevance.....	1
1.2 The aim of the work .....	2
1.3 Thesis structure .....	2
2 Structured sheet metals .....	3
2.1 Historical development of lightweight constructions.....	3
2.2 General information about structured plates .....	5
2.3 Definition and classification of structured plates.....	6
2.4 Classification and manufacturing of structured sheet metals.....	8
2.4.1 Classification according to DIN 8580 [66] .....	8
2.4.2 Classification according to Hoppe [9].....	10
2.4.3 Manufacturing using tools.....	10
2.4.4 Manufacturing of stiffened construction elements using active media [61, 62].....	14
2.5 Special features of structured plates.....	20
2.5.1 The geometry of hydroformed structured sheets produced by BTU .....	20
2.5.2 Honeycombs arrangement.....	22
2.5.3 Bending .....	22
2.5.4 Welding process of structured and flat sheet.....	24
2.5.5 Types of sandwiches .....	26
2.5.6 Structured sheets material properties.....	27
2.6 Application of structured sheets.....	30
2.6.1 Automotive applications.....	30
2.6.2 Structural applications .....	31
3 C-sectioned lightweight steel beams.....	35
3.1 Introduction.....	35
3.2 Material properties .....	35
3.2.1 Flat plates .....	35
3.2.2 Structured sheet metals.....	37



## Contents

3.3	Laboratory experiments .....	38
3.3.1	General information .....	38
3.3.2	Manufacturing of specimens .....	38
3.3.3	Experimental setup and boundary conditions.....	41
3.3.4	Displacement transducers (IWANs).....	42
3.3.5	Loading.....	43
3.3.6	Results .....	43
3.3.7	Conclusion.....	51
3.4	FEM simulations .....	53
3.4.1	General information .....	53
3.4.2	Geometry and material properties .....	53
3.4.3	Connections between elements of the model .....	54
3.4.4	Boundary conditions and loading.....	55
3.4.5	Mesh.....	56
3.4.6	Imperfections and buckling analysis .....	57
3.4.7	Riks analysis.....	60
3.4.8	Simulation results .....	61
3.4.9	Conclusion.....	65
3.5	Evaluation of simulation and experiment results .....	67
3.5.1	General information .....	67
3.5.2	Beam type 1: flat 0.75 mm + flat 0.75 mm .....	67
3.5.3	Beam type 2: flat 1.00 mm + flat 0.50 mm .....	69
3.5.4	Beam type 3: flat 0.75 mm + structured 0.50 mm.....	72
3.5.5	Beam type 4: flat 1.00 mm + structured 0.50 mm.....	74
3.5.6	Conclusion.....	77
3.6	Parametric modelling .....	78
3.6.1	General information .....	78
3.6.2	Parametric research and results .....	79
3.6.3	Conclusion.....	81
3.7	Conclusions to chapter 3 .....	81
4	Square-sectioned lightweight steel beams .....	83
4.1	Introduction.....	83
4.2	Materials and methods .....	83
4.3	Laboratory experiments .....	84
4.3.1	General information and manufacturing process of specimens.....	84
4.3.2	Experimental setup and boundary conditions.....	86
4.3.3	Displacement transducers (IWANs).....	86
4.3.4	Loading.....	87

## Contents

4.3.5 Results .....	87
4.3.6 Conclusion.....	92
4.4 FEM simulations .....	93
4.4.1 General information and material properties.....	93
4.4.2 Connections between elements of the model, boundary conditions and loading ...	94
4.4.3 Mesh .....	95
4.4.4 Imperfections and buckling and riks analysis.....	95
4.4.5 Simulation results .....	96
4.4.6 Conclusion.....	99
4.5 Evaluation of simulation and experiment results .....	100
4.5.1 General information .....	100
4.5.2 Beam type 1: flat 1.25 mm .....	100
4.5.3 Beam type 2: flat 1.50 mm .....	102
4.5.4 Beam type 3: flat 0.75 mm + structured 0.50 mm.....	104
4.5.5 Beam type 4: flat 1.00 mm + structured 0.50 mm.....	106
4.5.6 Conclusion.....	107
4.6 Analytical analysis .....	109
4.7 Conclusions to chapter 4 .....	110
5 Overall conclusions.....	113
6 References.....	115
7 Appendixes .....	123
Appendix A to Chapter 3: Laboratory experiments of C-sectioned beams (at the end of loading) .....	123
A.1 Beam 1.....	123
A.2 Beam 2.....	124
A.3 Beam 3.....	125
A.4 Beam 4.....	126
A.5 Beam 5.....	127
A.6 Beam 6.....	128
A.7 Beam 7.....	128
A.8 Beam 8.....	129
Appendix B to Chapter 3: FEM simulations of C-sectioned beams (under maximal force).....	131
B.1 Beam type 1.....	131
B.2 Beam type 2.....	132
B.3 Beam type 3.....	134
B.4 Beam type 4.....	135

## Contents

Appendix C to Chapter 4: Laboratory experiments of squared-sectioned beams (at the end of loading).....	137
C.1 Beam 1.....	137
C.2 Beam 2.....	138
C.3 Beam 3.....	139
C.4 Beam 4.....	139
C.5 Beam 5.....	140
C.6 Beam 6.....	141
C.7 Beam 7.....	142
C.8 Beam 8.....	142
Appendix D to Chapter 4: FEM simulations of squared-sectioned beams (under maximal force).....	144
D.1 Beam type 1.....	144
D.2 Beam type 2.....	145
D.3 Beam type 3.....	146
D.4 Beam type 4.....	148

## List of figures

Figure 2.1. Junkers F13 covered with corrugated sheets .....	4
Figure 2.2. Stress-test of a Junkers G-23 plane [26].....	4
Figure 2.3. Effects to be expected due to new shaping according to Bräunlich [91].....	5
Figure 2.4. Classification of structured thin sheets according to Hoppe [9] based on Hufenbach [20], Neubauer [19], Vollertsen [21].....	7
Figure 2.5. Corrugated sheet manufacturing using rotating tools [53] .....	11
Figure 2.6. Corrugated iron sheets as facade elements [65] .....	12
Figure 2.7. Roll structuring [9] .....	12
Figure 2.8. Bump structuring [9] .....	13
Figure 2.9. Structured plate produced by Dr. Mirtsch GmbH; Miele & Cie. GmbH&Co [71]....	14
Figure 2.10. Bump-structured sheet metal: in lighting technology: (a, b) hexal lamp [59] and in household appliance construction: (c) washing machine's drum [60] .....	14
Figure 2.11. Bump plate.....	15
Figure 2.12. Spherical structuring [9] .....	17
Figure 2.13. Ball-structured thin sheet: arrangement of the steel balls in the tool [9].....	17
Figure 2.14. Schematic representation of hydroforming process (a-f) [77].....	18
Figure 2.15. Molding tool for structuring sheet metals by hydroforming in BTU [80].....	19
Figure 2.16. Press with membrane and mould for production of a sheet metal with a honeycomb diameter of 33 mm in BTU [79] .....	19
Figure 2.17. Schematic representation of hydraulic deep-drawing (hydroforming) process of honeycomb sheets [82] .....	20
Figure 2.18. Honeycomb sheets after hydraulic deep-drawing process [82].....	20
Figure 2.19. Structured sheets manufactured by: a) Borit® company and b) by FQZ GmbH, Eisenhüttenstadt (right).....	20
Figure 2.20. Definitions of structured sheet metal and geometrical dimensions [83] .....	21
Figure 2.21. Position definition for the sheet metal (a), definition of structure (b) [83] .....	21
Figure 2.22. Structure lines of honeycomb structured sheet metal: lines with center point in the web crossing (a), lines with center point in the honeycomb (b) [83].....	22
Figure 2.23. 4 bending positions (a) and used bending press (b) [80] .....	23

## List of figures

Figure 2.24. Structural position of the structured sheet: a) ‘positive’, b) ‘negative’ [80].....	24
Figure 2.25. Spot welding machine, Düring company, type X-100 E-602/1, Panta Rhei, BTU	24
Figure 2.26. Sheet’s plane (a) and normals of the sheet metal surface (b) [83].....	25
Figure 2.27. Electrode positioning: a) orthogonal to the sheet-metal plane with deformation in the joining zone (pairs FS or FW); b) corrected electrode positioning orthogonal to the sheet surface (pairs FS or FW); c) orthogonal to the sheet plane with deformation in the welding zone, (pairs WW); d) electrode positioning taking into account the structure orthogonal to the sheet surface, (pairs WW). [83] .....	25
Figure 2.28. Welding of flat sheet and structured sheet (a) positive orientated and (b) negative orientated .....	26
Figure 2.29. Tensile test specimen of the structured sheet metal according to DIN EN ISO 6892-1[95].....	28
Figure 2.30. Specimen widths for structured sheet metals (structure position 0°) [95] .....	28
Figure 2.31. Stress-strain curves for a selected specimen dimension for the three tested structure positions and a flat sheet metal with corresponding deformation images [95].....	29
Figure 2.32. Characteristic range of stress-strain curves for the tested structure positions with corresponding deformation images [95] .....	29
Figure 2.33. Figure Mercedes SLK (a) and vault-structured sheet with a hexagonal staggered pattern (b) [87] .....	30
Figure 2.34. The designed underbody car element, Munich, Germany [88]. .....	31
Figure 2.35. The racing car (a, b), BTU Cottbus, Germany .....	31
Figure 2.36. A honeycomb-structured can body called ‘hexacan’ increases axial stiffness about 15 % (b) and radial stiffness about 50 % (a) as compared with a creased can body [87].....	32
Figure 2.37. Washing-machine drum made of structured plates [88].....	33
Figure 2.38. The lighting system Hexal LED [88] .....	33
Figure 2.39. The multi-purpose sports hall in Yuzhniy, a suburb of Odessa, resembles a giant turtle with bright tanks .....	34
Figure 3.1. Geometric parameters of samples cut from flat plate steel grade DC01 [98].....	36
Figure 3.2. Technical and true stress-strain curve, flat sheet metal DC01 .....	36
Figure 3.3. Technical and true stress-strain curve, flat (before forming) and structured (after forming) sheet metal DC04.....	37
Figure 3.4. Dimensions of original plate and cut (red line) structured plate.....	39

## List of figures

Figure 3.5. Cross sections of specimen types 1,2,3 and 4.....	39
Figure 3.6. Axonometric front and back view of specimens .....	41
Figure 3.7. Laboratory setup, front view .....	41
Figure 3.8. Laboratory setup, back view.....	42
Figure 3.9. Location of displacement transducers on specimen: front and side views .....	42
Figure 3.10. Displacement transducers at initial position (a), positive (b) and negative (c) moving direction .....	43
Figure 3.11. Force-time diagram from laboratory experiments, C-profiles of specimens.....	44
Figure 3.12. Force-displacement diagram from laboratory experiments, vertical displacement of lower part of the web, transducer IWAN 1 .....	45
Figure 3.13. Force-displacement diagram from laboratory experiments, vertical displacement of upper flange, transducer IWAN 2 .....	46
Figure 3.14. Force-displacement diagram from laboratory experiments, horizontal displacement of web, transducer IWAN 3 .....	47
Figure 3.15. Force-displacement diagram from laboratory experiments, horizontal displacement of web, transducer IWAN 7 .....	47
Figure 3.16. Force-displacement diagram from laboratory experiments, horizontal displacement of web, transducer IWAN 4 .....	48
Figure 3.17. Force-displacement diagram from laboratory experiments of IWAN 5 displacement transducers .....	49
Figure 3.18. Force-displacement diagram from laboratory experiments of IWAN 6 displacement transducers .....	50
Figure 3.19. Vertical stiffnesses of web beams 1-8 calculated by results captured by IWAN 2	52
Figure 3.20. Horizontal stiffness of web beam 1-8 calculated by results captured by IWAN 4.	52
Figure 3.21. Geometry AutoCAD (left) imported in ABAQUS (right) honeycomb [79] .....	53
Figure 3.22. Numbers of additional steel plates introduced to experiments .....	54
Figure 3.23. The weld points modeling for structured and flat web specimens: with structured sheets (a) and flat plates (b) .....	55
Figure 3.24. Areas where boundary conditions are applied: front(a) and back (b) side of specimen .....	56
Figure 3.25. The displacements color range for eigenmodes for the C-sectioned specimen in mm .....	59

## List of figures

Figure 3.26. First eigenmode for the C-sectioned specimen.....	60
Figure 3.27. Second eigenmode for the C-sectioned specimen .....	60
Figure 3.28. Third eigenmode for the C-sectioned specimen .....	60
Figure 3.29. Force-displacement (vertical) curves for lower flange (IWAN 1) of FEM simulation results .....	61
Figure 3.30. Force-displacement (vertical) curves for upper flange (IWAN 2) of FEM simulation results .....	62
Figure 3.31. Force-displacement (horizontal) curves for web (IWAN 4) of FEM simulation results.....	63
Figure 3.32. Force-displacement (horizontal) curves for web (IWAN 7) of FEM simulation results.....	63
Figure 3.33. Force-displacement (horizontal) curves for web (IWAN 3) of FEM simulation results.....	63
Figure 3.34. Stresses in MPa of C-profiles beam types a - 1, b - 2, c - 3, d - 4 under the maximal loading.....	64
Figure 3.35. Stresses in MPa of C-profile 2 mm thick under the maximal loading.....	65
Figure 3.36. Vertical stiffnesses of web beams 1-8, simulation results.....	66
Figure 3.37. Horizontal stiffness of web beam 1-8, simulation results.....	66
Figure 3.38. Force-displacement (vertical) curves for upper flange (IWAN 2): experimental results for Beam 1 and 2 and FEM results of Beam type 1.....	68
Figure 3.39. Force-displacement (horizontal) curves for web (IWAN 4): experimental results for Beam 1 and 2 and FEM results of Beam type 1.....	68
Figure 3.40. Force-displacement (vertical) curves for lower flange (IWAN 1): experimental results for Beam 1 and Beam 2 and FEM results of Beam type 1 .....	68
Figure 3.41. Force-displacement (horizontal) curves for web (IWAN 7): experimental results for Beam 1 and Beam 2 and FEM results of Beam type 1 .....	69
Figure 3.42. Force-displacement (horizontal) curves for web (IWAN 3): experimental results for Beam 1 and Beam 2 and FEM results of Beam type 1 .....	69
Figure 3.43 Force-displacement (vertical) curves for upper flange (IWAN 2): experimental results for Beam 3 and Beam 4 and FEM results of Beam type 2 .....	70
Figure 3.44. Force-displacement (horizontal) curves for web (IWAN 4): experimental results for Beam 3 and Beam 4 and FEM results of Beam type 2 .....	70

## List of figures

Figure 3.45. Force-displacement (vertical) curves for lower flange (IWAN 1): experimental results for Beam 3 and Beam 4 and FEM results of Beam type 2 .....	71
Figure 3.46. Force-displacement (horizontal) curves for web (IWAN 7): experimental results for Beam 3 and Beam 4 and FEM results of Beam type 2 .....	71
Figure 3.47. Force-displacement (horizontal) curves for web (IWAN 3): experimental results for Beam 3 and Beam 4 and FEM results of Beam type 2 .....	71
Figure 3.48. Force-displacement (vertical) curves for upper flange (IWAN 2): experimental results for Beam 5 and 6 and FEM results of Beam type 3.....	72
Figure 3.49. Force-displacement (horizontal) curves for web (IWAN 4): experimental results for Beam 5 and 6 and FEM results of Beam type 3.....	72
Figure 3.50 Force-displacement (vertical) curves for lower flange (IWAN 1): experimental results for Beam 5 and Beam 6 and FEM results of Beam type 3 .....	73
Figure 3.51. Force-displacement (horizontal) curves for web (IWAN 7): experimental results for Beam 5 and Beam 6 and FEM results of Beam type 3 .....	74
Figure 3.52. Force-displacement (horizontal) curves for web (IWAN 3): experimental results for Beam 5 and Beam 6 and FEM results of Beam type 3 .....	74
Figure 3.53. Force-displacement (vertical) curves for upper flange (IWAN 2): experimental results for Beam 7 and Beam 8 and FEM results of Beam type 4 .....	75
Figure 3.54. Force-displacement (horizontal) curves for web (IWAN 4): experimental results for Beam 7 and Beam 8 and FEM results of Beam type 4 .....	75
Figure 3.55. Force-displacement (vertical) curves for lower flange (IWAN 1): experimental results for Beam 7 and Beam 8 and FEM results of Beam type 3 .....	75
Figure 3.56. Force-displacement (horizontal) curves for web (IWAN 7): experimental results for Beam 7 and Beam 8 and FEM results of Beam type 4 .....	76
Figure 3.57. Force-displacement (horizontal) curves for web (IWAN 3): experimental results for Beam 7 and Beam 8 and FEM results of Beam type 4 .....	76
Figure 3.58. Vertical stiffnesses of web experiments and simulation results .....	78
Figure 3.59. Vertical stiffnesses of web experiments and simulation results .....	78
Figure 3.60. Stiffness increase factor – total specimen thickness dependence .....	80
Figure 4.1. Stress-strain curves for steel DC04 with different thicknesses.....	84
Figure 4.2. Laboratory setup, front view .....	86
Figure 4.3. Geometrical parameters of specimens and transducers locations.....	86



## List of figures

Figure 4.4. Force-time diagram from laboratory experiments, square-sectioned beams .....	87
Figure 4.5. Force-displacement diagram from laboratory experiments, horizontal displacement of web (from the left side), transducer IWAN H1 .....	88
Figure 4.6. Force-displacement diagram from laboratory experiments, horizontal displacement of web (from the right side), transducer IWAN H2 .....	89
Figure 4.7. Beam 2 buckling area, laboratory experiments .....	90
Figure 4.8. Beam 5 buckling area, laboratory experiments .....	90
Figure 4.9. Force-displacement diagram from laboratory experiments, vertical displacement of web (in the middle), transducer IWAN M .....	91
Figure 4.10. Force-displacement diagram from laboratory experiments, vertical displacement of web (from the left side), transducer IWAN L .....	91
Figure 4.11. Force-displacement diagram from laboratory experiments, vertical displacement of web (from the right side), transducer IWAN R .....	92
Figure 4.12. Areas where boundary conditions are applied .....	94
Figure 4.13. The displacements color range for eigenmodes for the squared-sectioned specimen, mm .....	96
Figure 4.14. First eigenmode for the squared-sectioned specimen .....	96
Figure 4.15. Second eigenmode for the squared-sectioned specimen .....	96
Figure 4.16. Third eigenmode for the squared-sectioned specimen .....	96
Figure 4.17. Force-displacement diagram, simulations results, vertical displacement in middle of the web .....	97
Figure 4.18. Force-displacement diagram, simulations results, horizontal displacement of web (from the left side) .....	98
Figure 4.19. Force-displacement diagram, simulations results, horizontal displacement of web (from the right side) .....	98
Figure 4.20. Square-sectioned beams: a - 2mm thickness and b – 3 mm thicknesses .....	99
Figure 4.21. Force-displacement (vertical) curves for lower flange in the middle of the beam (IWAN M): experimental results for Beam 1 and Beam 2 and FEM results of Beam type 1 ..	101
Figure 4.22. Force-displacement (horizontal) curves for web (IWAN H1), left side: experimental results for Beam 1 and Beam 2 and FEM results of Beam type 1 .....	102
Figure 4.23. Force-displacement (horizontal) curves for web (IWAN H2), right side: experimental results for Beam 1 and Beam 2 and FEM results of Beam type 1 .....	102

## List of figures

Figure 4.24. Force-displacement (vertical) curves for lower flange in the middle of the beam (IWAN M): experimental results for Beam 3 and Beam 4 and FEM results of Beam type 2 ..	103
Figure 4.25. Force-displacement (horizontal) curves for web (IWAN H1), left side: experimental results for Beam 3 and Beam 4 and FEM results of Beam type 2 .....	104
Figure 4.26. Force-displacement (horizontal) curves for web (IWAN H2), right side: experimental results for Beam 3 and Beam 4 and FEM results of Beam type 2 .....	104
Figure 4.27. Force-displacement (vertical) curves for lower flange in the middle of the beam (IWAN M): experimental results for Beam 5 and Beam 6 and FEM results of Beam type 3 ..	105
Figure 4.28. Force-displacement (horizontal) curves for web (IWAN H1 and H2), left and right sides: experimental results for Beam 6 and FEM results of Beam type 3 .....	105
Figure 4.29. Force-displacement (vertical) curves for lower flange in the middle of the beam (IWAN M): experimental results for Beam 7 and Beam 8 and FEM results of Beam type 4 ..	106
Figure 4.30. Force-displacement (horizontal) curves for web (IWAN H1), left side: experimental results for Beam 7 and 8 and FEM results of Beam type 4.....	107
Figure 4.31. Force-displacement (horizontal) curves for web (IWAN H2), right side: experimental results for Beam 7 and 8 and FEM results of Beam type 4.....	107
Figure 4.32. Graphic presentation of experimental and FEM stiffnesses, calculated from results captured by horizontal (IWAN H) and vertical (IWAN M) set up transducers.....	108
Figure 4.33. Stiffnesses of beams 1-8 and beam types 1-4 calculated from experiments, simulations and analytical results. ....	110
Figure 7.1. Beam 1 side view (flat 0.75 mm + flat 0.50 mm).....	123
Figure 7.2. Beam 1 back view (flat 0.75 mm + flat 0.50 mm).....	123
Figure 7.3. Beam 2 side view (flat 0.75 mm + flat 0.50 mm).....	124
Figure 7.4. Beam 2 back view (flat 0.75 mm + flat 0.50 mm).....	124
Figure 7.5. Beam 3 side view (flat 1.00 mm + flat 0.50 mm).....	125
Figure 7.6. Beam 3 back view (flat 1.00 mm + flat 0.50 mm).....	125
Figure 7.7. Beam 4 side view (flat 1.00 mm + flat 0.50 mm).....	126
Figure 7.8. Beam 4 back view (flat 1.00 mm + flat 0.50 mm).....	126
Figure 7.9. Beam 5 side view (flat 0.75 mm + structured 0.50 mm) .....	127
Figure 7.10. Beam 5 back view (flat 0.75 mm + structured 0.50 mm).....	127
Figure 7.11. Beam 6 side view (flat 0.75 mm + structured 0.50 mm) .....	128
Figure 7.12. Beam 7 side view (flat 1.00 mm + structured 0.50 mm) .....	128

## List of figures

Figure 7.13. Beam 7 back view (flat 1.00 mm + structured 0.50 mm) .....	129
Figure 7.14. Beam 8 side view (flat 1.00 mm + structured 0.50 mm) .....	129
Figure 7.15. Beam 8 back view (flat 1.00 mm + structured 0.50 mm) .....	130
Figure 7.16. Beam type 1 (flat 0.75 mm+flat 0.50 mm), stress distribution in MPa .....	131
Figure 7.17. Beam type 1 (flat 0.75 mm+flat 0.50 mm), Y-distribution displacement in mm .	131
Figure 7.18. Beam type 1 (flat 0.75 mm+flat 0.50 mm), Z-distribution displacement in mm..	132
Figure 7.19. Beam type 2 (flat 1.00 mm+flat 0.50 mm), stress distribution in MPa .....	132
Figure 7.20. Beam type 2 (flat 1.00 mm+flat 0.50 mm), Y-distribution displacement in mm .	133
Figure 7.21. Beam type 2 (flat 1.00 mm+flat 0.50 mm), Z-distribution displacement in mm..	133
Figure 7.22. Beam type 3 (flat 0.75 mm+structured 0.50 mm), stress distribution in MPa.....	134
Figure 7.23. Beam type 3 (flat 0.75 mm+structured 0.50 mm), Y-distribution displacement in mm .....	134
Figure 7.24. Beam type 3 (flat 0.75 mm+structured 0.50 mm), Z-distribution displacement in mm .....	135
Figure 7.25. Beam type 4 (flat 1.00 mm+structured 0.50 mm), stress distribution in MPa.....	135
Figure 7.26. Beam type 4 (flat 1.00 mm+structured 0.50 mm), Y-distribution displacement in mm .....	136
Figure 7.27. Beam type 4 (flat 1.00 mm+structured 0.50 mm), Z-distribution displacement in mm .....	136
Figure 7.28. Beam 1 side view (flat 1.25 mm) .....	137
Figure 7.29. Beam 1 front view (flat 1.25 mm) .....	137
Figure 7.30. Beam 1 back view (flat 1.25 mm) .....	137
Figure 7.31. Beam 2 side view (flat 1.25 mm) .....	138
Figure 7.32. Beam 2 front view (flat 1.25 mm) .....	138
Figure 7.33. Beam 2 back view (flat 1.25 mm) .....	138
Figure 7.34. Beam 3 side view (flat 1.5 mm) .....	139
Figure 7.35. Beam 3 back view (flat 1.5 mm) .....	139
Figure 7.36. Beam 4 side view (flat 1.5 mm) .....	139
Figure 7.37. Beam 4 back view (flat 1.5 mm) .....	140
Figure 7.38. Beam 5 side view (flat 0.75 mm + structured 0.5 mm) .....	140

List of figures

Figure 7.39. Beam 5 front view (flat 0.75 mm + structured 0.5 mm)..... 140

Figure 7.40. Beam 5 back view (flat 0.75 mm + structured 0.5 mm)..... 141

Figure 7.41. Beam 6 side view (flat 0.75 mm + structured 0.5 mm) ..... 141

Figure 7.42. Beam 6 back view (flat 0.75 mm + structured 0.5 mm)..... 141

Figure 7.43. Beam 7 side view (flat 1.00 mm + structured 0.5 mm) ..... 142

Figure 7.44. Beam 7 back view (flat 1.00 mm + structured 0.5 mm)..... 142

Figure 7.45. Beam 7 front view (flat 1.00 mm + structured 0.5 mm)..... 142

Figure 7.46. Beam 8 back view (flat 1.00 mm + structured 0.5 mm)..... 143

Figure 7.47. Beam type 1 (flat 1.25 mm), stress distribution in MPa..... 144

Figure 7.48. Beam type 1 (flat 1.25 mm), Y-distribution displacement in mm..... 144

Figure 7.49. Beam type 1 (flat 1.25 mm), Z-distribution displacement in mm ..... 144

Figure 7.50. Beam type 1 (flat 1.25 mm), magnitude displacement in mm, at the end of loading  
..... 145

Figure 7.51. Beam type 2 (flat 1.5 mm), stress distribution in MPa..... 145

Figure 7.52. Beam type 2 (flat 1.5 mm), Y-distribution displacement in mm..... 145

Figure 7.53. Beam type 2 (flat 1.5 mm), Z-distribution displacement in mm ..... 146

Figure 7.54. Beam type 2 (flat 1.5 mm), magnitude displacement in mm, at the end of loading  
..... 146

Figure 7.55. Beam type 3 (flat 0.75+structured 0.50 mm), stress distribution in MPa..... 146

Figure 7.56. Beam type 3 (flat 0.75+structured 0.50 mm), Y-distribution displacement in mm  
..... 147

Figure 7.57. Beam type 3 (flat 0.75+structured 0.50 mm), Z-distribution displacement in mm  
..... 147

Figure 7.58. Beam type 3 (flat 0.75+structured 0.50 mm), magnitude displacement in mm, at the  
end of loading ..... 147

Figure 7.59. Beam type 4 (flat 1.00+structured 0.50 mm), stress distribution in MPa..... 148

Figure 7.60. Beam type 4 (flat 1.00+structured 0.50 mm), Y-distribution displacement in mm  
..... 148

Figure 7.61. Beam type 4 (flat 1.00+structured 0.50 mm), Z-distribution displacement in mm  
..... 148

List of figures

Figure 7.62. Beam type 4 (flat 1.00+structured 0.50 mm), magnitude displacement in mm, at the end of loading ..... 149

## List of tables

Table 2.1. Classification of the processes for the structured thin sheets production [9].....	10
Table 2.2. Geometric dimensions of the structured sheets with the depth 33 mm [83].....	21
Table 2.3. Sandwiches with pictures and stiffnesses according to [85].....	26
Table 3.1. Sample dimensions for tensile tests .....	36
Table 3.2. DC01 steel parameters for sheet thicknesses 0.50; 0.75; 1.00 mm.....	37
Table 3.3. Structured sheet metal parameters before and after forming [95].....	38
Table 3.4. Dimensions of tested beams.....	38
Table 3.5. List of additional plates for specimens .....	40
Table 3.6. List of displacement transducers.....	43
Table 3.7. Maximal force, corresponding time according to laboratory experiments for C-profiles of specimens .....	44
Table 3.8. Maximal force for each specimen and corresponding displacements, results for IWAN 1 transducer.....	45
Table 3.9. Maximal force for each specimen and corresponding displacements, results for IWAN 2 transducer.....	46
Table 3.10. Maximal force for each specimen and corresponding displacements, results for IWAN 3 and IWAN 7 transducers.....	47
Table 3.11. Maximal force for each specimen and corresponding displacements, results for IWAN 4 transducer.....	49
Table 3.12. Maximal force for each specimen and corresponding displacements, results for IWAN 5 transducer.....	50
Table 3.13. Maximal force for each specimen and corresponding displacements, results for IWAN 6 transducer.....	51
Table 3.14. Specimens maximal forces, corresponding displacements from transducers (IWANs) and stiffnesses, experimental results.....	51
Table 3.15. Connection of specimen elements.....	55
Table 3.16. Boundary conditions and their degrees of freedom .....	56
Table 3.17. General information about models.....	57
Table 3.18. Equivalent geometric imperfections: Table C.2 from Annex C of EN 1993-1-5: [102].....	58

## List of tables

Table 3.19. Modelling of equivalent geometric imperfections: Figure C.1 from EN 1993-1-5 [102].....	58
Table 3.20. Eigenvalues for each of the model types. ....	59
Table 3.21. Simulation results for beam types 1-4, vertical deformation of lower model flange	62
Table 3.22. Simulation results for beam types 1-4, vertical deformation of upper model flange	62
Table 3.23. Simulation results for beam types 1-4, horizontal deformation of web in the center of model .....	63
Table 3.24. Simulation results for beam types 1-4, horizontal deformation of web on the left (IWAN 7) and right (IWAN 3) sides of model .....	64
Table 3.25. Beam types and corresponding stresses under the maximum loading .....	64
Table 3.26. Specimens maximal forces, corresponding displacements (from points where transducers are placed in experiments) and stiffnesses, simulation results for C-sectioned beams .....	66
Table 3.27. Comparison of experimental and simulation results (IWAN 2 and IWAN 4), Beam type 1.....	68
Table 3.28. Comparison of experimental and simulation results (IWAN 1), Beam type 1 .....	69
Table 3.29. Comparison of experimental and simulation results (IWAN 7 and IWAN 3), Beam type 1.....	69
Table 3.30. Comparison of experimental and simulation results (IWAN 2 and IWAN 4) for Beam type 2 .....	70
Table 3.31. Comparison of experimental and simulation results (IWAN 1), Beam type 2 .....	71
Table 3.32. Comparison of experimental and simulation results (IWAN 7 and IWAN 3), Beam type 2.....	72
Table 3.33. Comparison of experimental and simulation results (IWANs 2 and 4) for Beam type 3 .....	72
Table 3.34. Comparison of experimental and simulation results (IWAN 1), Beam type 3 .....	73
Table 3.35. Comparison of experimental and simulation results (IWAN 7 and IWAN 3), Beam type 3.....	74
Table 3.36. Comparison of experimental and simulation results (IWAN 2 and IWAN 4) for Beam type 4 .....	75
Table 3.37. Comparison of experimental and simulation results (IWAN 1), Beam type 4 .....	76

## List of tables

Table 3.38. Comparison of experimental and simulation results (IWAN 7 and IWAN 3), Beam type 4.....	76
Table 3.39. Comparison of experimental and FEM simulations results, C-sectioned beams.....	77
Table 3.40. Data for parametric research.....	79
Table 3.41. Results of parametric modelling.....	80
Table 4.1. DC04 steel parameters for sheet thicknesses 0.50; 0.75; 1.00 and 1.50 mm.....	84
Table 4.2. List of tested specimens and sheets that are their components.....	85
Table 4.3. List of displacement transducers.....	87
Table 4.4 Maximal force and corresponding time according to laboratory experiments for square-sectioned beams.....	88
Table 4.5. Maximal force for each specimen, corresponding displacements, stiffnesses, results from IWAN H1 and IWAN H2 transducers.....	89
Table 4.6. Location of visible web buckling area for specimens.....	90
Table 4.7. Maximal force for each specimen and corresponding displacements, results of IWAN L, IWAN M and IWAN L transducers.....	92
Table 4.8. Specimens maximal forces, corresponding displacements (from points where transducers are placed in experiments) and stiffnesses, simulation results for squared-sectioned beams.....	93
Table 4.9. Connection of specimen elements.....	94
Table 4.10. Boundary conditions and their degrees of freedom.....	94
Table 4.11. General information about models.....	95
Table 4.12. Eigenvalues for each of the model types.....	95
Table 4.13. Simulation results for beam types 1-4, vertical deformation in the middle of the beam.....	98
Table 4.14. Maximal force for each beam type, corresponding displacements and stiffnesses, simulation results.....	98
Table 4.15. Specimens maximal forces, corresponding displacements (from points where transducers are placed in experiments) and stiffnesses, simulation results for squared-sectioned beams.....	100
Table 4.16. Comparison of Beam 1 and 2 experimental and beam type 1 simulation results (IWAN M).....	101



## List of tables

Table 4.17. Comparison of experimental and simulation results (IWAN H1 and IWAN H2), Beam type 1 .....	102
Table 4.18. Comparison of Beam 3 and 4 experimental and beam type 2 simulation results (IWAN M) .....	103
Table 4.19. Comparison of experimental and simulation results (IWAN H1 and IWAN H2), Beam type 2 .....	104
Table 4.20. Comparison of Beam 5 and 6 experimental and beam type 3 simulation results (IWAN M) .....	105
Table 4.21. Comparison of experimental and simulation results (IWAN H1 and IWAN H2), Beam type 3 .....	106
Table 4.22. Comparison of Beam 7 and 8 experimental and beam type 4 simulation results (IWAN M) .....	106
Table 4.23. Comparison of experimental and simulation results (IWAN H1 and IWAN H2), Beam type 2 .....	107
Table 4.24. Comparison of experimental and FEM simulations results, square-sectioned beams .....	108
Table 4.25. Experimental, simulation and analytical stiffnesses .....	109

## Nomenclature

### Formula symbols

$h_C$	Comb height
$D_C$	Comb Depth
$t$	Sheet thickness
$l_C$	Length
$b_W$	Web gap
$l_{side}$	Comb side length
$s_{E0^\circ}$	Distance between two centers of honeycomb structural directions $0^\circ$
$s_{E90^\circ}$	Distance between two centers of honeycomb structural directions $90^\circ$
$\alpha_W$	Angle between curved comb and flat web
$E$	Young's Modulus
$R_{p0,2}$	Conventional limit of elasticity 0,2%
$R_m$	Tensile strength
$R_{plocal}$	Local yield strength
$R_{pglobal}$	Global yield strength
$b$	Flange width
$t$	Thickness of beams web
$L_c$	Specimen length according DIN EN ISO 6892-1 and DIN 50125
$L_0$	Gauge length according DIN EN ISO 6892-1 and DIN 50125
$w/l$	Width to length ratio of specimen according to Fritzsche [95]
$a$	Thickness of flat products according to DIN 50125
$b_0$	Sample width according to DIN 50125
$B$	Head width according to DIN 50125
$h$	Head length according to DIN 50125
$L_t$	Overall length according to DIN 50125
$\sigma_t$	True stress
$\sigma_n$	Nominal stress
$\varepsilon_n$	Engineering strain
$\varepsilon_t$	True strain
$\varepsilon_n$	Engineering strain
$\varepsilon_e$	Elastic strain
$\varepsilon_t$	True strain
$\varepsilon_p$	Plastic strain
$F$	Force
$UX(U1)$	Displacement in the X direction
$UY(U2)$	Displacement in the Y direction

## Nomenclature

UZ(U3)	Displacement in the Z direction
URX(UR1)	Rotational displacement in the X direction
URY(UR2)	Rotational displacement in the Y direction
URZ(UR3)	Rotational displacement in the Z direction
A	Beam type
B	Number of parametric beam
A.B	Beam full number
$t_{C-p}$	Thickness of C flat profile
$t_{3p}$	Thickness of 3 flat plates
k	Stiffness increase factor
$S_{BT1}$	Stiffness of beam type 1
$S_{BT2}$	Stiffness of beam type 2
$k_{BT2}$	Stiffness increase factor of beam type 2
$k_{flat}$	Stiffness increase factor for C-sectioned specimens manufactured from only flat plates
$k_{str}$	Stiffness increase factor for C-sectioned specimens manufactured from flat and structured plates
S	Bending stiffness
d	Deflection
F	Force
I	Moment of inertia of the beam
L	Beam length

## Abbreviations

ECCS	European Convention for Constructional Steelwork
FE/ FEM	Finite Elemente Methode
FQZ®	Germ. Forschungs- und Qualitätszentrum Oderbrücke gGmbH
Borit®	Borit® Leichtbau-Technik GmbH
CAE	Computer Aided Engineering
DAST	Deutscher Ausschuss für Stahlbau
IMP	Imperfection
ICE	Intercity-Express
FQZ	Research and quality center; germ.: Forschungs- und Qualitätszentrum
FMPA	Research and material testing institute; germ.: Forschungs- und Materialprüfanstalt)
BT	Beam type
GB	Flat single sheet connection; germ.: Glatt Blech Verbindung
GG	Two flat sheets connection; germ.: Glatt - Glatt Blech Verbindung
SG	Flat sheet-web connection; germ.: Glatt Blech-Steg Verbindung
WG	Flat sheet-comb connection; germ.: Waben-Glatt Verbindung
FS	Flat surface - web connection; germ.: flächige Auflage - Steg Verbindung
FW	Flat surface - comb connection; germ.: flächige Auflage - Wabe Verbindung
SSA	Web-web variant A connection; germ.: Steg-Steg, Variante A Verbindung
SSB	Web-web variant B connection; germ.: Steg-Steg, Variante B Verbindung
SW	Web-comb connection; germ.: Steg-Waben Verbindung
WW	Comb-comb connection; germ.: Wabe-Wabe Verbindung
3D	Three Dimension
IWAN	Displacement transducers; germ.: Induktive Wegaufnehmer
TIG	Tungsten inert gas
GTAW	Gas tungsten arc welding

# 1 Introduction

## 1.1 Motivation and relevance

The main purpose of an engineer is to provide the safety and to increase the economy of a construction. The main idea of lightweight constructions is to ensure economy and ecology with a low weight compared to other building constructions.

Since the end of the 1980s, a new so-called ‘structured thin sheets’- a light-weight product, have been produced to the construction industry. The aim of these lightweight elements is to increase the stiffness of sheet metal components by defining geometrical structures in the thickness direction of the sheet metal [1-6]. The stiffening leads to a weight saving of up to 50% without losing the load-bearing capacity of the construction, only through the attainable reduction of the sheet thickness. The structures themselves are inserted into the starting plate by means of a shaping technique, without additional material. This leads to an additional, significant weight reduction in the overall concept of passenger cars [7, 8].

Nowadays, special different technology allows people to produce thin steel plates with a three-dimensional structure - hexagonal staggered pattern (honeycombs or cells). These sheets are currently used in automotive and household industry and even aerospace. As honeycomb plates have a potential for using it in different parts of our live, the question is: will they find the application in building field.

Provided by different techniques, the mechanical transformation process of sheet metals leads to material structure changes. The structured metal sheets have higher bending stiffness than flat metal sheets, which can offer a certain application in steel construction. They are used as a basic material with increased buckling resistance to create new structural elements.

Some basic research already have been done. For example, in Germany, a group of professors, research workers and graduate students conducting basic research for the further production of structured sheets. The research group was established at the Brandenburg Technical University (BTU – germ. Brandenburgische Technische Universität) in Cottbus. Studies have focused mainly on the production of sheets of structured design, as well as the study of their carrying capacity, strength properties, aerodynamic properties, corrosion resistance. The overall objective of the research project is the accumulation of knowledge and experience to further the production and processing of structured sheets.

According to preliminary investigations it is possible to believe that this topic is relevant to this day. So that, the behavior of structured plates under external loads must be studied more detailed.

## **1.2 The aim of the work**

This thesis is created inside the complex research project DESTRUCT/S, based on the idea of sandwich structured sheets fundamental properties research. Some basic questions in different subject areas about structured material are investigated. The study is held in such areas as economy, acoustic, welding, corrosion, material engineering, structure building.

To provide a fundamental study in the area of light steel thin-walled structures, sandwich structured sheet metals as parts of the investigated specimens are chosen. The aim of the work is to find out the advantages of sandwich structured sheets over flat ones. To achieve this aim, several goals are set. First one is to manufacture specimens for the research and to find out their material properties by means of tensile tests. In general, for 2 series of point-bending tests 16 specimens with different wall thicknesses are created: 8 C-sectioned beams and 8 square-sectioned. There are following parameters for each of the specimens are found out from laboratory results: maximal forces with corresponding displacements, load bearing capacity and stiffnesses. After that, FEM simulations are conducted and evaluated with experimental results. Also, analytical and parametric studies are made in order to predict the behavior of similar-shaped specimens.

The results obtained are supposed to give a base for researchers about structured sandwich plates manufacturing and their properties and behaviour in different cases. Also, the topic structured sheet metals research will give a lot of possibilities to use such kind of material in steel constructions area of building.

## **1.3 Thesis structure**

Chapter 2 is an overview of the structured sheet metals. Special attention has been given to classification, manufacturing, forming, welding, properties and applications of structured plates.

Chapter 3 presents the laboratory and FEM experiments on lightweight steel C-sectioned beams. Similar structure has Chapter 4: same experiments are made, but for square-sectioned specimens. Also, Chapter 3 and Chapter 4 discuss the parametric modelling and analytical analysis of made experiments.

Finally, Chapter 5 contains overall conclusions of this work, based on obtained results from all previous chapters.

## 2 Structured sheet metals

### 2.1 Historical development of lightweight constructions

The use of stiffening elements in the steel industry has been known for over 150 years. Both the development and the requirements of the technology have been the driving force of the technical progress. For example, corrugated sheets made of steel could have only been manufactured after the rolling of the iron or steel sheet has become possible. The written below brief literature overview of the discovery and development of lightweight constructions is intended to illustrate this in more detail. [9]

In 1829 Henry Palmer took out a patent for ‘corrugated metallic sheets’. To solve the problem of roofing massive warehouses such as London Dock, he came up with light-weight corrugated iron sheets – though he quickly sold on the patent to a carpenter, Richard Walker, who was a contractor in the New Docks. [109]

The Turpentine Shed, built about 1830, was the first building to be roofed with iron sheets pressed through fluted rollers. Other large-span structures followed in the 1840s such as the Eastern Counties Railway Station in London. [109]

In 1844, Spencer rationalized the production of corrugated iron by the fact that the product was produced in a rolling mill, so that all sheets of metal could be stamped at once. With the corrugated plate principle, the bending stiffness of the material in the transverse direction can be increased substantially. In this case bearing load on the construction with such plates may increase more than one hundredfold. The new product significantly facilitates the construction of buildings; it is used as a cover or as a wall of sheds, garages, barracks and even to the plane [22].

In 1875 Wesenfeld invented the actual self-supporting corrugated sheet. [22] The lightweight potential of the corrugated sheet was already recognized in 1850. First mathematical approaches of the corrugated roofs and ceilings design had been made and became available in combined tables. However, the use of the corrugated sheets was limited by the restricted manufacturing possibilities. The influence of the corrugated sheets geometry, in particular of the cross-section, on the stiffness, was well-known. The advantage of the corrugated sheets compared to flat plates could not be exhausted completely. [23]

Constructive and stability-theoretical demands of the lightweight construction for the industry appeared at the beginning of the 20th century first in aircraft industry and became really necessary there. The first element for the airplane was stamped with the help of the timber-framed machine and the application of corrugated sheet. [9]

Junkers (see Figure 2.1 and Figure 2.2) was a very advanced aircraft: an aerodynamically clean all-metal low-wing cantilever (without external bracing) monoplane [24]. An aluminium

## Structured sheet metals

alloy (duralumin) structure was used for the aircraft. It was entirely made of corrugated and stressed duralumin skin.



Figure 2.1. Junkers F13 covered with corrugated sheets

Since about 1920 the shell and solid wall construction method prevailed over the others. Junkers, Dornier and Zeppelin were the leaders in using the modern lightweight constructions. Nevertheless, by while the shell and solid wall construction method was being used, the new stability questions were appearing. These were mostly solved by stress tests in the 1920s [25].



Figure 2.2. Stress-test of a Junkers G-23 plane [26]

Another shape optimization method is crimping of flat and curved metal sheets [27]. From the 1950 Oehler [28-30] carried out investigations of corrugated metal sheets dealing with production engineering aspects. But the first investigations of life expectancy were mainly carried out in the 1990s [31, 32].

In the 1960s, Kienzle investigated profiled steel bands and corrugated sheets, in order to demonstrate the stiffening effect of hat channel profiles, among other ones. He also researched the bead profiles with the biggest resisting moment and with the lowest material consumption. [33] Schapitz also presented new results of firmness calculations for lightweight construction [25]. The stiffening effect of the beads still interests the scientists.

However, at the present time, stiffening is being manufactured not only for beading and corrugated plates, but for sheet metals in general. Since the beginning of the 80s scientists have been searching for new possibilities of making building elements stiffer, to improve the products optical properties, to make higher sound and heat emission and also for decorative purposes [34, 35].



The structured thin sheets also provide a driving force for innovative light-weight solutions not only in machinery and vehicle construction but also construction building. Nevertheless, the development of complex lightweight construction elements, is very difficult, because usually they cannot be made according to guidelines and catalogues [9].

## 2.2 General information about structured plates

Due to the fast industry development, there is a need for new innovative components, such lightweight structures which have already come to the market in recent years. Even though they appeared not long ago, they still need to be investigated and described more carefully. [79]

Nature has perfected lightweight construction. With minimal use of energy and materials, it has produced a variety of stable and lightweight constructions.

The honeycomb structures of the bees have an extremely high stability and at the same time have an extremely low weight. Loads are distributed over the honeycomb walls on the entire honeycomb construction and thus do not act punctually. The hexagonal honeycombs give the construction its stability. [92].

Furthermore, a honeycomb shaping of sheet metal gives rise to various positive effects, which are shown in Figure 2.3.

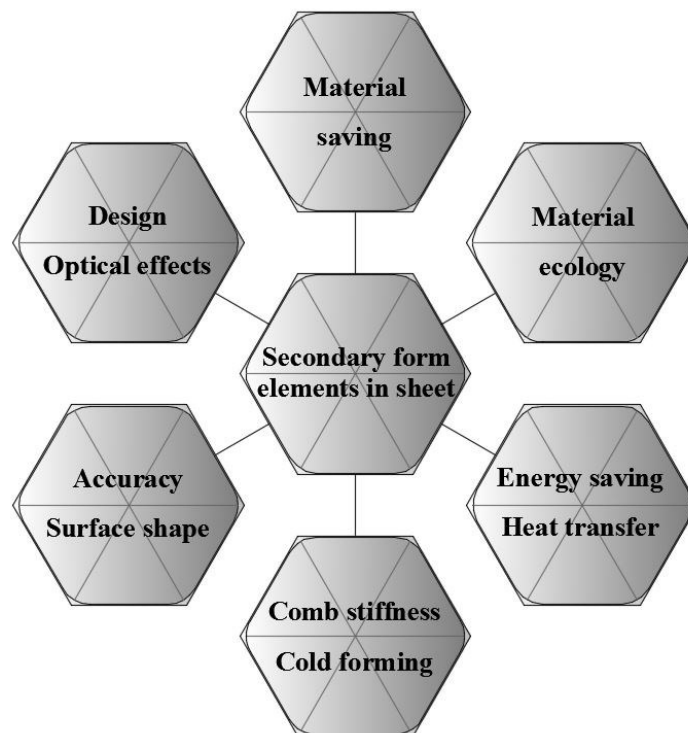


Figure 2.3. Effects to be expected due to new shaping according to Bräunlich [91]

To achieve the honeycomb (cell) shape, sheet metal is cold formed. By the means of structured thin sheets, it is possible to create innovative lightweight solutions and to produce new semifinished products for specific requirements. However, the structured sheets have not been implemented in guidelines yet, so that the industry and potential users should use them without concerns.

Exactly these concerns had to be solved aiming the practical implementation of the developed structured sheets. Sheets are already implemented in lighting technology or in the manufacture of household appliances (see chapter Application of structural sheets). In present time, only roof or facade elements with structured sheet metal have been implemented in steel construction. There are no limits to the use different materials in the structuring process - cardboard or even paper can be the reshaped or structured [93].

### 2.3 Definition and classification of structured plates

The word 'structure' comes in English from old French, or from Latin '*structura*', which in its turn comes from the verb '*struere*' - to build. The verb was rarely found before the 20th century.

The term 'structure' may be found in literature of different disciplines, so, there is a variety of definitions. There are some of them:

- Structure is the specific organization or system of interrelated elements, all of which implement a particular function [10]
- Structure is the way in which the parts of system or objects are arranged or organized or the system itself [11]

In the technical sense, structures are used to build a technical structure. The simplest technical constructions are individual parts. Each component has three influencing features: material, shape, dimensions [9].

The shape of the individual part is one of the essential factors for the implementation of lightweight construction. It has also brought a big influence to the dimensions of the individual part and the material consumption [12-15].

The structural sheets investigated in this study offer a high potential to reduce the weight of lightweight construction. Lightweight constructions can generally be divided into beam and shell support structures. A further classification takes place according to the function of the structure in tensile structures, tensile-push-thrust structures and bending-torsion structures [0]. The lightweight constructions offer optimal possibilities for low-cost production of optimized stiffeners and are classified according to their technological characteristics and conditions into integral, differential or composite construction. According to the geometric form, Hufenbach divides structural stiffening into local and global rigidity [17]. Bleicher determinates three construction strategies in the effort to minimize the dead weight of a construction in the above-mentioned structural design: to change the shape, the material and the working conditions of the constructions [18].

According to Neubauer [74], structures can be referred to as so-called 'secondary forming elements' including crimping, stiffening plates, folding etc. [9].

Secondary form elements are special material-geometric units, which can almost always be assigned to a production type. They define the main shape. The main shape is the flat or

## Structured sheet metals

curved sheet. Secondary form elements can have the various structural shapes such as truncated pyramid, truncated cone, half sphere. The properties of the whole plate depend on the orientation and the geometrical dimension of the secondary fold elements, located on the surface of the sheet. The arrangement of the form elements can be different: regularly or irregularly, symmetrically or asymmetrically in relation to the centre of the sheet metal. [9]

Structured fine sheets are planar light-weight structures, in which planar or curved sheet metal components have been stiffened by secondary forming elements. [9]

These structures of lightweight construction may consist of beads, ribs, folds, cells or other secondary features. The overview below – the classification made by Hoppe in Figure 2.4, explains the assignment of the structured sheets. [9]

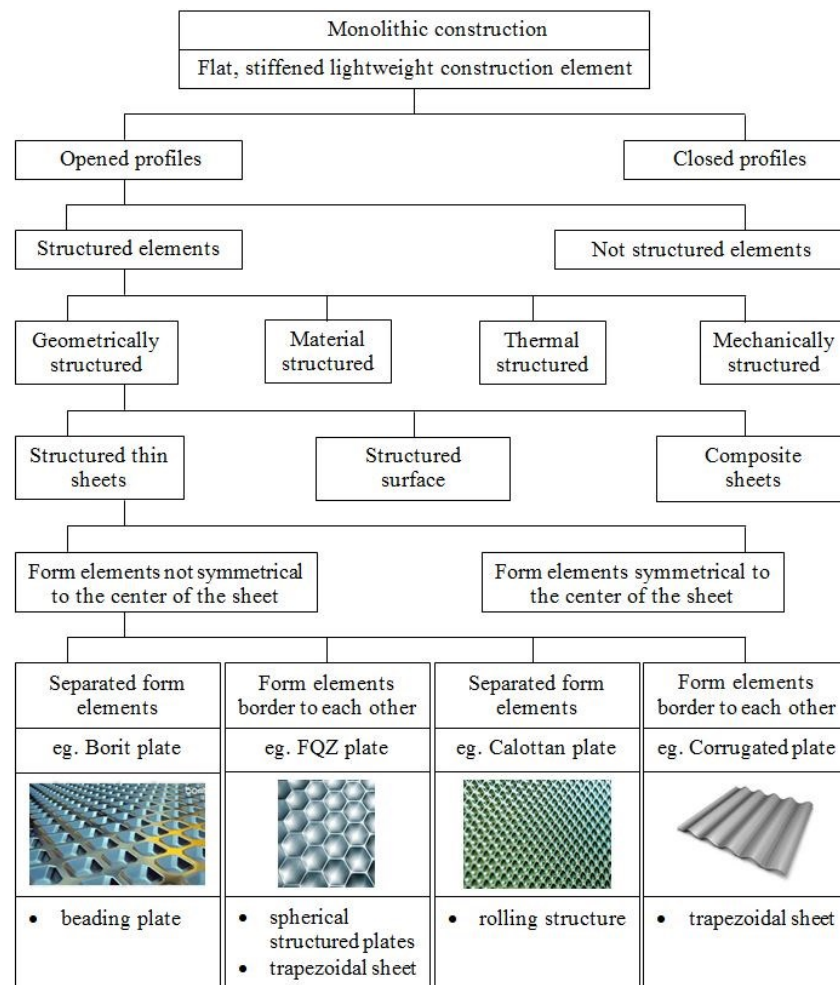


Figure 2.4. Classification of structured thin sheets according to Hoppe [9] based on Hufenbach [20], Neubauer [19], Vollertsen [21]

According to Figure 2.4, the structured thin sheets investigated in the present study are surface structures from the area of form-fit construction. The investigated structures, rolling structure, spherical structure and protruded structure are assigned to the group of geometrically structured fine sheets. Raw material forms an open profile. Structured sheets are produced using light-weight manufacturing processes. Also have a great importance the type of shaping and the forming history for the subdivision of the structural sheets. Structured sheets are low-reworking or even-free. A particular feature of these structures is to give a single-piece component a global

stiffening, particularly with reference to increase in torsional strength and/or buckling stability [9].

## **2.4 Classification and manufacturing of structured sheet metals**

In this part the metal manufacturing processes are classified according to DIN 8580 [66]. Some of them are used exactly for creating metal sheets. These processes are described in detail.

### **2.4.1 Classification according to DIN 8580 [66]**

According to DIN 8580 [66], the manufacturing processes are subdivided into six main groups, which focus on metal processing. Specific feature of the division is the cohesion of solid body particulate. The cohesion is either created (casting) or maintained (forming, rearrangement of solid particle) or reduced (separating, removing of solid particle) or increased (joining, coating, introducing of solid particle) [66].

1. Casting (create cohesion) includes all manufacturing processes in which a workpiece is manufactured from shapeless material, referred to as a primary molding process. In these methods, the cohesion of the particles is created. Formless material includes all starting material whose form is not defined, such as a liquid which adapts to the inner walls of the container. The most important process of the group is casting with molten base material. Otherwise powders, pastes and granules are used for sintering. The various generative manufacturing processes, some of which are also known as 3D printing or rapid prototyping, are not yet categorized as comparatively young methods in the DIN standards; in the special literature, however, they are mostly assigned to the original forms [66].
2. Forming (maintaining cohesion) combines all manufacturing processes in which workpieces are produced from solid workpiece by permanent deformation, only in case the material is neither added nor removed. The mass of the workpiece is equal to the mass of the finished item. The most important processes of the group are rolling, swaging (or drop forging), impact extrusion, extrusion molding, deep drawing and bending [66].
3. Separation (reduce cohesion) involves all processes in which the shape of a workpiece is changed by the damage of the material cohesion at the processing point and thus the total material amount is reduced. The most important group is machining, where the material is removed like chip scrap, e.g. sawing, planing, milling, drilling [66].
4. Joining (increasing cohesion) is the long-term connecting of several workpieces. This includes in particular welding, soldering and bonding but also riveting, screwing or assembling [66].
5. Coating (increasing cohesion) Coating is process in which a strongly adhering layer of shapeless material applies to a workpiece, e.g., painting, electroplating, powder coating, hot dip galvanizing [66].
6. Change material properties of a workpiece includes hardening and baking, e.g. softening for further processing) [66].

## Structured sheet metals

Forming should be considered more carefully, because exactly this type of manufacturing process was used in this work to get the structured plates for further investigation.

The individual procedures in the main group 'forming' may be divided according to different criteria [66]:

- I. Dimension of the workpieces:
  - A. Massive forming
  - B. Sheet metal forming
  - C. Wire forming
- II. Temperature of the processing
  - A. Cold forming, in which the strength of the workpieces increases during processing:
    - Impact extrusion
    - Spin forming (metal turning)
  - B. Hot forming:
    - Forging
    - Swaging
    - Extrusion molding
- III. Mechanical stress that act in the workpieces according to DIN 8580 [66]
  - A. Compression forming (DIN 8583 [68])
    - Rolling
    - Forging
    - Swaging
    - Embossing
    - Impact extrusion
    - Extrusion molding
  - B. Tension and compression forming (DIN 8584 [64])
    - Drawing
    - Deep drawing
    - Spin forming (metal turning)
    - Hydroforming
  - C. Tension forming (DIN 8585 [49])
    - Stretching
  - D. Bending (DIN 8586 [69])
    - Bending with straight tool
    - Bending with rotating tool
  - E. Shear forming (DIN 8587 [70])
    - Rotating
    - Shifting

### 2.4.2 Classification according to Hoppe [9]

Beside the replacement of classical materials with the aluminium materials and modern lightweight structural steels, structured thin sheets may significantly reduce the material use in the field of automobile manufacturing [36, 37]. According a lot of different articles and various publications, a great potential of structured thin sheets was discovered, which may be proved by many industrial applications [5, 7, 38-45]. Structured thin sheet metals are produced with the help of cost-effective, transforming manufacturing processes from thin or bent thin plates, which, in addition to defined mechanical properties, also must meet all requirements from the fields of design and safety of lightweight construction [32, 39, 44, 46, 47].

According to the manufacturing methods in Table 2.1 for the structured sheet metals manufacturing the corresponding semifinished products have been used. In compliance with ISO 3134, semifinished products are products which are produced, for example, by hot and / or cold forming (by warming and / or cold rolling) [9]. This includes profiles, sheets and strips. As written in DIN EN 1386, products with moulded patterns are called sheets if they are made from smooth sheet metals [48]. Structured sheets are produced by cold-forming processes and belong to the semifinished products category.

Table 2.1. Classification of the processes for the structured thin sheets production [9]

	Manufacturing process	Semifinished product
<u>Manufacturing using tools</u>		
Draw-forming method		
Deep drawing - Embossing using a rigid tool	Embossing	Waffle structured sheet metal
Bending forming method		
Bending using rotating tool - Roll bending	Roll bending (wavy forming)	Corrugated sheet
Tension and compression forming method		
Deep drawing, using tools - Deep drawing using a rigid tool (with rigid roller)	Roll structuring	Rolled sheet metal
Special process for sheet metal manufacturing		
Forming using tool with elastomer -Bump structure	Bump structuring	Bump structured sheet
<u>Manufacturing using active media</u>		
Tension and compression forming method		
Special process for sheet metal manufacturing		
Forming using active media -Combination of stretching and deep drawing	Hydrostatic stretch forming with rolling out	Hump sheet
Deep drawing using active media		
-Deep drawing using active media with force impact (with liquid)*	Spherical structuring	Spherical structured sheet
-Forming with negative molding tool and liquid under the pressure	Hydroforming	Structured sheet

### 2.4.3 Manufacturing using tools

#### 2.4.3.1 Embossing using rigid tool

The embossing is assigned to the deep-drawing group according to DIN 8585. It is a stamping process for producing raised or sunken relief in sheet metal with insignificant change

in metal thickness made by passing sheet or a strip of metal between rolls of desired pattern [49].

During stretching, recesses appear on the surface of a flat or bent plate. The sheet thickness decreases due to the surface expansion. Waffle structure sheets are often produced on simple presses with a column frame by hollow embossing with the help of a rigid tool. For this purpose, the lower embossing instrument with the arranged shaping elements is brought into the sub-tool. The upper tool is manufactured with embossed formed elements [9].

The flat sheet is inserted into the tool, and then when the tool is closed, the sheet is pulled or bent into the recess. The waffle structure forms symmetrically in relation to the centre of the sheet from both sides. The shape of the structure that was formed in the upper and lower tool depends on the shaping elements. But the embossing of structured thin sheets has disadvantage - the tool size and the press size limit the blank size of the area to be structured. These structures are used in heat shielding technology [50-52].

### 2.4.3.2 Roll bending

The bending process of moulded semifinished products is one of the most common types of metal forming. [69]

Sheet curving is similar to bending forming process and cold forming process in which patterned structural sheets, that are produced from flat sheet metal with a help of profiled-determining roller pair, for example, so-called corrugated sheets, by one or more steps are generated –Figure 2.5.



Figure 2.5. Corrugated sheet manufacturing using rotating tools [53]

This deformation makes a thin piece of steel or aluminium sheet a semifinished product with high stiffness and load bearing capacity with a very low net weight and material use. The disadvantage of the corrugated sheets is the so-called corrugated sheet metal effect - the dependence of the stiffening direction, which is still enormous [9].

As this method is concerned with a bending process, there is no intentional sheet thickness change. Thin-walled and with large area structured thin sheets can be produced economically with high productivity. This is an incontestable advantage of this method. Modern equipment deforms the sheet to profiles with the speed over 70 m/min for sheets up to 200 mm

height. Corrugated sheets are characterized by the corrugated profile introduced perpendicular to the feed direction of the sheet Figure 2.6 [9].



Figure 2.6. Corrugated iron sheets as facade elements [65]

For demanding objects, it is possible to find smaller wave profiles, with so-called mini waves. These mini-waved profiles are often used to build exhibition and shop halls. The mini waves may be manufactured in steel, stainless steel and aluminium may be used indoors and outdoors. [54].

#### 2.4.3.3 Roll structuring

In the case of the rolling structuring, planar thin plates are guided through a roller frame with two so-called ‘spiked wheels’, Figure 2.7.

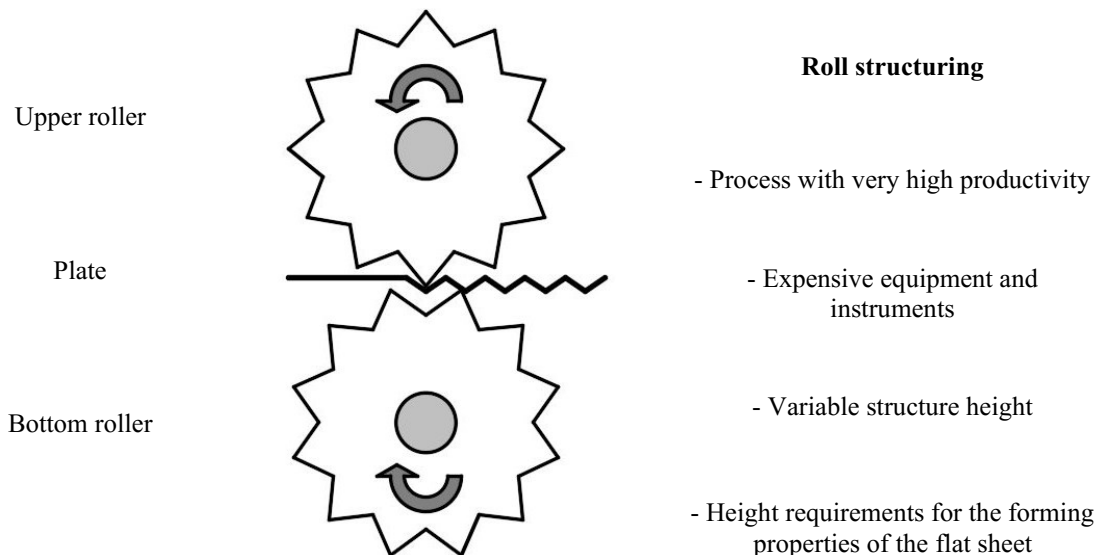


Figure 2.7. Roll structuring [9]

The rollers shaping elements are usually truncated cone or pyramids. The shaping elements create the characteristic roller structures. These shaping elements create the characteristic rolled structures. The quality and stiffness of rolled sheet is defined by the sizes of engagement depth and roller friction that is the proportion of the upper and lower rollers velocities. The proportion of the sheet thickness to the structural height is maximum 1:10. A



characteristic feature of the roll structuring is the bilateral symmetrical structure formation taking place in the centre of the sheet metal plate. An important precondition of the heat shields or warm protective shields production is the possibility of structuring also thin sheets in the area of 0.1 mm [9].

Due to geometric and mechanical conditions, aluminium materials up to 2 mm, normal steel type up to 1 mm and higher steel quality up to 0.6 mm thickness are manufactured. By means of the roll patterning, perforated plates can also be produced. They are also used for the production of multilayer interconnections to form heat shields [9].

#### 2.4.3.4 Bump structuring

Bump structuring is an innovative, patented process [55]. A flat sheet metal prestressed between two rollers is linearly transformed into an instability state, so that the so-called bump structure is formed continuously over the width.

The lower roll is made of an elastomer, similar to that of the bossing roll, and the upper roll is made of steel and is a base for the shaping elements [52]. In the forming process, only a plastic deformation occurs like a bending edge on the border of the bumps, so that the deformability of the base material is largely retained and the stress on surface dip remains poor [56], Figure 2.8.

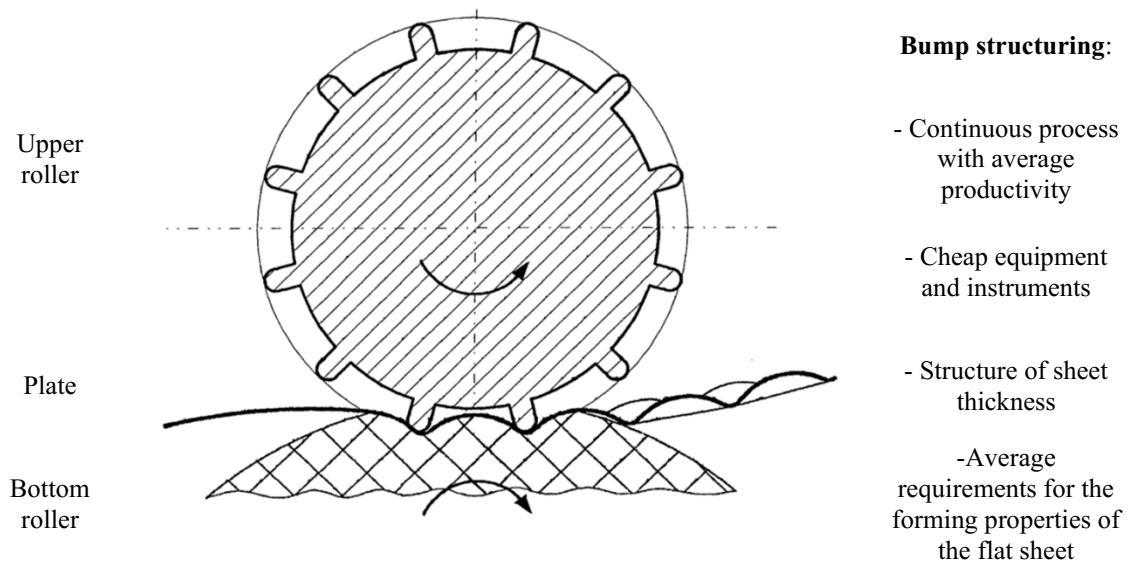


Figure 2.8. Bump structuring [9]

The structure of the bending plate looks like cells (or honeycombs) – see Figure 2.9.

## Structured sheet metals



Figure 2.9. Structured plate produced by Dr. Mirtsch GmbH; Miele & Cie. GmbH&Co [71]

Bump structures are currently used in car industry and container construction [43], in the packaging industry [45, 57], in lighting technology, in heat exchangers [58] and household appliance constructions, see Figure 2.10.

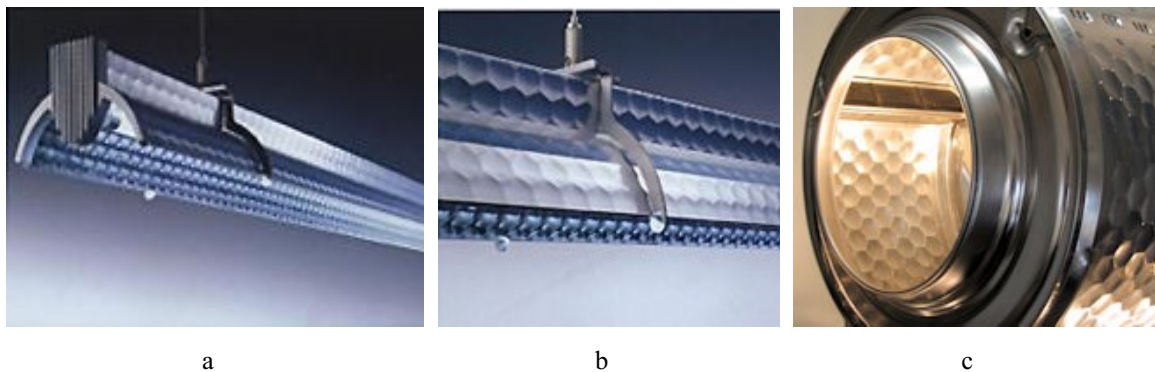


Figure 2.10. Bump-structured sheet metal: in lighting technology: (a, b) hexal lamp [59] and in household appliance construction: (c) washing machine's drum [60]

### 2.4.4 Manufacturing of stiffened construction elements using active media [61, 62]

According to DIN 8584, the tensile-strain-press forming of a sheet pre-cut part (film, plate, panel, segment or section) into an opened on one side hollow body or into a hollow body, that reduced to a smaller cross-section without a desired change in the sheet thickness [63]. The thermoforming process also includes inverting. Stretching is assigned to the group of deep drawing according to DIN 8585, T4 and is a method of tensile deformation to introduce the depressions into a flat or corrugated fine sheet [49]. The surface extension relates to the sheet metal thickness reduction.

Cupping processes with the use of an active media are divided according to DIN 8584 [64]. The depth, in particular the stretching, could also been done with active media. A shaping half (stamp or matrix) of the conventional tools is replaced with active media by a formless solid medium, a liquid or a gas. The forming processes with liquids are practically important, for example, with water emulsions or gases (as nitrogen or air). Both these methods are used in the production of structured fine sheets. Not only aluminium but also steel may be both found in base material group [9].

#### 2.4.4.1 Hydrostatic stretch forming with rolling out (Metallwerk GmbH) [72]

Approximately 50 years ago a technology with the stretching techniques of bump plates production began to develop. These bump plates were developed by the companies Krupp Maschinenteknik GmbH as employer and Stephan Witte GmbH & Co. KG as a manufacturer. Bump plates are manufactured from flat semifinished products, the regular located bump-shaped protrusions are pressed to one side, see Figure 2.11 [9].



Figure 2.11. Bump plate

By means of the deep drawing and the pure hydrostatic stretching transformation of the secondary formed elements, the sufficient high quality bump plates can not be manufactured, because the achievable sheet thicknesses in the bottom area became too small. Therefore, the production of the bump plates is predominantly carried out with the hydrostatic stretch-back forming according to the patented technique. This is a combined process. [73, 74]

First, only the body surface of the secondary forming element is stretched by forming. The sheet bottom area remains largely unformed. Then, the active medium (water) is reversed (redirected) and everted the resulting sheet shape. The final shape is almost reached, but in the bottom of the secondary shaping element the full forming capacity is still available and can be used for the complete shaping of the secondary shaping element. A further pressure increasing to a maximum of 3000 bar leads to the complete formation of the desired secondary shaping element. [9]

Bump plates consist of flat areas and bump-shaped deepenings, which are spanned with the same interval and in one side. With small and middle-sized truncated cone of bumps, their insertion in row occurs in such a way, that the row always ends with one whole bump. The production of each next bump row happens after the sheet is moved in longitudinal direction. Special tools which determine the geometry of the bumps are required to pull out the bumps [75]. This method may be applied to the materials from an initial sheet thickness from 0.1 mm up to 2.0 mm. Greater sheet thicknesses are technologically feasible but need higher pressures to apply. The materials must have excellent forming characteristics. The pronounced extensibility is particularly important.

Bump plates can be produced from coil. The desired board lengths are cut after the bumps are finished. Today the production of the bump plates takes place with feed motion. This also

allows reducing a cost-effective width variation of the circuit boards and also partial structuring [19].

Bump plates, like many other structured sheets, have a wide range of application, mainly through the shaping of interconnections or so-called hollow structures. Due to the simple manufacturing process, the application fields of the single bump plate as a flat lightweight construction element are realized first of all in the construction industry (façades), transportation (container) and rail vehicle construction (ICE trains) [76].

The bump-plates have advantages. Compared to the smooth sheets, a heat exchange surface of up to 30% higher and the stability or compressive strength (according to the picture experiments) of the double bump sheets is 7.5 times higher than welded together flat with bump plates and in 55 times higher than for flat plate. Bump plates also are good and easy to store by parallel arrangement because of their structure [75].

### **2.4.4.2 Deep drawing using active media**

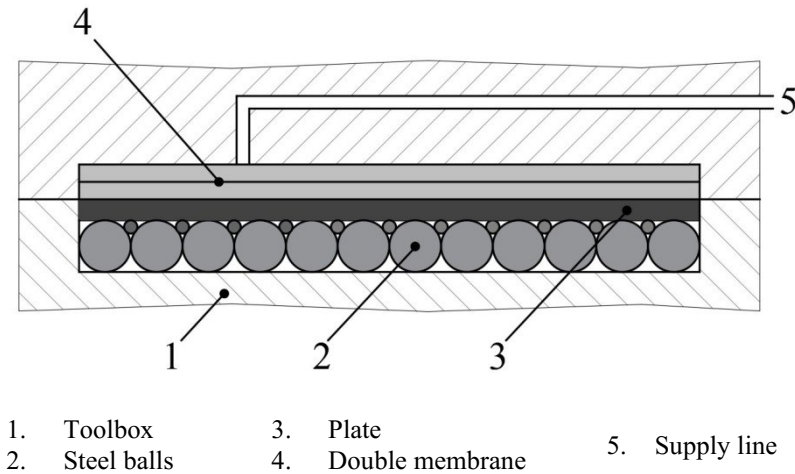
The deep-drawing processes using active medium may be divided, on the one hand, if a membrane is applied or not and, on the other hand, if the pressure comes by the tool movement or from the outside. One form of thermoforming with the active medium is the fluid cell method. It was developed at the end of the 50s especially for the aircraft industry for the production of low drawing depths [52].

#### **2.4.4.2.1 Spherical structuring based on the fluid cell method**

The manufacturing process of the so-called spherical structure is shown in Figure 2.12. The pressure is carried out externally like in the case of the fluid cell process. The double membrane is used for force transmission. Forming elements are steel balls.

In Figure 2.12 the tool consists of a toolbox (1) and a double membrane (4) which can be acted on by a working medium. Steel balls (2) are arranged in two different sizes in the tool box, Figure 2.12. The size of the structure depends on the size of the used steel balls. By selecting the steel balls diameters, it should be taken into account that the proportion of the ball diameter 1 to the ball diameter 2 should correspond to the 1:3 respectively. If the balls are arranged as shown in Figure 2.12 and the ball diameter is selected in a proportion of 1:3, it is ensured, that an approximately equal height of structure that was made by the implemented balls on the surface is achieved. The insertion of the smaller balls takes place in order to minimize the structured parts warping.

The flat plate (3) is loosely inserted into the tool over the steel balls, the tool is closed. An active medium is brought into the double membrane via a supply line (5). Due to the high active medium pressure, the structure is extruded from the initial material. Then the pressure from the double membrane is taken off, the tool is opened, and the ball-shaped thin sheet is removed as a semifinished product [9].



**Spherical structuring:**

- Discontinuous process with average productivity
- Expensive equipment and instruments
- Variable structure geometry
- Average requirements for the forming properties of the flat sheet

Figure 2.12. Spherical structuring [9]

Due to the variation of the ball sizes and the membrane pressure different structures can be produced flexibly without high tools costs. This method provides the partial structuring of elements or structuring of individual sheets. At this time these structures are used in manufacturing of floors and radiators, Figure 2.13.

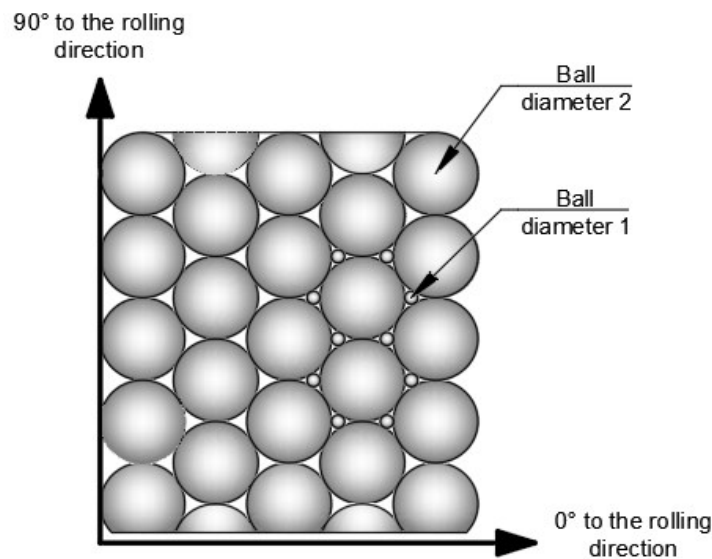


Figure 2.13. Ball-structured thin sheet: arrangement of the steel balls in the tool [9]

**2.4.4.2.2 Hydroforming**

Hydroforming is another type of shaping metals. Exactly this way of shaping is used to get honeycomb structured plates, that are investigated in present work.

The sheet hydroforming process is based on the 1950s patent for hydramolding by Fred Leuthesser, Jr. and John Fox of the Schaible Company of Cincinnati, Ohio in the United States. It was originally used in producing kitchen spouts [77, 78].

A negative form (molding tool) is in a press. The sheet to be structured is placed on that form and fixed. In a closed camera, a pressure is exerted on the sheet by means of a fluid, so that the sheet abuts to the negative molding tool and is structured, as shown in Figure 2.13. [77].

## Structured sheet metals

The forming tool used for sheet metal uses a diaphragm and closed camera to build up pressure. The advantage of hydroforming is that the workpiece is separated from the active medium and the need of a subsequent cleaning disappears. [79]

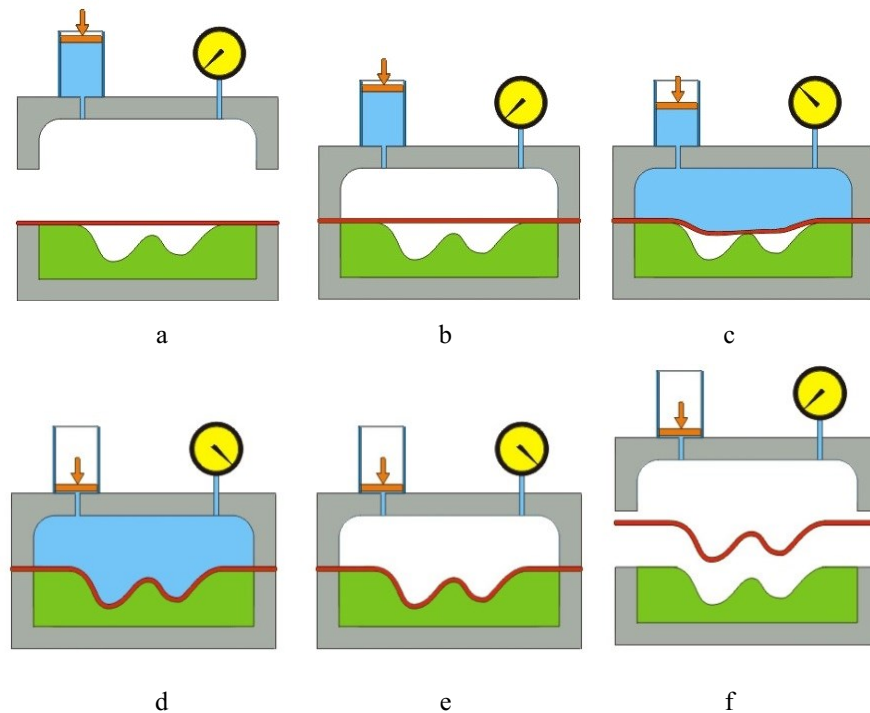


Figure 2.14. Schematic representation of hydroforming process (a-f) [77]

The structured sheet investigated in this the work has a honeycomb structure made by hydroforming. During the structuring process showed in Figure 2.14, the smooth sheet metal that should be formed is located between the matrix (Figure 2.14a) with the desired hexagonal support elements geometry and a pressure membrane. In BTU the structuring process is carried out using a deep-drawing press HYDRAP 'type HPDZb500. The pressing force is 3100 kN. Water is pumped into a rubber membrane with a compressed air operated high pressure pump – MAXIMATOR (Figure 2.14 b,c,d). The membrane expands under pressure (Figure 2.14c) and is forms the sheet (Figure 2.14d). The edge area is located under the hold-down area remains flat. The structure height is adjusted by the water pressure. For the structuring of DC04 steel the pressure is 50 bar. [80] The used forming method has an advantage - the structure height can be specifically adjusted for the different sheet thicknesses and materials. The limitations are the formability of the material, the maximum media pressure and the pressing force of the machine. [80]

## Structured sheet metals

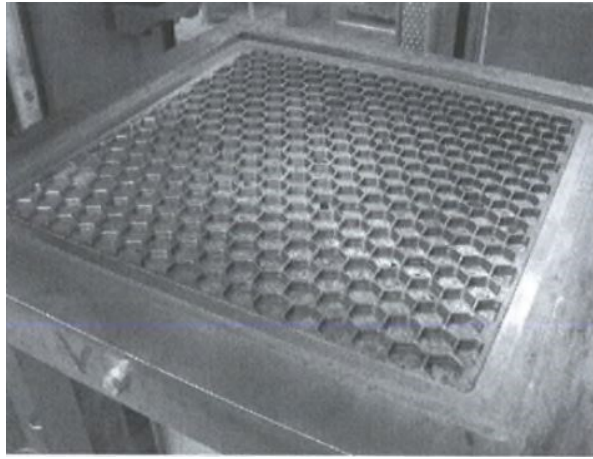


Figure 2.15. Molding tool for structuring sheet metals by hydroforming in BTU [80]

Flat sheets that are placed under the press have size of 600 mm x 600 mm. So that, structured pattern manufactured by pressing has size of 585 mm x 585 mm. For the investigation, special samples are produced. They are measured with the roughness and contour measuring device in order to guarantee process-reliable production with low tolerances and to create reproducible structure heights. The minimum height of a honeycomb could be achieved with allowed deviation of less than 5%, a value of 3.0 mm. This applies to the case, when the structured sheet - honeycomb size is 33 mm and a sheet thickness is 0.5 mm [81]. This illustrates a high process reliability of hydroforming structuring. Exactly these structured sheet parameters are used in present work.

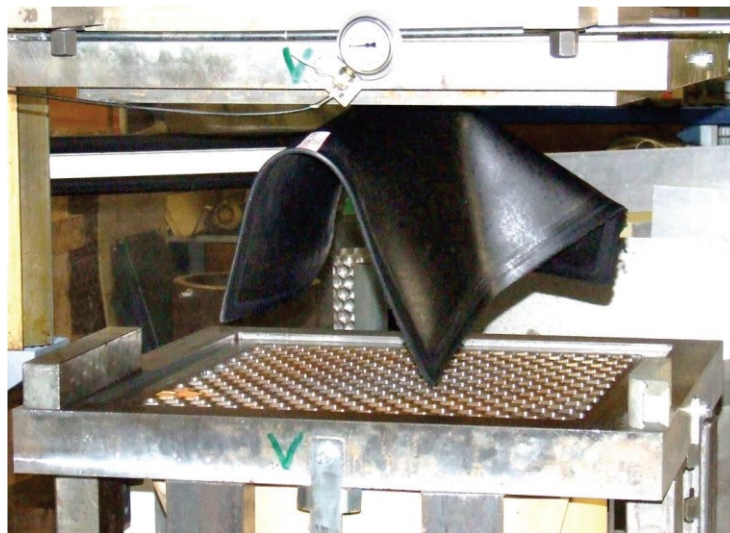


Figure 2.16. Press with membrane and mould for production of a sheet metal with a honeycomb diameter of 33 mm in BTU [79]

A similar principle of hydraulic deep drawing by means of water pressure, but for larger dimensions of sheet metal, the companies Borit® uses and FQZ GmbH, Eisenhüttenstadt. The process is shown in the Figure 2.17, the manufactured structured plates are shown in the Figure 2.18 and Figure 2.19.

## Structured sheet metals

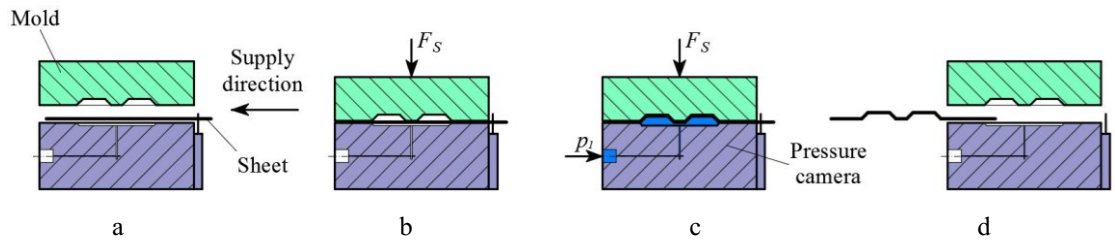


Figure 2.17. Schematic representation of hydraulic deep-drawing (hydroforming) process of honeycomb sheets [82]

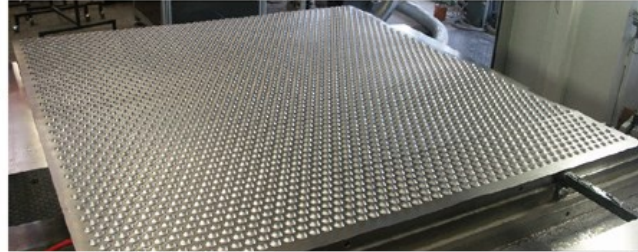


Figure 2.18. Honeycomb sheets after hydraulic deep-drawing process [82]

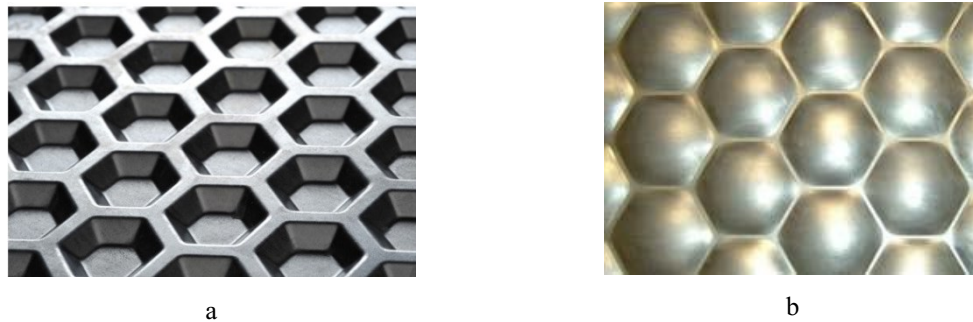


Figure 2.19. Structured sheets manufactured by: a) Borit® company and b) by FQZ GmbH, Eisenhüttenstadt (right)

## 2.5 Special features of structured plates

### 2.5.1 The geometry of hydroformed structured sheets produced by BTU

The structure consists of stiffening elements with a hexagonal basic shape, which resemble the honeycomb. The structured sheet has different areas and characteristic points. The elements of the structure are differentiated with webs - for the flat sheet metal areas - and with honeycombs - for the curved areas. Characteristic points in these areas are points, where the webs cross and the honeycomb centers. The webs crossing points are flat and the honeycomb circled centers area with a diameter of about 5 mm is almost flat. [83]

These areas have different dimensions and characterize the structure. They depend on the wrench size and the height of the structure. If two straight lines go through the middle of the honeycomb, one runs through the web and the other – at the  $90^\circ$  angle to the first one, then two characteristic directions will be built. In one direction, the webs are cut with a line and the honeycombs line up. This structural direction is indicated as  $0^\circ$ . In the other direction, after cutting the honeycomb, the webs will pass longitudinally and then another honeycomb goes. The structural direction is indicated by  $90^\circ$ . [83]



## Structured sheet metals

The characteristics of structured sheets are depth, side length and web gap, corner length and the dimensions  $S_{E0^\circ}$  or  $S_{E90^\circ}$  - the distance between two centers of honeycomb stiffening elements in structural directions  $0^\circ$  and  $90^\circ$  respectively. The terms and the characteristic measures are shown in Figure 2.20. [83]

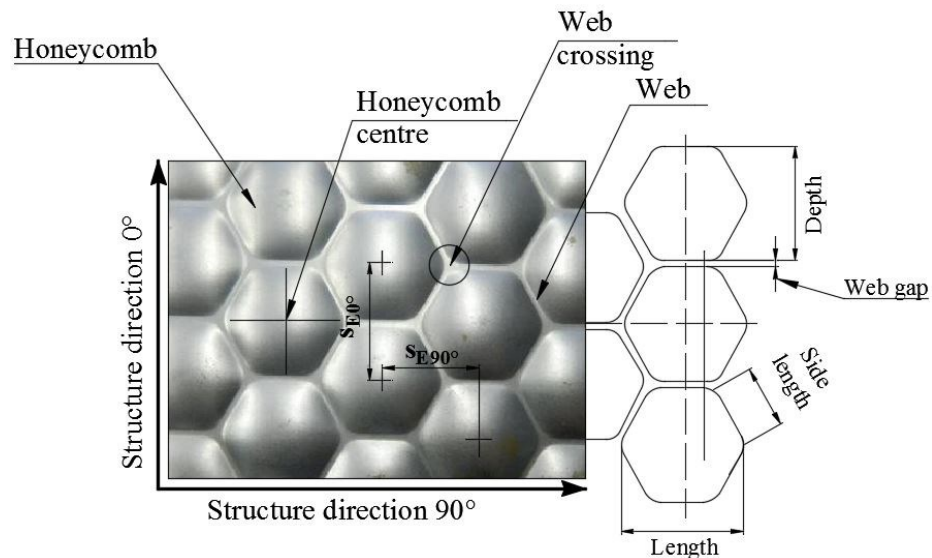


Figure 2.20. Definitions of structured sheet metal and geometrical dimensions [83]

The geometry after hydroforming is a structure which is asymmetrical in relation to the sheet surface - see Figure 2.21, which is referred as a positive structure in the case of upwardly arched structural element and a negative structure in the case of a downwardly curved / arched structural element, see Figure 2.21. The plane in the middle of the sheet before deformation is called sheet metal. The nominal thickness of the sheet indicates the starting sheet thickness of the flat sheet. The geometrical dimensions are summarized in Table 2.2. These sizes are valid to sheets with a nominal sheet thickness of 0.5 mm, a comb height of approximately 3.0 mm [83].

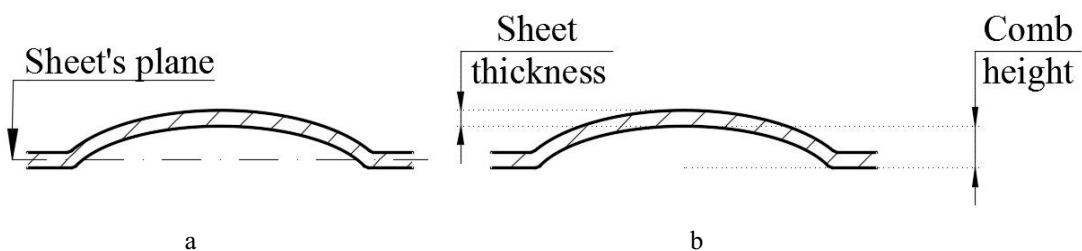


Figure 2.21. Position definition for the sheet metal (a), definition of structure (b) [83]

Table 2.2. Geometric dimensions of the structured sheets with the depth 33 mm [83]

Dimension title	Dimension	Dimension title	Dimension
Comb height, $h_c$	3.0 mm	Comb side length, $l_{side}$	~20.0 mm
Depth, $D_c$	33.0 mm	Distance between two centers of honeycomb structural directions $0^\circ$ , $S_{E0^\circ}$	35.0 mm
Sheet thickness, $t$	0.5 mm	Distance between two centers of honeycomb structural directions $90^\circ$ , $S_{E90^\circ}$	33.3 mm
Length, $l_c$	40.2 mm	Angle between curved comb and flat web, $\alpha_w$	~15°
Web gap, $b_w$	2.0 mm		

### 2.5.2 Honeycombs arrangement

Figure 2.22 shows the structure lines. They mark the lines, in which the same geometric conditions exist, so that some structural directions repeat others. As shown in Figure 2.22b the geometry structure in the direction  $90^\circ$  repeats itself at the angles of  $30^\circ$  and  $150^\circ$ . The angles of  $60^\circ$  and  $120^\circ$  illustrate the structural direction  $0^\circ$ . [83]

Structural curves are different; they depend on the structural directions  $0^\circ$  and  $90^\circ$ . As can be seen in Figure 2.22b, starting from the center of the honeycomb, the structural direction  $0^\circ$  runs a perpendicular web and then crosses over the honeycomb in the maximum height structure and after comes to the next web. Since here the depth  $D$  is smaller than the length  $l$  of the hexagon, the angle  $\alpha_w$  at the beginning of the honeycomb, is greater than in the structural direction  $90^\circ$ . In the direction of  $90^\circ$ , after the honeycomb a straight sheet metal web with the side length  $l_{\text{side}}$  follows. [83]

Therefore, higher requirements are presented to the processes in the structural direction  $0^\circ$  compared to those in  $90^\circ$ . [83] There are much fewer requirements for all other structural curves in directions deviating from  $0^\circ$  and  $90^\circ$  because the maximum height of the structure and/or high rise from the honeycomb to web transition are not included. [83]

The structural direction  $90^\circ$  contains both the maximum comb height and only slightly smaller angles of rise in places of transition from the web to the honeycomb as well as flat sheet metal areas and as a result covers almost the full complexity of the structure in cut. Therefore, the structural directions  $0^\circ$  and  $90^\circ$  are the most interesting directions for the investigations. [83]

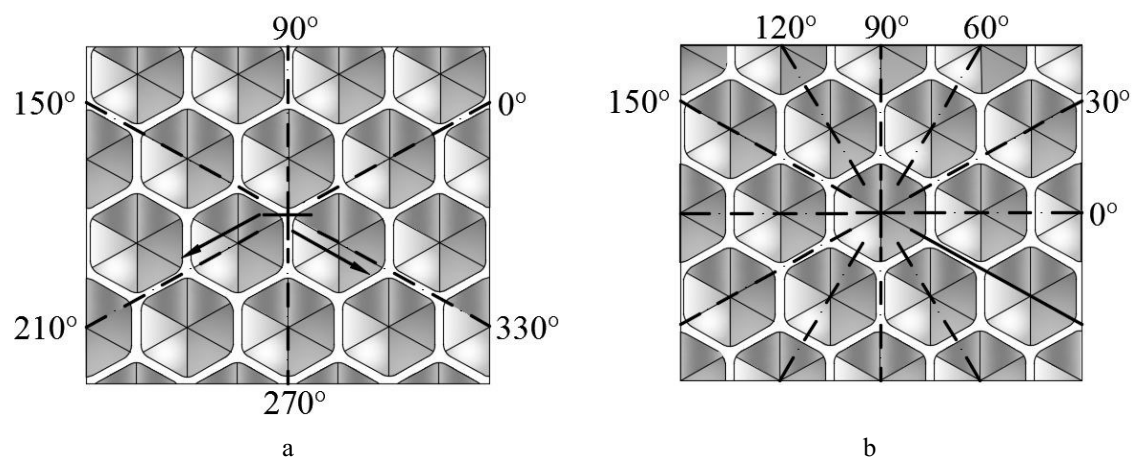


Figure 2.22. Structure lines of honeycomb structured sheet metal: lines with center point in the web crossing (a), lines with center point in the honeycomb (b) [83]

### 2.5.3 Bending

The structure sheet after forming processes which were described above, is only premade product. For a further use of the structured sheet flat areas around structured it must be cut and afterwards structured sheet could be bent. The bending procedure has been investigated in research work of Malikov, Ossenbrink, and Michailov [84].

In forming the structured sheets, a critical parameter is the bending point - in which line sheet metal will be formed. For this purpose, the 4 bending positions can be taken as shown in

## Structured sheet metals

Figure 2.23. In addition, with the use of bending machine, that is shown in Figure 2.23 the sample sheets sized 190 mm x 190 mm and a thickness of 0.5 mm by 90 ° are bent [84].

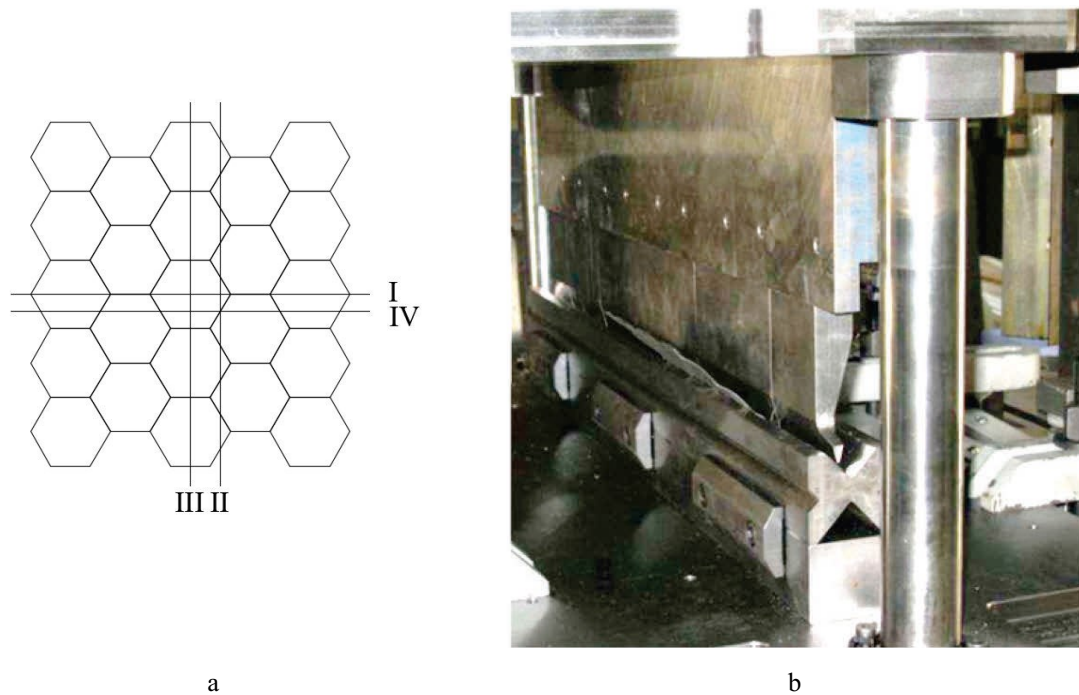


Figure 2.23. 4 bending positions (a) and used bending press (b) [80]

The investigations as well as the simulation of the hydroforming and bending process show that in fact the thickness of the sheets is negligible reduced during the these processes. In addition, the structured sheets behave differently with regard to the bending position and bending direction. There is an indirect proportion between die force and die opening and all tested structured sheets achieve larger die forces than the flat reference sheet. This depends on the one hand on the geometry and on the other hand on the plastic hardening from the manufacturing process. The largest measured stamping force must be applied to bend the positive orientated plate in direction III and the smallest in the II direction for negatively orientated plate. [80]

The largest measured stamping forces reach the sheets in the bending direction III, the smallest in the II direction. Comparing the values of the different structural layers, it will be seen that all ‘positively’ installed sheets achieve higher bending forces than those ‘negative’ of used sheets in structural position-see Figure 2.24. [80]

The structural elements are not symmetrical to the sheet surface. The orientation of the sheet in relation to the structural elements is called the structural position see Figure 2.24. The structure position ‘positive’ means that the honeycombs are oriented upwards. In the structural position ‘negative’ the honeycombs are oriented downwards. This distinction is necessary because of mechanical properties and the forming behaviour depend on the structural position. [80]

## Structured sheet metals

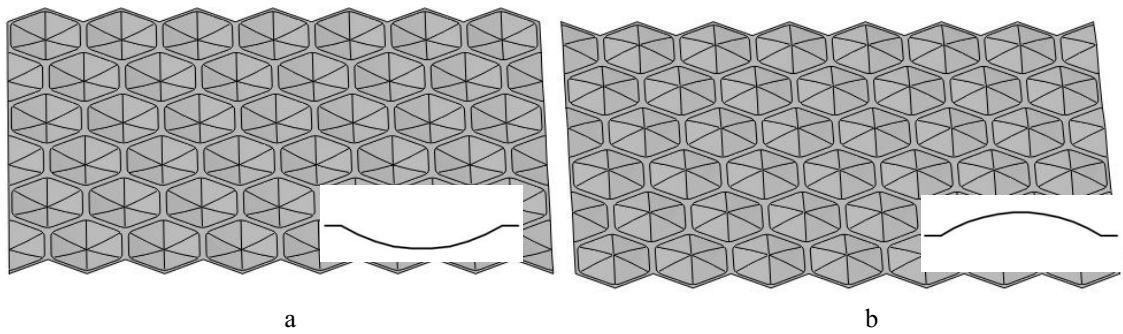


Figure 2.24. Structural position of the structured sheet: a) 'positive', b) 'negative' [80]

### 2.5.4 Welding process of structured and flat sheet

In this work, the steel type DC04 as the material for structured plates is chosen. From a technical point of view, the DC04 is a material with low electrical resistance and very good weldability for resistance point calibration. [83]

For current welding, a console hydraulic spot welding machine is used - Figure 2.25. The manufacturing company of the machine is Düring, the machine type is X-100 E-602/1.

The electrodes type that are used for point welding is B165R75T. The parameters of welding are the following: welding current (Hauptstrom): 7 kA, electrode force (Sollkraft): 1500 N, holding time (Vorhaltezeit): 100 ms.

For flat sheets, the electrode axes are orthogonal to the sheet plane in conventional processing. The electrodes can therefore be aligned well and in case of deviations of the position of a component in the sheet plane, the welding conditions vary marginally. [83]

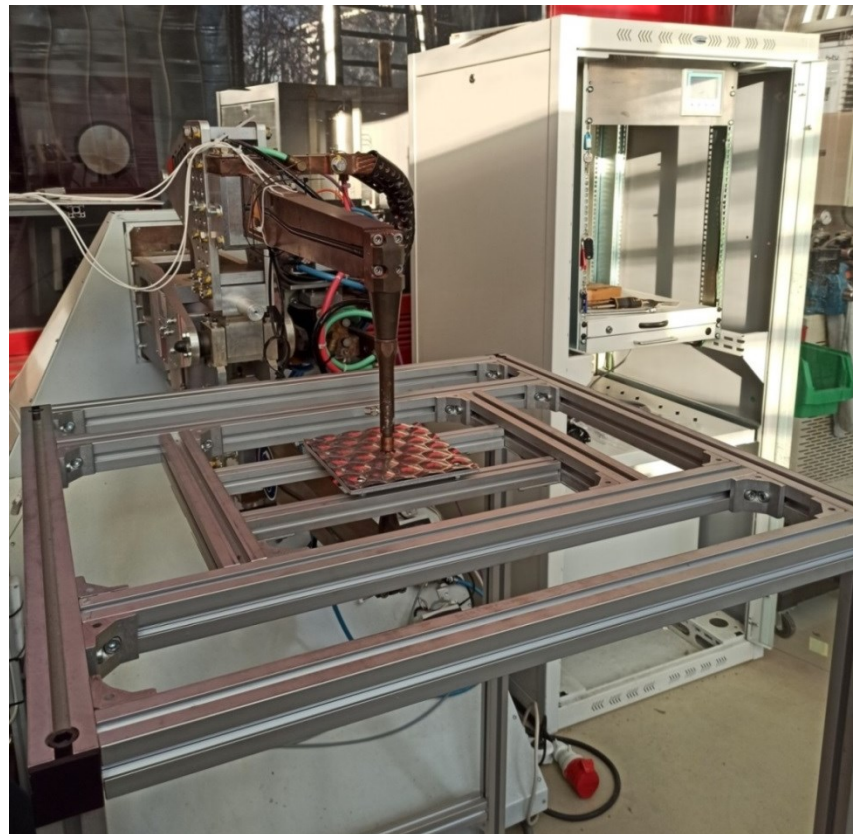


Figure 2.25. Spot welding machine, Düring company, type X-100 E-602/1, Panta Rhei, BTU

## Structured sheet metals

In the area of the joining zone (sheet-metal plane), the joining partners touch each other flatly. With structured sheets, the welding conditions change considerably compared to flat sheets. [83]

For joining 2 structured sheets together points A, B, C and D exist-see Figure 2.26. The honeycombs have curved areas that lie outside the sheet's plane (in positions B, C and D), see Figure 2.26a. With conventional adjustment, these curved areas changed welding conditions with electrode axes that are orthogonal to the sheet's plane (in positions B, C and D). [83]

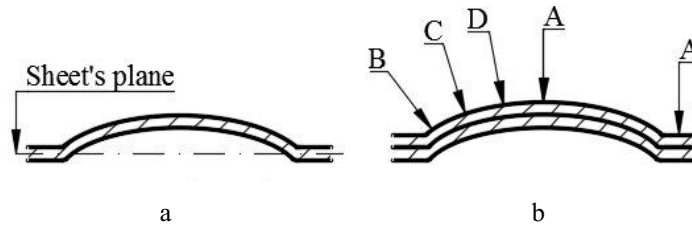


Figure 2.26. Sheet's plane (a) and normals of the sheet metal surface (b) [83]

Usually, the electrode alignment or the robot with electrode holders programming during welding of structured plates are carried out conventionally orthogonal to the flat areas of a sheet plane. But the angles and distances between sheet metal plane and sheet metal surface may lead to considerable deformations at the welding point. These deformations have three disadvantages: the welding point can be damaged by this deformation (introduction of unevenly distributed stresses); the welding parameters can be adversely affected (the current density and the force distribution in the joining zone); the cell structure is visually damaged [83]

An easy way to avoid these negative welding conditions is the electrode correction - the alignment of the welding electrodes orthogonal to the sheet surface instead of to the sheet metal plane. An example of a suitable matching of the joint location for a selected pairing is shown in Figure 2.27.

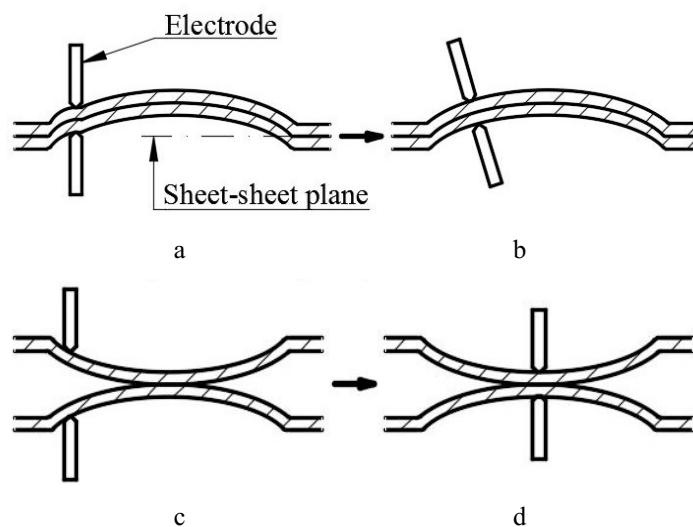


Figure 2.27. Electrode positioning: a) orthogonal to the sheet-metal plane with deformation in the joining zone (pairs FS or FW); b) corrected electrode positioning orthogonal to the sheet surface (pairs FS or FW); c) orthogonal to the sheet plane with deformation in the welding zone, (pairs WW); d) electrode positioning taking into account the structure orthogonal to the sheet surface, (pairs WW). [83]

## Structured sheet metals

The electrodes of console hydraulic spot welding machine (C-Rahmeu) that is used to weld sheets together for the investigations in this work cannot be rotated as it shown on Figure 2.27b. Therefore, there are 2 appropriate ways to weld flat and structured sheets together as shown in Table 2.3 (pairs SG and WG) and Figure 2.28. [83]

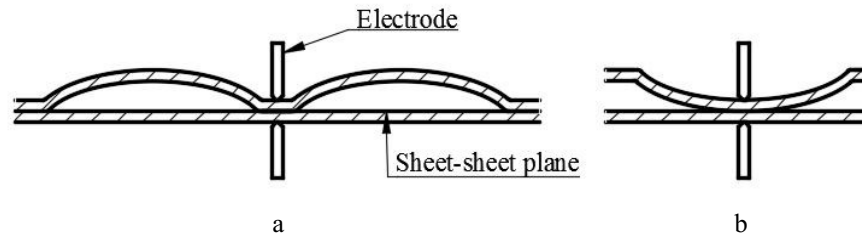


Figure 2.28. Welding of flat sheet and structured sheet (a) positive orientated and (b) negative orientated

### 2.5.5 Types of sandwiches

The development of steel sheet multi-layer composites dates back several years. Already in [20] these compounds were classified and presented how innovative these precursors are. Eight different arrangements for joining a sandwich by spot welding were found [83]. A special feature of structured sheets is the lap joint impact of the not flat surfaces of the parts to be joined – they have only local contact. [83]

In the Table 2.3 according to [85] are shown the results of 3 point bending tests - 1 reference sheet (№1) and 9 sandwiches (№2-10). 9 pairs of sandwich elements – from number 2 to 10 – 3 of them include structures with flat plates and 6 include two structured plates, differently orientated ( $0^\circ$  and  $90^\circ$ ) and welded in different points. In pairs from 2-10 the thickness of one sheet is 0.5 mm, that means the total pair thickness (of one sandwich element) is 1 mm. A reference sheet is a flat single sheet (abbreviation GB) with thickness 1 mm and stiffness 1.0. To create all sheet pairs the same material is used – steel, type DC04. Also, all pairs have the same dimensions. [83]

Table 2.3. Sandwiches with pictures and stiffnesses according to [85]

№	Abbreviation	Full name of the connection	Picture	Stiffness
1	GB	Flat single sheet		1.0
2	GG	Two flat sheets		-
3	SG	Flat sheet-web		1.81-2.28
4	WG	Flat sheet-comb		6.7-7.29
5	FS	Flat surface - web		-
6	FW	Flat surface - comb		-
7	SSA	Web-web variant A		2.59-3.7
8	SSB	Web-web variant B		-
9	SW	Web-comb		5.97-8.11
10	WW	Comb-comb		10.71-12.57

The pairs SG and SSA show the lowest bending stiffnesses, which increased only about 1.8 to 3.7 times compared to the reference sheet stiffness. By contrast, pairs SW and WG achieve stiffness of 5.9 to 8.1. Such a big difference arises because of the force application point change and the structural directions. The best pair is WAV (№10), stiffness increases from 10.7 to 12.6 times compared to the reference (№1) one. [83]

As can be seen from the above, stiffness of sandwiches with structured sheets (№ 2-10) is up to 12 times higher than stiffness of the flat sheet (№1). That way of using structured sandwiches which replace flat sheets a weight saving of about 56% can be achieved [85]. Another advantage of pairs with high stiffness is the bending force absorption at very low deflections and thereby reversible behavior under the load [85]. With the same stiffness, for example, an aluminum sheet with about 3.2 mm sheet thickness can be replaced by a sandwich lightweight structured steel component at the weight is reduced by approx. 10%. [83]

Unfortunately, due to the lack of structured plates it was impossible to use 5-10 types of sandwiches, presented in Table 2.3. The choice was between SG and WG pairs. For this work WG pair type (Flat sheet-comb) is chosen, as its stiffness is 3 times higher than similar SG pair type (Flat sheet-web).

### **2.5.6 Structured sheets material properties**

Steel material characteristics and mechanical properties could be found out from standardized tensile tests. Due to the fact that standard testing methods, were developed for flat (plain) steel sheets, they cannot be used for testing structural sheet metals.

The material properties of the cold forming sheets are affected by the processes of change of the material shape such as embossing, hydroforming or others similar. During the cold forming process, the materials are deformed at room temperature what increases the stress in deformed areas. For this reason, it is necessary to research the new material properties obtained after the forming process. [79]

At the BTU's Joining and Welding Technology Department, investigations were carried out to identify which sample geometries the structured sheet metal must have to correspond DIN EN ISO 6892, so that tensile tests could be carried out according that document. [79]

Sheet metals are usually tested according to DIN EN ISO 6892-1 [96]. This norm describes the test procedure and the specimen dimensions. For sheet metals up to 3 mm of thickness uniform specimen dimensions of 20 mm in width and 120 mm of test length are recommended. During testing the deformation of the specimen is measured with tensometers with an original gauge length of 80 mm. However, the described standard is inadequate for the investigated structured sheet metals as the width of a single structure element exceeds the recommended specimen width. [95]

In order to characterize the structured sheet metals and to test joined structured sheet metals, specimen dimensions must be adapted for structured sheet metals. Furthermore, it

identifies characteristic values to evaluate the structured sheet metal and detect specific load paths and load cases like elastic or plastic strain zones in the structured sheet metal. [95]

According to DIN EN ISO 6892-1 for sheet metals up to 3 mm thickness a uniform specimen with width  $b = 20$ , test length  $L_c = 120$  mm and original gauge length  $L_0 = 80$  mm is recommended. Transferring these small dimensions to a tensile test specimen of structured sheet metal would result in ‘destroyed’ structure elements with less stability. This is schematically shown in Figure 2.29. [95]

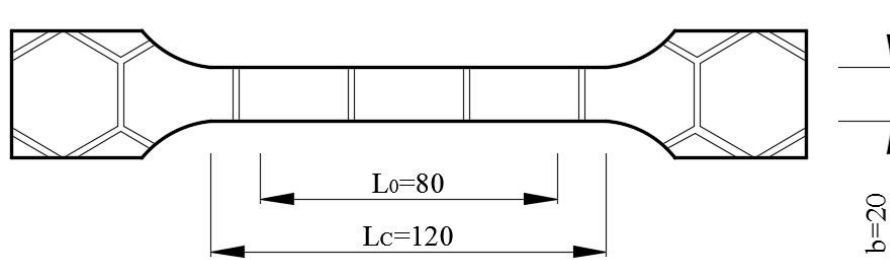


Figure 2.29. Tensile test specimen of the structured sheet metal according to DIN EN ISO 6892-1 [95]

Figure 2.30 shows the modified specimen with one, two and three structure elements over the specimen width. To achieve symmetrical specimen deformation the structure elements are arranged symmetrically in length and width. [95]

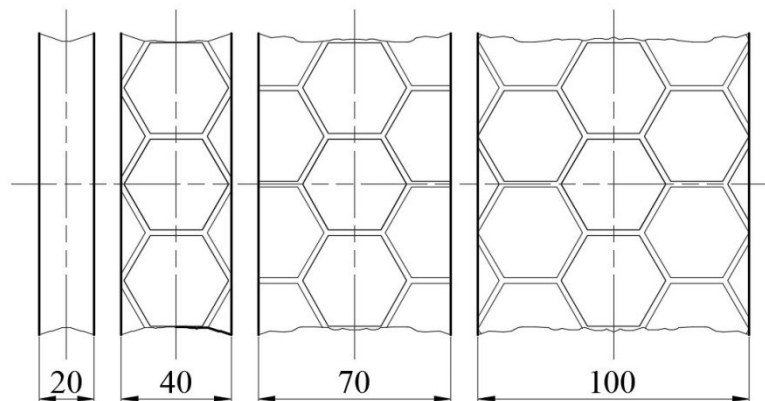


Figure 2.30. Specimen widths for structured sheet metals (structure position  $0^\circ$ ) [95]

Various test series of tensile tests are carried out by Fritzsche, Ossenbrink and Michailov with 3D optical strain displacement measurement and the software ARAMIS-system [96]. Stress-strain curves are recorded, as shown in Figure 2.31. For all tensile specimens structured steel DC04 (1.0338) are used. [95].

In this investigation the structure is a hexagonal regular bump structure with a small bridge of 2 mm between the bumps. The thickness of the sheet metal is 0.5 mm. During the hydroforming manufacturing process from a flat sheet metal to a structured sheet metal the material thickness reduces particularly [95].

As a result the specimen with 100 mm width and 200 mm test length is used for the further tests. Figure 2.31 shows the stress-strain curves for flat and structured specimens as a function of different structure positions [95].



## Structured sheet metals

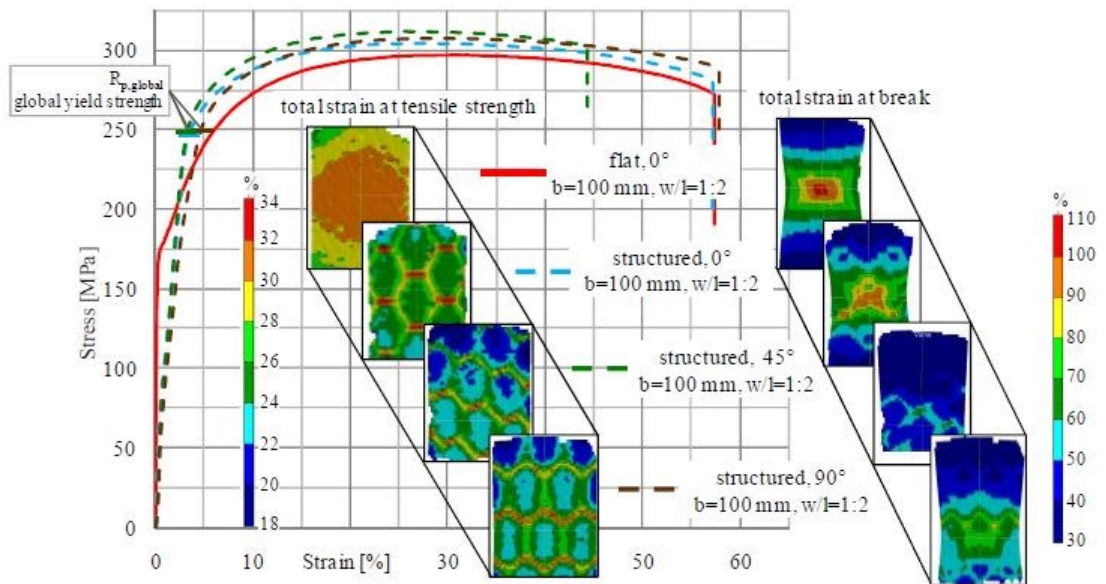


Figure 2.31. Stress-strain curves for a selected specimen dimension for the three tested structure positions and a flat sheet metal with corresponding deformation images [95]

The flat sheet metal has a uniform strain distribution until 30% and then necking occurs. For the structured sheet metals the strain characteristic is more complex. They show for all structure positions a strain concentration in the bridges (webs), with local values about 32-34 %. [95].

The structured sheet metals show specific characteristic stress-strain behavior before reaching the uniform strain. Global yield strength can be identified-see Figure 2.32. After exceeding this point the specimen shows a distinctive plastic behavior. The stress-strain curve before exceeding the global yield strength can be divided in three divisions, each with specific structure deformation behavior. The images in Figure 2.32 show the strain at end of each division for different structure positions. [95]

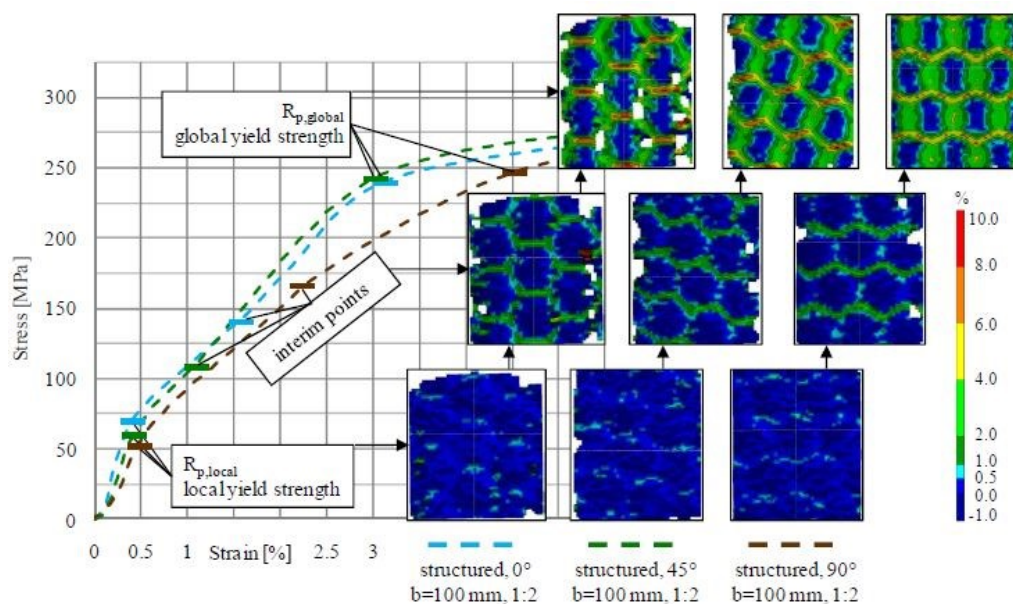


Figure 2.32. Characteristic range of stress-strain curves for the tested structure positions with corresponding deformation images [95]

The end of first division can be identified as the local yield strength. The deformation is mainly concentrated on the transverse bridges (webs) with approximately 0.4 %. The bumps of the structure elements are not deformed. In the second division begins the flattening of the structure elements through increasing strains in the bridges (webs). This part ends with the interim point as transition to the third division. After exceeding the interim point, the transverse bridges (webs) become unsteady and buckling begins. The origin hexagonal structure is extended, and the instability of the bridges (webs) produces a wave form in the sheet metal. For the 0° and 45° structure position the strain at this global yield strength is about 3 % for the 90° structure position 4.5 %. [95]

## 2.6 Application of structured sheets

The 3-D structure enhances the mechanical properties of components, primarily by increasing bending stiffness because of increased inertia (the higher the structure, the stiffer the sheet). Strain hardening, which occurs during the structuring process, also improves the rigidity of the product. Initially 3-D structured sheet is used for making products that required increased rigidity. However, now these materials are used in a wider range of products. [86]

### 2.6.1 Automotive applications

According to consumers and the government demand of fuel-efficient vehicles to achieve higher safety and environmental standards, structured rear panel on a 2004 Mercedes SLK® was made – Figure 2.33. It was made from vault-structured sheet with a hexagonal staggered pattern – this structure improves the sheet's rigidity with low weight and an extremely small space requirement with simultaneously advantageous acoustic properties. [88] This panel adds stiffness and improves the car's acoustic behaviour by dampening noise from the trunk and rear of the automobile, which can enter the passenger compartment. [86]. Since 2004, Dr. Ing. Mirtsch Wölbstrukturierung GmbH is a supplier of the vaulted aluminium ( $Al_6O_{16}$ ) boards of thickness 1.15 mm with the key width 50 mm of the hexagon for the SLK series. [86]



Figure 2.33. Figure Mercedes SLK (a) and vault-structured sheet with a hexagonal staggered pattern (b) [87]

In Munich, Germany structured plates are used as an underbody car element – see Figure 2.34. The realization of the underfloor represents the first part of the implementation of the body outer skin. This was designed according to aerodynamic aspects, so that the buoyancy of the vehicle can be minimized even at high speeds and without extra elements. In addition, as low a

## Structured sheet metals

weight with a high degree of stiffness is required, this is achieved by a specially processed aluminium sheet with a vault structure. [88]

The underbody has been manufactured in the workshop of the chair in Technical University in Munich and is now attached to the vehicle. Presumably, the outer skin is manufactured based on fibre composite materials. [88]



Figure 2.34. The designed underbody car element, Munich, Germany [88].

The racing car constructed in Brandenburg Technical University (BTU) was also made from structured sheet metal – it covers the bottom part of the car under the driver's seat –see Figure 2.35 a,b.



Figure 2.35. The racing car (a, b), BTU Cottbus, Germany

## 2.6.2 Structural applications

Structured sheet also can be used in thermal engineered products. In heat exchangers, for example, increased fluid turbulence along 3D structured surfaces, combined with a larger surface area, significantly improves the rate of heat transfer. Other applications for structured sheet include building construction and architectural products (ceilings, walls, and door panels) and packaging (cans, containers, and bottles). [88]

### 2.6.2.1 Thin-walled detector tubes in particle accelerators

For high accuracy, aluminium detector tubes, used in particle accelerators, are designed to be as thin as possible. These tubes are maintained under high internal vacuum. The thin-walled

tubes must be very rigid to avoid collapsing under atmospheric pressure. Additionally, these tubes undergo thermal stresses caused by temperature changes.

The walls of the detector tubes can be strengthened by vault structuring, which ensures rigidity to prevent collapsing under vacuum and high axial flexibility to accommodate thermal expansion. [89].

### 2.6.2.2 Cans and containers

Structuring or beading the wall of cans increases their rigidity, thus allowing wall thickness reduction to decrease weight and save material. Use of structured high-strength materials has helped reduce wall thickness by 29 % over the last 24 years. With the vault-structuring technique, an additional reduction of 24 % in sheet thickness can be obtained. [89]

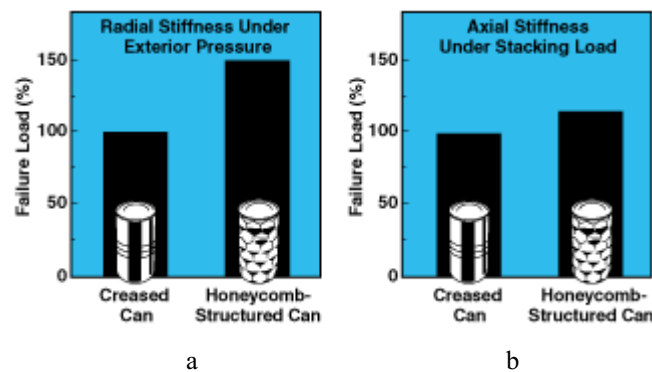


Figure 2.36. A honeycomb-structured can body called ‘hexacan’ increases axial stiffness about 15 % (b) and radial stiffness about 50 % (a) as compared with a creased can body [87]

A honeycomb-structured can body called ‘hexacan’ increases axial stiffness about 15 % and radial stiffness about 50 % as compared with a creased can body (see Figure 2.36). High-strength materials that cannot be structured conventionally because of low formability can be vault-structured, which induces relatively little plastic deformation. [89]

### 2.6.2.3 Washing-machine drum

Washing machine drums are designed for high-speed rotations of up to 1.800 revolutions per minute. Structuring of the drum surface increases its rigidity. Also, washing machine drum has due to a convex structure less and smaller holes than the conventional one. Figure 2.37 shows a washing machine drum made from hexagonally vault-structured stainless steel. The staggered and soft-curved hexagonal structure is designed to help improve fluid flow behaviour both for gentle and quick washing.

By virtue of the smoothed out and 3D structured surface the clothes may be dried more gently than before. In addition, the rinsing process continues faster and becomes easier due to more intensive flow close to the drum wall. High stiffness, even at the highest spin speed is also provided. [88]

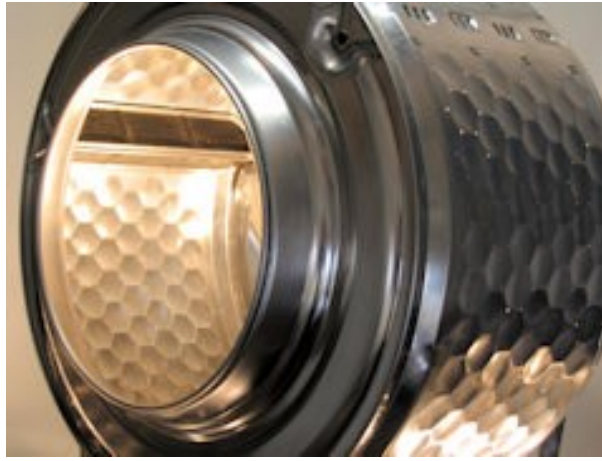


Figure 2.37. Washing-machine drum made of structured plates [88]

#### 2.6.2.4 Lightning

The lighting system Hexal LED (see Figure 2.38) is made from structured plates and shows which elegant and functionally convincing solutions with vault-structured materials are possible. It is characterized by its extremely low weight and exceptional appearance. A mirroring layer is initially applied on the surface of sheet metal by anodizing. This sheet then is Vault-structured. Every hexagonal structure on the sheet surface acts like a single mirror. [88]



Figure 2.38. The lighting system Hexal LED [88]

Due to the special processing and materiality of the compact luminaire modulus, which body is made of extremely thin aluminium and at the same time performs as a reflector. The light is diffused by the vault structures and allows with the aid of light scatter on 3D structures a glare-free illumination. The trunking rail, luminaire insert and reflector are integrated in a compact unit, because the high rigidity of the arched reflector does not require a housing, for this reason it saves up to 80 % of the weight. [88]

### 2.6.2.5 Roof

The roof of sports hall in Odessa, Ukraine is covered with corrugated sheets-see Figure 2.39. The unusual shape of the building evokes memories of space, that is why it was called ‘UFO in metal forming - futuristic sports center on the Black Sea’. [90]

The 6000 m<sup>2</sup> 3D roof construction made of lacquered (by Novelis firm), rolled and assembled (by Böhme Haustechnik firm) arched aluminium sheet with approximately 30% weight saving compared to the conventionally smooth construction. The damage, that was coursed by hail earlier, now is hardly visible because high stiffness and the diffuse refraction due to the vault structures. [90]



Figure 2.39. The multi-purpose sports hall in Yuzhniy, a suburb of Odessa, resembles a giant turtle with bright tanks

### 3 C-sectioned lightweight steel beams

#### 3.1 Introduction

The use of structured sheets as components of steel constructions is currently very low. In order to find a suitable area of application, different variants were initially discussed in the course of the work. Since the structured sheet metals are used as surface elements in the automotive industry, a facades or roof elements were also considered to study. Nevertheless, the decision was made to use the structured sheets as webs in lightweight steel beams. At the beginning of the work, a suitable form of the test sample had to be found. There were several basic conditions that were decisive. In addition, various literature sources describe how the test bodies were defined in various investigations carried out in the past. Based on the task, ideal forms are found.

In this part material properties of structured and flat sheet metals are described. The steel type of flat plates is DC01 (1.0330) and for structured- DC04 (1.0338) - non-alloy steel. These are both cold rolled steel, which usually is used in building industry and also they are ideal for cold forming: steel grade DC01 is usually used for simple forming work, such as beading, bending, embossing, drawing, DC04 is used when high requirements are placed on the forming of the product. [93]

#### 3.2 Material properties

##### 3.2.1 Flat plates

The material properties of flat plates (steel grade DC01) are determined from tensile tests, which are conducted by tensile test machine, the manufacturer is Hegewald & Peschke with a 250 kN load, Schimadzu company. Tests are made according to DIN EN ISO 6892 [96]. Samples for tensile tests are prepared according to DIN 50125 [98]. 20 samples (10 in longitudinal direction and 10 in transverse) are cut from 3 big sheet metals DC01 with different thickness of 1, 0.75, 0.5 mm. The geometric parameters are shown in Figure 3.1. They correspond to sample form H from DIN 50125 [98] for flat products with the thickness (a) between 0.1 mm and 3 mm - Eq. (3.1):

$$0,1 \text{ mm} \leq a \leq 3 \text{ mm} \quad 3.1$$

### C-sectioned lightweight steel beams

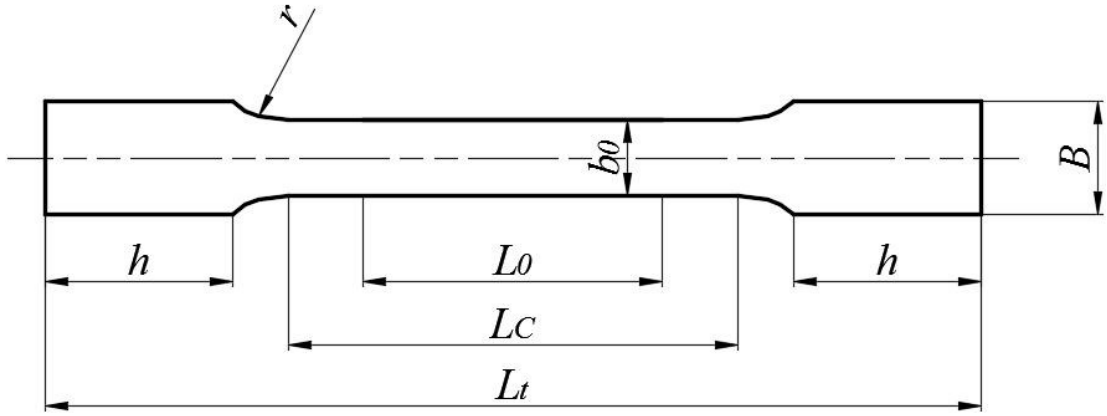


Figure 3.1. Geometric parameters of samples cut from flat plate steel grade DC01 [98]

Legend:  $b_0$  - sample width;  $B$  - head width;  $h$  - head length;  $L_0$  - original sample length

$L_C$  - test length, ( $L_C = L_0 + 2 b$ );  $L_t$  - overall length

The exact samples dimensions in mm for tensile tests are presented in Table 3.1.

Table 3.1. Sample dimensions for tensile tests

$b_0$	$L_0$	$B$	$r$	$h$	$L_C$	$L_t$
20	80	30	20	50	120	250

After conducting tensile tests, resulting stress-strain curves are presented in Figure 3.2 – true and technical curves for steel DC01 with thicknesses 0.50; 0.75 and 1.00 mm are shown.

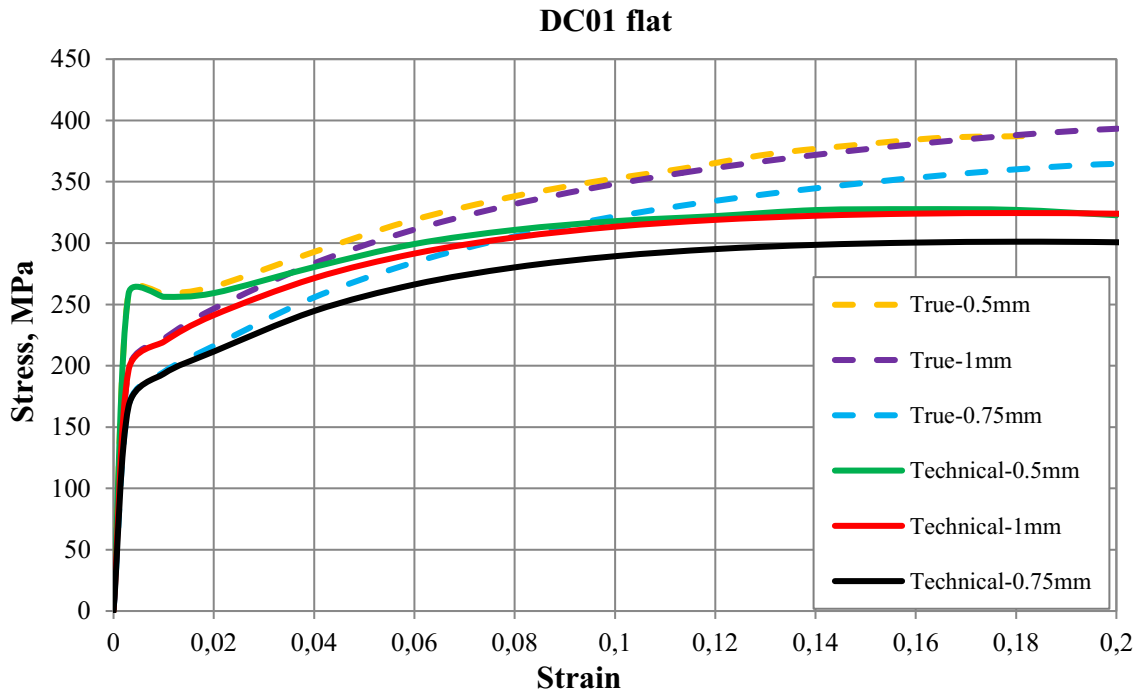


Figure 3.2. Technical and true stress-strain curve, flat sheet metal DC01

The technical stress-strain curve is determined directly from the tensile tests. For the conversion into the true stress ( $\sigma_t$ ), nominal stress ( $\sigma_n$ ) and engineering strain ( $\epsilon_n$ ) from tensile tests – Eq. 3.2. True strain ( $\epsilon_t$ ) is calculated from engineering strain ( $\epsilon_n$ ) – see Eq. 3.3). Elastic strain ( $\epsilon_e$ ) is ratio of true strain ( $\epsilon_t$ ) to Young's Modulus ( $E$ ) – Eq. 3.4 ). And finally, plastic strain ( $\epsilon_p$ ) is difference between true strain ( $\epsilon_t$ ) and elastic strain ( $\epsilon_e$ ) – see Eq. 3.5).

$$\sigma_t = \sigma_n \cdot (1 + \epsilon_n) \quad 3.2$$



### C-sectioned lightweight steel beams

$$\varepsilon_t = \ln(1 + \varepsilon_n) \quad 3.3$$

$$\varepsilon_e = \frac{\varepsilon_t}{E} \quad 3.4$$

$$\varepsilon_p = \varepsilon_t - \varepsilon_e \quad 3.5$$

The main parameters corresponding to curves illustrated in Figure 3.2 are shown in Table 3.2.

Table 3.2. DC01 steel parameters for sheet thicknesses 0.50; 0.75; 1.00 mm

Steel thickness, mm	Parameter, MPa	
0.50	E- Modulus	186904.95
	R <sub>p0.2</sub>	240.74
	R <sub>m</sub>	304.76
0.75	E- Modulus	189621.57
	R <sub>p0.2</sub>	154.27
	R <sub>m</sub>	284.71
1.00	E- Modulus	197380.59
	R <sub>p0.2</sub>	177.85
	R <sub>m</sub>	302.47

### 3.2.2 Structured sheet metals

The detailed material properties study is written in chapter 2.5.6 Structured sheets material properties

Stress-strain curves are shown in Figure 3.3 taken from Fritzsche, Ossenbrink, Michailov study. [95]

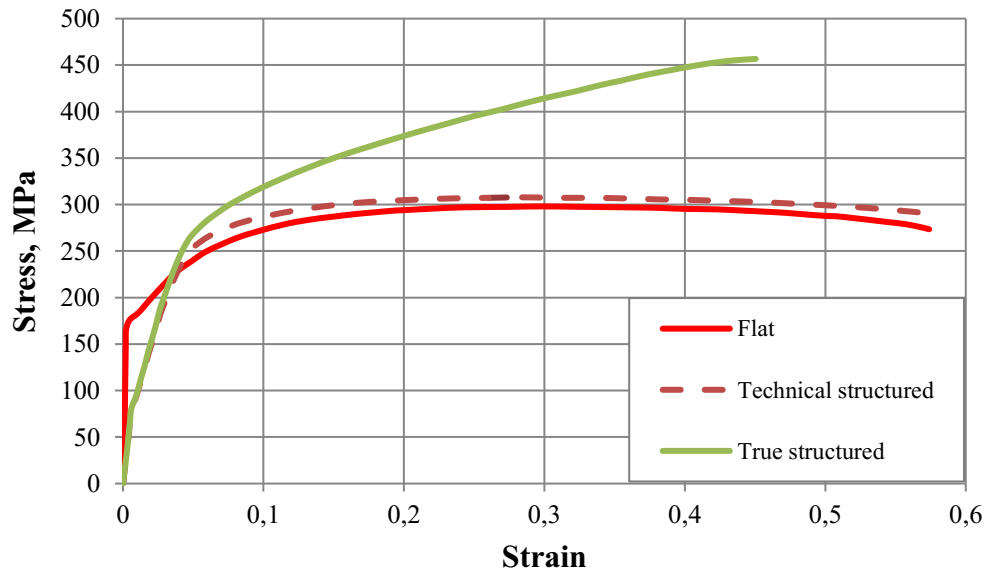


Figure 3.3. Technical and true stress-strain curve, flat (before forming) and structured (after forming) sheet metal DC04

The main parameters corresponding to curves are shown in Table 3.3.

## C-sectioned lightweight steel beams

Table 3.3. Structured sheet metal parameters before and after forming [95]

Flat (before forming)		Structured (after forming)	
Parameter, MPa		Parameter, MPa	
E- Modulus	165000	E- Modulus	13455*
$R_{p0.2}$	170	$R_{plocal}$	65
$R_m$	295	$R_{pglobal}$	240
		$R_m$	305

\* E- Modulus is calculated based on the following conclusion from the study: The stress-strain curves for the structured sheet metals show a specific stress-strain curve before exceeding the global yield strength. The deformation behavior is classified in three characteristic divisions. Only in the first division the deformation is fully elastic. [95]

### 3.3 Laboratory experiments

#### 3.3.1 General information

The experiments are carried out at the Brandenburg Technical University Cottbus in research and material testing institute – FMFA (Germ. Forschungs- und Materialprüfanstalt). For laboratory experiments 8 specimens are created. All specimens are C-sectioned beams. The height is 364 mm, the length is 1260 mm, the width of flanges is 65 mm each (upper and lower). Specimen types and numbers are listed in Table 3.4. Specimens 1-4 are made only of flat plates, specimens 5-8 – of flat and structured. The specimens 5-8 consist of in one sheet of C-sectioned flat plate and structured connected to the flat one so that webs pattern can be seen.

Table 3.4. Dimensions of tested beams

Experiment number	Type	Beam number	Plate №1 - C-profile			Plates №2 – 3 squared plates		
			Type	Thickness, mm	Steel type	Type	Thickness, mm	Steel type
1	1	1	flat	0.75	DC01	flat	0.75	DC01
2		2						
3		3						
4	4							
5	3	5		0.75		structured	0.50	DC04
6		6						
7	4	7		1.00				
8		8						

#### 3.3.2 Manufacturing of specimens

The choice of the investigated beams geometric parameters is narrowed by the geometric parameters of its steel components – structured sheets. The size of the future structured plates is selected as the key factor. During the production of structured sheets by hydroforming process (see chapter 2.4.4.2.2 Hydroforming), the maximum flat sheet size is 670 mm x 670 mm is used (size of sheets before pressing). After manufacturing process with the deduction of the molding tool edges that remain flat, the size of structured sheets is 585 mm x 585 mm.

The height and the width of the beams are chosen so, that one plate contained 11 whole combs. Also, the plate is cut so to get rid of possible combs that height varies in comparison to the other combs. Usually, such ‘defective’ combs situated on the edge of the structured plate. [83] The cut plate has dimensions 420 mm x 364 mm – see Figure 3.4.

## C-sectioned lightweight steel beams

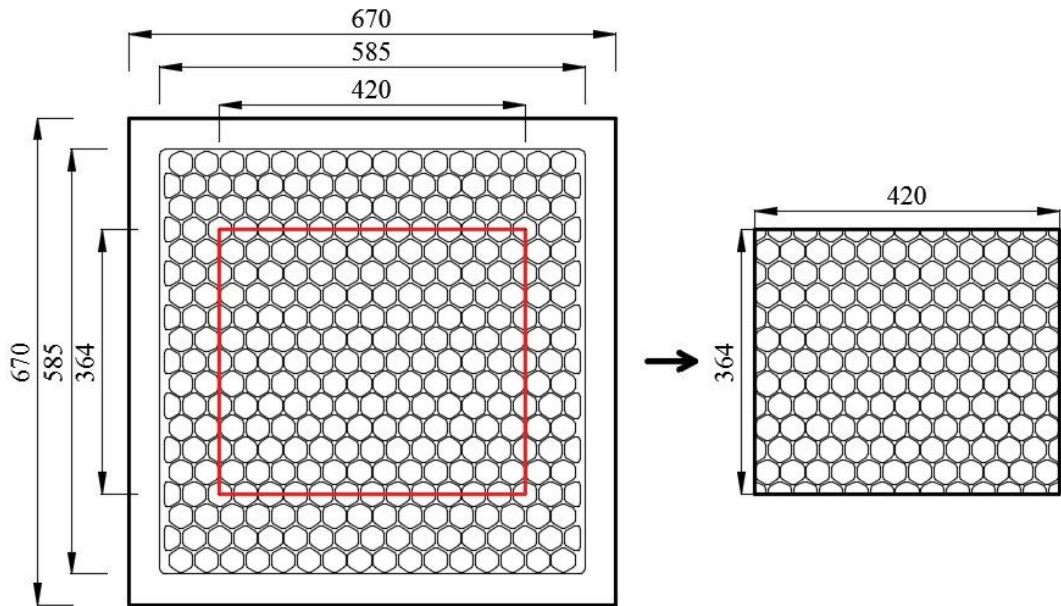


Figure 3.4. Dimensions of original plate and cut (red line) structured plate

The chosen beams consisted of 3 structured plates welded with laser along the edge with one another and of the flat plate with C-profile connected by point-welding. Combs are orientated negative to the surface of the flat plate and have structural direction of 90°. The dimensions of beams are shown in a Figure 3.5 and in Table 3.4.

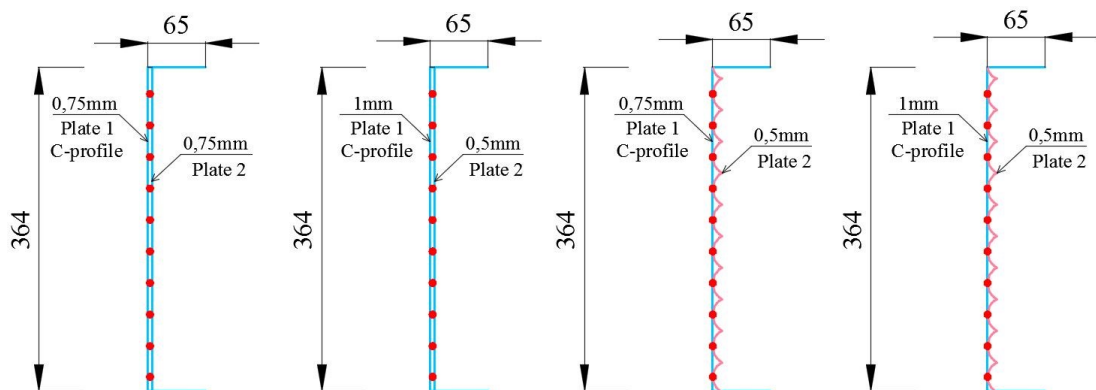


Figure 3.5. Cross sections of specimen types 1,2,3 and 4

Figure 3.5 shows specimens numbers and thicknesses of all sheets - components of investigated specimens.

The length of beams is multiple of one structured sheet length and consists of 3 plates, 420 mm length each. The whole length is 1260 mm, the flange of 65 mm is chosen according to Eurocode 3 [100] – Eq. (3.5):

$$\frac{b}{t} \leq 50 \quad 3.6$$

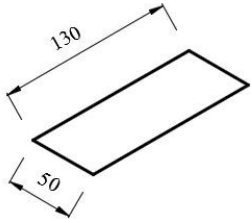
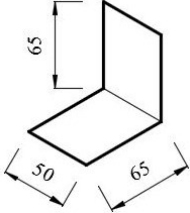
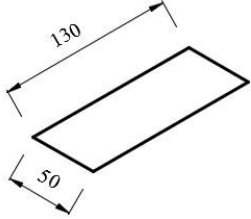
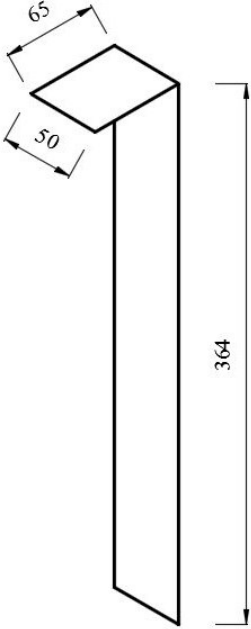
Legend: b-width of flange; t-thickness of beams web.

The tested beams differ from each other in the second plate geometry and in web thicknesses. Types 1 and 2 (see Figure 3.5) are created in order to make a comparison in behaviour of flat and structured plates.

### C-sectioned lightweight steel beams

There are 6 additional plates are used in experiments in order to make specimens more stable and to prevent local web buckling-see Table 3.5. All plates are made from steel type DC01.

Table 3.5. List of additional plates for specimens

Number	Shape and dimensions in mm	Thickness, mm	Function
1,2		5	For holding the beam on the support, connect plates 3 and 4 to 1 and 2
3,4		1	To make beam stable on the support
5		5	Area for machine stamp to apply the load, connects beam and plate 6
6		1	To transfer the load to the beams web

In Figure 3.6 additional plates for specimens from Table 3.5 are shown.

### C-sectioned lightweight steel beams

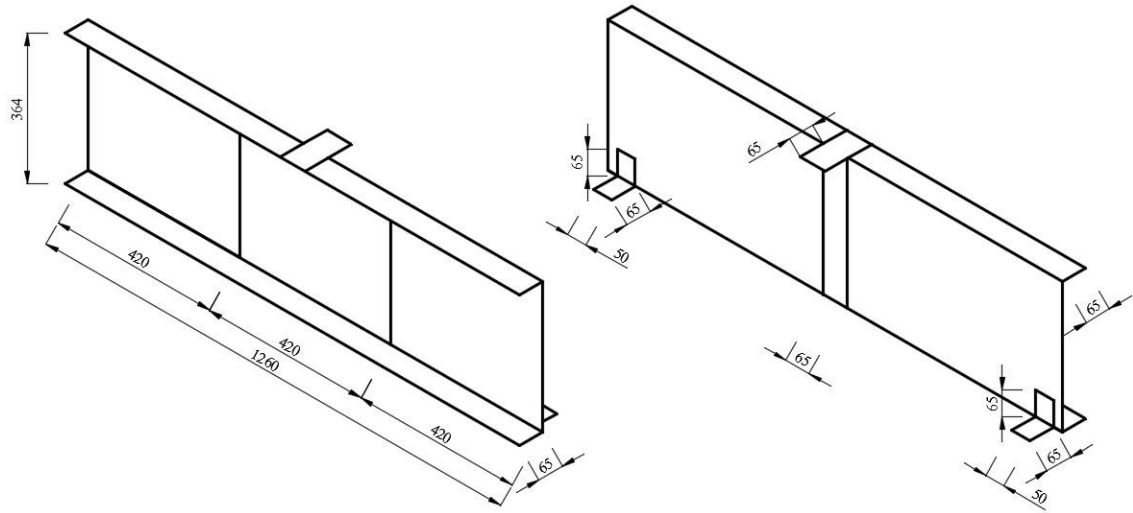


Figure 3.6. Axonometric front and back view of specimens

### 3.3.3 Experimental setup and boundary conditions

For the laboratory experiments a special setup is created. All specimens are simply supported beams. As a base and as supporting structure I-beam is used, it holds other supports of the setup and the specimen itself. Four lateral supports – small T-beams are welded to the base – in order to support flange of specimen in front and back sides. The supports in front side consist of two parts - welded to the base and movable, connected to fixed one. By means of untwisting the washers from the bolts, which are welded to plates, it is possible to remove the movable part of support to set the specimen in place. The specimen is placed on two steel rods 5 mm in radius each - one of them is welded to the base beam, the other is not. They are pin and roller support respectively.

The experimental setup is same for all specimens – see Figure 3.7 (front view) and Figure 3.7 (back view). In Figure 3.7 on the left side stands the vertical steel beam, which is used to support the displacement transducers. In the middle of the specimen the steel plate connected to the upper flange – it transfers the load to the beams web.



Figure 3.7. Laboratory setup, front view

In Figure 3.8 in the middle (the load point) of the specimen it is seen the hydraulic jack of testing machine. Also on the back side of the setup 2 displacement transducers are located.

## C-sectioned lightweight steel beams

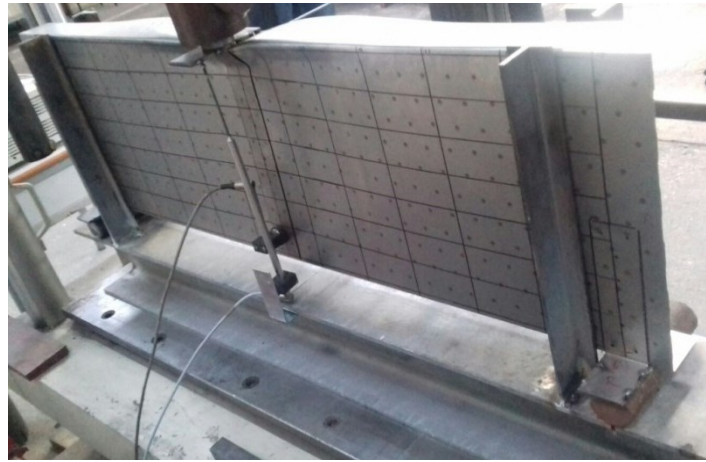


Figure 3.8. Laboratory setup, back view

### 3.3.4 Displacement transducers (IWANs)

In each of 8 experiments, 7 displacement transducers are used. The short name of transducer is IWAN (germ. Induktive Wegaufnehmer). The location of transducers is shown in Figure 3.9. In general, there are used 7 transducers-5 measured horizontal displacement (IWANs 5,7,4,3,6) and 2 – vertical (IWANs 1,2).

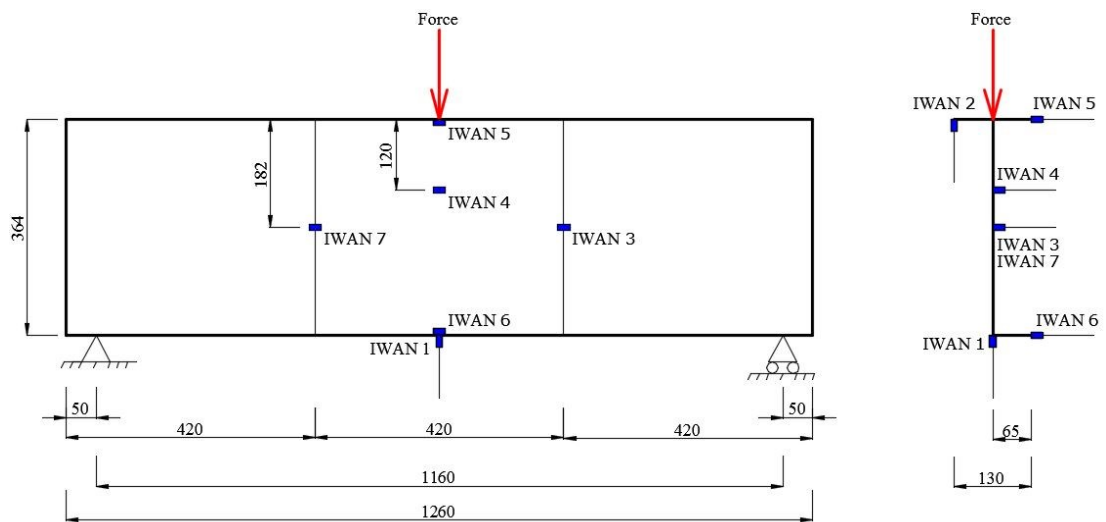


Figure 3.9. Location of displacement transducers on specimen: front and side views

Displacement transducers that are used in this research consist of several parts: movable part, fixed part and a wire which connect transducer to computer. Movable part is set to a certain part of specimen and when they start to move under loading applied on specimen, computer records the displacement. Each transducer can capture only horizontal or only vertical displacements. Furthermore, displacement recorded by computer can be both positive and negative. It depends on which way the movable part of transducer goes: in or out (see Figure 3.10).

### C-sectioned lightweight steel beams

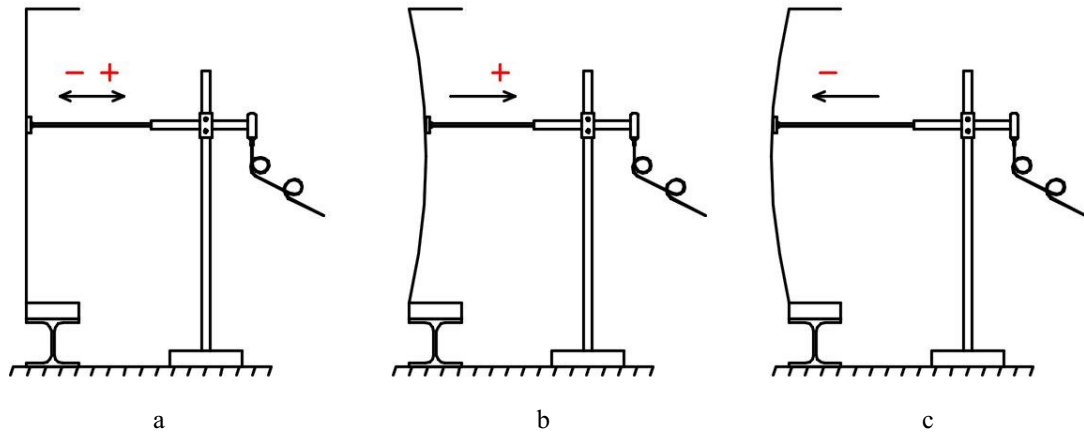


Figure 3.10. Displacement transducers at initial position (a), positive (b) and negative (c) moving direction

In Table 3.6 is described what type of displacement (vertical or horizontal) transducers measure and on which part of the beam they are fixed.

Table 3.6. List of displacement transducers

Name of the transducer	Measured displacement	Location on the beam
IWAN 1	vertical	Lower part of web
IWAN 2		Upper flange
IWAN 3	horizontal	Web right
IWAN 4		Web in the middle
IWAN 5		Web near upper flange
IWAN 6		Lower flange
IWAN 7		Web left

### 3.3.5 Loading

For loading 3 points bending test are chosen. This type of bending is basic and one of the simplest one. The main idea is to investigate the behaviour of sandwich (flat and structured) web of the beam. In case of, for example 4-points bending tests, this idea would fail because the loading points would be wright above (or near) the welding joint of structured plates. As a result the welding joints will be under load, but not the web itself. This can lead to incorrect results of the web bending tests.

The load is introduced by means of a testing machine hydraulic jack with a limit of maximum applied force of 500 kN via a load transferring plate welded in the middle of upper flange. The speed of loading is 10 mm/min and 5 mm/min.

### 3.3.6 Results

This chapter present results captured by displacement transducers. Force-time diagram in Figure 3.11 shows also the speed of loading (see Table 3.7). The jump of the curve in the time interval from 0 to 5 seconds occurs due to the fact that movable part of the machine (hydraulic jack) meets the beam surface. This is called 'force closure' and in present case it is 0.6 kN.

### C-sectioned lightweight steel beams

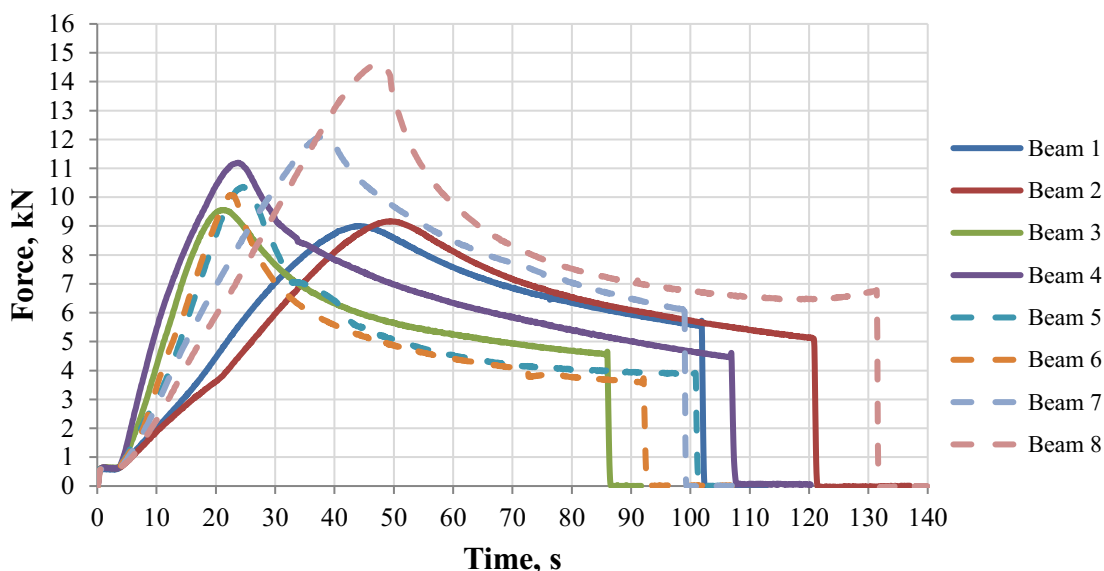


Figure 3.11. Force-time diagram from laboratory experiments, C-profiles of specimens

Table 3.7. Maximal force, corresponding time according to laboratory experiments for C-profiles of specimens

Specimen №	Force <sub>max</sub> , kN	Corresponding time, s
Beam 1	9.01	44.1
Beam 2	9.17	49.4
Beam 3	9.56	21.5
Beam 4	11.20	23.8
Beam 5	10.36	24.5
Beam 6	10.12	17.3
Beam 7	12.10	38.2
Beam 8	14.62	47

Figure 3.12 shows dependence of force and vertical displacement of lower beams web – the global deflection of the beam (results from transducer IWAN 1). The highest maximal force is reached by Beam 8 – 14.62 kN, the lowest – Beam 1 (9.01 kN) (see Table 3.8). Beam 3, Beam 5 and Beam 6 curves differ from others - at first, displacement increases and after reaching the maximal force it begins to decrease (displacement on other curves grows). That means that transducers captured the change of the displacements direction of the lower part of the web. It is caused due to the fact that the web of these beams bents in the positive direction and then changes to negative (see Figure 3.10). As it is seen on Figure 3.12, displacements of lower beams web with structured plates (Beams 5 and 6) are less than in flat ones (Beams 1 and 2).



## IWAN 1

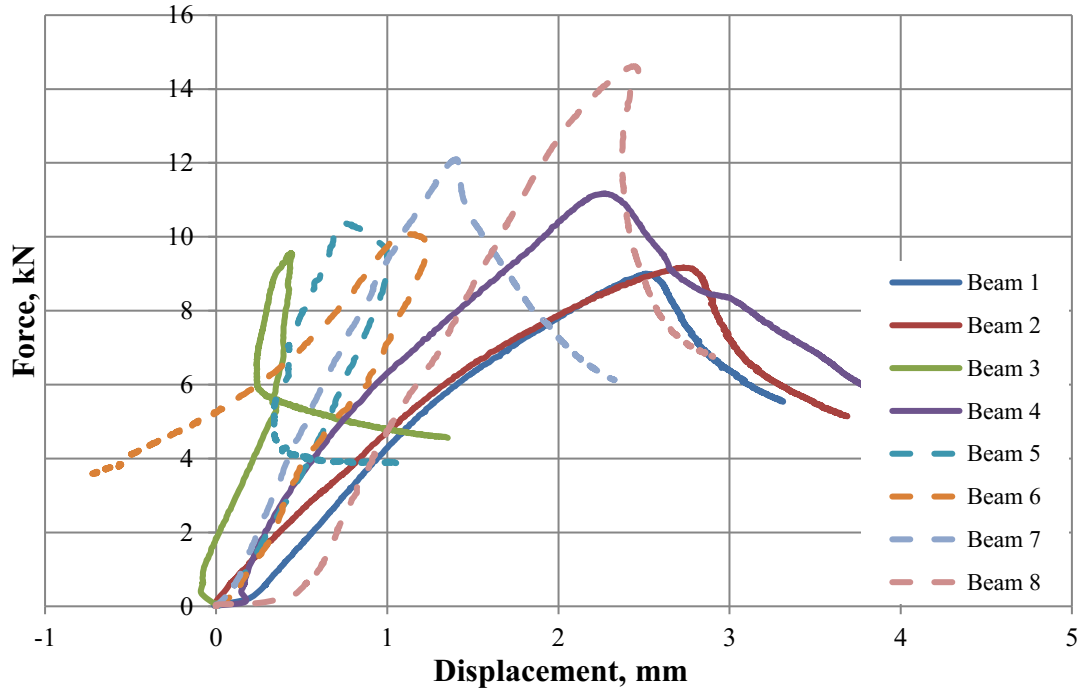


Figure 3.12. Force-displacement diagram from laboratory experiments, vertical displacement of lower part of the web, transducer IWAN 1

In Table 3.8 maximal force and corresponding displacement captured by IWAN 1 are summarized.

Table 3.8. Maximal force for each specimen and corresponding displacements, results for IWAN 1 transducer

Specimen №	Force <sub>max</sub> , kN	Corresponding displacement, mm
Beam 1	9.01	2.51
Beam 2	9.17	2.73
Beam 3	9.56	0.44
Beam 4	11.20	2.27
Beam 5	10.36	0.76
Beam 6	10.12	1.16
Beam 7	12.10	1.40
Beam 8	14.62	2.43

Transducer IWAN 2 captured one of the most important displacements – the displacement of the upper beam flange – see Figure 3.13, where load is applied. These results contain important information about the research subject – stiffness and load bearing capacity of structured sandwich sheet (the sandwich web of the specimen).

Displacements of this part are larger than in lower web. The reason is that both local and global deformations take place in area of loading. In general, displacements of the beams with structured plates (Beams 5-8) are less than flat ones (Beams 1-4). That means, that the beams made of sandwich members with structured plates have up by 47% higher stiffness (see Table 3.9) and load bearing capacity is maximum 53% higher comparing to beams with flat sandwich web (if comparing beams with same total thickness).

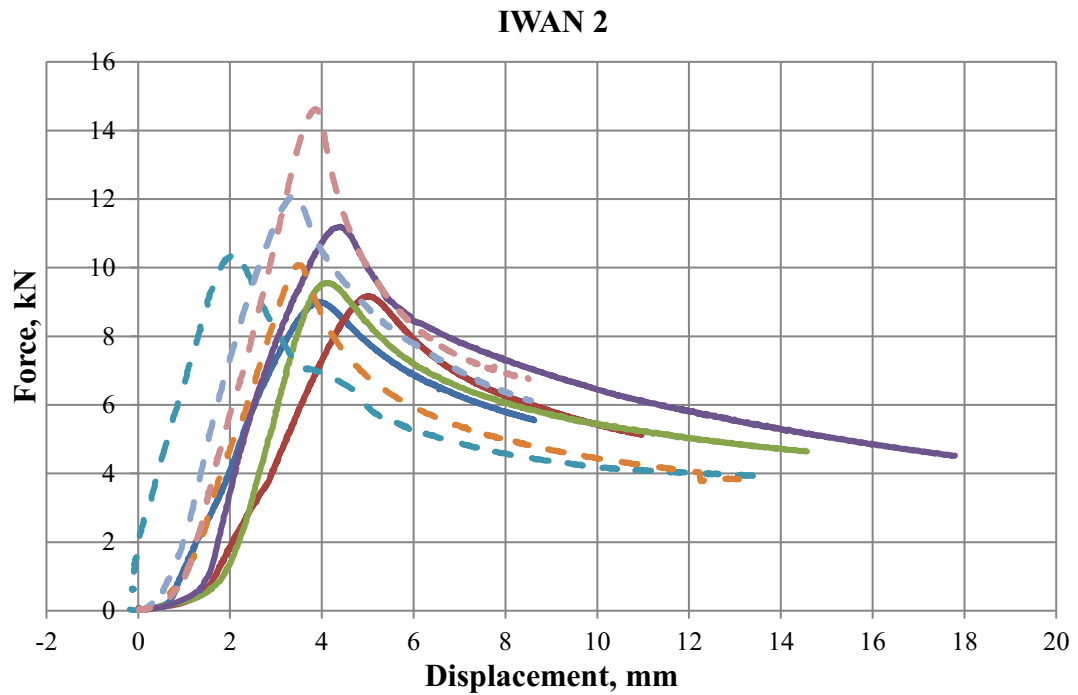


Figure 3.13. Force-displacement diagram from laboratory experiments, vertical displacement of upper flange, transducer IWAN 2

In Table 3.9 maximal force and corresponding displacement are summarized. Maximal forces are reached by loading specimens with sandwich web of flat plate 1mm connected to structured 0.5 mm. The forces are 14.62 kN - Beam 8 and 12.10 kN – Beam 7.

In Table 3.9 stiffnesses of specimens webs are calculated. In order to except the initial deformations, that took place in the experiments (curves jumpings, see Figure 3.13), stiffness of experiments is defined as an inclination of sharp straight line (in elastic zone) between approximately 2 and 8 kN. That is the initial gradient, which shows realistic experiment results.

Table 3.9. Maximal force for each specimen and corresponding displacements, results for IWAN 2 transducer

Specimen №	Force <sub>max</sub> , kN	Corresponding displacement, mm	Web stiffness (vertical), kN/mm
Beam 1	9.01	3.94	3.34
Beam 2	9.17	5.01	3.16
Beam 3	9.56	4.15	4.74
Beam 4	11.20	4.40	4.78
Beam 5	10.36	2.06	4.64
Beam 6	10.12	3.46	4.46
Beam 7	12.10	3.42	5.29
Beam 8	14.62	3.84	5.25

Transducer IWAN 3 is located symmetric to IWAN 7. They both situated at the distance of 1/3 of the beams edges and show the horizontal displacement (global) of the beams web - see Figure 3.14 and Figure 3.15.

C-sectioned lightweight steel beams

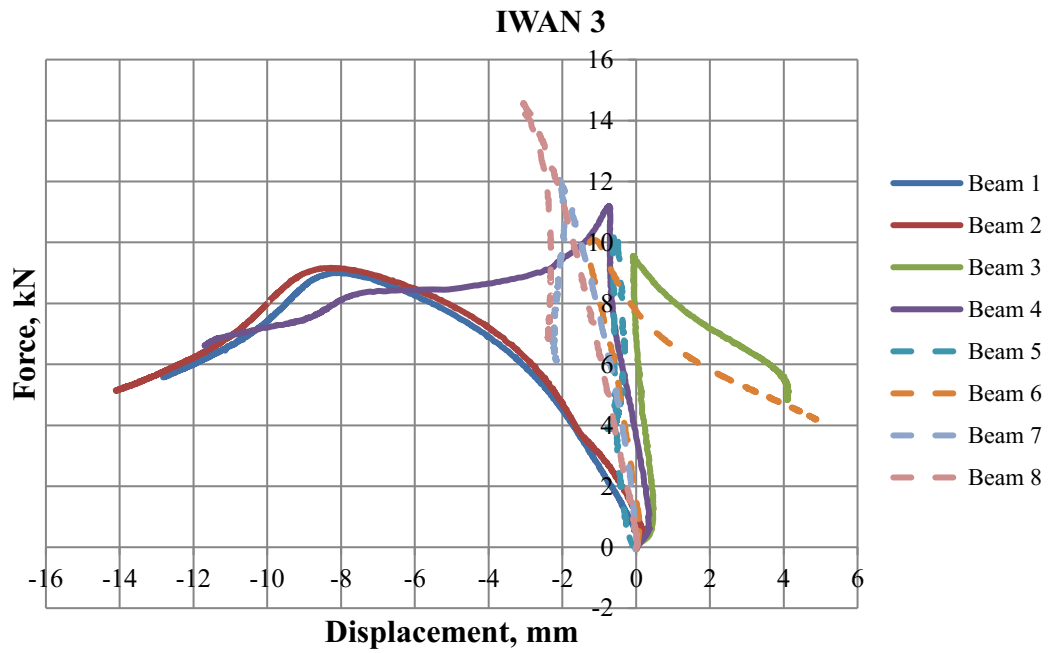


Figure 3.14. Force-displacement diagram from laboratory experiments, horizontal displacement of web, transducer IWAN 3

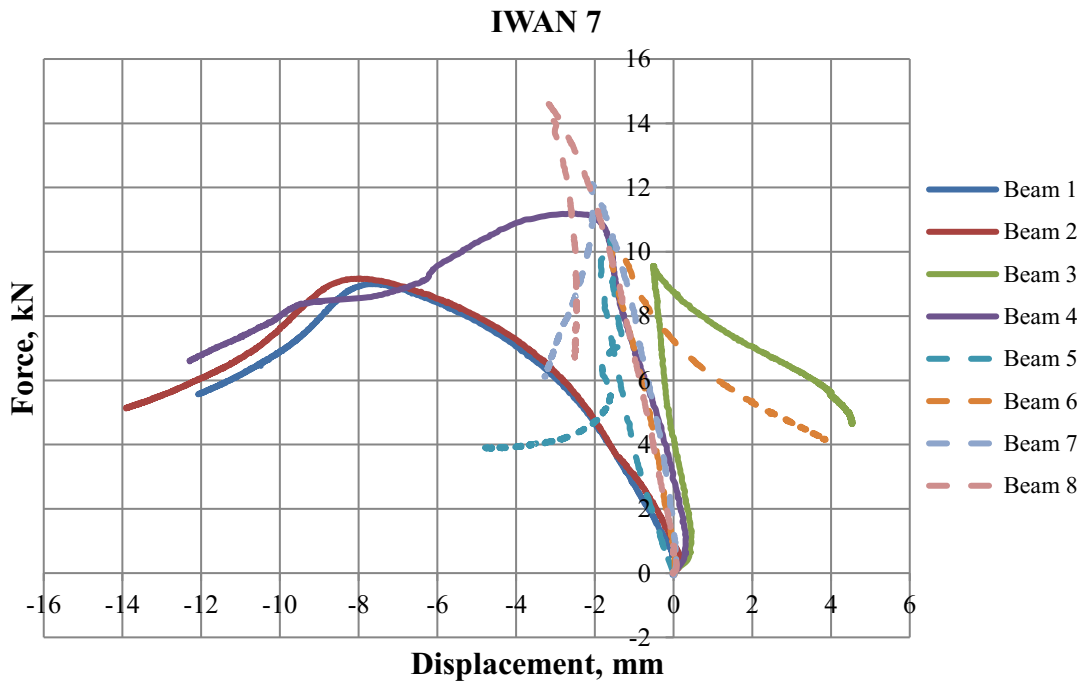


Figure 3.15. Force-displacement diagram from laboratory experiments, horizontal displacement of web, transducer IWAN 7

As it is seen from Table 3.10, the global horizontal displacement of each beams web occurs rather symmetrical. The highest web displacements have Beams 1 and 2, that means the web buckling process runs more active compared to other specimens and therefore Beams 1 and 2 webs are less stable, than webs of other beams. In general, beams with structured sheets show more stable behavior than beams with flat sandwich web.

Table 3.10. Maximal force for each specimen and corresponding displacements, results for IWAN 3 and IWAN 7 transducers

### C-sectioned lightweight steel beams

Specimen №	Force <sub>max</sub> , kN	Corresponding displacement, mm	
		IWAN 3	IWAN 7
Beam 1	9.01	-8.07	-7.61
Beam 2	9.17	-8.27	-7.98
Beam 3	9.56	-0.07	-0.52
Beam 4	11.20	-0.74	-2.63
Beam 5	10.36	-0.58	-1.61
Beam 6	10.12	-1.21	-1.49
Beam 7	12.10	-2.11	-2.08
Beam 8	14.62	-3.10	-3.17

IWAN 4 (see Figure 3.16) captures horizontal displacement of web in the middle of the beam. It is located at the distance of 120 mm from upper beam flange. Transducers IWANs 3,7 and 4 show the deformation appeared on beams web. It can be seen, that webs behavior of flat and structured specimens is different. In case of beams 1-4 (with only flat plates) webs displacement increases while force changes, so web deformation occurs smoothly. Beams 5-8 show another behavior: while force increases, displacement practically does not change, but increases only after reaching maximal force. That means, sandwich web made of structured plates is stiffer than sandwich made of flat plates.

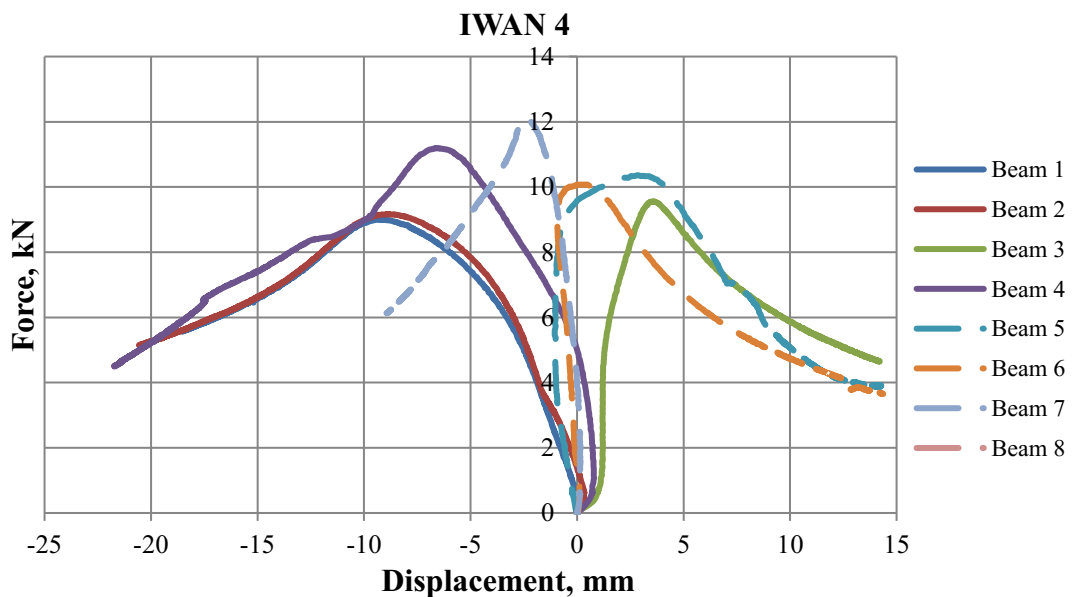


Figure 3.16. Force-displacement diagram from laboratory experiments, horizontal displacement of web, transducer IWAN 4

As Table 3.11 shows, all beams except Beam 3 and Beam 5 bend in negative direction (see Figure 3.10). That may happen because of pre-deformations that are caused by point-welding. The displacements of Beams 1-4 web are higher than Beams 5-8. That means, that the horizontal buckling field of Beams 1-4 (with flat plates) is higher, than field of Beams 5-8 (with structured plates).

According to Table 3.10 and Table 3.11 horizontal deformation distributes evenly on specimens webs and reaches maximum value in cases of Beam 1 and 2 – 9,15 mm and 8,84 mm (see Table 3.11).

### C-sectioned lightweight steel beams

In Table 3.11 stiffnesses in absolute values of specimens webs (horizontal) are calculated. In order to except the initial deformations, that took place in the experiments (curves jumpings, see Figure 3.16), stiffness of experiments is defined from sharp straight line (elastic zone) between approximately 2 and 6 kN. As it can be seen from Table 3.11, the web stiffness in horizontal direction of specimens 5-8 (with sandwich structured sheets) is up to 7 times higher than specimens 1-4 (with sandwich flat plates).

Table 3.11. Maximal force for each specimen and corresponding displacements, results for IWAN 4 transducer

Specimen №	Force <sub>max</sub> , kN	Corresponding displacement, mm	Web stiffness (horizontal), kN/mm
Beam 1	9.01	-9.15	1.42
Beam 2	9.17	-8.84	1.53
Beam 3	9.56	3.63	2.17
Beam 4	11.20	-6.61	2.18
Beam 5	10.36	2.87	6.27
Beam 6	10.12	-0.03	6.28
Beam 7	12.10	-2.44	7.01
Beam 8	14.62	-3.94	7.06

Figure 3.17 shows results from IWAN 5 displacement transducer – the horizontal displacement of upper beam flange. According to graph, the displacements are very small – maximum 1.16 mm (Beam 3) and minimum (in absolute value) – 0.05 mm. That means upper beam flange practically has no horizontal movement, but only vertical. Therefore, practically pure compression takes place.

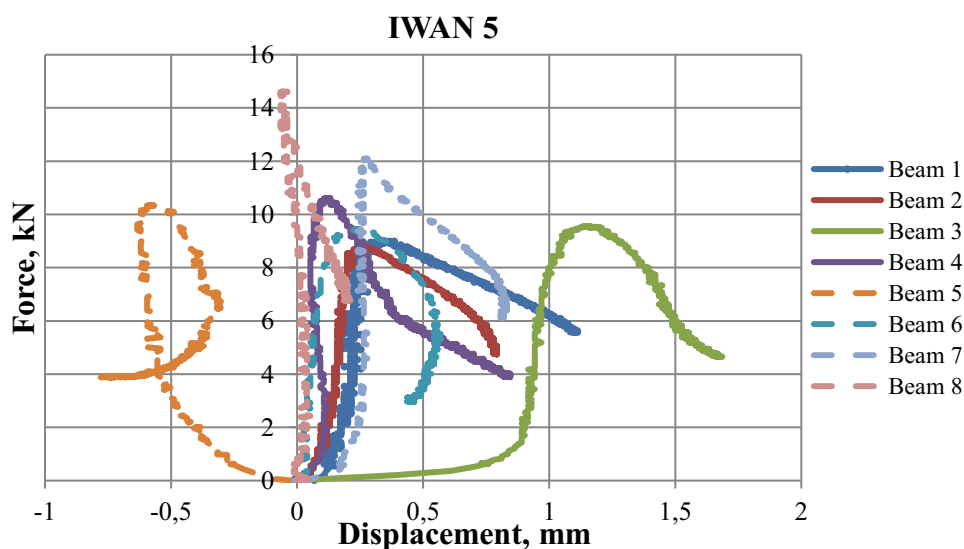


Figure 3.17. Force-displacement diagram from laboratory experiments of IWAN 5 displacement transducers

In Table 3.12 maximal force and corresponding displacement are summarized (captured by IWAN 5).

### C-sectioned lightweight steel beams

Table 3.12. Maximal force for each specimen and corresponding displacements, results for IWAN 5 transducer

Specimen №	Force <sub>max</sub> , kN	Displacement, mm
Beam 1	9.01	0.34
Beam 2	9.17	0.52
Beam 3	9.56	1.16
Beam 4	11.20	0.58
Beam 5	10.36	-0.58
Beam 6	10.12	0.52
Beam 7	12.10	0.28
Beam 8	14.62	-0.05

IWAN 6 captures the horizontal displacement of specimens lower flange – see Figure 3.18.

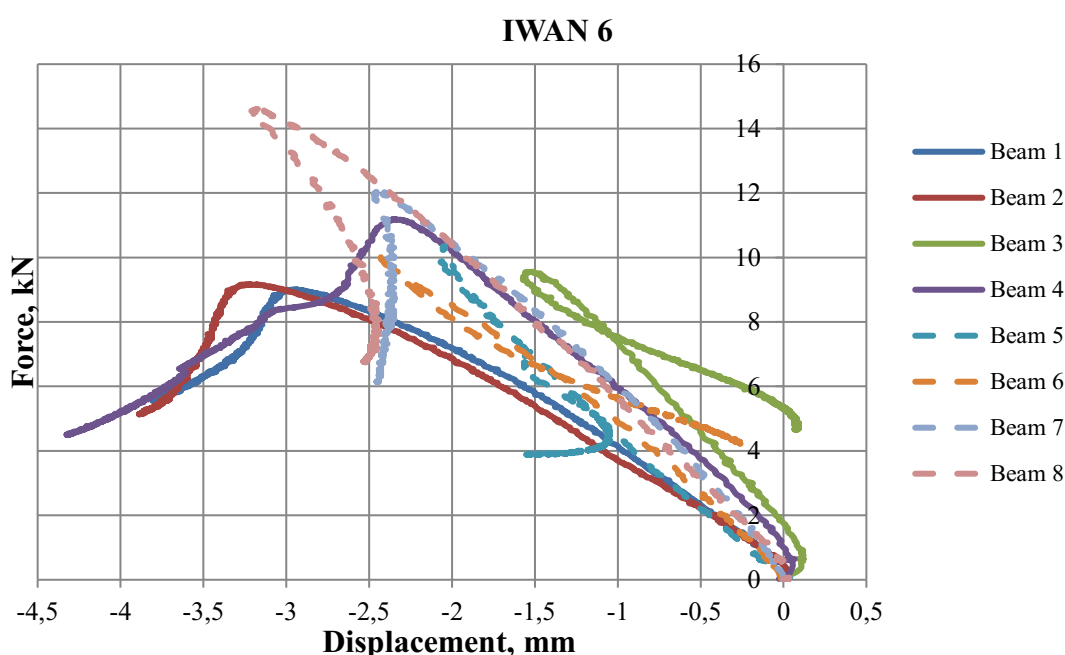


Figure 3.18. Force-displacement diagram from laboratory experiments of IWAN 6 displacement transducers

In Table 3.13 maximal force and corresponding displacement are shown. As it is seen from the Table 3.13 and Figure 3.18 lower flange of all beams has negative displacement. One direction movement have Beams 1, 2 and 4. Change the direction displacement movement occurs by Beams 3, 5, 6 and 7 (after reaching max force, displacement decreases). It means that the flange of those beams moves at first in negative direction and then in positive (see Figure 3.10). Absolute maximal displacement has Beam 2 – 3.22 mm, practically same displacement has Beam 8 – 3.17 mm, but loading capacity is 60% higher than Beam 2.

## C-sectioned lightweight steel beams

Table 3.13. Maximal force for each specimen and corresponding displacements, results for IWAN 6 transducer

Specimen №	Force <sub>max</sub> , kN	Displacement, mm
Beam 1	9.01	-2.93
Beam 2	9.17	-3.22
Beam 3	9.56	-1.55
Beam 4	11.20	-2.35
Beam 5	10.36	-2.04
Beam 6	10.12	-2.46
Beam 7	12.10	-2.45
Beam 8	14.62	-3.17

### 3.3.7 Conclusion

In this chapter the experimental results of 8 C-profiled beams welded together with 3 plates are presented. The experiments are carried out at the BTU, Cottbus in research and material testing institute – FMPA (Germ. Forschungs- und Materialprüfanstalt). Beams 1-4 are made only of flat plates, specimens 5-8 – of flat and structured. All specimens have same geometrical parameters (except thickness) and are loaded under the same boundary conditions. The variable is thickness of panel (see Table 3.4). In Table 3.14 the force-displacement results captured by 7 displacement transducers are presented. For every beam transducers (IWANs) are put in the same places to receive displacements of characteristic points and to have an opportunity to compare them.

Table 3.14. Specimens maximal forces, corresponding displacements from transducers (IWANs) and stiffnesses, experimental results

Beam	F <sub>max</sub> , kN	IWAN									
		1	2		4		7	3	5	6	
		Displ., mm	Displ., mm	Stiffness, kN/mm	Displ., mm	Stiffness, kN/mm	Displ., mm				
1	9.01	2.51	3.94	3.34	-9.15	1.42	-7.61	-8.07	0.34	-2.93	
2	9.17	2.73	5.01	3.16	-8.84	1.53	-7.98	-8.27	0.52	-3.22	
3	9.56	0.44	4.15	4.74	3.63	2.17	-0.52	-0.07	1.16	-1.55	
4	11.20	2.27	4.40	4.78	-6.61	2.18	-2.63	-0.74	0.58	-2.35	
5	10.36	0.76	2.06	4.64	2.87	6.27	-1.61	-0.58	-0.58	-2.04	
6	10.07	1.16	3.46	4.46	-0.03	6.28	-1.49	-1.21	0.52	-2.46	
7	12.10	1.40	3.42	5.29	-2.44	7.01	-2.08	-2.11	0.28	-2.45	
8	14.62	2.43	3.84	5.25	-3.94	7.06	-3.17	-3.10	-0.05	-3.17	

As it can be seen from the table above, if compare specimens with same total thickness, load bearing capacity by beams 5 and 6 is up to 15% higher, than by beams 1 and 2, and by beams 7 and 8 – up to 53% higher, than by beams 3 and 4. Also, stiffnesses, that are calculated based on results, captured by IWAN2 (vertical displacement of specimens web) are also higher by beams with structured sheets: up to 46% and 12% higher by beams 5,6 and 7,8 respectively comparing to beams 1,2 and 3,4. That proves the specimen web made of flat and structured plates is stiffer and bears higher force, than web made of 2 flat plates. Figure 3.19 describes graphically stiffnesses of beams web.

**IWAN 2**

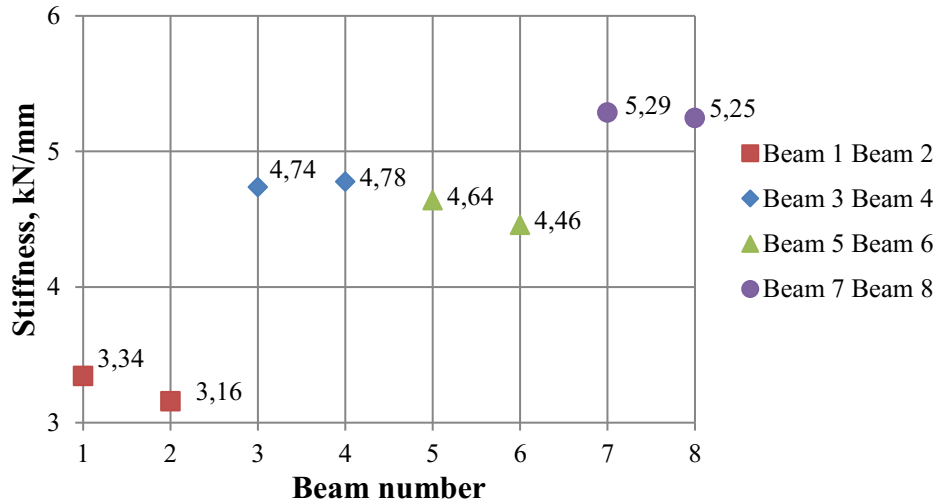


Figure 3.19. Vertical stiffnesses of web beams 1-8 calculated by results captured by IWAN 2

Stiffness calculated from results captured by IWAN 4 is horizontal web stiffness, it shows how big the buckling displacement (horizontal) is. From Table 3.14, it is seen, that beams 5-8 (with structured web) web stiffness is much (from 4 to 7 times) higher, than beams 1-4. That happens due to higher out of plane rigidity of structured plates compare to flat ones. Figure 3.20 describes visually the stiffnesses of beams 1-8. From diagram presented in Figure 3.20 is clearly seen how big is the difference of beams 1-4 and beams 5-8 stiffnesses.

**IWAN 4**

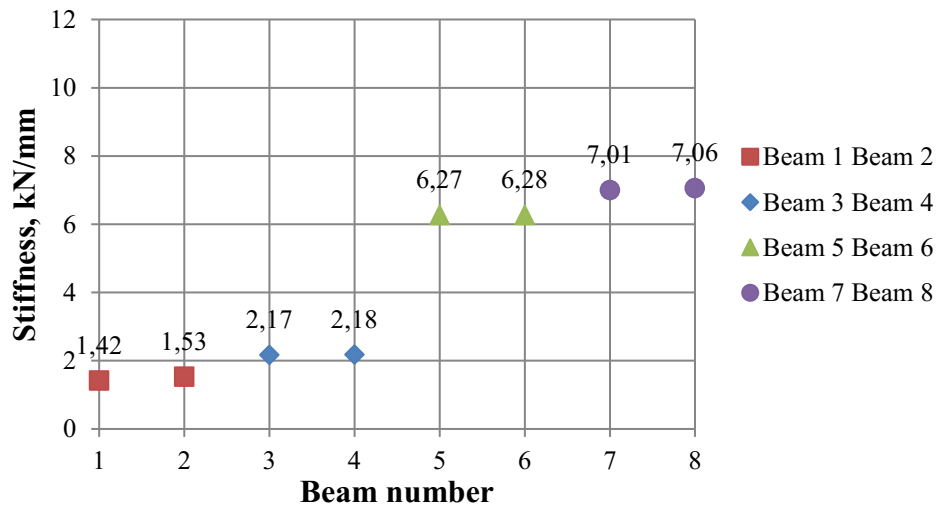


Figure 3.20. Horizontal stiffness of web beam 1-8 calculated by results captured by IWAN 4

The general aim of experimental research is to seek a determination of relationship between two variables – the dependent variable (in this research: load bearing capacity of specimens) and the independent variable (thickness of investigated sheets). To conduct the experiments several steps are made: all plates are processed (cut, bent, hydroformed, laser welded) for further point-welding connection with each other. Afterwards, additional details are manufactured in order to create certain boundary conditions that would be able to provide for the setup an acceptable environment for studying the research object (load bearing capacity of



specimens). These steps of preparations for experiments give more fundamental knowledge about investigated subject (beam) and more details, that should be introduced in future FEM simulation model.

In following chapters, information collected while manufacturing and loading of specimens is integrated in software ABAQUS in order to verify FEM simulations. The simulations are described in next chapter and in following chapters FEM simulations and experimental results are compared. The conclusions from verification control are used for parametric modelling and give an opportunity to predict the behavior of specimens similar to the studied ones.

### 3.4 FEM simulations

#### 3.4.1 General information

For finite element analysis (FEM) simulations of the laboratory tests the software package ABAQUS/CAE, Standard Version 6.14 is used. ABAQUS/CAE, or Complete ABAQUS Environment, is a software application used for both the modeling and analysis of mechanical components and assemblies (pre-processing) and visualizing the finite element analysis results. [98]

The basic properties of the component, such as geometry, storage conditions and material are defined and assigned to the specified elements. The following applies to all experiments: modeling space is 3-dimensional, modeling type – deformable shell elements [79], modeling steps: Buckling and Riks.

For each type of investigated beams, an FE model is created and analyzed. Comparative values are all simulation and laboratory results such as the critical loads, reactions of the supports, displacements and deflections.

Beam types 1-4 (see Table 3.4) are created in software ABAQUS according to chosen dimensions written above (see Figure 3.6). For beam types 3 and 4 the main element – a single comb was created with the help of the ProEngineer software and imported into the ABAQUS via the AutoCAD software (see Figure 3.21). [79]

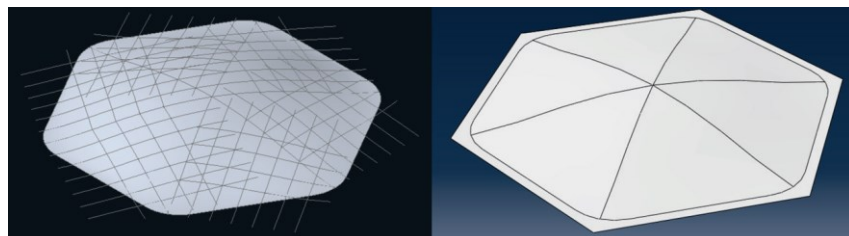


Figure 3.21. Geometry AutoCAD (left) imported in ABAQUS (right) honeycomb [79]

#### 3.4.2 Geometry and material properties

The geometry of 4 types created models is shown in Figure 3.6 and copies the geometry of laboratory specimens. Specimen types and numbers are listed in Table 3.4.

## C-sectioned lightweight steel beams

The characteristic values of used materials are determined by tensile tests (see 3.2 Material properties), adapted to the input in ABAQUS with true stress-strain relationship and implemented to the software. In tests, material characteristics are used as elastically plastic bilinear material law. In chapter 3.2 Material properties, the stress-strain curves for flat (Figure 3.2) and structured (Figure 3.3) plates are shown and main sheet metal parameters are summarized in Table 3.2 and Table 3.3.

For the implementation of the material laws for used elements, the integration according to Gauss with six integration points across the thickness is chosen. This has the advantage that more complex non-linear problems can be solved with higher accuracy [101].

### 3.4.3 Connections between elements of the model

There are 6 additional plates are used in experiments in order to make studied beams more stable and to prevent local web buckling, to see their functions Table 3.5. Figure 3.22 illustrates additional steel plates with its numbers.

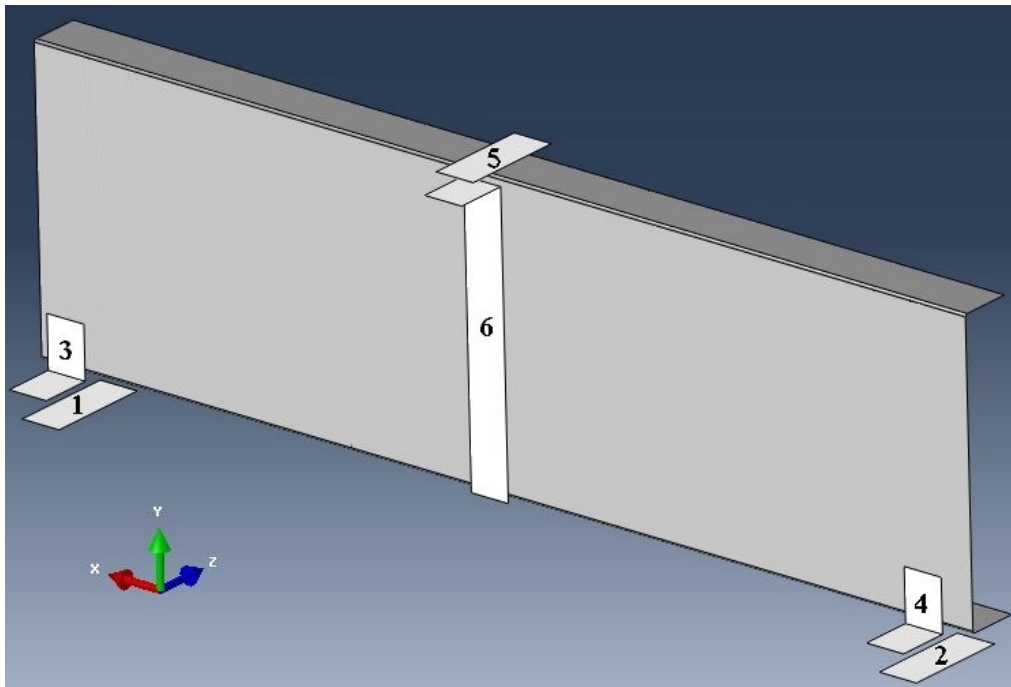


Figure 3.22. Numbers of additional steel plates introduced to experiments

After creating main (C-profiled beam and 3 rectangular) and additional model parts, it should be put together in order to make final model (specimen) in Assembly mode. By modelling sandwich elements, investigated in this work, 2 types of connections are simulated: laser and point welding.

Laser welding connect 3 rectangular plates (flat and structured) with one another along the edge, so that 1 big sheet is made. To model laser welding function 'Tie' is used. It is also used to model connection between additional steel plates and C-profile. After joining 3 plates in one big, point welding is simulated. In order connect to 1 big sheet to C-profiled beam the 'Fastener' option is chosen, type: Discrete and Point-based correspondingly. For structured plates, fastener points located in the centre of the honeycomb, exactly at the highest point of the

## C-sectioned lightweight steel beams

comb. Fastener points of flat plates are geometrically located just like in the case of structured. Fasteners option allows also insert the geometric properties of real model – the radius of the welding points – 3 mm. Connection of specimen elements and types of connections are listed in Table 3.15.

Table 3.15. Connection of specimen elements

Plate number/ name	Connected element(s)	Connected areas	Type of connection
1	Lower beam flange- Plate 3	Surface	Constraint: Tie, surface to surface
2	Lower beam flange- Plate 4		
3	Beam web-Plate 1		
4	Beam web-Plate 2		
5	Upper beam flange- Plate 6		
6	Beam web		
Flat plate	Flat plate	Edge	Tie, Analysis default
Structured plates	Structured plates		
Flat plate	Beam web	Points	Fasteners; Attachment method: face to face; Physical radius: 3 mm; Connector section: beam
Structured plates	Beam web		

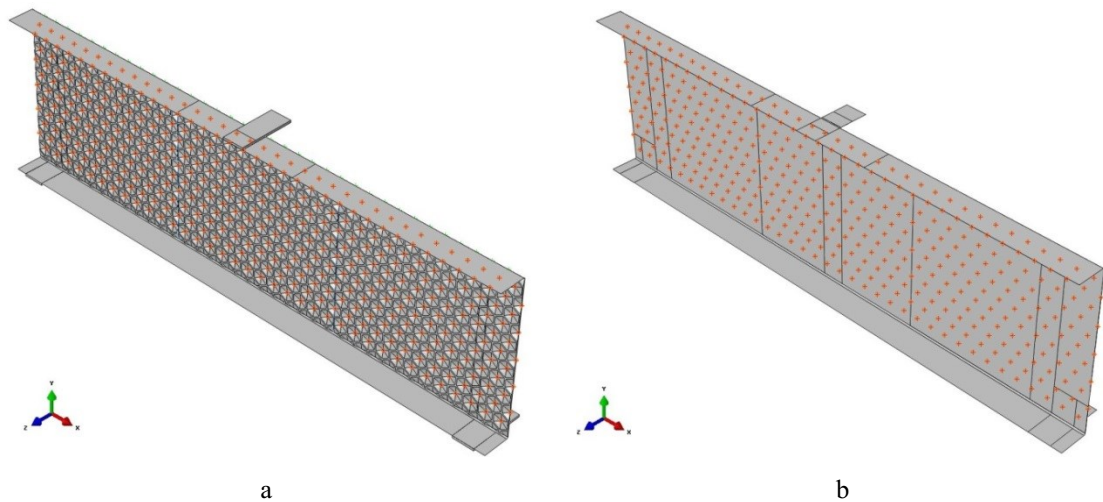


Figure 3.23. The weld points modeling for structured and flat web specimens: with structured sheets (a) and flat plates (b)

### 3.4.4 Boundary conditions and loading

The support conditions designed in the model duplicate conditions from the laboratory tests. For the support 1, the degrees of freedom 1 and 2 are fixed, that means, the movements in the X, Y directions are blocked. The rotation in all three directions is free. For the support 2, only degrees of freedom 2 are fixed – the displacements in Y direction are blocked. The rotation in all three directions is also free. The stall protection is realized by holding the front (Areas 3 and 4) and back (Areas 5 and 6) surfaces of the specimens webs in Z-direction. Area 7 is the place of load application, introduced in model by displacement in Y-direction. Plate in the

## C-sectioned lightweight steel beams

middle of the specimens upper flange is fixed in Z-direction (Area 8). Boundary conditions areas are shown in Figure 3.24 and their degrees of freedom are listed in Table 3.16.

Table 3.16. Boundary conditions and their degrees of freedom

Name	$U_x(U_1)$	$U_y(U_2)$	$U_z(U_3)$	$UR_x(UR_1)$	$UR_y(UR_2)$	$UR_z(UR_3)$
Line 1	0	0	-	-	-	-
Line 2	-	0	-	-	-	-
Area 3	-	-	0	-	-	-
Area 4	-	-	0	-	-	-
Area 5	-	-	0	-	-	-
Area 6	-	-	0	-	-	-
Area 7	-	-1	-	-	-	-
Area 8	-	-	0	-	-	-

Note: U-translational displacement, UR-rotational displacement, 0 - movement is not allowed, '-'-movement is allowed

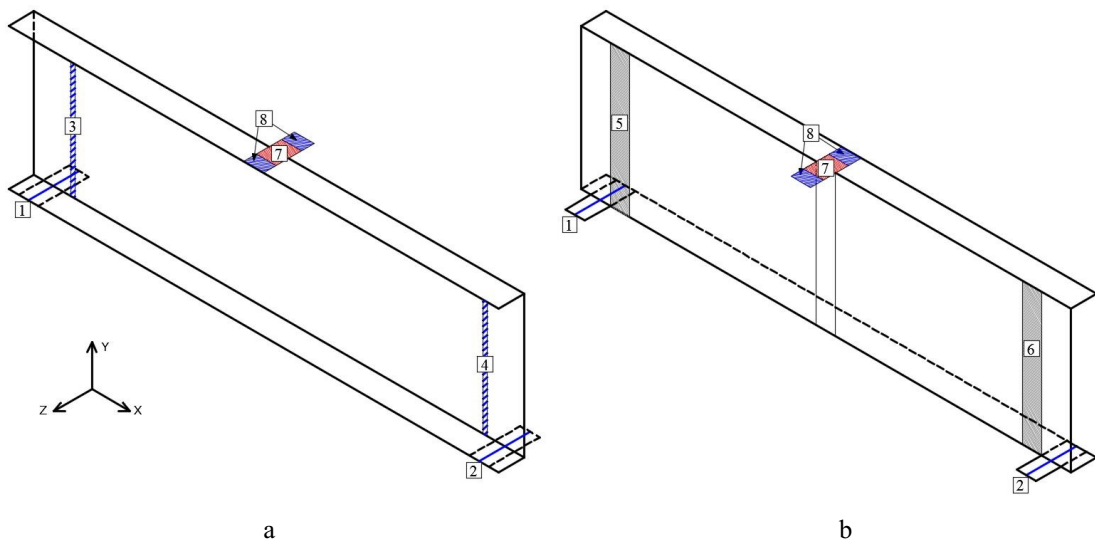


Figure 3.24. Areas where boundary conditions are applied: front(a) and back (b) side of specimen

The applied force is a point load, which model the hydraulic jack of the testing machine. It is applied on Area 7 – in the middle of beams upper flange. Load is introduced by displacement control.

### 3.4.5 Mesh

One of the most important steps till completed simulation is meshing process. Size of the mesh depends on the size of the whole model. Small elements of mesh lead to more accurate analysis compared to the bigger ones. However, the smaller elements are created in a model, the more time will the analysis take. So that the calculation of the investigated models with extra small mesh elements can take days, whereas the calculation time with optimal mesh size will take approximately an hour or even less.

For this investigation for the beam with sizes 1260 mm x 364 mm the general optimal mesh size is chosen – 5x5 mm. For structured areas it was reduced to 3x3 mm. It is necessary due to the curved honeycomb surface. For solid plates with 5 mm thickness (on upper flange, where load is applied and bottom flanges, where rollers are located) the mesh size is 5x6.5x6.5 mm. General information about models each of the beam types is summarized in Table 3.17.

## C-sectioned lightweight steel beams

Table 3.17. General information about models

Beam type	Number of		Types of elements	Size of the element, mm
	nodes	elements		
1	46433	45328:	S4R C3D8R	5x5 5x6.25x7
2		44848 480		
3	88949	88580:	S4R S3 C3D8R	5x5 3x3 5x6.25x7
4		85437 2663 480		

S4R and S3 are general-purpose shells, elements that allow transverse shear deformation. The thick shell theory is used as the shell thickness increases and become discrete Kirchhoff thin shell elements as the thickness decreases; the transverse shear deformation becomes very small as the shell thickness decreases. [101]

S4R is a linear quadrilateral elements 4-node general-purpose shell, reduced integration with hourglass control and a large strain formulation:

S – conventional stress/displacement shell;

4 – number of nodes;

R – reduced integration. [101]

S4R is element type used for meshing of flat and structured plates.

S3 – is 3-node triangular general-purpose shell, this element is a degenerated triangle version of S4R that is fully compatible with S4R. [101]

C3D8R is one of the stress/displacement element types, is used for 3D solid additional plates 1, 2 and 5 – see Table 3.5. C3D8R is three-dimensional continuum hexahedral elements, 8-node linear brick, reduced integration (1 integration point). [101]

C – continuum stress/displacement solid element;

3D – three-dimensional;

8 – number of nodes;

R – reduced integration. [101]

### 3.4.6 Imperfections and buckling analysis

Imperfections are from 2 different origins: geometric imperfections (due to fabrication and construction tolerances) and residual stresses (due to fabrication process: steel plate cutting, bending, welding). For combination of both effects, the equivalent geometric imperfection method is applied, consisting of increasing the amplitude of the geometric imperfections in order to cover also the residual stresses. For some basic cases – see Table 3.18 (Table C2 from EN 1993-1-5) and (Figure C.1 from EN 1993-1-5) give recommendations for defining the deformed shapes and amplitudes of these equivalent imperfections. [103]

## C-sectioned lightweight steel beams

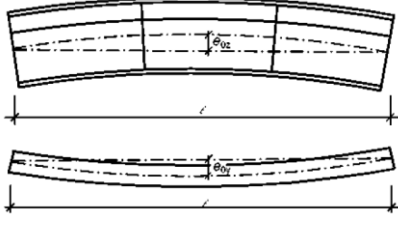
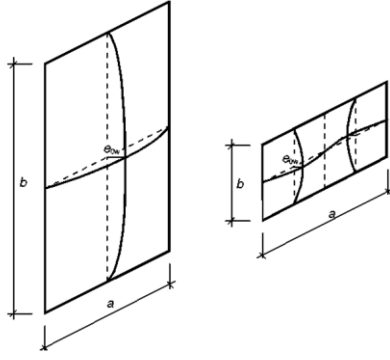
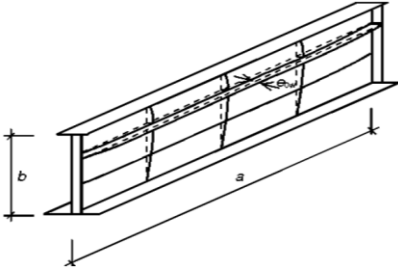
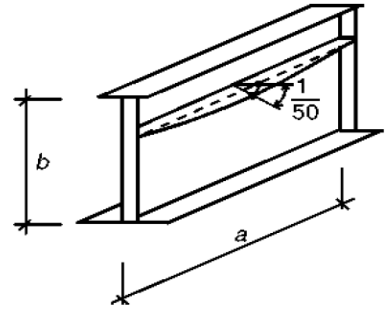
Table 3.18. Equivalent geometric imperfections: Table C.2 from Annex C of EN 1993-1-5: [102]

Type of imperfection	Component	Shape	Magnitude
global	member with length $l$	bow	see EN 1993-1-1, Table 5.1
global	longitudinal stiffener with length $a$	bow	$\min(a/400, b/400)$
local	panel or subpanel with short span $a$ or $b$	buckling shape	$\min(a/200, b/200)$
local	stiffener or flange subject to twist	bow twist	1/50

The elementary imperfection shapes from Table 3.19 can be obtained by using the buckling modes of the structure taken from a buckling analysis (Buckling step). An appropriate combination of these shapes should be used. [103]

EN 1993-2-5 indicates that in combining imperfections a leading imperfection should be chosen (100%) and the accompanying imperfections may have their values reduced to 70% [102].

Table 3.19. Modelling of equivalent geometric imperfections: Figure C.1 from EN 1993-1-5 [102]

Type of imperfection	Component	Type of imperfection	Component
global member with length $l$		local panel or subpanel	
global longitudinal stiffener with length $a$		local stiffener or flange subject to twist	

Geometric and imperfections from residual stresses used in analysis are determined by using buckling mode analysis in ABAQUS software. The imperfection according to the first buckling mode comprises global imperfection of the plate and local twist of the stiffener, while the imperfection according to second buckling mode consists of local twist of the stiffener. [103]

In order to detect the buckling of thin-walled beams, eigenvalues are determined by means of a buckling analysis. They are implemented into the Riks analysis. These eigenmodes useful for the respective supports are shown in Figure 3.26, Figure 3.27 and Figure 3.28. To

### C-sectioned lightweight steel beams

make the further connection of Buckling and Riks analysis, in Keywords of Buckling the following before ‘\*End step’ must be written:

\*NODE FILE

U

These two lines will extract the eigenvalue in Riks analysis and place them in a file with the name of job that is submitted. Table 3.20 lists the eigenvalues are found. They represent the value of applied load, which is necessary to achieve the respective eigenform on the perfect system with displacement of 1 mm.

The imperfections 1-3 are modelled according to Annex C5 of EN 1993-1-5 [102]. Combination of these 3 basic imperfections is done, where IMP 1(100%) is a leading global imperfection and IMP 2 and IMP 3 are accompanying ones with reduced values of amplitudes (70 % of nominal value). [102].

Table 3.20. Eigenvalues for each of the model types.

Model type	Sandwich members	Total thickness; mm	Ultimate load, kN		
			IMP 1	IMP 2	IMP 3
1	flat 0.75 mm+ flat 0.50 mm	1.25	0.058	0.079	0.091
2	flat 1.00 mm+ flat 0.50 mm	1.5	0.093	0.128	0.159
3	flat 0.75+ structured 0.50 mm	1.25	0.107	0.148	0.181
4	flat 1.00mm+ structured 0.50 mm	1.5	0.142	0.198	0.251

Figure 3.26, Figure 3.27 and Figure 3.28 show eigenforms from Buckling analysis. These deformation forms are same to each of the model type case. The difference is in the load that must be applied to each of the beams in order to deform it by 1 mm (see Table 3.20). To observe more clearly which part of the beam is being deformed, the deformation scale factor for eigenforms is increased up to 100 (in Figure 3.26, Figure 3.27 and Figure 3.28).

The displacements color range vary from red (maximal displacement – 1 mm) to blue (minimal displacement 0 mm) is shown in Figure 3.25.

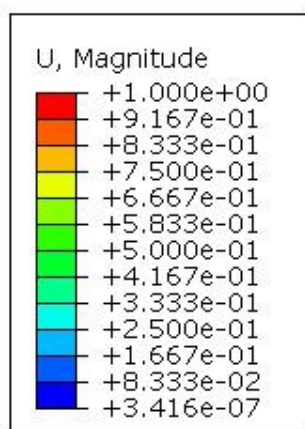


Figure 3.25. The displacements color range for eigenmodes for the C-sectioned specimen in mm

### C-sectioned lightweight steel beams

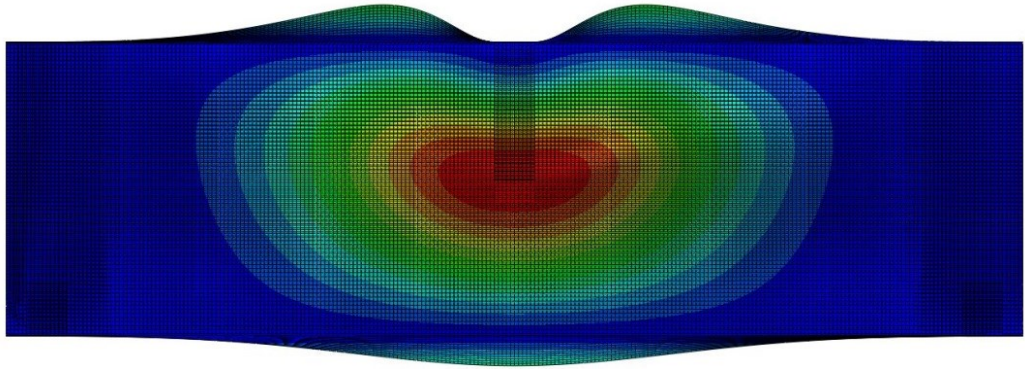


Figure 3.26. First eigenmode for the C-sectioned specimen

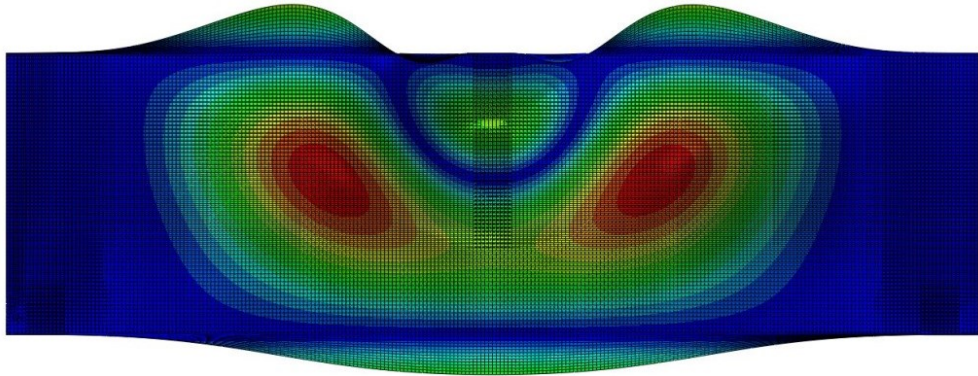


Figure 3.27. Second eigenmode for the C-sectioned specimen

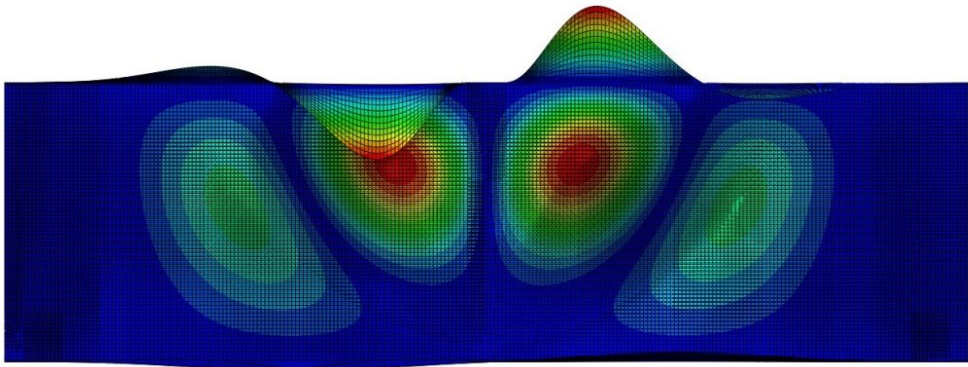


Figure 3.28. Third eigenmode for the C-sectioned specimen

#### 3.4.7 Riks analysis

To implement the found eigenforms (imperfections of the models) to Riks analysis, the following text is added in the input Keywords after words 'End Assembly':

```
*IMPERFECTION,FILE=BUCKLING JOB,
```

```
STEP=1
```

```
1,1
```

```
2,0.7
```

```
3,0.7
```

'FILE=BUCKLING JOB' is a link for ABAQUS to the results of found buckling eigenvalues and 'STEP=1' informs which Step contains this information. Numbers from 1 to 3 are numbers of the respective eigenmodes.



According to EN 1993-1-5: Eurocode 3 [102], to combine imperfections a leading imperfection should be chosen (100%) and the accompanying imperfections may have their values reduced to 70% [102]. According to this, the first eigenform is selected as a main one and the second and the third - accompanying imperfections. Pictures from RIKS analysis are presented in Appendix A.

### 3.4.8 Simulation results

In this chapter FEM simulation results for beam types 1, 2, 3 and 4 are presented. Simulation results are presented in Appendix B. In general, there are 5 pictures - Figure 3.29- Figure 3.33 with 4 force-displacement curves are presented. Also in Table 3.21-Table 3.24 for each of the beam types maximal force, corresponding displacement and stiffness are summarized.

Simulation comparison and analysis of points deformations located in the same places of investigated samples is very important. Transducers define these special points. So that, Figure 3.29 - Figure 3.33 present results from FEM simulations for points where transducers in experiments are placed. As it can be seen further, figures present results for IWANs 1, 2, 4, 7 and 3. Horizontal deformations of upper and lower flanges of models corresponding to transducers IWAN 5 and IWAN 6 are equal to zero and are not presented.

Figure 3.29 shows the behavior of lower flange (also a vertical displacement of web). For all models vertical displacement is rather small – maximum is 0.29 mm by beam type 1. Anyway, the behavior of types 3 and 4 (with structured plates) differ from behavior of types 1 and 2: blue and green curves are practically vertical, so displacement grows slower than in case of purple and red ones.

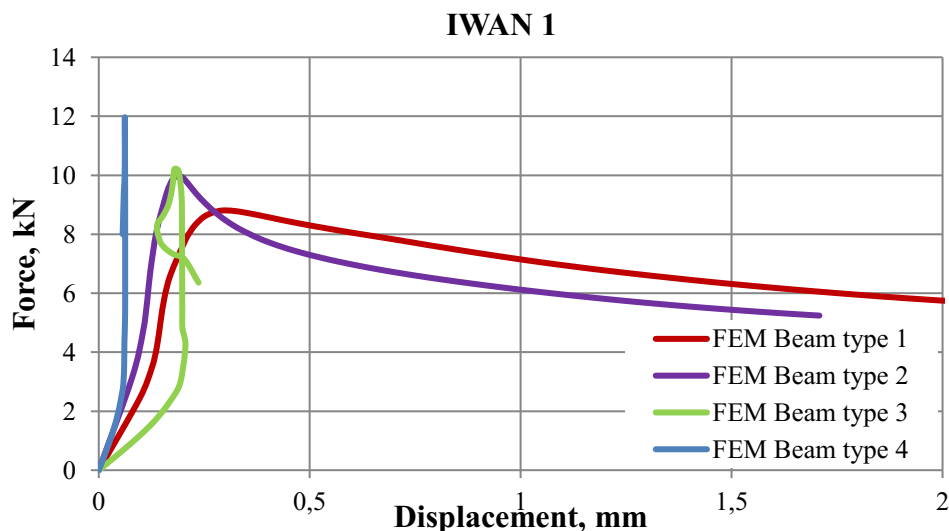


Figure 3.29. Force-displacement (vertical) curves for lower flange (IWAN 1) of FEM simulation results

In Table 3.21 maximal forces and corresponding displacement are collected. The smallest deflection has beam type 4 with maximal force 11.97 kN and practically zero displacement.

### C-sectioned lightweight steel beams

Table 3.21. Simulation results for beam types 1-4, vertical deformation of lower model flange

Beam type	F <sub>max</sub> , kN	IWAN 1	
		Corresponding displacement, mm	
1	8.80	0.29	
2	10.17	0.19	
3	10.20	0.18	
4	11.97	0.06	

In Figure 3.30 force-displacement results of vertical displacement of models upper flange are shown. As it is expected, the smallest stiffness – see Table 3.22, has beam type 1 with total thickness 1.25 mm and consist of only flat plates. Then, 30% higher stiffness have beam types 2 (flat plates only) and 3 (flat and structured plates) with total thickness 1.5 mm and 1.25 mm respectively. The highest stiffness has beam type 4 (46 % higher than beam type 1) with total thickness 1.5 mm consist of flat C-profile and structured plates.

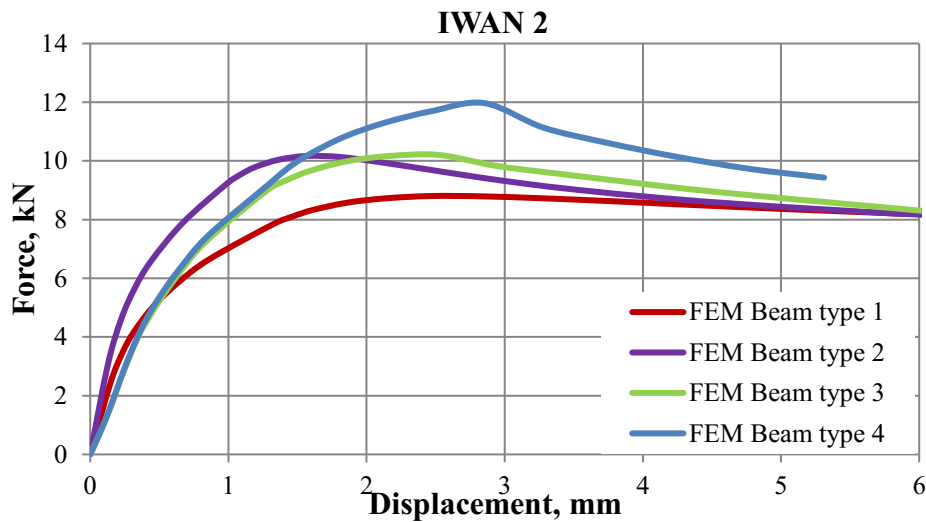


Figure 3.30. Force-displacement (vertical) curves for upper flange (IWAN 2) of FEM simulation results

As expected, beam types 3 and 4 in general have higher stiffnesses, than beams types 1 and 2 with same thicknesses – see Table 3.22. That means there is some contribution to the total beam stiffness of structured sheets. And based upon research, this contribution is greater than from flat plates with the same geometrical parameters.

Table 3.22. Simulation results for beam types 1-4, vertical deformation of upper model flange

Beam type	Total thickness, mm	F <sub>max</sub> , kN	IWAN 2	
			Corresponding displacement, mm	Stiffness, kN/mm
1	1.25	8.80	2.47	3.64
2	1.50	10.17	1.57	4.74
3	1.25	10.20	2.53	4.74
4	1.50	11.97	2.85	5.33

According to results shown in Figure 3.31 and Table 3.23 – model flanges horizontal displacement of beams with (types 3 and 4) structured sheets have much higher stiffnesses than beams without (types 1 and 2). Also, the character of webs deflection is also differ from each other – by types 1 and 2 it is flattened curve, but for types 3 and 4 curves rise sharply, practically vertical. That happens due to high stiffness of structured plates.

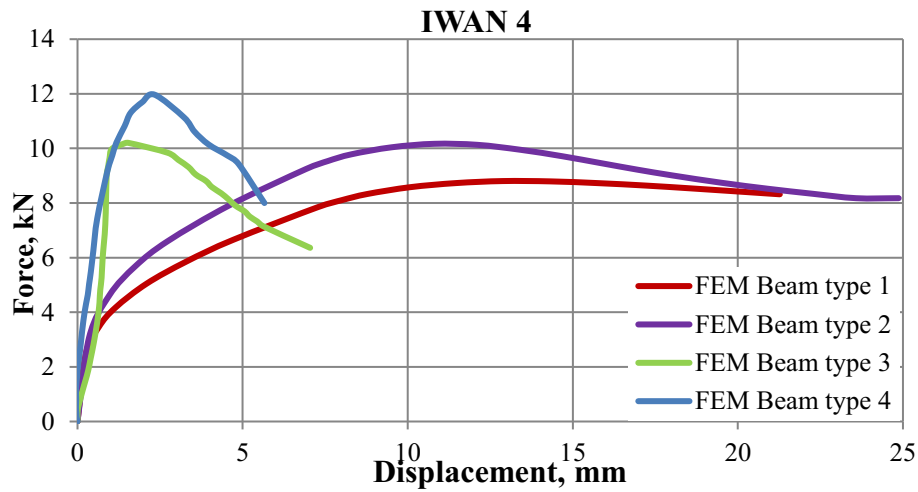


Figure 3.31. Force-displacement (horizontal) curves for web (IWAN 4) of FEM simulation results

According to Table 3.23, displacements correspond to maximal forces of types 1 and 2 are 2-4 times lower than for beam types 3 and 4. At the same time, the maximal reached forces are higher, as a result, stiffnesses are also higher. The fact of higher stiffness of sandwich plates made of structured plates proves calculated stiffnesses in Table 3.23 – it is up to 4.6 times higher than flat beams.

Table 3.23. Simulation results for beam types 1-4, horizontal deformation of web in the center of model

Beam type	$F_{max}$ , kN	IWAN 4	
		Corresponding displacement, mm	Stiffness, kN/mm
1	8.80	12.88	1.41
2	10.17	10.81	2.51
3	10.20	1.54	6.56
4	11.97	2.33	7.59

Figure 3.32 and Figure 3.33 present displacement results of web points located in the 1/3 of the specimen length. The behavior of models in these points is similar to the point in the middle of the web.

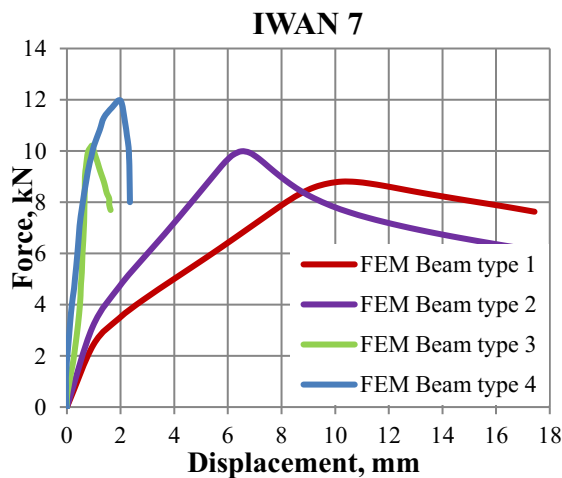


Figure 3.32. Force-displacement (horizontal) curves for web (IWAN 7) of FEM simulation results

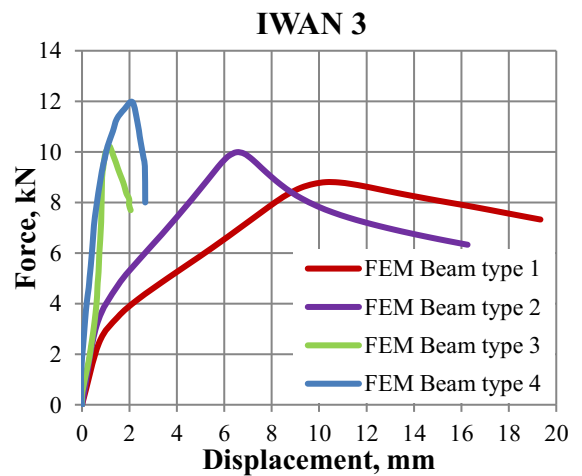


Figure 3.33. Force-displacement (horizontal) curves for web (IWAN 3) of FEM simulation results

## C-sectioned lightweight steel beams

According to the Table 3.24, the displacements for each beam type are close to each other. Moreover, as expected, the vertical deflection of the beam in the center of the beam is bigger, than on the sides – see Table 3.23 and Table 3.24.

Table 3.24. Simulation results for beam types 1-4, horizontal deformation of web on the left (IWAN 7) and right (IWAN 3) sides of model

Beam type	F <sub>max</sub> , kN	Corresponding displacement, mm	
		IWAN 7	IWAN 3
1	8.80	10.25	10.29
2	10.17	6.50	6.52
3	10.20	0.94	1.32
4	11.97	2.00	2.13

The collapsing of construction in simulations and in laboratory experiments happen due to material properties – the plastic failure of the web and upper chord occurs. One of the ways of avoiding that type of failure is to make the whole flat C-profile thicker.

According to the Figure 3.34 , it can be seen, that the collapsing of the beams happens due to the plasticity of the flat sheets material – the stresses under the maximal force is much higher than the 0.2% limit of elasticity.

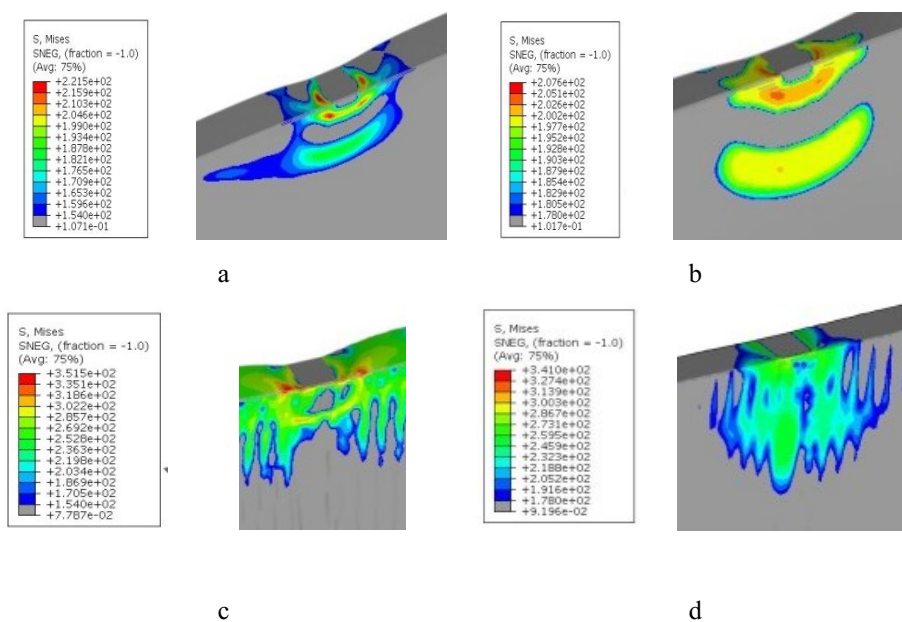


Figure 3.34. Stresses in MPa of C-profiles beam types a - 1, b - 2, c – 3, d – 4 under the maximal loading

In Table 3.25 Stresses of all beam types under the maximal loading are listed.

Table 3.25. Beam types and corresponding stresses under the maximum loading

Beam type	C-plate thickness, mm	Maximal stress, MPa	R <sub>0,2</sub> ,MPa
1	0,75	210	154
2	1,00	200	178
3	0,75	270	154
4	1,00	240	178

## C-sectioned lightweight steel beams

The way to avoid this type of collapsing is to make C-profile thicker, for example, the material properties used for beam type 4 are taken and 2 mm thickness of C-profile is given instead of 1 mm.

There is no plastic collapse occurs when C-flat profile's thickness is 2 mm and thicker. As it is shown in Figure 3.35, when the web and the upper chord of the beam 2 mm thick, the stress of the web is lower or equal to the 0.2% limit of elasticity, so that the C-profile still works in elastic zone under the maximal load.

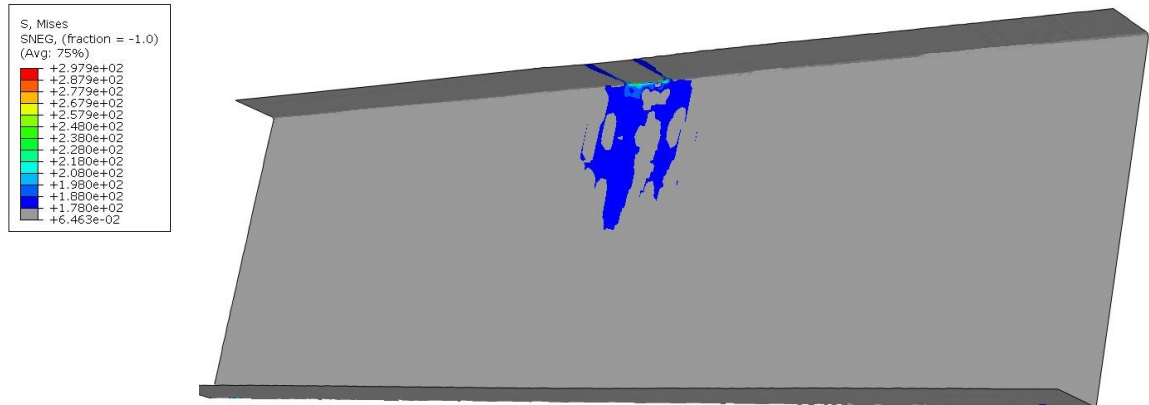


Figure 3.35. Stresses in MPa of C-profile 2 mm thick under the maximal loading

### 3.4.9 Conclusion

In this chapter FEM simulation process in software ABAQUS software is described: geometry of beams, material properties, boundary conditions and loading are simulated based on experiments. In experiments 8 specimens are investigated: there are 4 types of specimens geometry and each of it is made in 2 copies. So, there are 4 types of beams for simulations are created – see Table 3.26.

In order to compare simulations and experimental results, data processed from FEM results correspond to experimental results captured by transducers. In Table 3.26 simulation results for beam types 1-4 are presented.

According to simulations, load bearing capacity of beam types 3 and 4 (models with structured plates) is 16% and 18% higher than beam types 1 and 2 respectively. Also, Table 3.26 shows that if comparing specimens with same total thickness, stiffnesses (of IWAN 2) are also higher by beams with structured sheets: up to 30% and 12% higher by beam type 3 and 4 respectively comparing to types 1 and 2.

In Table 3.26 also stiffness of IWAN 4 is calculated, by beam types 3 and 4 it is higher than by types 1 and 2.

### C-sectioned lightweight steel beams

Table 3.26. Specimens maximal forces, corresponding displacements (from points where transducers are placed in experiments) and stiffnesses, simulation results for C-sectioned beams

Beam type	F <sub>max</sub> , kN	IWAN						
		1	2		4		7	3
		Displ., mm	Displ., mm	Stiffness, kN/mm	Displ., mm	Stiffness, kN/mm	Displ., mm	Displ., mm
1	8.80	0.29	2.47	3.64	12.88	1.41	10.25	10.29
2	10.17	0.19	1.57	4.74	10.81	2.51	6.50	6.52
3	10.20	0.18	2.53	4.74	1.54	6.56	4.18	3.77
4	11.97	0.06	2.85	5.33	2.33	7.59	2.36	2.28

Figure 3.36 and Figure 3.37 describe graphically stiffnesses of beams web: vertical and horizontal respectively.

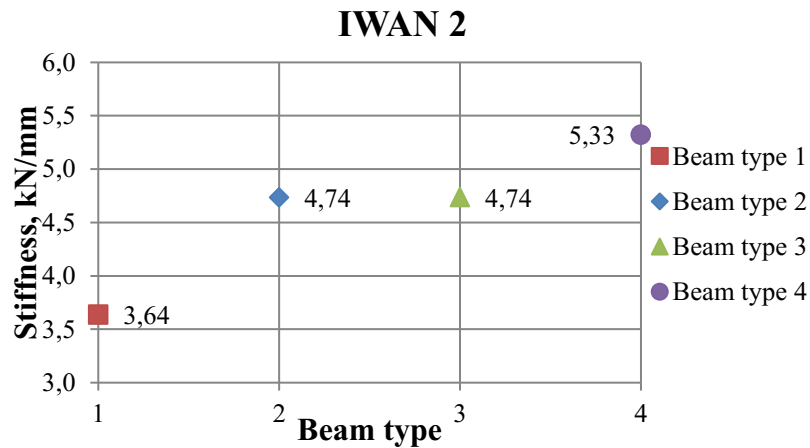


Figure 3.36. Vertical stiffnesses of web beams 1-8, simulation results

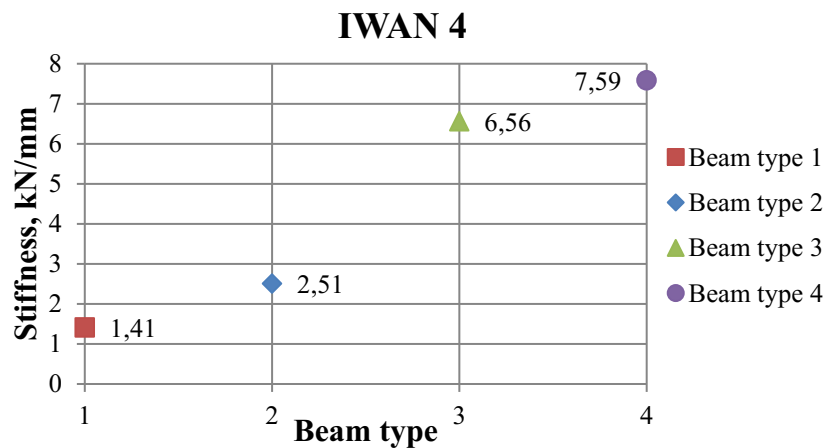


Figure 3.37. Horizontal stiffness of web beam 1-8, simulation results

Simulations provide an important method of analysis which is easily verified, communicated and understood. It provides valuable solutions by giving clear insights into complex systems.

Comparison with experimental results indicates the accuracy of assumptions that are introduced in simulations and gives an opportunity to understand if more fundamental knowledge by conducting experiments is needed. Experiments together with verified simulation results give a strong base for further study and development of many scientific topics.

## 3.5 Evaluation of simulation and experiment results

### 3.5.1 General information

The beam Type 1 with a flat C-profile 0.75 mm thickness and flat plates 0.50 mm thickness is the first model that is created with the software package ABAQUS/CAE, Standard Version 6.14. At the beginning the various parameters are changed so that the results from the experiments and simulation match. Important role for final displacement-load curve play such parameters as: material properties, boundary conditions, connections between elements (constraints), load application, imperfections. Finally, all final found parameters are described above.

### 3.5.2 Beam type 1: flat 0.75 mm + flat 0.75 mm

Beam type 1 consists of flat plates: C-profiled (0.75 mm thickness) and 3 structured plates 0.5 mm thick. To compare FEM and experimental results, in ABAQUS, the points which displacement is shown in the Figure 3.38-Figure 3.42, corresponded to the locations of installed transducers.

Figure 3.38 shows results corresponding to vertical displacement of upper beam flange. As it is seen, in experiments initial deformations take place, but they are absent in FEM results. The reason is that simulation results are always close to ideal type of loading – the moment of unloaded flange and after, the ‘meeting’ of hydraulic jack and upper flange is excluded. As can be seen in Figure 3.38, the curves of the experiment and the FEM analysis converge very well. Anyway, the most important is stiffness which is calculated as the slope of the force-displacement curve – see Table 3.27.

In Figure 3.39, horizontal displacement of web is shown. FEM curve has opposite displacement direction than curves of Beam 1 and 2 in experiment results. That might be caused by initial deformations from manufacturing process or/and by slight displacement of the pressing machine hydraulic jack relative to the beam web axis.

As it can be seen, the behavior of specimens and FEM model looks similarly, also stiffnesses in Table 3.27 have good convergence.

C-sectioned lightweight steel beams

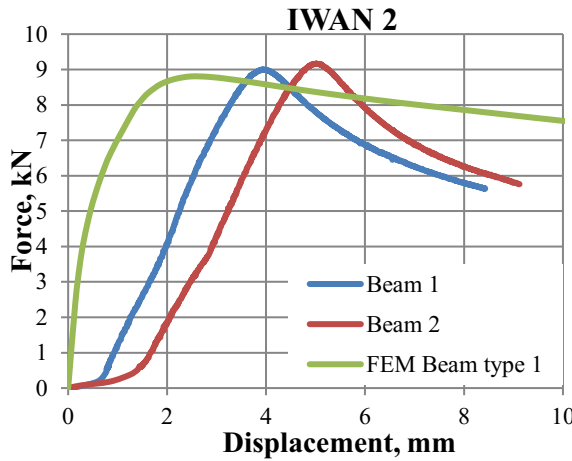


Figure 3.38. Force-displacement (vertical) curves for upper flange (IWAN 2): experimental results for Beam 1 and 2 and FEM results of Beam type 1

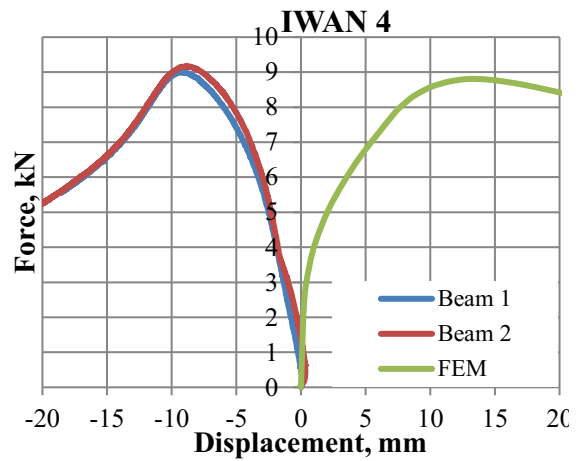


Figure 3.39. Force-displacement (horizontal) curves for web (IWAN 4): experimental results for Beam 1 and 2 and FEM results of Beam type 1

As it is seen from Table 3.27, the stiffness of simulated model for upper flange vertical displacement is 10-15 % higher than the stiffness of experimental beams (IWAN 2 column). In case of horizontal web behavior, stiffnesses are very close to each other (IWAN 4 column).

Table 3.27. Comparison of experimental and simulation results (IWAN 2 and IWAN 4), Beam type 1

	$F_{max}$ , kN	IWAN 2		IWAN 4	
		Corresponding displacement, mm	Stiffness, kN/mm	Corresponding displacement, mm	Stiffness, kN/mm
Beam 1	9.01	3.94	3.34	-9.15	1.42
Beam 2	9.17	5.01	3.16	-8.84	1.53
FEM	8.80	2.47	3.64	-12.88	1.41

Figure 3.40 illustrates the vertical behavior of lower beams flange. Simulation and experimental results differ from each other: FEM model have much smaller vertical displacement, than it is in experiments. Anyway, in general, both deflections, compare to other parts where displacements are captured, are rather small.

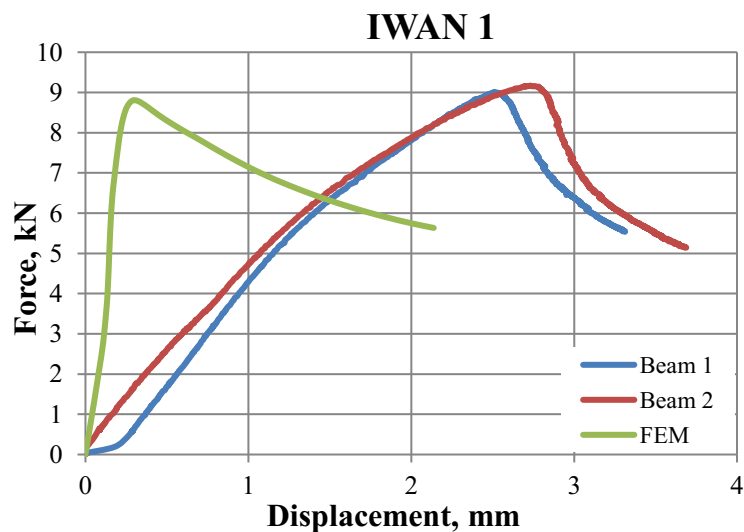


Figure 3.40. Force-displacement (vertical) curves for lower flange (IWAN 1): experimental results for Beam 1 and Beam 2 and FEM results of Beam type 1



### C-sectioned lightweight steel beams

In Table 3.28 vertical displacements of lower specimens flange at maximal force are collected. FEM beam is much stiffer in present case, than experimental.

Table 3.28. Comparison of experimental and simulation results (IWAN 1), Beam type 1

	$F_{max}$ , kN	IWAN 1
		Corresponding displacement, mm
Beam 1	9.01	2.51
Beam 2	9.17	2.73
FEM	8.80	0.29

Symmetrical located on the vertical weld line of structured plates transducers IWAN 7 and 3 capture horizontal displacement of the specimen web. According to Figure 3.41, Figure 3.42 and Table 3.29 both simulations and experimental results show the same symmetrical webs displacement of the model and beams.

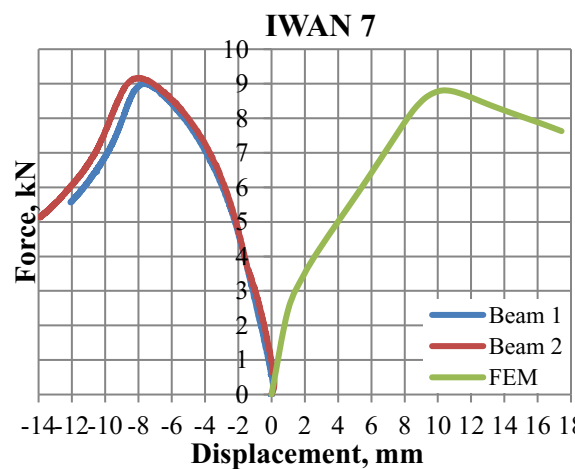


Figure 3.41. Force-displacement (horizontal) curves for web (IWAN 7): experimental results for Beam 1 and Beam 2 and FEM results of Beam type 1

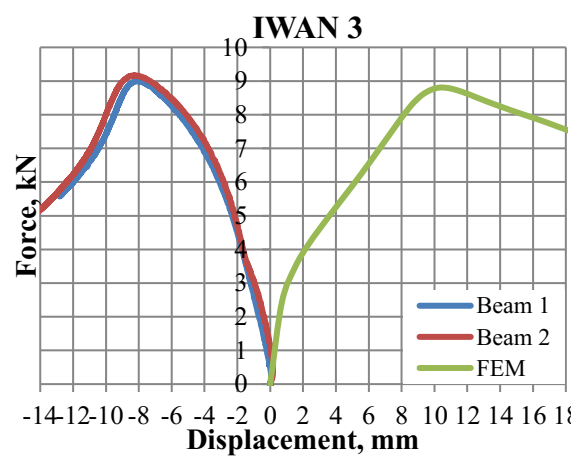


Figure 3.42. Force-displacement (horizontal) curves for web (IWAN 3): experimental results for Beam 1 and Beam 2 and FEM results of Beam type 1

Table 3.29. Comparison of experimental and simulation results (IWAN 7 and IWAN 3), Beam type 1

	$F_{max}$ , kN	IWAN 7	IWAN 3
		Corresponding displacement, mm	
Beam 1	9.01	-7.61	-8.07
Beam 2	9.17	-7.98	-8.27
FEM	8.80	-10.25	-10.29

Displacements that are captured by IWAN 5 and IWAN 6 in laboratory experiments in simulations equal to 0. That means upper and lower beam flanges have no horizontal movement, but only vertical.

### 3.5.3 Beam type 2: flat 1.00 mm + flat 0.50 mm

Beam type 2 is specimens made of flat plates: C-profiled 1 mm thick and 3 structured plates 0.5 mm thick. Figure 3.43 shows experimental and FEM displacement-force curves for upper flange of specimen (transducer IWAN 2). As in case of beam type 1, initial deformations (curves jumpings till approximately 2 mm) also take place in experiments. Like in case of beam

type 1, stiffness for each of the curves is calculated. According to Table 3.31, stiffnesses of experimental and FEM results have excellent agreement.

In Figure 3.44 curves correspond to horizontal displacement of web are presented. As it can be seen, curve of Beam 3 has opposite displacement direction than curves of Beam 4 and simulation results. That might be caused by initial deformations from manufacturing process or/and by slight displacement of the pressing machine hydraulic jack relative to the beam web axis.

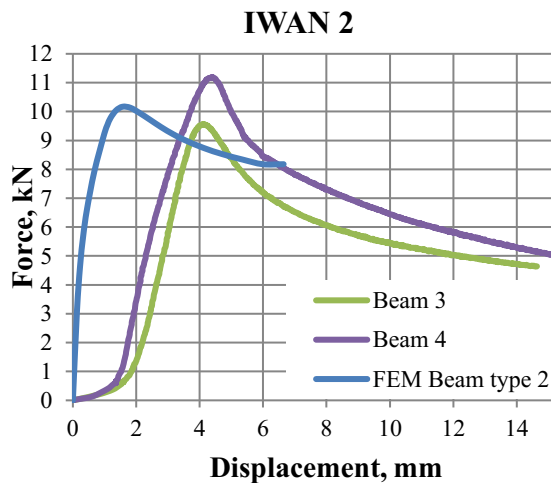


Figure 3.43 Force-displacement (vertical) curves for upper flange (IWAN 2): experimental results for Beam 3 and Beam 4 and FEM results of Beam type 2

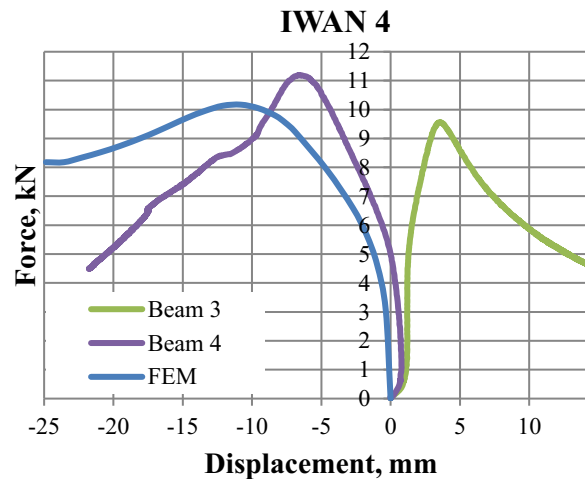


Figure 3.44. Force-displacement (horizontal) curves for web (IWAN 4): experimental results for Beam 3 and Beam 4 and FEM results of Beam type 2

In Table 3.30 it is seen that stiffnesses for specimens web of computer model and experimental ones have good agreement – FEM stiffness is only 11% higher.

Table 3.30. Comparison of experimental and simulation results (IWAN 2 and IWAN 4) for Beam type 2

	F <sub>max</sub> , kN	IWAN 2		IWAN 4	
		Corresponding displacement, mm	Stiffness, kN/mm	Corresponding displacement, mm	Stiffness, kN/mm
Beam 3	9.56	4.15	4.74	3.63	2.17
Beam 4	11.20	4.40	4.78	-6.61	2.18
FEM	10.17	1.57	4.74	-10.81	2.42

Figure 3.45 the vertical behavior of lower beams flange is presented. In case of beam type 2 simulations and Beam 4 curve have big difference in behavior. Transducer IWAN 1 of specimens captures vertical movement of beams web, is fixed on the lower part of beams web. As beams web deforms in and out of plane, transducer repeats webs movement – it captures displacement in plane (vertical), but not the horizontal one. So that, the web, while deforming drags it along, causing corrupted displacement results captured by transducer.

C-sectioned lightweight steel beams

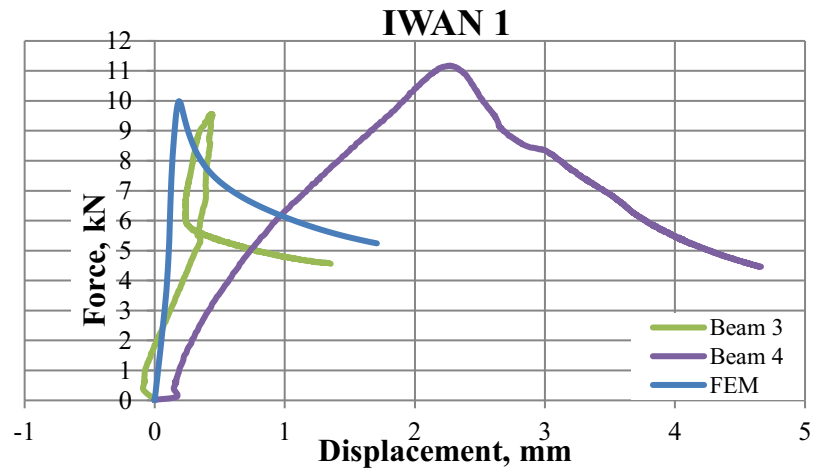


Figure 3.45. Force-displacement (vertical) curves for lower flange (IWAN 1): experimental results for Beam 3 and Beam 4 and FEM results of Beam type 2

Anyway, the displacements captured by IWAN 1 are relatively small in relation to other displacements captured by transducers. In Table 3.31 displacements captured by transducer IWAN 1 are summarized.

Table 3.31. Comparison of experimental and simulation results (IWAN 1), Beam type 2

	F <sub>max</sub> , kN	IWAN 1
		Corresponding displacement, mm
Beam 3	9.56	0.44
Beam 4	11.20	2.27
FEM	10.17	0.19

Figure 3.46 and Figure 3.47 illustrate curves correspond to horizontal displacements of specimen webs, captured by transducers IWAN 7 and 3. In present case displacements in experimental results are pretty symmetrical – see

Table 3.32. Beam 4 has a little bigger displacement of the left side, than the right one. It could be caused, for example, by a slight offset from the middle on the right side of hydraulic jack.

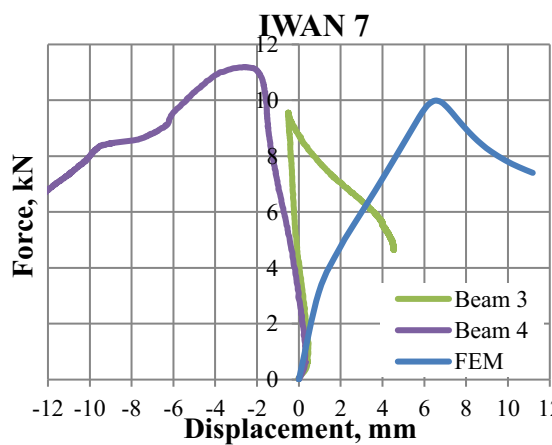


Figure 3.46. Force-displacement (horizontal) curves for web (IWAN 7): experimental results for Beam 3 and Beam 4 and FEM results of Beam type 2

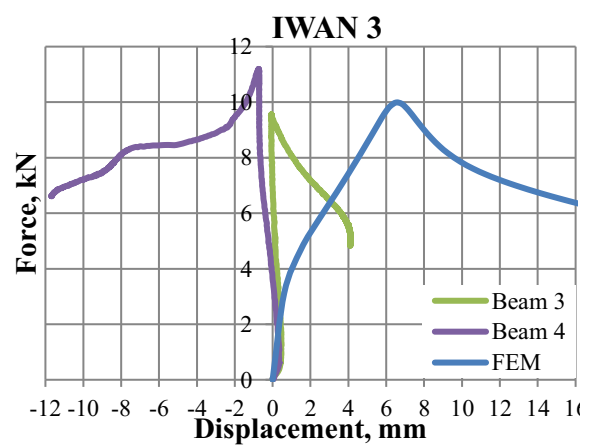


Figure 3.47. Force-displacement (horizontal) curves for web (IWAN 3): experimental results for Beam 3 and Beam 4 and FEM results of Beam type 2

## C-sectioned lightweight steel beams

Table 3.32. Comparison of experimental and simulation results (IWAN 7 and IWAN 3), Beam type 2

	$F_{max}$ , kN	IWAN 7	IWAN 3
		Corresponding displacement, mm	
Beam 3	9.56	-0.52	-0.07
Beam 4	11.20	-2.63	-0.74
FEM	10.17	-6.50	-6.52

Displacements that are captured by IWAN 5 and IWAN 6 in laboratory experiments in simulations equal to 0. That means upper and lower beam flanges have no horizontal movement, but only vertical.

### 3.5.4 Beam type 3: flat 0.75 mm + structured 0.50 mm

Beam type 3 specimens consist of flat C-profiled flat plate with 0.75 mm thickness and 3 structured sheets 0.5 mm thickness. Conducted simulations and experiments have good agreement – see Figure 3.48 and Table 3.33. Beam types 1 and 3 have same total thickness – 1.25 mm, but vertical stiffness of beam type 3 compared to type 1, as it is shown in Table 3.33, is up to 50% higher. Otherwise, beam types 2 and 3 have close vertical stiffnesses, but different total thicknesses – specimens of beam type 2 are 0.25 mm thicker (total thickness is 1.5 mm) than specimens of beam type 3 (1.25 mm total).

In Figure 3.49 curves of horizontal displacement for FEM and experiments are shown. In general behavior is similar: within 2 mm displacement and upon reaching max force, together model and specimens show rather stable web behavior with no sharp jumpings. In spite that, according to Table 3.33, horizontal stiffness of models web is 30% lower, than in experiments.

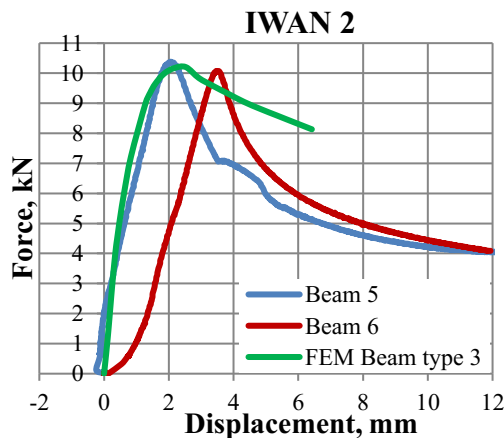


Figure 3.48. Force-displacement (vertical) curves for upper flange (IWAN 2): experimental results for Beam 5 and 6 and FEM results of Beam type 3

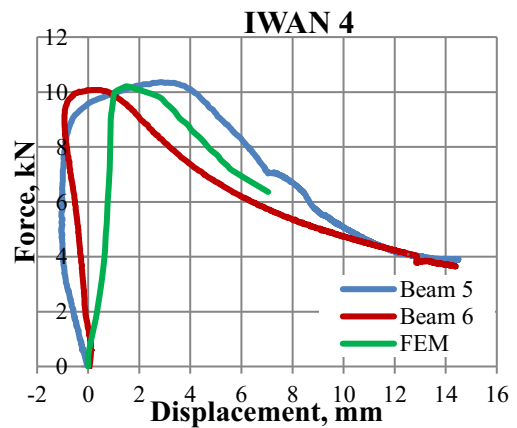


Figure 3.49. Force-displacement (horizontal) curves for web (IWAN 4): experimental results for Beam 5 and 6 and FEM results of Beam type 3

Table 3.33. Comparison of experimental and simulation results (IWANs 2 and 4) for Beam type 3

	$F_{max}$ , kN	IWAN 2		IWAN 4	
		Corresponding displacement, mm	Stiffness, kN/mm	Corresponding displacement, mm	Stiffness, kN/mm
Beam 5	10.36	2.06	4.64	2.87	9.13
Beam 6	10.12	3.46	4.46	-0.03	9.72
FEM	10.20	2.53	4.74	1.54	6.56

### C-sectioned lightweight steel beams

Force-displacement (vertical) results captured by transducer IWAN 1 are shown in Figure 3.50. Vertical displacement of lower flange is close to zero that means deformations extinguished by the web of the beam and has more local, rather global character.

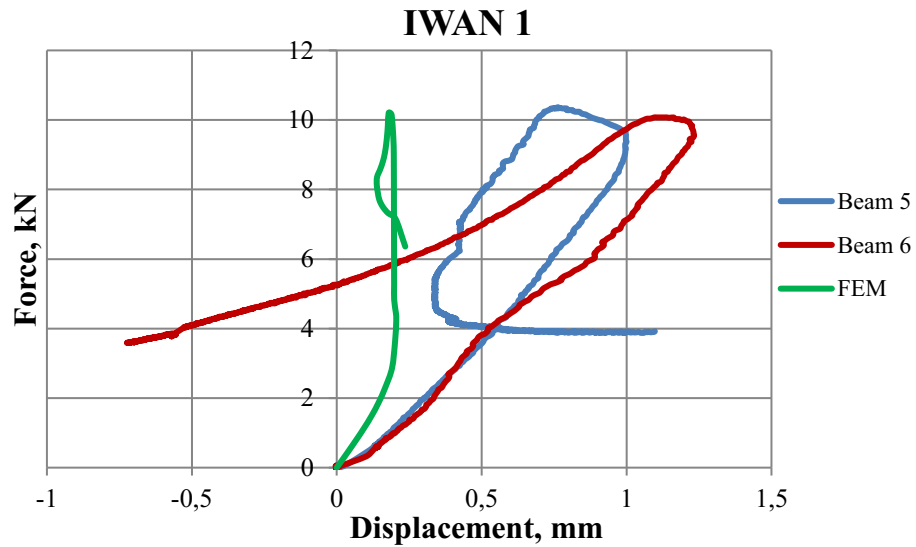


Figure 3.50 Force-displacement (vertical) curves for lower flange (IWAN 1): experimental results for Beam 5 and Beam 6 and FEM results of Beam type 3

According to Table 3.34, maximum displacement is 1.16 mm of Beam 6. In general, these vertical displacements of lower flange are the smallest ones of all beams.

Table 3.34. Comparison of experimental and simulation results (IWAN 1), Beam type 3

	$F_{\max}$ , kN	IWAN 1
		Corresponding displacement, mm
Beam 5	10.36	0.76
Beam 6	10.12	1.16
FEM	10.20	0.18

In Figure 3.51 and Figure 3.52 are force-displacement results of symmetrical located points on the beams webs. According to figures, behavior of beams and model webs differ. Deformation distributes evenly in experimental results. In FEM the web behavior distributes by jumpings – at first, it grows and then practically no displacement takes place until reach the maximum force. But, according to FEM, web behavior on the left and right sides from the center logically repeats the webs behavior in the center of the beam – see Figure 3.51 and Figure 3.52 and Table 3.35.

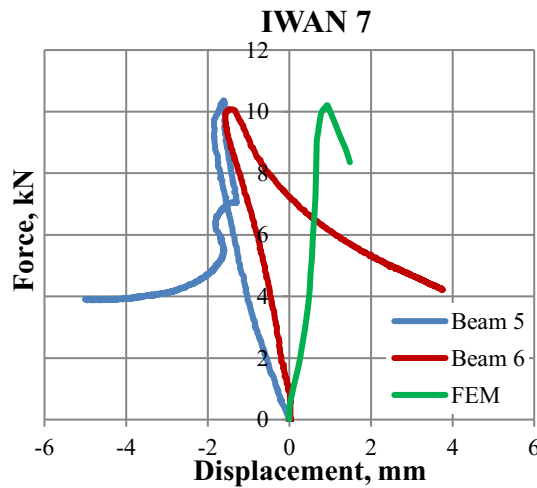


Figure 3.51. Force-displacement (horizontal) curves for web (IWAN 7): experimental results for Beam 5 and Beam 6 and FEM results of Beam type 3

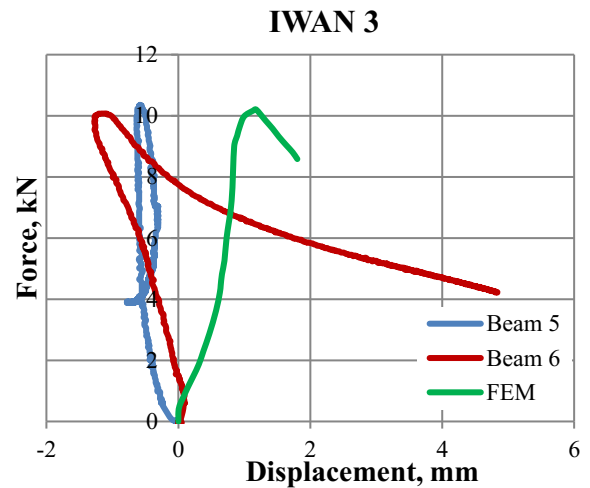


Figure 3.52. Force-displacement (horizontal) curves for web (IWAN 3): experimental results for Beam 5 and Beam 6 and FEM results of Beam type 3

Table 3.35 summarizes displacements captured by transducers IWAN 7 and IWAN 3.

Table 3.35. Comparison of experimental and simulation results (IWAN 7 and IWAN 3), Beam type 3

	$F_{max}$ , kN	IWAN 7	IWAN 3
		Corresponding displacement, mm	Corresponding displacement, mm
Beam 5	10.36	-1.61	-0.58
Beam 6	10.12	-1.49	-1.21
FEM	10.20	0.94	1.32

Displacements that are captured by IWAN 5 and IWAN 6 in laboratory experiments in simulations equal to 0. That means upper and lower beam flanges have no horizontal movement, but only vertical.

### 3.5.5 Beam type 4: flat 1.00 mm + structured 0.50 mm

Beam type 4 specimens consist of flat C-profiled flat plate with 1 mm thickness and 3 structured sheets 0.5 mm thickness. Total thickness of the specimen is 1.5 mm – same as specimens of beam type 2. However, vertical stiffness of beam type 4 specimens is 13% higher, than stiffness of beam type 2 – see Figure 3.53 and Table 3.36. FEM and experimental results have an excellent agreement – see Figure 3.53 and Table 3.36.

Otherwise, the horizontal behavior of beams web of FEM differs from experimental ones. In experiments horizontal deformation of the web occurs smoothly – see Figure 3.54. By FEM simulations web buckles approximately 2 times faster, than in experiments till 3 mm and after stays constantly rigid till reaching maximal force. Another outstanding difference is between simulations and experiments – the direction of webs buckling. The reasons could be similar to what is described for beam type 2: initial deformations from manufacturing process or/and slight displacement of the pressing machine hydraulic jack relative to the beam web axis.

C-sectioned lightweight steel beams

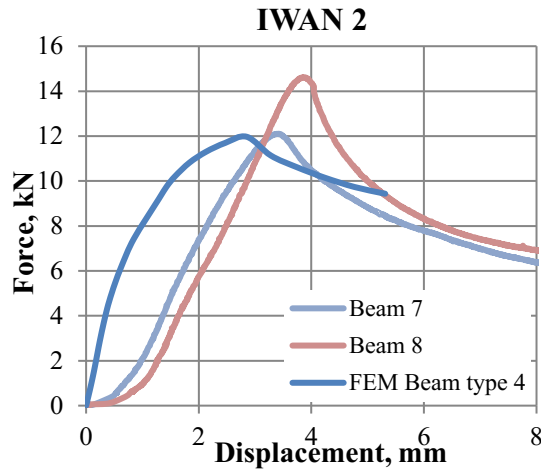


Figure 3.53. Force-displacement (vertical) curves for upper flange (IWAN 2): experimental results for Beam 7 and Beam 8 and FEM results of Beam type 4

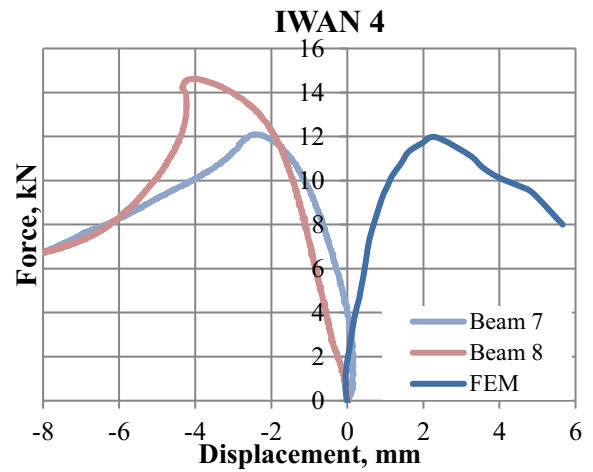


Figure 3.54. Force-displacement (horizontal) curves for web (IWAN 4): experimental results for Beam 7 and Beam 8 and FEM results of Beam type 4

Table 3.36. Comparison of experimental and simulation results (IWAN 2 and IWAN 4) for Beam type 4

	$F_{max}$ , kN	IWAN 2		IWAN 4	
		Corresponding displacement, mm	Stiffness, kN/mm	Corresponding displacement, mm	Stiffness, kN/mm
Beam 7	12.10	3.42	5.29	-2.44	9.41
Beam 8	14.62	3.84	5.25	-3.94	10.04
FEM	11.97	2.85	5.33	2.33	7.59

In Figure 3.55 are shown FEM and experimental specimens curves of force-displacement (vertical) results captured by transducer IWAN 1. Vertical displacement of lower flange is close to zero that means deformations extinguished by the web of the beam and has more local, rather global character.

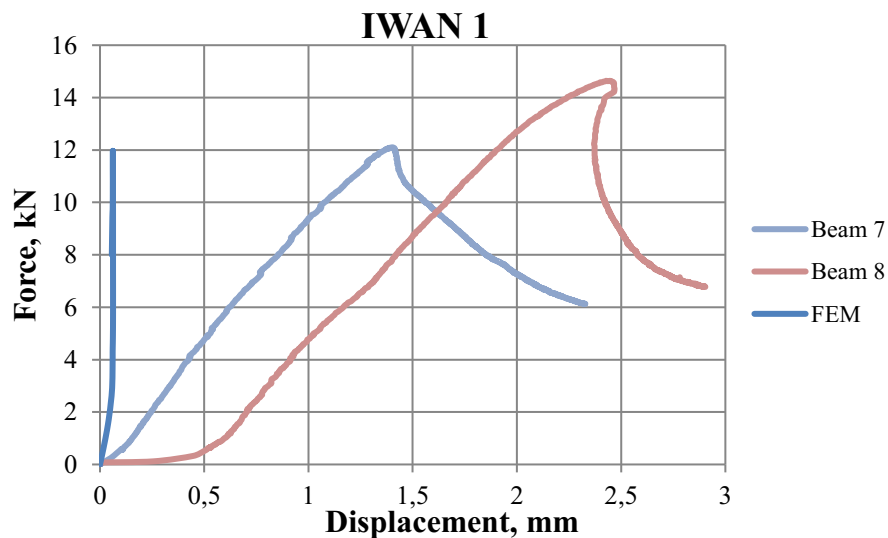


Figure 3.55. Force-displacement (vertical) curves for lower flange (IWAN 1): experimental results for Beam 7 and Beam 8 and FEM results of Beam type 3

In Table 3.37, FEM displacement is practically zero that confirms the idea, that the vertical deflection of lower flange of beam does not take place. In experiments the maximal deflection is 2.5 mm – could be inaccuracy of measurements.

### C-sectioned lightweight steel beams

Table 3.37. Comparison of experimental and simulation results (IWAN 1), Beam type 4

	$F_{max}$ , kN	IWAN 1
		Corresponding displacement, mm
Beam 7	10.36	1.40
Beam 8	10.12	2.43
FEM	10.20	0.06

In Figure 3.56 and Figure 3.57 are force-displacement results of symmetrical located points on the beams webs – on the left and right side from the center of specimen. According to figures, behavior of beams and model webs is similar to behavior of Beams 5 and 6 and Beam type 3. Deformation distributes evenly in experimental results. In FEM the web behavior on the left and right sides from the center, logically repeats the webs behavior in the center of the beam. Compare the stiffnesses (IWAN 4) from Table 3.36 and Table 3.33, it is seen, that beam type 4 stiffness is higher, than beam type 3. This includes both simulations and experimental results.

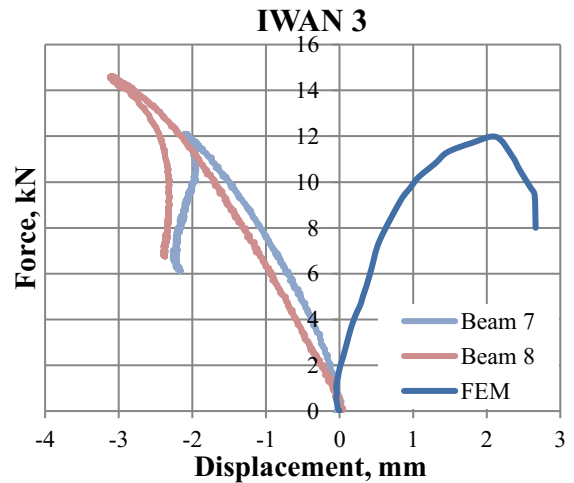
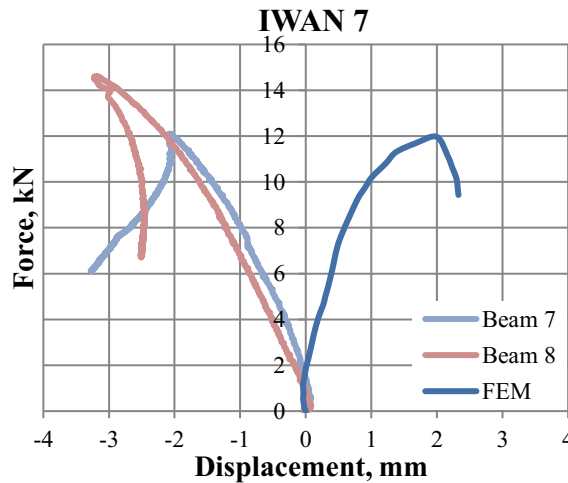


Figure 3.56. Force-displacement (horizontal) curves for web (IWAN 7): experimental results for Beam 7 and Beam 8 and FEM results of Beam type 4

Figure 3.57. Force-displacement (horizontal) curves for web (IWAN 3): experimental results for Beam 7 and Beam 8 and FEM results of Beam type 4

In Table 3.38 results of experiments and FEM simulations are collected.

Table 3.38. Comparison of experimental and simulation results (IWAN 7 and IWAN 3), Beam type 4

	$F_{max}$ , kN	IWAN 7	IWAN 3
		Corresponding displacement, mm	Corresponding displacement, mm
Beam 5	10.36	-2.08	-2.11
Beam 6	10.12	-3.17	-3.10
FEM	10.20	2.00	2.13

Displacements that are captured by IWAN 5 and IWAN 6 in laboratory experiments in simulations equal to 0. That means upper and lower beam flanges have no horizontal movement, but only vertical.



### 3.5.6 Conclusion

In this chapter the comparison between FEM simulations and experiment results is described. For every of the specimens resulting experimental force-displacement curves are compared with simulations. In Table 3.39 resulting data from experimental and simulation results is collected. The deviation of simulation vertical stiffness (see column IWAN 2 in Table 3.39) from experimental is maximal 15% (between stiffnesses of beam 2 and beam type 1). The average deviation is of calculated simulation stiffness from experimental is 5.77%. In Figure 3.58 stiffnesses calculated from simulation and experiment results are illustrated and it is seen, that they have good agreement.

Comparing horizontal stiffnesses is calculated from results captured by IWAN 4, it can be seen, that stiffnesses of simulation and experimental results are really close to each other. For beams made of structured plates stiffness is up to 4 times higher, than for flat beams. That means, beam made of flat and structured plate is much stiffer and more stable under loading, than beam made of 2 flat plates.

Table 3.39. Comparison of experimental and FEM simulations results, C-sectioned beams

Name	$F_{max}$	IWAN										
		1		2		4		7		3	5	6
		Displ., mm	Displ., mm	Stiffness, kN/mm	Displ., mm	Stiffness, kN/mm	Displ., mm					
Beam 1	9.01	2.51	3.94	3.34	-9.15	1.42	-7.61	-8.07	0.34	-2.93		
Beam 2	9.17	2.73	5.01	3.16	-8.84	1.53	-7.98	-8.27	0.52	-3.22		
Beam type 1	8.80	0.29	2.47	3.64	12.88	1.41	10.25	10.29	-	-		
Beam 3	9.56	0.44	4.15	4.74	3.63	2.17	-0.52	-0.07	1.16	-1.55		
Beam 4	11.20	2.27	4.40	4.78	-6.61	2.18	-2.63	-0.74	0.58	-2.35		
Beam type 2	10.17	0.19	1.57	4.74	10.81	2.51	6.50	6.52	-	-		
Beam 5	10.36	0.76	2.06	4.64	2.87	6.27	-1.61	-0.58	-0.58	-2.04		
Beam 6	10.07	1.16	3.46	4.46	-0.03	6.28	-1.49	-1.21	0.52	-2.46		
Beam type 3	10.20	0.18	2.53	4.74	1.54	6.56	0.94	1.32	-	-		
Beam 7	12.10	1.40	3.42	5.29	-2.44	7.01	-2.08	-2.11	0.28	-2.45		
Beam 8	14.62	2.43	3.84	5.25	-3.94	7.06	-3.17	-3.10	-0.05	-3.17		
Beam type 4	11.97	0.06	2.85	5.33	2.33	7.59	2.00	2.13	-	-		

Figure 3.58 and Figure 3.59 illustrate stiffness values from IWAN 2 and IWAN 4 graphically to present more clearly the good agreement between simulations and experiments.

## C-sectioned lightweight steel beams

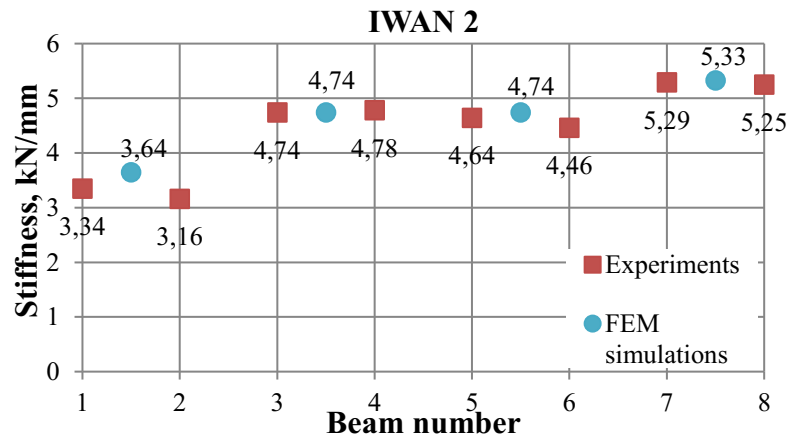


Figure 3.58. Vertical stiffnesses of web experiments and simulation results

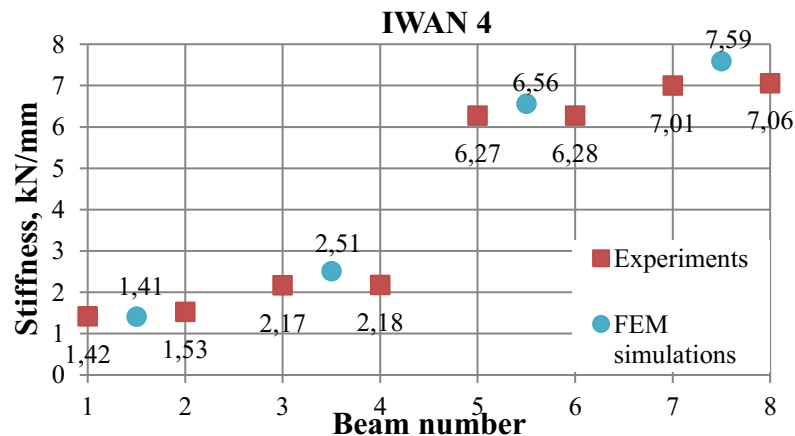


Figure 3.59. Vertical stiffnesses of web experiments and simulation results

From all described above, it can be concluded that simulations and experiments have good agreement. That fact gives the base for future researchers and investigations to develop present topic based on simple FEM simulations avoiding complicated manufacturing process and laboratory investigations.

## 3.6 Parametric modelling

### 3.6.1 General information

Parametric modeling is a modeling process with the ability to change the geometry of model as soon as the one or several dimensions are modified. The model is visualized in 3D software to resemble the attributes of the real behavior of the original project. [104] In present research it is implemented through the software package ABAQUS for faster changing the dimensions of the models.

Based on experiments and validated FEM models, parametric modelling is one of the fastest ways to get a model performance prediction by changing several model parameters. Indeed, parametric modeling has advantages over tests in situ, such as more accurate parameters change and control, more precise results for all design parameters and of course, lowers costs, less material waste, less transportation of unnecessary products and saving time.

### 3.6.2 Parametric research and results

In FEM simulations there are 4 beam types are created and validated. Choosing the geometry of parametric models is based on the manufactured specimens. Each beam type is a base for 4 similar models. Parametric models differ from each other in total plates thicknesses, which are taken with the step 0.5 mm.

In general, all models are divided in 4 groups: made of flat plates (beam types 1 and 2) and with structured members (beam types 3 and 4) and each of them is also divided in 2 groups – with thickness difference (0.25 and 0.5 mm) between C-profiled member and 3 web plates.

Full beam numbers of parametric models consist of two numbers: first one shows the beam type (made flat or structured members) and sequential number, which goes in ascending order of plates thickness. All data is collected in Table 3.40.

According to Table 3.40, simulations are conducted and vertical stiffness of all models is calculated and collected in Table 3.41. The stiffness of the beam type 1 with total thickness 1.25 mm (C-profile 0.75 mm and 3 squared plates – 0.5 mm each –see Table 3.41) is taken as 1. According to this, stiffness increase factors are calculated for other beams.

Table 3.40. Data for parametric research

Beam types (A)	Number (B)	Beam full number (A.B)	Thickness, mm			
			C profile flat, $t_{C-p}$	3 flat plates, $t_{3p}$	Total	Difference, $t_{C-p}-t_{3p}$
1			0.75	0.5	1.25	0.25
	1	1.1	1	0.75	1.75	
	2	1.2	1.25	1	2.25	
	3	1.3	1.5	1.25	2.75	
	4	1.4	1.75	1.5	3.25	
2			1	0.5	1.5	0.5
	1	2.1	1.25	0.75	2	
	2	2.2	1.5	1	2.5	
	3	2.3	1.75	1.25	3	
	4	2.4	2	1.5	3.5	
3			0.75	0.5	1.25	0.25
	1	3.1	1	0.75	1.75	
	2	3.2	1.25	1	2.25	
	3	3.3	1.5	1.25	2.75	
	4	3.4	1.75	1.5	3.25	
4			1	0.5	1.5	0.5
	1	4.1	1.25	0.75	2	
	2	4.2	1.5	1	2.5	
	3	4.3	1.75	1.25	3	
	4	4.4	2	1.5	3.5	

So that, for beam type 2 stiffness increase factor ( $k_{BT2}$ ) is the ratio of two stiffnesses - beam type 1 ( $S_{BT1}$ ) and 2 ( $S_{BT2}$ ) – Eq. (3.7):

C-sectioned lightweight steel beams

$$k_{BT2} = \frac{S_{BT1}}{S_{BT2}} \quad 3.7$$

Correspondingly, for beam number 1.1 – Eq. (3.8):

$$k_{BT2} = \frac{S_{BT1}}{S_{1.1}} \quad 3.8$$

And similarly for all other beams.

Results from Table 3.41 are illustrated in Figure 3.60 as stiffness increase factor - total specimen thickness dependence for flat specimens and structured.

To create formulas, which includes all calculated factors from Table 3.41, linear trend line is used. Obviously, there are 2 dependencies are created: for specimens consist only of flat plates and for specimens consist of flat and structured plates.

Table 3.41. Results of parametric modelling

total	Thickness, mm		Beam type/ Full number	$k = S_{BT1}/S_{A.B}$	Beam/ Full number	$k = S_{BT1}/S_{A.B}$
	C-profile, flat	3 square plates				
1.25	0.75	0.50	Beam type 1	1.00	Beam type 3	1.35
1.50	1.00	0.50	Beam type 2	1.27	Beam type 4	1.49
1.75	1.00	0.75	1.1	1.63	3.1	1.91
2.00	1.25	0.75	2.1	1.88	4.1	2.28
2.25	1.25	1.00	1.2	2.21	3.2	2.46
2.50	1.50	1.00	2.2	2.54	4.2	2.97
2.75	1.50	1.25	1.3	2.86	3.3	3.12
3.00	1.75	1.25	2.3	3.24	4.3	3.52
3.25	1.75	1.50	1.4	3.40	3.4	3.82
3.50	2.00	1.50	2.4	3.72	4.4	4.05

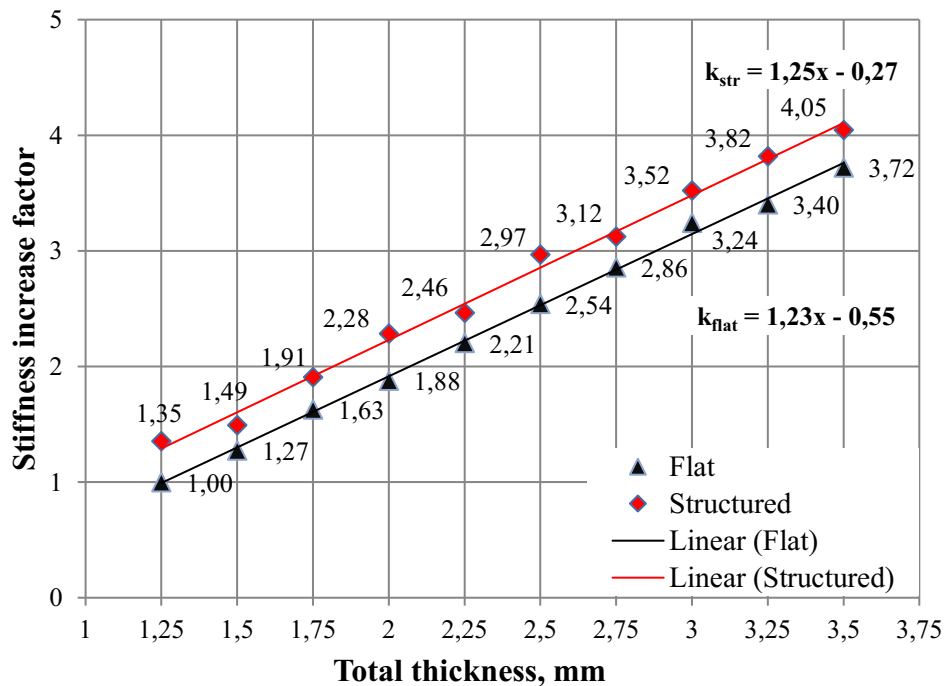


Figure 3.60. Stiffness increase factor – total specimen thickness dependence

## C-sectioned lightweight steel beams

As it is seen from Figure 3.60, the stiffness of specimens depends linear from thickness of plates. Since the lines of distribution of stiffness are parallel, that stiffnesses of specimens consist of structured plates are in average 32% higher than stiffnesses of plates made only of flat plates. It can be predicted that such a dependence will persist for stiffnesses of such beams with higher panel thicknesses (assumed that the thickness difference of C-profile and 3 plates is 0.25 and 0.5 mm). But anyway, to prove this idea further research is needed.

For specimens manufactured from only flat plates, formula for stiffness increase factor ( $k_{flat}$ ) is the following - Eq. (3.9):

$$k_{flat} = (1.23 \cdot x - 0,55) \quad 3.9$$

For specimens manufactured from flat and structured plates, formula for stiffness increase factor ( $k_{str}$ ) is the following - Eq. (3.10):

$$k_{str} = (1.25 \cdot x - 0,27) \quad 3.10$$

Where x-is the total panel thickness, in interval - Eq. (3.11):

$$1.25mm \leq x \leq 3.5mm \quad 3.11$$

And also x depends on 3 plates thickness - Eq. (3.12):

$$x = t_{c-p} + t_{3p} \quad 3.12$$

After addition of similar terms - Eq. (3.13):

$$x = 3 \cdot t_{3p} + 0.25mm \text{ or } x = 3 \cdot t_{3p} + 0.5mm, \quad 3.13$$

Where 0.25 mm and 0.5 mm are thickness difference between C-profile and 3 plates.

### 3.6.3 Conclusion

This chapter contains information about parametric modelling based on both conducted experimental and laboratory experiments.

A parametric model is a computer representation of a design made with geometric shapes with constant and variable properties. In present work, constant properties are shapes of models, material properties and boundary conditions, variable are thicknesses of panels. Variable attributes are called parameters. It is changed in the parametric model to search for the thickness-stiffness relationship to predict the performance of similar models.

The parametric model is obtained automatically by changing the only thicknesses without needing to change the whole model geometry or redrawing it. [105]

Based on parametric modelling results, 2 formulas of stiffness increase factors for C-profiled beams welded together with squared plates are presented. One formula is applicable for specimens consist only of flat plates, the other one should be used for specimens made of flat and structured plates. Also, the range of stiffness increase factor is defined.

## 3.7 Conclusions to chapter 3

This chapter describes the investigations of C-sectioned structured steel beams properties: load bearing capacity and stiffnesses.

## C-sectioned lightweight steel beams

The first parts of this chapter present research of material properties used sheet metals and laboratory experiments (3-points bending tests) of manufactured specimens. All specimens are manufactured in laboratory of BTU Cottbus. The production of specimens is a time-consuming process for the reasons of multi-steps processing of the original material to the final test piece: cutting, bending, positioning of point-welding machine, manual point-welding itself. To simplify and reduce the manufacturing time, it is necessary to automate the most time-taking processes in particular, machine tool positioning and point-welding. Also, one of the ways to shorten the assembly process is to change the shape of the specimens: instead of C-sectioned beams with additional plates make I-beams. Unfortunately, it was not possible in present work because of the lack of structured sheets.

For laboratory tests 8 specimens are made: 2 specimens for each of the type: type 1 and 2 are 2 welded together flat sandwiches with thicknesses (0.75+0.75) mm and (1.00+0.50) mm correspondingly. Types 3 and 4 are sandwiches made of also C-flat plates and structured ones: (0.75+0.50) mm and (1.00+0.50) mm correspondingly. Despite the fact, that received results within 1 type are close to each other, to have more accurate results, it is necessary to test more than 2 specimens of each type. Again, unfortunately in this work it was not possible by the reason of small number of structured sheet metals.

According to laboratory experiments, load bearing capacity of sandwiches made of structured sheets is up to 50% higher than flat ones. Elastic stiffnesses of sandwiches with structured plates are also higher than sandwiches with flat ones: up to 46% higher for vertical web stiffness and from 4 to 7 times higher for horizontal. That means the rigidity of structured plates is higher than flat ones and that is why sandwich web made of flat and structured plates is stiffer and bears higher force, than web made of 2 flat plates.

The fourth part of this chapter is about FEM modelling of laboratory experiments in software package ABAQUS/CAE, Standard. The fifth part is comparison of laboratory and simulation results. It was found that according to simulation results the deflection shapes and stress distribution are similar to the experimental results. Also, according to simulations, calculated elastic stiffnesses and load bearing capacity of sandwiches with structured sheets are higher, than with flat ones. Simulations results are close to experiments and could be used as a base for future investigations with similar topics.

The last part of this chapter is parametric modelling based on received simulation results. By changing the thicknesses of specimen sheets, the dependence between thickness of sandwich plates and stiffness increase factor is found out. 2 formulas of stiffness increase factor are presented for C-sectioned beams made of only flat plates and for both flat with structured plates. It is found out that stiffness-sandwich thickness relationship is linear, and the stiffness of structured sandwiches is in average 32% higher than stiffnesses of sandwiches made only of flat plates.

## **4 Square-sectioned lightweight steel beams**

### **4.1 Introduction**

For further investigations of structured steel plates behavior, it was decided to conduct more experiments with structured sheets, but as elements of another specimens shapes. So that in this chapter the research of squared beams is described. Similar to previous chapter, the main objective of this one is to find out the load bearing capacity of beams made of sandwich structured plates and flat plates, conduct laboratory experiments, make simulations. Also, compare experimental and simulation results, calculate stiffness of all specimens analytical using results of experiments and simulations.

### **4.2 Materials and methods**

For investigations, the following methods are used: laboratory experiments (testing) – for finding the relationships between load bearing capacity and thicknesses of beams webs. A single variable - the thickness of beam wall is changed while other variables are kept constant. The FEM modelling process is also a method of investigations, which helps clearly understand how specimen under loading behaves, or to show some parameters that are not captured in experiments. For each specimen one model is done.

The models match the produced specimens: material properties, geometrical sizes, boundary conditions, load application. These models give an opportunity to compare results from laboratory and from simulations, and also to make parametric study of other variables, that are not studied during the experiments. Based on results from laboratory and simulations, it is possible to predict the change of variables and in general, to predict the behaviour of whole system, which include them.

The material of structured plates is steel DC04, the flat plates – steel DC01. The material properties tests procedure is described in chapter 3.2 Material properties.

In Figure 4.1 nominal and true stress-strain curves for steel DC04 with thicknesses 0.75, 1.00, 1.25, 1.50 mm are presented.

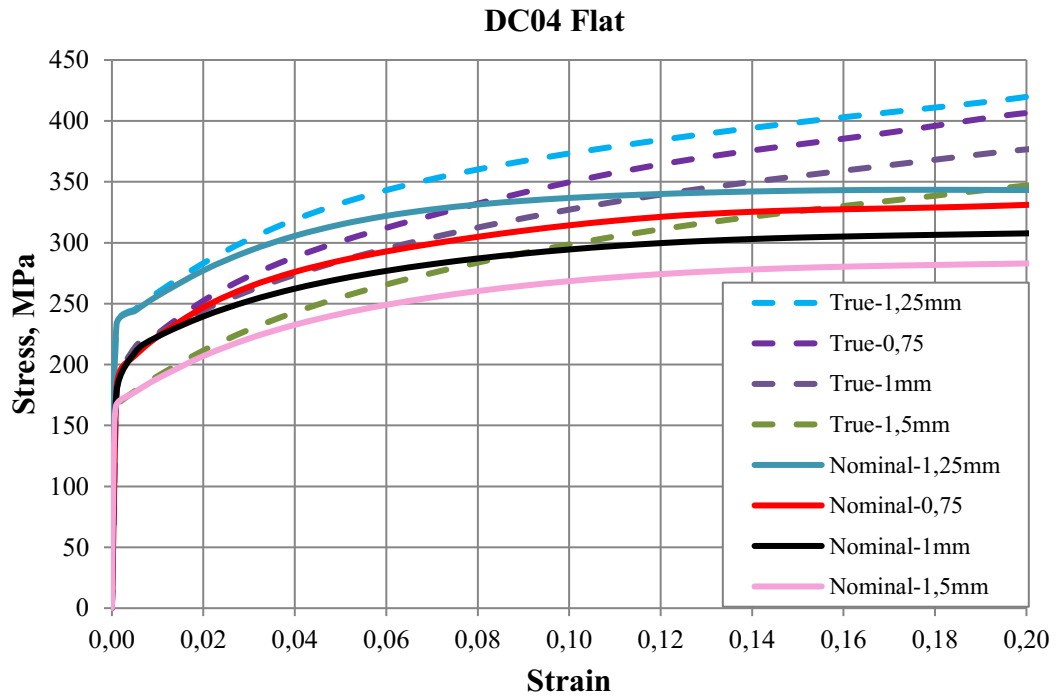


Figure 4.1. Stress-strain curves for steel DC04 with different thicknesses

The main parameters corresponding to curves illustrated in Figure 4.1 are shown in Table 3.2.

Table 4.1. DC04 steel parameters for sheet thicknesses 0.50; 0.75; 1.00 and 1.50 mm

Steel thickness, mm	Parameter, MPa	
0.75	E- Modulus	180419.12
	R <sub>p0.2</sub>	191.75
	R <sub>m</sub>	332.86
1.00	E- Modulus	177210.56
	R <sub>p0.2</sub>	212.87
	R <sub>m</sub>	309.12
1.25	E- Modulus	188497.15
	R <sub>p0.2</sub>	230.56
	R <sub>m</sub>	342.50
1.50	E- Modulus	183320.37
	R <sub>p0.2</sub>	169.75
	R <sub>m</sub>	289.04

The material properties of structured sheet metals are described in chapter 3.2.2 Structured sheet metals.

### 4.3 Laboratory experiments

#### 4.3.1 General information and manufacturing process of specimens

Similar to previous series of experiments described in chapter 3 C-sectioned lightweight steel beams, experiments from this chapter also are carried out at the Brandenburg Technical University Cottbus in FMFA.

For laboratory experiments 8 specimens are created. All specimens are square-sectioned beams. The height is 105.6 mm, the length is 1365 mm. Specimen types and numbers are listed



### Square-sectioned lightweight steel beams

in Table 4.2. Specimens 1-4 are made only of flat plates and specimens 5-8 – of flat and structured plates. The specimens 5-8 consist of structured plates covered with flat ones and not the reverse. This is made by several reasons. The first one is force transfer. By loading flat sheet, the force is transferred uniformly on the surface of the beam. In case of structured plate loading, the surface of specimen will be loaded only in high points where structure plate is curved. The second reason is the difficulties by laser welding of 2 structured plates along the edges. The problem is the following: when 2 structured plates edges are located on one surface it is easier to position them relative to one another. But even in that case the possibility of small ‘holes’ after welding is very high. These ‘holes’ mean that laser did not weld locally edges of plates. The reason is that the edges of the two plates did not fit tightly against each other at the moment of welding. That usually happens while manufacturing process: the combs height from plate to plate varies [83], the displacement of cutting axis 1-2 mm moves etc. When the angle between structured plates is 90° the processes of positioning and welding seems practically impossible.

Table 4.2. List of tested specimens and sheets that are their components

Experiment number	Beam type	Specimen (beam) number	Plate 1			Plate 2		
			type	thickness, mm	steel type	type	thickness, mm	Steel type
1	1	1	flat	1.25	DC01	-		
2		2						
3	2	3						
4		4						
5	3	5		structured		0.50	DC04	
6		6						
7	4	7		1.00				
8		8						

The creation of specimens is quite time-taking process. The structured sheet investigated in this the work has a honeycomb structure made by hydroforming – see 2.4.4.2.2 Hydroforming.

Flat sheets are cut to the required size and form and bent in the middle in order to have L-form. These two workpieces with same geometrical parameters are main parts of future specimen. The flat edges of structured plates are also cut off in order to have size of plates 211.2 x 455 mm. After that they are welded together at the shortest side by laser and also bent in the middle. To connect flat sheets and structured, a console hydraulic spot-welding machine is used. The orientation of honeycombs corresponding to the flat plate is negative and 90°-see Figure 2.24 and Figure 2.22.

For joining 2 L-workpieces together TIG (tungsten inert gas) welding unit is used. Gas tungsten arc welding (GTAW), also known as tungsten inert gas (TIG) welding, is an arc welding process that uses a non-consumable tungsten electrode to produce the weld. It is particularly suitable for alloyed steels or light metals.

### 4.3.2 Experimental setup and boundary conditions

Special setup for laboratory is created. All specimens are simply supported beams - they are supported at both ends with the 50 mm offset from the edges and free to rotate. Vertical webs are fixed lateral in order to prevent the horizontal global displacements. To conduct the experiments 4-point bend method is used. The load is applied in the middle of additional I-beam, which is used for transferring it by means of 2 rollers which are located from 471 mm of the specimen edges – see Figure 4.2 and Figure 4.3.

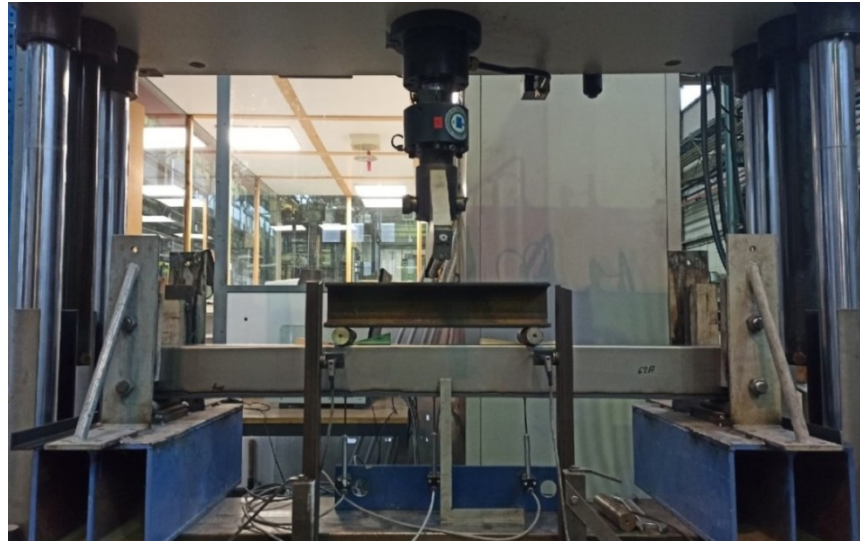


Figure 4.2. Laboratory setup, front view

### 4.3.3 Displacement transducers (IWANs)

To capture beams deflection 5 displacement transducers - IWAN (germ. Induktive Wegaufnehmer) are used. There are 3 transducers to capture vertical global displacements- located in the middle (IWAN M) of the specimens lower chord and 2 symmetrical (IWAN L and IWAN R) are located under the load points. IWAN H1 and IWAN H2 are also placed under the loading lines, and they capture the local buckling of specimens web – see Figure 4.3.

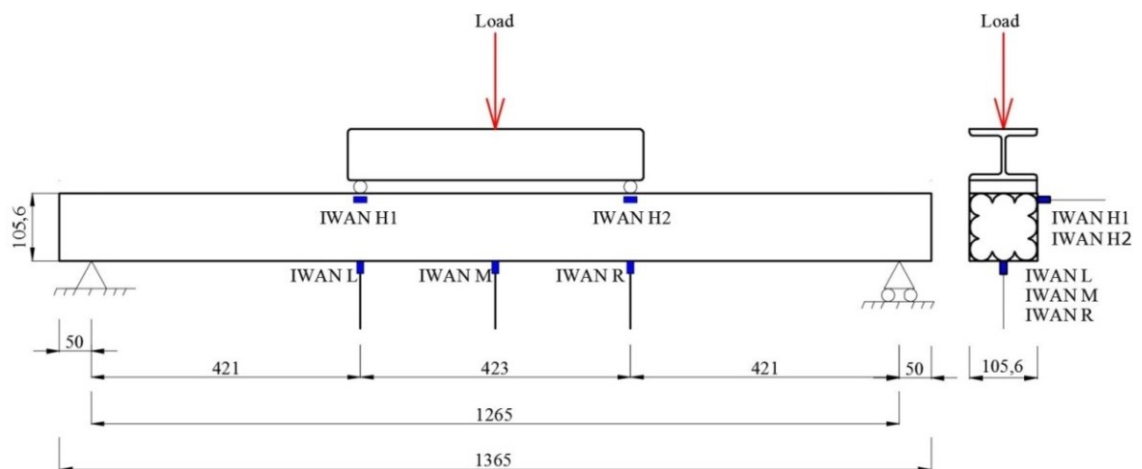


Figure 4.3. Geometrical parameters of specimens and transducers locations

In Table 4.3 all transducers are collected, and the locations are described.

## Square-sectioned lightweight steel beams

Table 4.3. List of displacement transducers

Name of the transducer	Measured displacement	Location on the beam
IWAN M	vertical	Middle of lower flange
IWAN L	vertical	Lower flange, left side
IWAN R	vertical	Lower flange, right side
IWAN H1	horizontal	Web near upper flange under the load, left side
IWAN H2	horizontal	Web near upper flange under the load, right side

### 4.3.4 Loading

For loading 4 points bending test are chosen. In the case of 4-points bending tests, the specimen volume under stress is larger than the one under 3-point bending. The major difference between 4 and 3-points bending tests is that 4 points tests the part of the beam between two loading points is put under maximum stress, as opposed to material which located directly underneath the centre support in the case of a 3-points test. The setup is shown in Figure 4.2.

Thereby the preference is given to 4-points bending tests. The load is applied on the upper chord of the beam with the same offset from the edges – 471 mm. The speed of hydraulic machine jack (loading) is 5 mm/min. For simulations, the same loading speed is used.

### 4.3.5 Results

In this chapter results captured by displacement transducers are described. Force-time diagram in Figure 4.4 shows the general time that is spent for conducting one experiment. The small curve jumping at the beginning also takes place in experiments. The reason is the same as in previous test series - movable part of the machine (hydraulic jack) meets the beam surface. This is called ‘force closure’ and equal to 0.6 kN.

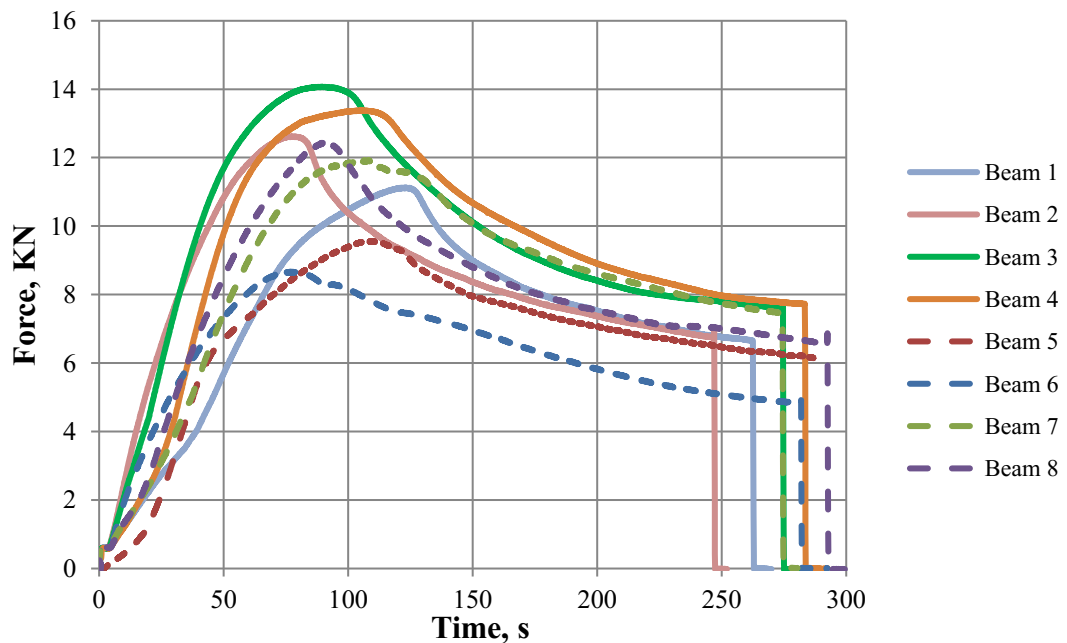


Figure 4.4. Force-time diagram from laboratory experiments, square-sectioned beams

### Square-sectioned lightweight steel beams

In Table 4.4 maximal forces and to it corresponding time are presented. Maximal force in experiments is reached by Beam 3, consisted of flat plates – 14.07 kN. This is correspondingly 20 and 12 % higher than maximal force of beams with same total thickness - Beam 7 and 8.

Table 4.4 Maximal force and corresponding time according to laboratory experiments for square-sectioned beams

Specimen №	Force <sub>max</sub> , kN	Corresponding time, s
Beam 1	11.13	123.2
Beam 2	12.62	77.60
Beam 3	14.07	89.40
Beam 4	13.39	105.00
Beam 5	9.56	109.24
Beam 6	8.67	78.90
Beam 7	11.92	123.20
Beam 8	12.45	90.40

Figure 4.5 and Figure 4.6 illustrate force-(horizontal) displacement dependence for specimens web near upper flange, where force is applied, results captured by transducers IWAN H1 and IWAN H2. As it is seen from Figure 4.5 and Figure 4.6 and also Table 4.5, maximal displacements captured by symmetrical located transducers are more or less same. But the force-displacement curves of the specimens web have different shapes after reaching maximal force. That means web buckling occurs not symmetrical: one side buckling area is more defined than on the other. All photos from laboratory experiments are collected in Appendix C.

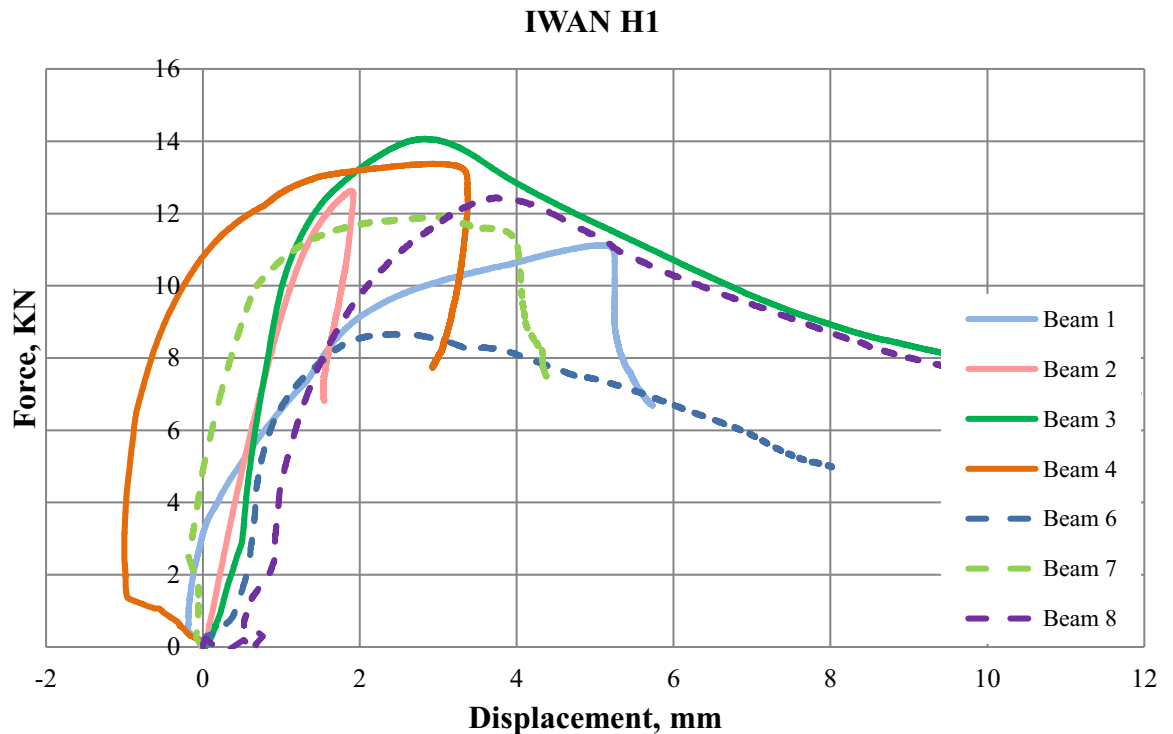


Figure 4.5. Force-displacement diagram from laboratory experiments, horizontal displacement of web (from the left side), transducer IWAN H1

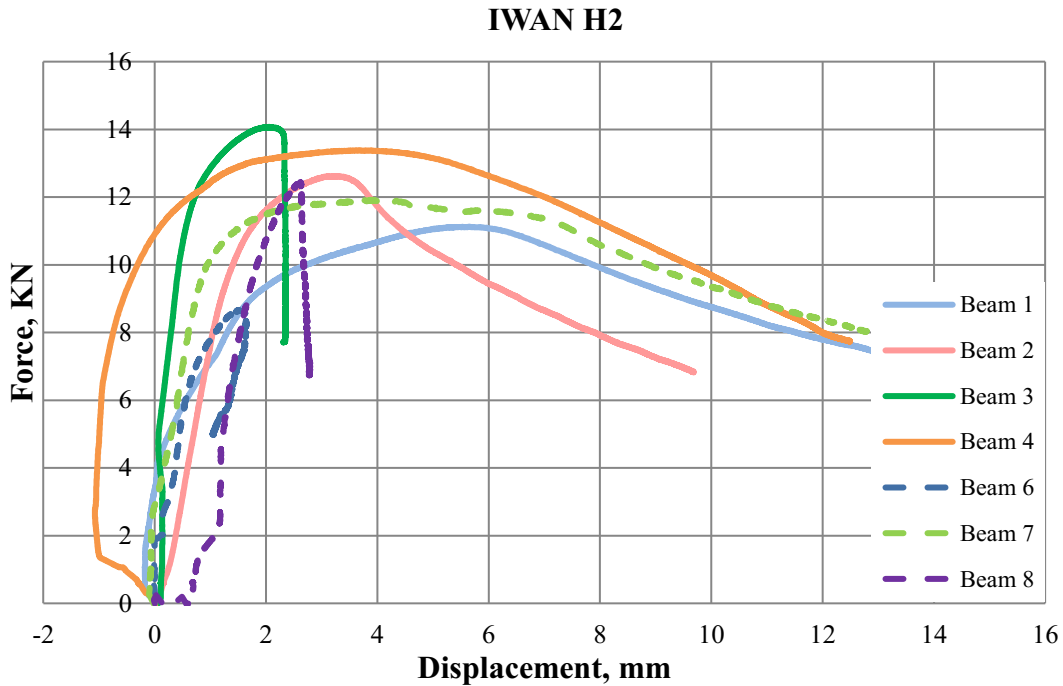


Figure 4.6. Force-displacement diagram from laboratory experiments, horizontal displacement of web (from the right side), transducer IWAN H2

In Table 4.5 maximal forces with corresponding displacements and also horizontal stiffnesses for specimens webs are collected. Stiffnesses are defined according to the same principle as described in chapter 3.3.6 Results for C-sectioned beams: is calculated as an inclination of a straight curve part, which is taken from elastic zone between approximately 2 and 6 kN. As it is seen from the Table 4.5, stiffnesses of the web on left and right sides are practically same (in elastic zone). Average values of specimen stiffnesses show that in general, horizontal stiffness of beams web made of structured plates is higher, than beams made of flat ones. In average, Beam 6 stiffness is 10% higher than Beam 1 and 2, Beams 7 and 8 average stiffness is 6% higher than Beams 3 and 4.

Table 4.5. Maximal force for each specimen, corresponding displacements, stiffnesses, results from IWAN H1 and IWAN H2 transducers

Beam №	Force <sub>max</sub> , kN	Corresponding displacement, mm		Stiffness, kN/mm		
		WA H1	WA H2	WA H1	WA H2	Average
Beam 1	11.13	5.10	5.64	10.46	9.92	10.19
Beam 2	12.62	1.89	3.21	10.17	9.19	9.68
Beam 3	14.07	2.83	2.06	12.86	12.43	12.65
Beam 4	13.39	2.93	3.65	12.52	12.27	12.39
Beam 5	9.56	_*	_*	_*	_*	_*
Beam 6	8.67	2.52	1.56	11.04	11.27	11.16
Beam 7	11.92	3.07	4.05	13.32	12.93	13.12
Beam 8	12.45	3.74	2.60	13.30	13.28	13.29

\* Beam 5 was the first tested beam in this series of experiments. Tests were conducted separately from all the rest experiments as pilot experiments and only 3 displacement transducers were used – IWANs L, M and R.

In Table 4.6 location of web buckling area under load points are presented. Buckling area is located either under the left loading point (see Table 4.6 and Figure 4.7 and Figure 4.8) or under right point (see Appendix C).

## Square-sectioned lightweight steel beams

Table 4.6. Location of visible web buckling area for specimens

Beam №	Side of the beam, area under load points	
	left	right
Beam 1		✓
Beam 2		✓
Beam 3	✓	
Beam 4		✓
Beam 5		✓
Beam 6	✓	
Beam 7		✓
Beam 8	✓	

Figure 4.7 and Figure 4.8 illustrate the size of buckling area, in general by flat plates it is approximately 10 cm in width, but for structured is 7-5 cm. As examples, Beam 2 has 10 cm buckling area width, Beam 5 buckling area is 6 cm width.



Figure 4.7. Beam 2 buckling area, laboratory experiments



Figure 4.8. Beam 5 buckling area, laboratory experiments

The most important results are captured by transducers IWAN M (see Figure 4.9) which captures the deflection of the specimens in the middle of beam span.

## Square-sectioned lightweight steel beams

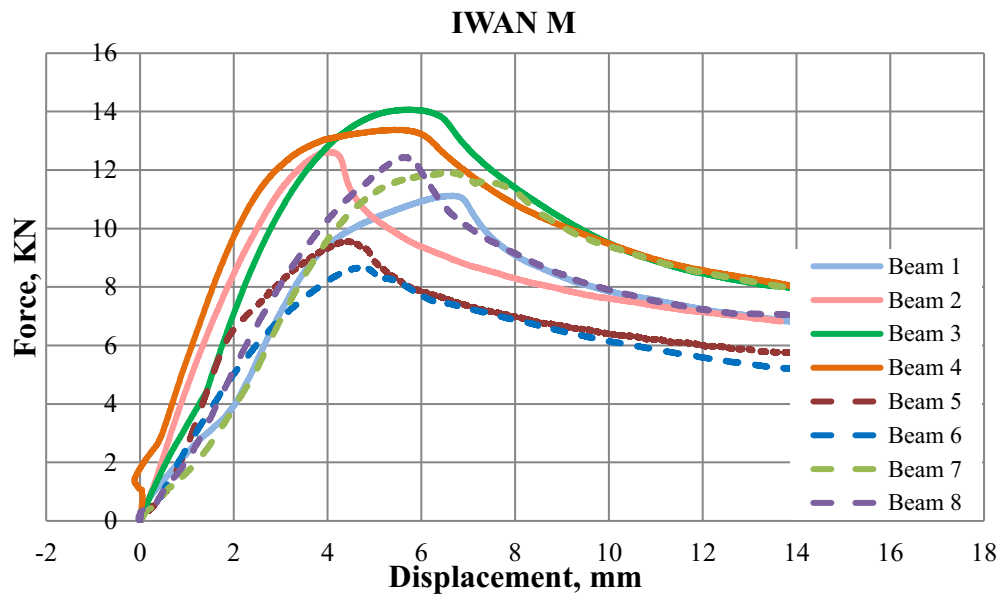


Figure 4.9. Force-displacement diagram from laboratory experiments, vertical displacement of web (in the middle), transducer IWAN M

Resulting curves from IWAN L and IWAN R are presented in Figure 4.10 and Figure 4.11. These curves have near resemblance with results presented in Figure 4.9. This proves that idea of symmetrical deflection of central part of all specimens and the fact that a larger portion of the material is involved in tests is achieved successfully.

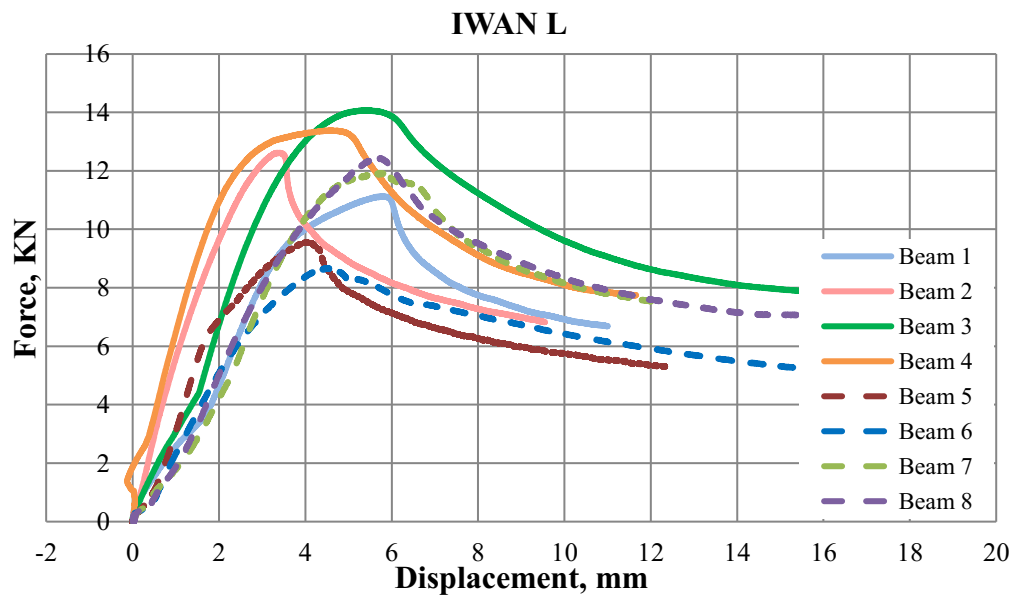


Figure 4.10. Force-displacement diagram from laboratory experiments, vertical displacement of web (from the left side), transducer IWAN L

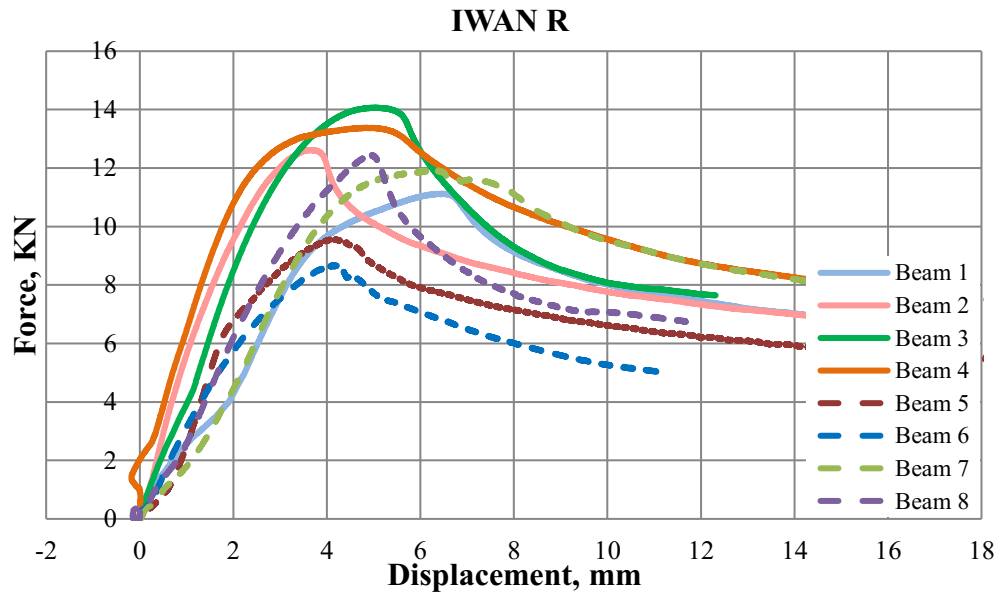


Figure 4.11. Force-displacement diagram from laboratory experiments, vertical displacement of web (from the right side), transducer IWAN R

In Table 4.7 maximal force, corresponding displacements captured by IWAN L, IWAN M and IWAN L transducers and stiffness, calculated from curves illustrated in Figure 4.9 are collected.

Table 4.7. Maximal force for each specimen and corresponding displacements, results of IWAN L, IWAN M and IWAN L transducers

Beam №	Force <sub>max</sub> , kN	Corresponding displacement, mm			Stiffness, kN/mm
		IWAN L	IWAN M	IWAN R	
Beam 1	11.13	5.81	6.67	6.47	3.21
Beam 2	12.62	3.38	4.02	3.65	3.91
Beam 3	14.07	5.42	5.74	5.04	4.53
Beam 4	13.39	4.58	5.43	4.85	4.74
Beam 5	9.56	4.05	4.43	4.15	3.27
Beam 6	8.67	4.57	4.75	4.18	3.07
Beam 7	11.92	5.82	6.64	6.30	3.31
Beam 8	12.45	5.64	5.63	4.92	3.29

#### 4.3.6 Conclusion

This chapter laboratory experiments are described. Specimens are 8 quadrat-sectioned beams with the 1365 mm and height 105.6 mm. For beams testing 4-points method is used: 2 line loads are applied in the 1/3 of beams edges on the upper flange. 4 different types of beams are tested: made of flat plates with thickness 1.25 and 1.50 mm and flat connected with structured with total thickness 1.25 and 1.50 mm (see Table 4.2). To compare the behavior of specimens, the setup for each beam is the same: each of the specimens is simply supported beam with the same located 5 displacement transducers, which capture displacements of beams parts (see Figure 4.3 and Table 4.3).

In Table 4.8 the results captured by transducers are summarized: maximal forces, corresponding displacements and calculated stiffnesses. As it is seen from the Table 4.8



## Square-sectioned lightweight steel beams

stiffnesses for Beams 1-4 calculated from results of transducer IWAN M, which captured general vertical specimen deflection in the middle of the beam are up to 25 % higher than stiffnesses of beams 5-8. But along with this, the average stiffness of beams 5-8 (with structured plates) calculated from results captures by horizontal transducers is up to 27% higher, than flat beams.

So that, according to experimental results, beams 1-4 (made of flat sheets) have higher bearing capacity loads and also out of plane stiffnesses comparing to beams 5-8, but their stiffnesses in plane are lower than beams 5-8.

Table 4.8. Specimens maximal forces, corresponding displacements (from points where transducers are placed in experiments) and stiffnesses, simulation results for squared-sectioned beams

Beam №	Force <sub>max</sub> , kN	Corresponding displacement, mm		Stiffness, kN/mm			Corresponding displacement, mm			Stiffness, kN/mm
		IWAN				Average	IWAN			
		H1(L)	H2(R)	H1(L)	H2(R)		L	M	R	
1	11.13	5.10	5.64	10.46	9.92	10.19	5.81	6.67	6.47	3.21
2	12.62	1.89	3.21	10.17	9.19	9.68	3.38	4.02	3.65	3.91
3	14.07	2.83	2.06	12.86	12.43	12.65	5.42	5.74	5.04	4.53
4	13.39	2.93	3.65	12.52	12.27	12.39	4.58	5.43	4.85	4.74
5	9.56	-*	-*	-*	-*	-*	4.05	4.43	4.15	3.27
6	8.67	2.52	1.56	11.04	11.27	11.16	4.57	4.75	4.18	3.07
7	11.92	3.07	4.05	13.32	12.93	13.12	5.82	6.64	6.30	3.31
8	12.45	3.74	2.60	13.30	13.28	13.29	5.64	5.63	4.92	3.29

\* Beam 5 was the first tested beam in this series of experiments. Tests were conducted separately from all the rest experiments as pilot experiments and only 3 displacement transducers were used – IWANs L, M and R.

## 4.4 FEM simulations

### 4.4.1 General information and material properties

Similarly to the described in chapter 3.4 FEM simulations, this chapter contains information of the simulated laboratory experiments by using the software package ABAQUS/CAE, Standard Version 6.14. The basic properties of the component, such as geometry, storage conditions and material are defined and assigned to the specified elements. The following applies to all experiments: modeling space – 3-dimensional, modeling type - deformable shell elements [79], modeling steps: Buckling and Riks.

For each type of investigated beams (see Table 4.2), an FE model is created and analyzed. Comparative values are taken from all simulations and laboratory results, they are maximal loads, reactions of the supports, displacements and deflections. Beams are created according to geometrical parameters that are illustrated in Figure 4.3. Specimen types are in Table 4.2.

The material properties are described in chapter 4.2 Materials and methods and implemented to ABAQUS by true stress-strain curves. In chapter 4.2 Materials and methods, the stress-strain curves for flat plates are presented in Figure 4.1, main sheet metal parameters are summarized in Table 4.1. For structured sheet metals, stress-strain curves and material parameters are described in chapter 3.2. Material properties.

### 4.4.2 Connections between elements of the model, boundary conditions and loading

Compared with above investigated C-sectioned beams, these pipe specimens (squared-sectioned) consist maximal (beam types 3 and 4) from following elements: 2 L-bent flat plates and 3 L-bent structured. There are no additional plates like in previous series of experiments. In Table 4.9 connections of specimen elements are listed.

Table 4.9. Connection of specimen elements

Plate name	Connected element(s)	Connected areas	Type of connection
L-formed flat plate 1	L-formed flat plate 2	2 edges	Constraint: Tie, Analysis default
L-formed structured plate	L-formed structured plate	4 edges	
L-formed structured plates	L-formed flat plates	Points	Fasteners; Attachment method: face to face; Physical radius: 3 mm; Connector section: beam

Geometrical parameters and boundary conditions are modelled exactly like in laboratory. Figure 4.12 illustrates lines and areas where boundary conditions are applied and in Table 4.10 their degrees of freedom are listed. Like in previous experiments, these specimens are simply supported beams: line 1 has pinned support and line 2 – roller. Also, areas 3 and 4 are fixed in Z-direction.

The applied forces are a line loads, applied in 1/3 of beam length webs – areas 5 (see Figure 4.12). Line loads are introduced in FEM simulations by means of displacement control.

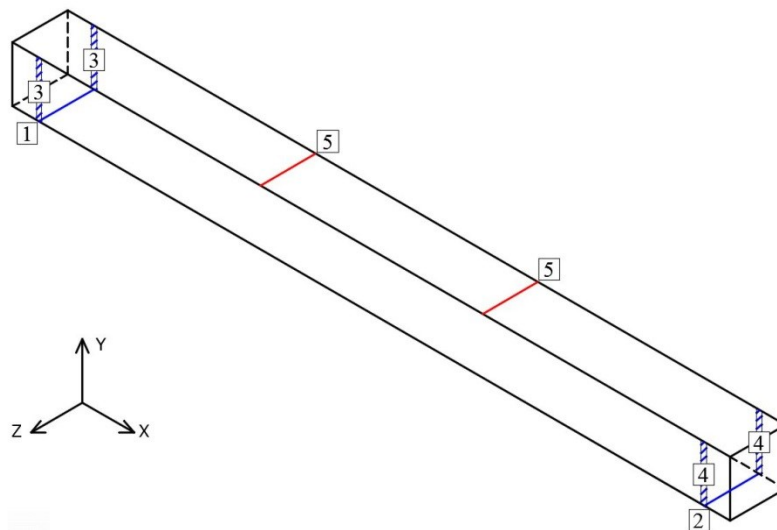


Figure 4.12. Areas where boundary conditions are applied

Table 4.10. Boundary conditions and their degrees of freedom

Name	$U_x(U_1)$	$U_y(U_2)$	$U_z(U_3)$	$UR_x(UR_1)$	$UR_y(UR_2)$	$UR_z(UR_3)$
Line 1	0	0	-	-	-	-
Line 2	-	0	-	-	-	-
Area 3	-	-	0	-	-	-
Area 4	-	-	0	-	-	-
Line 5	-	-1	-	-	-	-

Note: U-translational displacement, UR-rotational displacement, 0- movement is not allowed, blank space-movement is allowed

### 4.4.3 Mesh

For this FEM simulations investigation optimal mesh size is chosen - 10x10 mm for flat plates and for structured - 3x3 mm. General information about number of elements and nodes is listed in Table 4.11.

Table 4.11. General information about models

Beam type	Number of		Types of elements	Size of the element, mm
	nodes	elements		
1	6440	6116	S4R	10x10
2				
3	90224	91891:	S4R	10x10
4		85791 6100		

The meaning of elements names is described in chapter 3.4.5. Mesh.

### 4.4.4 Imperfections and buckling and riks analysis

The detailed information about imperfections, the way of choosing them and how to introduce them to analysis is presented in chapter 3.4.6 Imperfections and buckling analysis.

The imperfections 1-3 are modelled according to Annex C5 of EN 1993-1-5 [102]. The combination of these 3 basic imperfections is implemented to the software by function ‘Edit Keywords’ in Riks Step, where IMP 1(100%) is a leading global imperfection and IMP 2 and IMP 3 are accompanying ones with reduced values of amplitudes (70 % of nominal value). [102].

In Table 4.12 tree eigenvalues for each of Beam types are found. They represent the value of applied load, which is necessary to achieve the respective eigenform on the perfect system with displacement of 1 mm.

Table 4.12. Eigenvalues for each of the model types

Model type	Sandwich member	Total thickness; mm	Ultimate load, kN		
			IMP 1	IMP 2	IMP 3
1	flat 1.25 mm	1.25	-1.9748	1.9963	-2.1118
2	flat 1.50 mm	1.50	-2.5371	2.5681	-2.7039
3	flat 0.75+ structured 0.50 mm	1.25	-1.2752	1.2946	-1.3092
4	flat 1.00mm+ structured 0.50 mm	1.50	-1.7171	1.7426	-1.8263

Figure 4.14, Figure 4.15 and Figure 4.16 show the found eigenforms from Buckling analysis. To illustrate deformable parts of the beams, the deformation scale factor for the eigenforms is increased up to 150. These deformation forms are same to each of the model type case. The difference is in the load that must be applied to each of the beams in order to deform it by 1 mm – see Table 4.12.

The displacements color range varies from red (maximal displacement – 1 mm) to blue color (minimal displacement – 0 mm) is shown in Figure 4.13.

## Square-sectioned lightweight steel beams

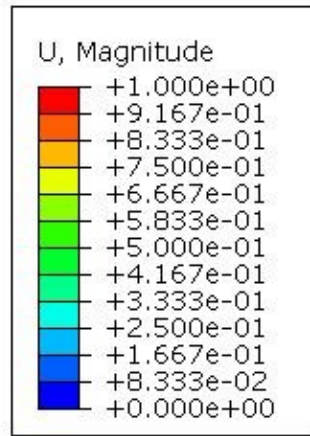


Figure 4.13. The displacements color range for eigenmodes for the squared-sectioned specimen, mm

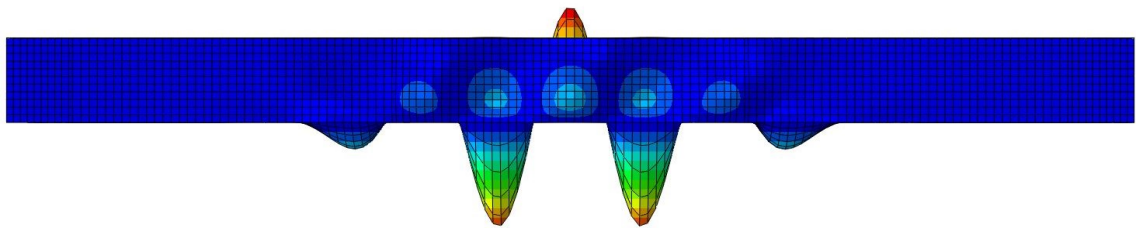


Figure 4.14. First eigenmode for the squared-sectioned specimen

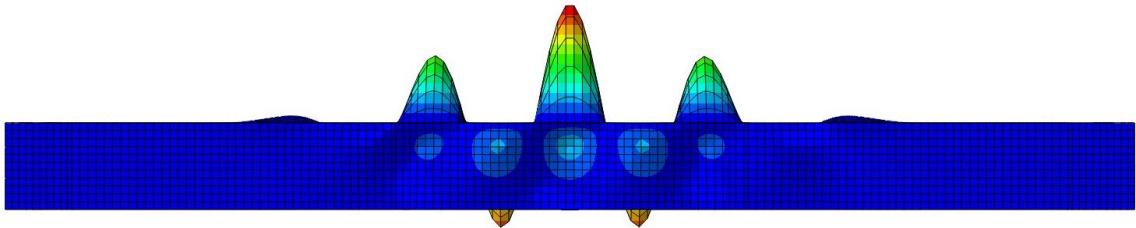


Figure 4.15. Second eigenmode for the squared-sectioned specimen

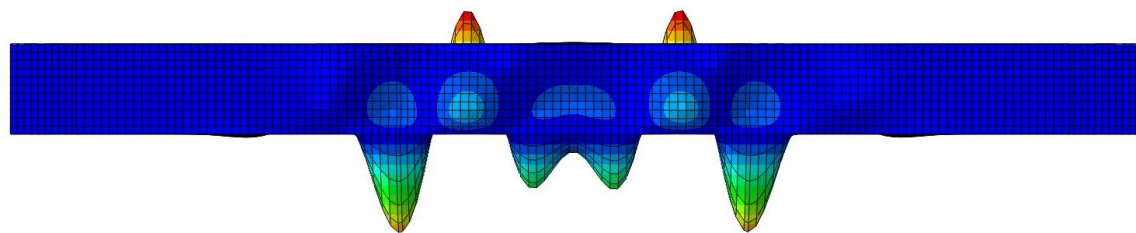


Figure 4.16. Third eigenmode for the squared-sectioned specimen

Three found eigenforms described above are introduced in Riks analysis by function 'Edit keywords' in a similar way that is described in chapter 3.4.7. Riks analysis.

According to EN 1993-1-5: Eurocode 3 [102], the combinations of imperfections is chosen so, that a leading imperfection is the first eigenform (IMP1 - 100%) and the accompanying imperfections values reduced to 70% - second and third eigenforms (IMP2 and IMP3) [102]. Pictures from Riks analysis are presented in Appendix D.

### 4.4.5 Simulation results

## Square-sectioned lightweight steel beams

In this chapter simulation results for each of the beam types are described. The most important results are captured by transducers IWAN M (see Figure 4.3) which captures the middle deflection of the specimens. Resulting displacement curves of FEM simulations of the left and right sides of the beam (basically, where IWAN L and IWAN R are located) are not presented by the reason of near resemblance with results of IWAN M. This proves successful idea achievement of symmetrical deflection of central part of all specimens and the fact that a larger portion of the material is involved in tests.

Simulation results presented for each of specimen. Force represents is total sum of forces in points where boundary conditions are applied. Displacement of simulation results is extracted from the center bottom chord of the specimens. In Figure 4.17 force-displacement curves from FEM simulation results are presented. Maximal load bearing force -14.15 kN is reached by the beam type 2 (flat squared-sectioned beam with 1.5 mm thickness). Maximal force for beam type 4 (flat with structured beam) with similar thickness 1.5 mm is 12 kN. That is 15% lower than for beam type 2. Beam type 3 maximal force (9.07 kN) is 33% lower, than beam type 1 – 13.59 kN.

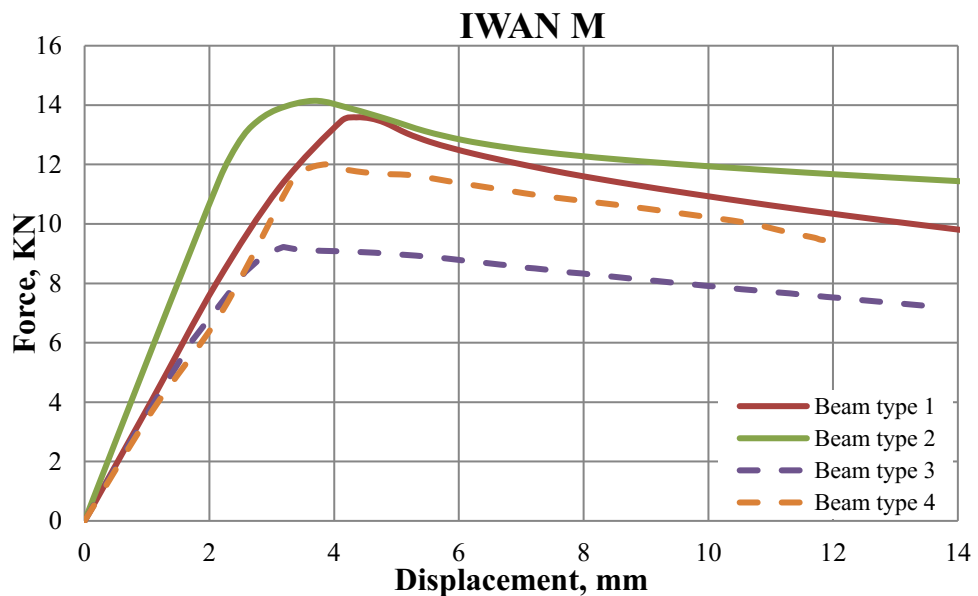


Figure 4.17. Force-displacement diagram, simulations results, vertical displacement in middle of the web

Table 4.13 summarizes vertical deformation in the middle of the beam from simulation results for each of the beam types according to force-displacement curves presented in Figure 4.17.

In Table 4.13 also calculated stiffnesses for each of beam types are presented. Stiffnesses are calculated for elastic zone of the resulting force-displacement curves in the similar way that is described in previous chapters.

## Square-sectioned lightweight steel beams

Table 4.13. Simulation results for beam types 1-4, vertical deformation in the middle of the beam

Beam type	Total thickness, mm	F <sub>max</sub> , kN	IWAN M	
			Corresponding displacement, mm	Stiffness, kN/mm
1	1.25	13.59	4.35	3.79
2	1.50	14.15	3.69	4.66
3	1.25	9.07	3.31	3.41
4	1.50	12.01	3.88	3.46

Figure 4.18 and Figure 4.19 illustrate force-displacement diagrams of left and right sides of specimens flange (where according to laboratory experiments transducers IWAN H1 and IWAN H2 are located). As expected, the horizontal flange buckling occurs practically symmetric. In simulations symmetric flange buckling is predictable, because all parameters (such as symmetry of the model, mesh, force appliance) are exact verified data by contrast with laboratory experiments.

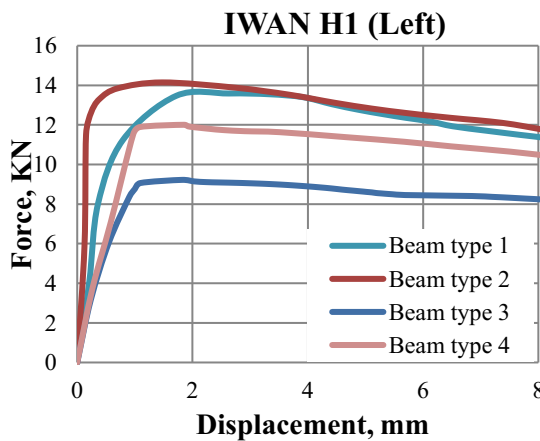


Figure 4.18. Force-displacement diagram, simulations results, horizontal displacement of web (from the left side)

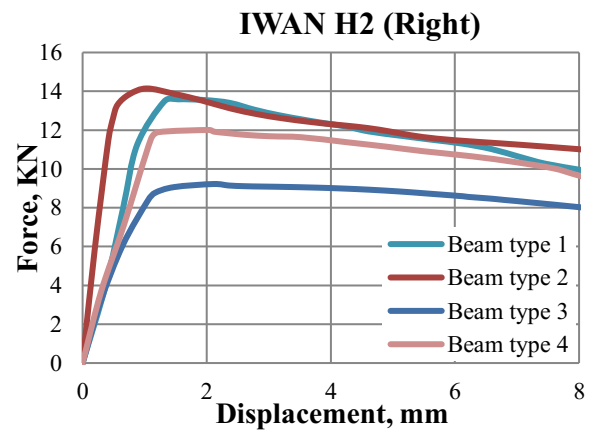


Figure 4.19. Force-displacement diagram, simulations results, horizontal displacement of web (from the right side)

In Table 4.14 maximal forces, corresponding displacements and stiffnesses from force-displacement curves presented in Figure 4.18 and Figure 4.19 are summarized. To have an opportunity to compare them with laboratory experiments, average stiffnesses are also calculated. In general, concerning the behavior of the specimens in elastic zone with same total thickness, according to the Table 4.14, average stiffnesses of all specimens are really close to each other and it is difficult to make conclusions based only on the vertical stiffness of the flange.

Table 4.14. Maximal force for each beam type, corresponding displacements and stiffnesses, simulation results

Beam type	Total thickness, mm	F <sub>max</sub> , kN	IWAN H1 (left)		IWAN H2 (right)		Average stiffness
			Corresponding displacement, mm	Stiffness, kN/mm	Corresponding displacement, mm	Stiffness, kN/mm	
1	1.25	13.59	1.72	12.33	1.31	10.05	11.19
2	1.50	14.15	1.48	13.66	1.03	14.20	13.93
3	1.25	9.07	1.82	11.04	2.11	10.92	10.98
4	1.50	12.01	1.86	14.18	2.04	12.32	13.25

## Square-sectioned lightweight steel beams

The loads are applied as a line loads (rollers, that are placed on the upper chord) and maximal stresses concentrate exactly under line loads. So that, the construction collapse starts exactly in those places. Due to the fact that the loads are not spread with the help of additional plates (this is possible to place additional steel plates under the rollers), stresses are concentrated on the upper chord even when the profile thickness is increased – see Figure 4.20.

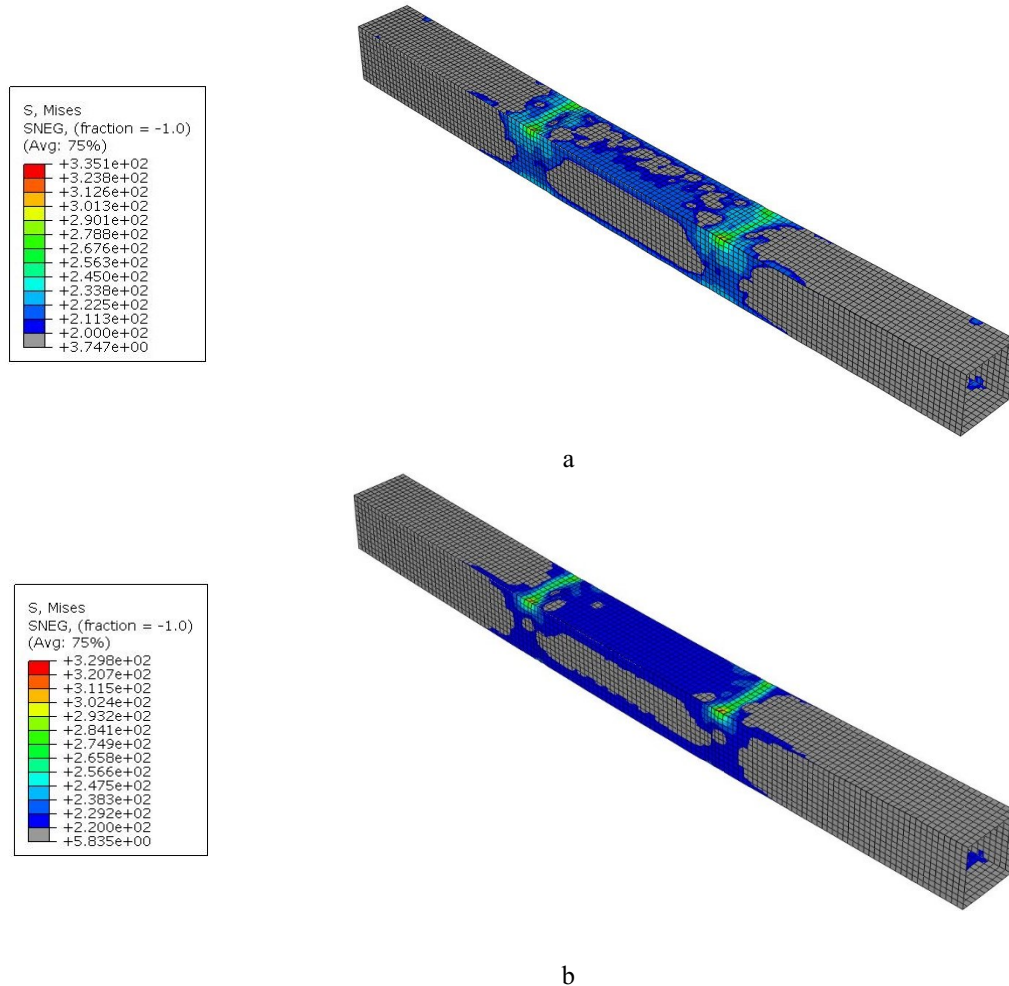


Figure 4.20. Square-sectioned beams: a - 2mm thickness and b – 3 mm thicknesses

### 4.4.6 Conclusion

This chapter describes FEM simulation process by using FEM software ABAQUS software. Geometry of specimens, material properties, boundary conditions and force application match to laboratory experiments. There are 4 types of specimens involved in research, for laboratory tests for each of the type 2 beams are constructed (so that there are 8 beams in total).

The output data of simulations is extracted for points, where transducers in laboratory are installed. In Table 4.15 simulation results for beam types 1-4 are presented.

According to simulations, load bearing capacity of beam types 1 and 2 (models made of flat plates) is 33% and 15% higher than beam types 3 and 4 respectively. According to Table 4.15 stiffnesses of flat beams (column IWAN M) are 10 to 25% higher, than of beams made of sandwich members.

## Square-sectioned lightweight steel beams

Comparing horizontal average stiffnesses, it can be seen, that for specimens with same total thickness (beam types 1 and 3; beam types 2 and 4), they are practically same. That means under in-plane deformations, flat plates and structured sandwich as a web part of specimen, behave similar.

However, specimens of flat plates show advantages compared to structured in load bearing capacity and in vertical stiffness – see Table 4.15.

Table 4.15. Specimens maximal forces, corresponding displacements (from points where transducers are placed in experiments) and stiffnesses, simulation results for squared-sectioned beams

Beam type	F <sub>max</sub> , kN	IWAN						
		M		H1 (left)		H2 (right)		H1 and H2 average stiffness, kN/mm
		Displ., mm	Stiffness, kN/mm	Displ., mm	Stiffness, kN/mm	Displ., mm	Stiffness, kN/mm	
1	13.59	4.35	3.79	1.72	12.33	1.31	10.05	11.19
2	14.15	3.69	4.66	1.48	13.66	1.03	14.20	13.93
3	9.07	3.31	3.41	1.82	11.04	2.11	10.92	10.98
4	12.01	3.88	3.46	1.86	14.18	2.04	12.32	13.25

To avoid plastic failure that occurs in simulations and experiments (similar to C-profiles beams), the thickness of the flat squared-sectioned can be increased.

## 4.5 Evaluation of simulation and experiment results

### 4.5.1 General information

The first modelled beam is Type 3 with a flat squared-profile 0.75 mm thickness and structured plates 0.50 mm thickness. It is chosen as the most complicated type for calculation because of structured sheets and the connections between them and flat plates. To create beam types 1 and 2 structured plates with connections are simply deleted from this model. For beam type 4 only thickness of flat plate is changed.

In order to compare experimental results and numerical simulations, elastic stiffness for each of the specimens is determined. The bending stiffness (S) is the resistance of a member against bending deformation or ratio of applied force (F) to deflection (d) – see Eq. 4.1:

$$S = \frac{F}{d} \quad 4.1$$

### 4.5.2 Beam type 1: flat 1.25 mm

Beam type 1 is a specimen made of 2 L-shaped flat plates, welded together. To the FEM model beam type 1 corresponds specimens Beams 1 and 2.

In Figure 4.21 are force-displacement curves from transducer IWAN M (vertical displacement) captured in the middle of the lower specimen flange. As it is illustrated, curves have good agreement with one another and stiffnesses calculated for elastic zone summarized in Table 4.16 confirm that.



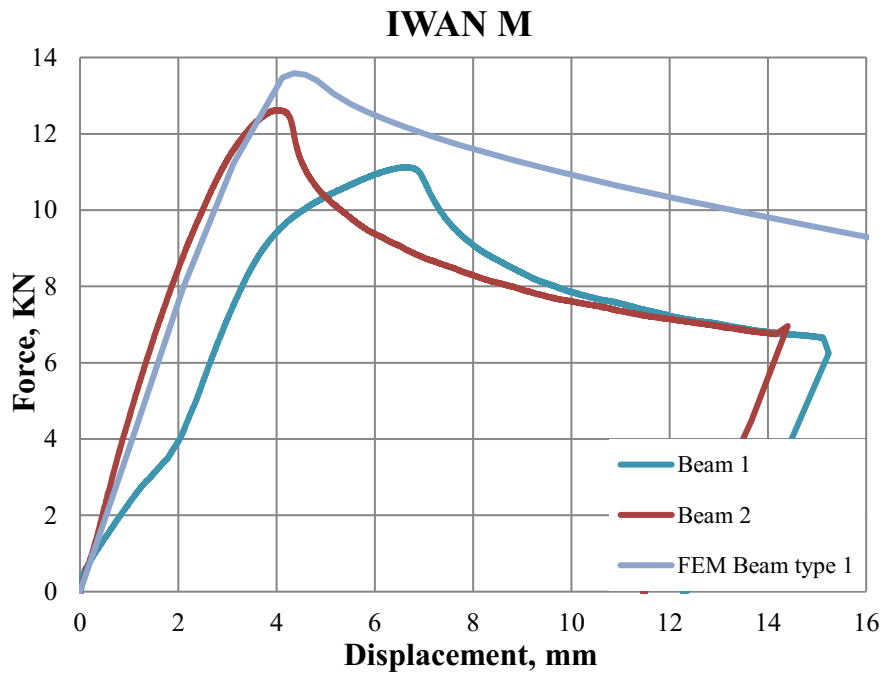


Figure 4.21. Force-displacement (vertical) curves for lower flange in the middle of the beam (IWAN M): experimental results for Beam 1 and Beam 2 and FEM results of Beam type 1

In Table 4.16 maximal forces and stiffnesses calculated based on laboratory tests and simulations are listed.

Table 4.16. Comparison of Beam 1 and 2 experimental and beam type 1 simulation results (IWAN M)

	$F_{max}$ , kN	IWAN M	
		Corresponding displacement, mm	Stiffness, kN/mm
Beam 1	11.13	6.67	3.21
Beam 2	12.62	4.02	3.91
FEM	13.59	4.35	3.79

Figure 4.22 and Figure 4.23 show the force - horizontal displacement diagrams made for left and right sides of specimens webs – laboratory and simulations results. It is important to mention, that according to simulation results, curves are pretty similar to each other, that means the horizontal buckling of left and right sides of the beams occurs simultaneously and symmetrical. Curves from laboratory show different behavior of left and right sides of the specimens: at the beginning it is practically same (one curve), but after reaching specific point, one of the curves sharply falls down and the second one smoothly goes further. In Appendix C photos from laboratory are collected and it is clearly seen, that horizontal buckling of web occurs asymmetrical. That could happen due to several factors such as inaccuracies in manufacturing of specimens, not absolutely symmetrical force application etc.

This buckling asymmetry takes place in all experiments. Table 4.6 shows on which side of the specimen the buckling area is visible.

## Square-sectioned lightweight steel beams

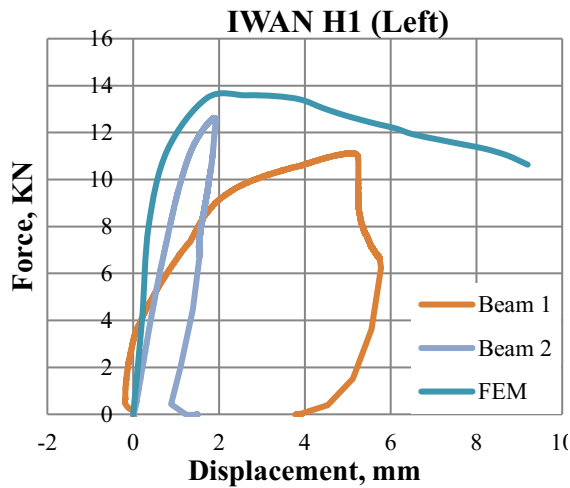


Figure 4.22. Force-displacement (horizontal) curves for web (IWAN H1), left side: experimental results for Beam 1 and Beam 2 and FEM results of Beam type 1

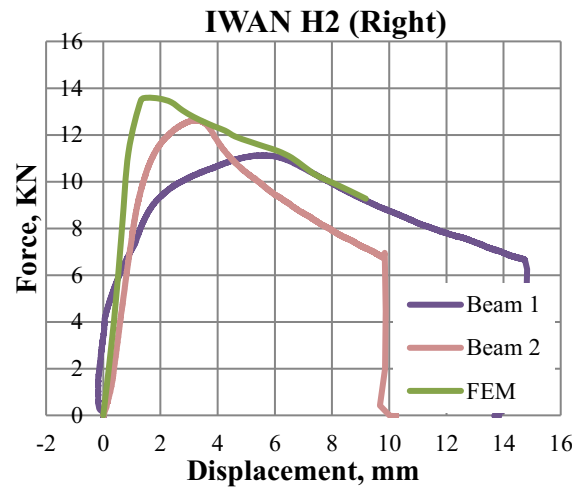


Figure 4.23. Force-displacement (horizontal) curves for web (IWAN H2), right side: experimental results for Beam 1 and Beam 2 and FEM results of Beam type 1

Table 4.17 shows maximal forces, corresponding displacements and horizontal stiffnesses of beams 1 and 2 and beam type 1. Average stiffness of the FEM model flange is a 10% higher, than in experiments.

Table 4.17. Comparison of experimental and simulation results (IWAN H1 and IWAN H2), Beam type 1

	$F_{\max}$ , kN	IWAN H1 (Left)		IWAN H2 (Right)		Average stiffness, kN/mm
		Corresponding displacement, mm	Stiffness, kN/mm	Corresponding displacement, mm	Stiffness, kN/mm	
Beam 1	11.13	5.10	10.46	5.64	9.92	10.19
Beam 2	12.62	1.89	10.17	3.21	9.19	9.68
FEM	13.59	1.72	12.33	1.31	10.05	11.19

### 4.5.3 Beam type 2: flat 1.50 mm

Beam type 2 is a squared-sectioned beam with the thickness 1.50 mm. Beam type 2 is a model of laboratory specimens Beam 3 and 4.

Force-displacement curves from Figure 4.24 are match to each other and according to Table 4.18, stiffnesses of experimental and FEM simulations have perfect agreement.

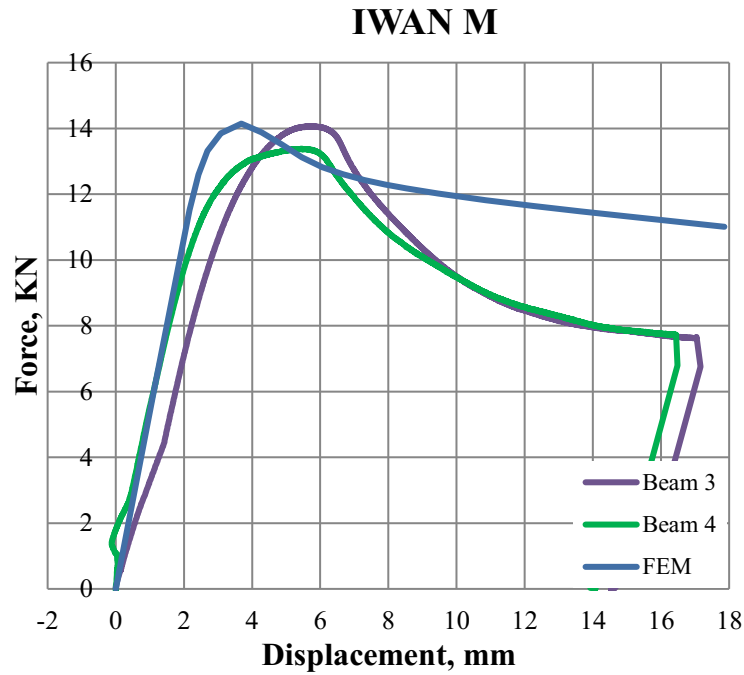


Figure 4.24. Force-displacement (vertical) curves for lower flange in the middle of the beam (IWAN M): experimental results for Beam 3 and Beam 4 and FEM results of Beam type 2

Table 4.18 present maximal forces and calculated stiffnesses for beams 3, 4 and beam type 2.

Table 4.18. Comparison of Beam 3 and 4 experimental and beam type 2 simulation results (IWAN M)

	$F_{max}$ , kN	IWAN M	
		Corresponding displacement, mm	Stiffness, kN/mm
Beam 3	14.07	5.74	4.53
Beam 4	13.39	5.43	4.74
FEM	14.15	3.69	4.66

Figure 4.25 and Figure 4.26 show force-displacement curves of IWAN H1 (left side of beams web) and IWAN H2 (right side of the beams web). As it is seen, till approximately 1 kN curve of Beam 4 goes to the direction of decreasing X-axis and then, gradually changing direction towards increasing the X-axis. In practice, it means that web buckles to one side and then to the other one. This deformation cannot be seen in photos, because the value of this initial buckling is really small (approximately 1 mm).

## Square-sectioned lightweight steel beams

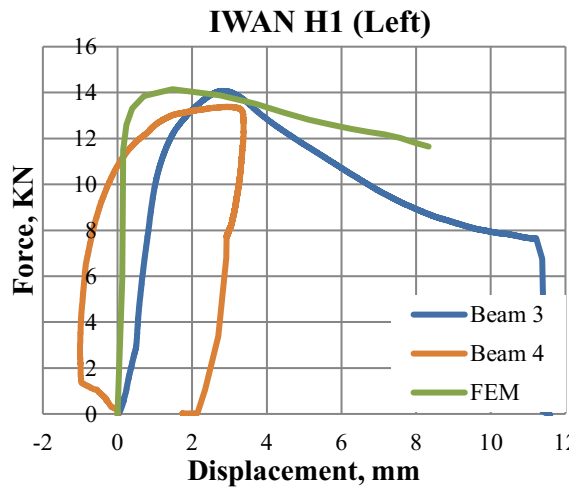


Figure 4.25. Force-displacement (horizontal) curves for web (IWAN H1), left side: experimental results for Beam 3 and Beam 4 and FEM results of Beam type 2

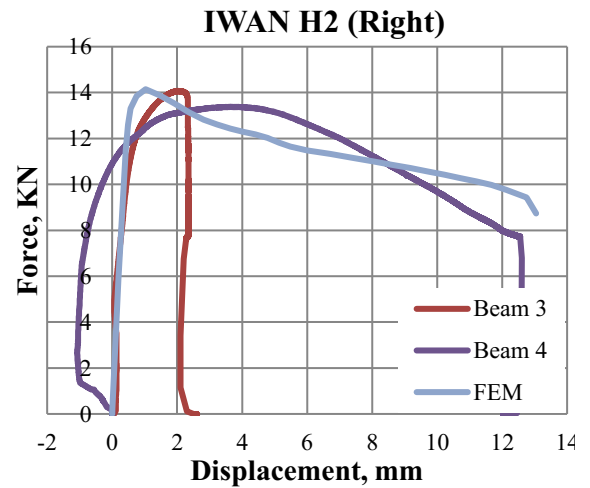


Figure 4.26. Force-displacement (horizontal) curves for web (IWAN H2), right side: experimental results for Beam 3 and Beam 4 and FEM results of Beam type 2

Table 4.19 shows good agreement between maximal forces - simulation result force is just 5 % higher than Beam 4 force. Average stiffnesses FEM and experimental values of the web are also very close to each other-maximal difference is 12%.

Table 4.19. Comparison of experimental and simulation results (IWAN H1 and IWAN H2), Beam type 2

	$F_{max}$ , kN	IWAN H1 (Left)		IWAN H2 (Right)		Average stiffness, kN/mm
		Corresponding displacement, mm	Stiffness, kN/mm	Corresponding displacement, mm	Stiffness, kN/mm	
Beam 3	14.07	2.83	12.86	2.06	12.43	12.65
Beam 4	13.39	2.93	12.52	3.65	12.27	12.39
FEM	14.15	1.48	13.66	1.03	14.20	13.93

### 4.5.4 Beam type 3: flat 0.75 mm + structured 0.50 mm

Beam type 3 consist of 2 L-formed flat plates with thickness 0.75 mm and of 3 L-formed structured plates with thickness 0.50 mm. All they are connected together in a squared-sectioned beam. Beam type 3 corresponds to Beam 5 and 6.

In Figure 4.27 there are force-displacement curves from simulation results and laboratory experiments. As it is seen, the inclination of the curves is close to each other and the Table 4.20 confirms that – difference in FEM and experiments stiffnesses is maximal 4%.

Square-sectioned lightweight steel beams

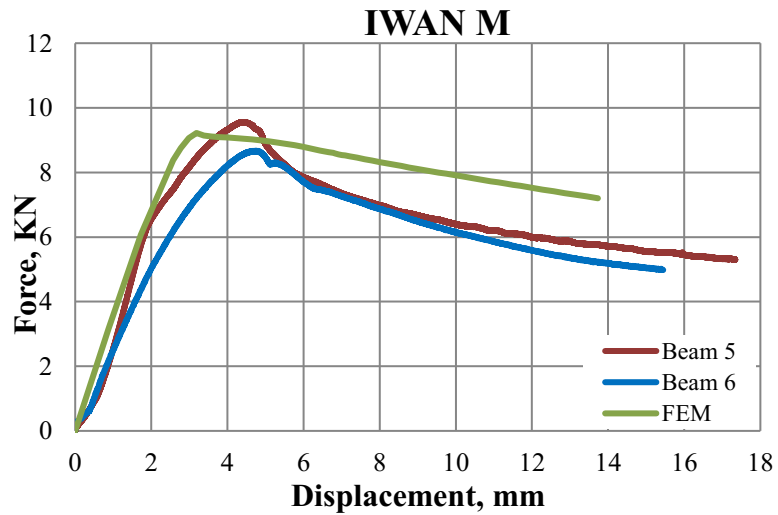


Figure 4.27. Force-displacement (vertical) curves for lower flange in the middle of the beam (IWAN M): experimental results for Beam 5 and Beam 6 and FEM results of Beam type 3

In Table 4.20 maximal forces, displacements and stiffnesses are listed. As it can be seen, values from Table 4.20 have good agreement.

Table 4.20. Comparison of Beam 5 and 6 experimental and beam type 3 simulation results (IWAN M)

	$F_{max}$ , kN	IWAN M	
		Corresponding displacement, mm	Stiffness, kN/mm
Beam 5	9.56	4.43	3.27
Beam 6	8.67	4.75	3.07
FEM	9.07	3.31	3.41

In Figure 4.28 force-displacement results of simulations and experiments are shown. Unfortunately, there are no results from horizontal transducers for Beam 5, because it was the pilot beam tested in laboratory, so that only transducers captured vertical displacements were installed.

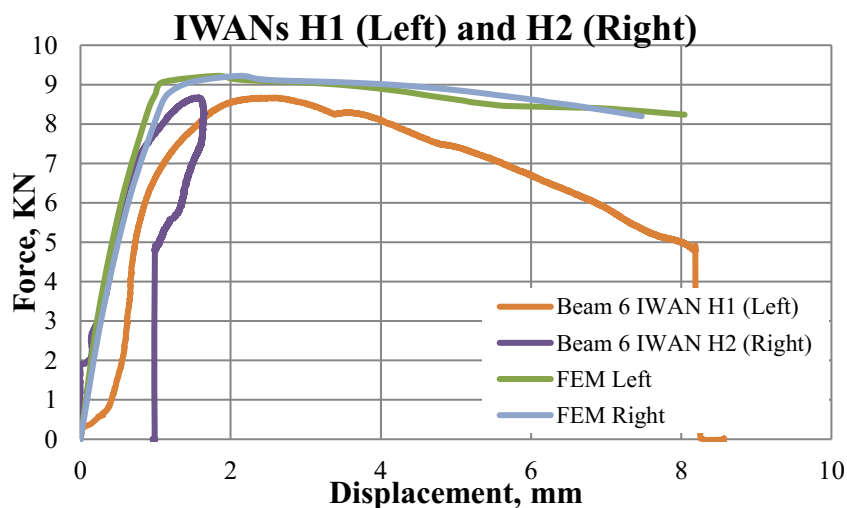


Figure 4.28. Force-displacement (horizontal) curves for web (IWAN H1 and H2), left and right sides: experimental results for Beam 6 and FEM results of Beam type 3

As it can be seen from Figure 4.28 and Appendix C the left side of the Beam 6 web is not visibly deformed. According to simulation results for beam type 3, maximal force is 4% higher

### Square-sectioned lightweight steel beams

than by Beam 6 and 5% lower than by Beam 5. In Table 4.21 experimental results for Beam 5 and 6 and simulation results for beam type 3 are presented.

Table 4.21. Comparison of experimental and simulation results (IWAN H1 and IWAN H2), Beam type 3

	$F_{max}$ , kN	IWAN H1 (Left)		IWAN H2 (Right)		Average stiffness, kN/mm
		Corresponding displacement, mm	Stiffness, kN/mm	Corresponding displacement, mm	Stiffness, kN/mm	
Beam 5	9.56	_*	_*	_*	_*	_*
Beam 6	8.67	2.52	11.04	1.56	11.27	11.16
FEM	9.07	1.82	11.04	2.11	10.92	10.98

#### 4.5.5 Beam type 4: flat 1.00 mm + structured 0.50 mm

Beam type 4 consist of 2 L-formed flat plates with thickness 1.00 mm and of 3 L-formed structured plates with thickness 0.50 mm. All they are connected in a squared-sectioned beam. Beam type 4 corresponds to Beam 7 and 8.

According to Figure 4.29 the agreement between simulation and experiments is good: force-displacement curves are really close to each other. So that according to Table 4.22, the stiffnesses are practically same and maximal forces also (the difference in loads is maximal 3.5%).

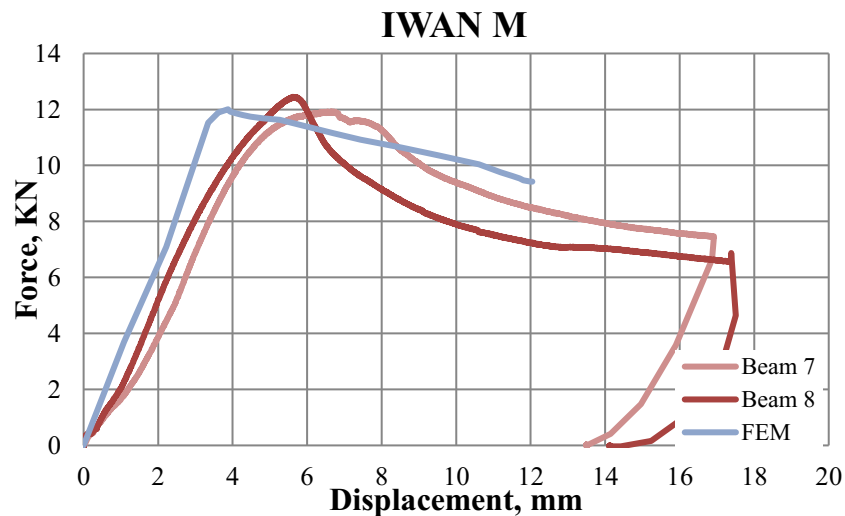


Figure 4.29. Force-displacement (vertical) curves for lower flange in the middle of the beam (IWAN M): experimental results for Beam 7 and Beam 8 and FEM results of Beam type 4

Table 4.22. Comparison of Beam 7 and 8 experimental and beam type 4 simulation results (IWAN M)

	$F_{max}$ , kN	IWAN M	
		Corresponding displacement, mm	Stiffness, kN/mm
Beam 7	11.92	6.64	3.31
Beam 8	12.45	5.63	3.29
FEM	12.01	3.88	3.46

Figure 4.30 and Figure 4.31 illustrate force-displacement curves from horizontal transducers set up on the left (IWAN H1 (L)) and right IWAN H1 (R)) sides of specimens web and also from simulation results. As it can be seen, according to symmetry of curves extracted from simulations, buckling of the model web occurs symmetrically. In Table 4.23 this is proved

## Square-sectioned lightweight steel beams

by displacement corresponding to maximal load and by calculated stiffnesses. Figure 4.30 and Figure 4.31 clearly show that Beam 7 deformed more on the right side and Beam 8 on the left side of the web.

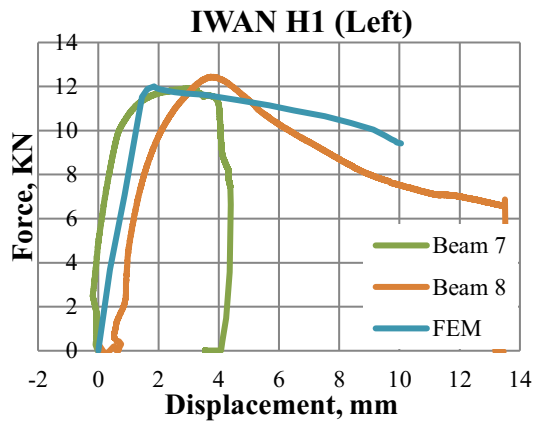


Figure 4.30. Force-displacement (horizontal) curves for web (IWAN H1), left side: experimental results for Beam 7 and 8 and FEM results of Beam type 4

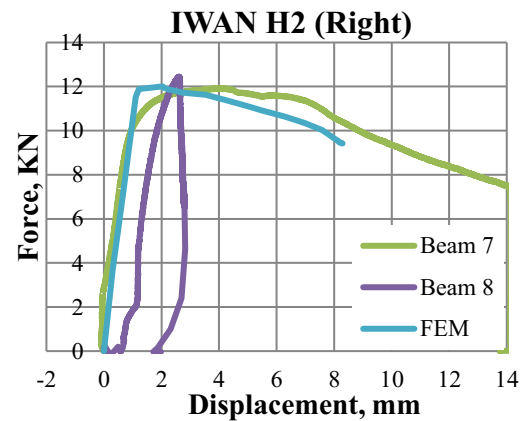


Figure 4.31. Force-displacement (horizontal) curves for web (IWAN H2), right side: experimental results for Beam 7 and 8 and FEM results of Beam type 4

Table 4.23. Comparison of experimental and simulation results (IWAN H1 and IWAN H2), Beam type 2

	$F_{\max}$ , kN	IWAN H1 (Left)		IWAN H2 (Right)		Average stiffness, kN/mm
		Corresponding displacement, mm	Stiffness, kN/mm	Corresponding displacement, mm	Stiffness, kN/mm	
Beam 7	11.92	3.07	13.32	4.05	12.93	13.12
Beam 8	12.45	3.74	13.30	2.60	13.28	13.29
FEM	12.01	1.86	14.18	2.04	12.32	13.25

### 4.5.6 Conclusion

This chapter contains the comparison of simulation and experimental results. Force-displacement results of each type of the beam modelled in FEM software is compared with received results from laboratory experiments.

All data is summarized in Table 4.24. Comparing calculated stiffnesses, it may be noted the following: elastic vertical stiffness (calculated from results captured by IWAN M-the last column in Table 4.24) of simulation results is maximal 18% (by beam type 1) higher than experimental ones. Maximal difference between horizontal stiffnesses has also beam type 1: calculated FEM stiffness is 15% higher than experimental one.

Figure 4.32 clearly presents the information from Table 4.24: stiffnesses calculated from simulations and experiment results.

## Square-sectioned lightweight steel beams

Table 4.24. Comparison of experimental and FEM simulations results, square-sectioned beams

Name	F <sub>max</sub> , kN	IWAN		Average stiffness (H1 L and H2 R), kN/mm	IWAN			Stiffness, kN/mm
		H1(L)	H2(R)		L	M	R	
		Displacement, mm						
Beam 1	11.13	5.10	5.64	10.19	5.81	6.67	6.47	3.21
Beam 2	12.62	1.89	3.21	9.68	3.38	4.02	3.65	3.91
Beam type 1	13.59	1.72	1.31	11.19	-	4.35	-	3.79
Beam 3	14.07	2.83	2.06	12.65	5.42	5.74	5.04	4.53
Beam 4	13.39	2.93	3.65	12.39	4.58	5.43	4.85	4.74
Beam type 2	14.15	1.48	1.03	13.93	-	3.69	-	4.66
Beam 5	9.56	-*	-*	-*	4.05	4.43	4.15	3.27
Beam 6	8.67	2.52	1.56	11.16	4.57	4.75	4.18	3.07
Beam type 3	9.07	1.82	2.11	10.98	-	3.31	-	3.41
Beam 7	11.92	3.07	4.05	13.12	5.82	6.64	6.30	3.31
Beam 8	12.45	3.74	2.60	13.29	5.64	5.63	4.92	3.29
Beam type 4	12.01	1.86	2.04	13.25	-	3.88	-	3.46

\* Beam 5 was the first tested beam in this series of experiments. Tests were conducted separately from all the rest experiments as pilot experiments and only 3 displacement transducers were used – IWANs L, M and R.

### Horizontal and vertical stiffnesses

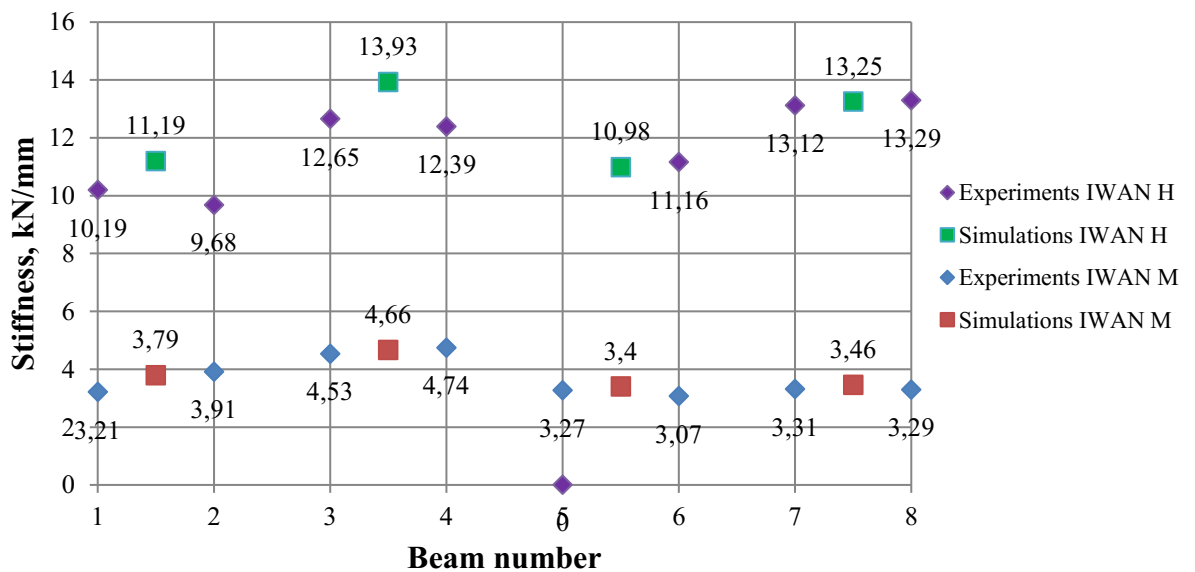


Figure 4.32. Graphic presentation of experimental and FEM stiffnesses, calculated from results captured by horizontal (IWAN H) and vertical (IWAN M) set up transducers

In general, simulations and experimental results have good agreement, which means the high precision of modeling within the framework of this study. That fact gives an opportunity for future investigations with the topic of ‘structured sheet metals’ to be based on FEM simulations, described in present work.



## 4.6 Analytical analysis

Previous chapters described laboratory experiments, simulations and also comparison of received results. In order to compare experimental results and numerical simulations, elastic stiffness for each of the specimens is calculated by formulas. To validate calculated stiffnesses based on laboratory and simulations results, analytical analysis is done.

The first way of calculation stiffness is used in experimental results and numerical simulations. The bending stiffness ( $s$ ) is the resistance of a member against bending deformation or ratio of applied force ( $F$ ) to deflection ( $d$ ) – see Eq. (4.2):

$$s = \frac{F}{d} \quad 4.2$$

The second way is the following: stiffness can be calculated based on the parameters of the material which is used to manufacture it. So that, stiffness ( $s$ ) can be presented by ratio of 56.4, Young's Modulus ( $E$ ) and area moment of inertia of the beam ( $I$ ) to beam length raised to the power of 3 ( $L$ ) – see Eq.4.3. Eq. 4.3 is used for simply supported beams and forces located on 1/3 of the beam length, which corresponds to this research specimen installation.

$$s = 56,4 \cdot \frac{E \cdot I}{L^3} \quad 4.3$$

Experimental, simulation and analytical calculated stiffnesses of every specimen and every type of specimen are collected in Table 4.25. Experimental and simulation stiffnesses are calculated for the elastic part of the curves (for IWAN M).

In order to except the initial deformations, that took place in the experiments, stiffnesses of laboratory experiments are defined from sharp straight line between approximately 1 and 6 kN. That is the initial gradient, which shows realistic experiment results.

Table 4.25. Experimental, simulation and analytical stiffnesses

Name	Description	Elastic stiffness, kN/mm		
		Experiments	Simulations	Analytical
Beam 1	Flat 1.25_1	3.57*	3.79	4.18
Beam 2	Flat 1.25_2	3.91		
Beam 3	Flat 1.5_3	4.53	4.66	4.94
Beam 4	Flat 1.5_4	4.74		
Beam 5	Structured 0.8+0.5_5	3.27	3.40	3.47
Beam 6	Structured 0.8+0.5_6	3.07		
Beam 7	Structured 1+0.5_7	3.31	3.46	3.68
Beam 8	Structured 1+0.5_8	3.29		

\* In spite the fact, that stiffness of Beam 1 is comparable to stiffness of Beam 2 which has same properties, simulation and analytical stiffnesses, it is considered as a failed attempt. By some reasons, experiment went wrong with Beam 1 (see Figure 4.4) – it stands out of the overall load-displacement picture for beams made of flat plates. It remains in the graphical representation, but is not considered any further (due to welding defects).

In general, as it is seen from the Table 4.25 beams with structured plates lose in stiffness with flat panels. That is shown in low stiffnesses values for beams 5-8 comparing to stiffnesses

## Square-sectioned lightweight steel beams

of beams 1-4. That probably happens due to the small contribution to the total beam 5-8 stiffness of structured sheets.

Figure 4.33 illustrate all stiffness values listed in Table 4.25 graphically to present more clearly the good agreement between simulations, experiments and analytical calculations.

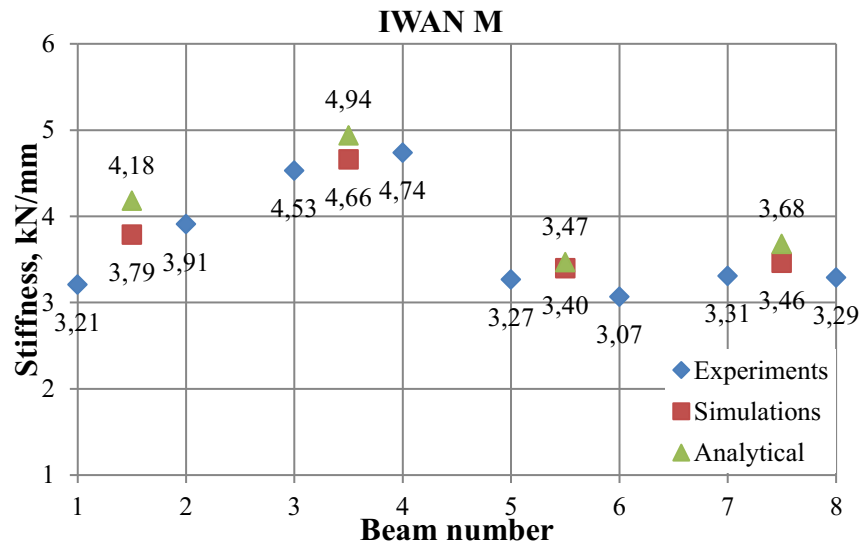


Figure 4.33. Stiffnesses of beams 1-8 and beam types 1-4 calculated from experiments, simulations and analytical results.

Anyway, simulations and analytical calculations have good agreement. The reason is same initial data that is introduced in simulations and used in calculations: Young's Modulus, moment of inertia and specimen length. As it is seen, stiffnesses from experimental results are a bit lower or a bit larger, than calculated and simulated ones. There are several reasons for that.

The first one – the experimental installation is a complicated system with unique material parameters, imperfections, connections etc. Of course, all these main parameters which describe the experimental model are implemented in simulation process. But there are still some random variables that are not taken into account, for example, manufacturing defects of materials, human factor (specimen making process and its setup, loading location etc.).

The other one logically comes out from the first one. Experiments can provide us with new empirical data, computer simulations cannot. Computer simulations can only produce results that are implied according to assumptions based on a theory. [106] Computer simulations are normally based on a theory, but experiments can prove it.

The last, but not least is the fact of experiments quantity. Of course, for statistical data 2 specimens of 1 type is not enough. At least, 10 are needed. Unfortunately, there was no such an opportunity. Due to lack of the main material – structured plates, its manufacturing difficulties and also high material consumption for 1 specimen (3 structured plates for 1 beam), manufacturing of more than 2 specimens with the same geometry was impossible.

## 4.7 Conclusions to chapter 4

Chapter 4 contains information about the square-sectioned structured steel beams study.

## Square-sectioned lightweight steel beams

The first part of this chapter describes the laboratory tests of material properties and 4 points bending tests of manufactured specimens. All specimens are manufactured in laboratory of BTU Cottbus. In present work the investigated specimens are manufactured by technical reasons so, that the beauty and extraordinariness of structured plates are hidden inside them. Unfortunately, it is impossible to see structured sheets. One way for solution of this problem is using of structural plates in construction of stands and boards at for example expositions and exhibitions.

The specimens production of square-sectioned beams is rather complicated and time-consuming process. It could be simplified by following actions: in order to avoid laser welding of structured plates along the edges and also to increase its size and thickness, hydroforming of flat plates could be replaced by cold-rolling process (steel plates up to 1 mm are manufactured) [9].

By the manufacturing process the following methods are used: hydroforming, laser and manual cutting, laser, point and manual (by using TIG apparatus) welding. There are 8 square-sectioned thin-walled specimens are manufactured. 4 types of specimens (2 specimens for each type) consist of flat sheets and flat sheets connected by point welding with structured are investigated. Each type of studied beams has its own total thicknesses: types 1 and 2 are compiled only from flat plates 1.5 mm and 1.25 mm thickness and types 3 and 4 consist of a flat and structured plates with thicknesses:  $(0.75+0.5)$  mm and  $(1+0.5)$  mm respectively. Force results of 4-point bending tests are collected from hydraulic-jack press machine and displacements of specimens are captured by transducers in characteristic points. The 4-points bending laboratory tests showed that load bearing capacity of beams made of flat plates is higher than beams with structured elements. Maximal reached force is 14.07 kN has Beam 3 (flat 1.5 mm plate), the lowest – Beam 6 (flat+structured plates  $0.8+0.5$  mm ) with 8.67 kN.

In the second part of this chapter, for each of type of the specimens computer models are created by using shell-elements in software package ABAQUS/CAE, Standard Version 6.14. Dimensions, material properties, boundary conditions, load points are implemented in software according to laboratory setup. Buckling numerical simulations and non-linear behavior of beams under static loading, based on the FE method are performed. Force-displacement results from simulations are collected of same characteristic points as in laboratory – points are chosen according to transducers locations. The simulation results indicate the similar maximal force picture: maximal force has beam type 2 (flat 1.5mm plate) – 15.5kN, the lowest – 9.07 beam type 3 (flat+structured plates  $0.75+0.5$ mm). That means, that the numerical results are rather close to laboratory investigations and may be used in similar future investigations.

The third big part contains information about evaluation of simulation and experimental results. According to comparison, they have good agreement what testifies about high quality of conducted simulations. But along with this, calculated web average stiffnesses (from horizontal transducers IWAN H1 (Left) and IWAN H2 (Right)) of Beams 1-4 (made only with flat sheets)

### Square-sectioned lightweight steel beams

and Beams 5-8 (made of sandwich members with flat and structured sheets) do not stand in stark contrast to each other. By comparison of different beam types with same thicknesses, it can be noted that maximal difference between simulation and experimental stiffnesses calculated from results of IWAN M is about 25% (between types 2 and 4) and about 20% between types 1 and 3.

However, in order to have wider perception picture of such experiments, more than 2 specimens for each type are needed. In spite of the lower stiffness values of beams with structured plates compare to flat ones, there are some ways to increase structured sheets stiffness: for example, to increase their thickness – again by choosing rolling forming process instead of hydroforming. [9]

The last part of this chapter is analytical analysis which proves the fact accuracy of test and simulation results. The divergence of stiffness numerical, analytical and simulation results is maximum 6% and 15% respectively (see Table 4.25). It proves the fact of good agreement between them.

## 5 Overall conclusions

This thesis presents a contribution to investigating the properties structured sandwich panels (flat and structured sheet metals welded together). This research is a part of a complex research project DESTRUCT/S. The base project idea is fundamental properties research of sandwich structured sheets in such areas as economy, acoustic, welding, corrosion, material engineering and structure building. To provide the investigations in area of structural building light steel thin-walled sandwich structures are chosen as a study object. The C- and square-sectioned beams are manufactured in order to conduct further investigations. The aim of this work is to find out load bearing capacity and elastic stiffnesses of manufactured beams by laboratory experiments, FEM simulations, analytical and parametric investigations.

Chapter 2 deals with detailed information about structured sheet metals: classification, geometry, manufacturing process and material properties of structured sheets, types of sandwiches made of structured sheets and their application. Hydroformed structured sheet metals with structural direction  $90^\circ$  (Figure 2.22) and ‘positively’ installed (Figure 2.24) are used as a basic material in this research. There are several reasons for that: the direction  $90^\circ$  covers almost the full complexity of the structure in cut [83], ‘positively’ installed sheets achieve higher bending forces than those ‘negative’ of used sheets in structural position (see Figure 2.24) [80]. Types of sandwiches to manufacture specimens are flat-structured with the flat sheet-comb connection (see Table 2.3). This type of connection is chosen due to lack of structured sheets (because of difficulties in hydroforming production) and due to the fact that it has one of the highest stiffnesses (after comb-comb sandwich – see Table 2.3) [85, 83, 79].

Chapter 3 describes study of C-sectioned beams, made of flat and both flat and structured sheets. Laboratory 3-points bending tests and simulation results have good agreement and prove the fact that for this shape of specimen, load bearing capacity of beams made of structured sheets is up to 2 times higher than flat ones. Also, according to calculations based on experiments and simulations the elastic stiffnesses of beams with structured plates are also higher than beams with flat ones: up to 2 times higher for vertical web stiffness and from 4 to 7 times higher for horizontal. That means that structured sandwich members used in C-sectioned beams as webs are stiffer and bear higher loads than webs made of only flat sheets. Based on these results, parametric modelling is conducted in order to find the sandwich thickness-stiffness relationship to have an opportunity to predict the behavior of similar models. Therefore, 2 formulas of stiffness increase factors for C-profiled beams are created: one is for beams consist only of flat plates, the other one - for specimens made of flat and structured plates. It is found out that the web stiffness of C-profiled structured beams is in average 32% higher than stiffness of similar beams made only of flat plates.

Chapter 4 presents information about investigation of square-sectioned flat and structured beams. Conducted 4-point bending laboratory tests show that load bearing capacity of beams

### Overall conclusions

with sandwich structured plates is 20-30% lower than flat ones. Simulation and analytical calculations have similar results and confirmed this fact. However, despite the clear superiority in load bearing capacity of flat sheets over structured sandwiches, their stiffnesses do not differ significantly. Vertical stiffness of lower beam flange made of structured sandwich sheets is approximately 20-30% lower, than of flat beams. When it comes to horizontal stiffness of flange, it is slightly higher by structured sandwiches than by flat sheets.

Despite the fact, that nowadays structured sheets are studied so that their application field is large because of their high rigidity, carried out investigations showed that structured sheet metal sheets behave variously in different load cases and as a components of different beams shapes [9, 79, 107, 108]. Unfortunately, structured plates are not completely studied in the context of application in structural building. Undoubtedly, structured plates have a big potential in building area and are worth future studying.

## 6 References

1. Bold J., Hoppe. M., Keller, S.:  
Bauteileigenschaften makrostrukturierter Feinbleche; Konferenz- Einzelbericht Band T 20; Fertigungsverfahren für den modernen Leichtbau, Fellbach 22./23 02 2000
2. Floß A., Hachmann B., Neubauer A.:  
Untersuchungen zur Anwendbarkeit hydrostatischer Umformverfahren für die Fertigung von versteiften, flächigen Formleichtbau-Komponenten und Prägeteilen aus Stahlfeinblech; Forschungsbericht p. 258; Studiengesellschaft Stahlanwendung e.V.; Verlag und Vertriebsgesellschaft GmbH, Düsseldorf 1998
3. Mirtsch F., Bränlich H.:  
Neuartige wölbstrukturierte Feinbleche - ein Beitrag zum Leichtbau im Fahrzeugbau  
Kolloquium Innovative Karosserieteilefertigung; Chemnitz, p. 17, 1996;
4. Kopp R.; Scholl C.:  
Metallische Hohlstrukturen; Konferenz Einzelbericht 10 Aachener Stahlkolloquium  
Umformtechnik— mit Kreativität zu innovativen Lösungen; Aachen 23 /24 03 95;  
p. 2.2-1 to 2.2-7
5. Casajus A.:  
Einsatz von strukturierten Blechen im modernen Stahlleichtbau, Konferenz Einzelbericht  
Band T 20; Fertigungsverfahren für den modernen Leichtbau; Hannover, 2000
6. Kopp. R., Lempnauer, K., Scholl, C.:  
Untersuchung der Fertigung und der Umformmöglichkeiten von doppellagigen, an  
einzelnen Stellen durch ein geeignetes Fügeverfahren verbundenen Blechtafeln  
(Twinbleche); Forschungsbericht P 260; Studiengesellschaft für Stahlanwendung e V.,  
Verlag und Vertriebsgesellschaft GmbH; Düsseldorf, 1997
7. Fertigung Nopal, Werkzeugbau; Firmenschrift Fa H. Diedrichs, Darmstadt, BRD
8. Vehlow, B.; Hillmann, J.; Welsch, F., Oehlerking, C.; Blümel, K. W.:  
Gewichtsreduzierung im Fahrzeugbau durch den Einsatz neuartiger Doppelblechstrukturen,  
In: VDI-Bericht Nr. 1398; VDI Verlag, Düsseldorf 1999; S. 283-300.
9. Hoppe, M.:  
Umformverhalten strukturierter Feinbleche. Dissertation Lehrstuhl Konstruktion und  
Fertigung BTU Cottbus, 2002.
10. N. N.: Meyers Taschenlexikon, Weltbild Verlag GmbH; Augsburg, 1999.
11. Website, address: <https://dictionary.cambridge.org/dictionary/english/structure>. Accessed:  
09.06.2017
12. Koller, R.:  
Konstruktionslehre für den Maschinenbau; Grundlagen zur Neu- und Weiterentwicklung  
technischer Produkte, 4 Auflage, Springer Verlag, Berlin, 1998.

## References

13. Conrad, K. J.:  
Grundlagen der Konstruktionslehre; Carl Hanser Verlag; München, 1998.
14. Hoppe, M.:  
Erarbeitung eines Formelemente-Kataloges für die automatische Zeichnungserkennung,  
Diplomarbeit; TU Dresden, 1991.
15. Sawilla, E.:  
Geometriestruktur technischer Produkte und ihr Informationsgehalt; Dissertation;  
Universität Stuttgart, 1988.
16. Wiedemann, J.:  
Leichtbau, Band 1; Elemente; 2. Auflage; Springer Verlag; Berlin, 1996.
17. Hufenbach, W.:  
Leichtbau mit höherfesten Stahlblechen und Tailored Blanks für eine innovative PKW-  
Fertigung; Konferenz-Einzelbericht, Band 733; Stahl für moderne Automobile;  
Einladungskolloquium, 2000, S. 63-71
18. Bleicher, W.:  
Konstruieren mit Aluminium; Aluminium-Taschenbuch, Düsseldorf, 1974.
19. Hellwig, U.; Neubauer, A.:  
Umformen von Nebenformelementen für Leichtbau— Strukturkomponenten In:  
Maschinenmarkt; Heft 21/97; S.26-31.
20. Hufenbach, W., Adam, F.:  
Strukturierung und Klassifizierung von Stahl Mehrschichtverbunden; Forschung für die  
Praxis P. 307; Studiengesellschaft für Stahlanwendung e.V.; Verlag und  
Vertriebsgesellschaft mbH; Düsseldorf, 1996.
21. Vollertsen, F., Hollmann, F.:  
Umformen strukturierter Platinen mit Mehrfachmembranen im Sinne eines robusten  
Fertigungsprozesses; DFG-Vorhaben SPP 1098; Wirkmedienbasierte Fertigungstechniken  
zur Blechumformung; Internetpräsentation 2001.
22. N. N. Chronik der Technik:  
Bertelsmann Lexikon Verlag GmbH; Gütersloh; München, 1995.
23. Königer, O.:  
Die Konstruktionen in Eisen; 6. Auflage; J. M. Gebhardt's Verlag; Leipzig, 1902.
24. Turner, P. St. J., Nowarra, H. J.:  
Junkers: an aircraft album No.3, Airco Publishing Co. pp. 17–20, New York, 1971
25. Schapitz, E.:  
Festigkeitslehre für den Leichtbau; VDI-Verlag GmbH; Düsseldorf, 1963
26. Schäfke, W.; Schleper, T.; Tauch, M.:  
Aluminium. Das Metall der Moderne; Kölnisches Stadtmuseum; Köln, 1991
27. Oehler, G.; Weber, A.:



## References

- Steife Blech- und Kunststoffkonstruktionen; Konstruktionsbücher, Band 30; Springer Verlag; Berlin, 1972
28. Oehler, G.:  
Fehlerhaftes und richtiges Gestalten gebogener und gezogener Blechteile; Referatauszug zur Arbeitsgruppentagung am 03.03.1955
29. Oehler, G.:  
Die Versteifung von Karosserie-Bleefeldern durch Sicken und Querschnittsgestaltung selbsttragender Schalen; In ATZ 61; Heft 5/59
30. Oehler, G.:  
Sickenversteifte Blechkonstruktionen; In Konstruktion; Heft 12/70; p. 481.
31. Herrmann, F.; Kiehn, H.; Stäblein, R.:  
Lebensdauer von Blechen mit Sicken; FAT-Bericht Nr. 128; Frankfurt am Main, 1996.
32. Herrmann, F., Maiwald, J.; Schriever, T.:  
Festigkeits- und Steifigkeitsverhalten von dünnen Blechen mit Sicken; FAT-Bericht Nr.06, Frankfurt am Main, 1994
33. Kienzle, O.:  
Versteifung ebener Böden und Wände; DFBO-Mitteilung; Hell 7/55; p. 77-83 u. Heft13/55; S. 153-160.
34. Werkzeugbau; Firmenschrift Fa. Ecrans Thermiques; Thourace, France
35. Systeme für die Fahrzeugtechnik und die Innenausstattung; Firmenschrift Fa. Faist Automotive; Krumbach, BRD
36. Kainer, K. U., von Buch, F.:  
Moderne Entwicklungen von Legierungen für den Leichtbau; In: Materialwissenschaft und Werkstofftechnik, Heft 30/99, S. 159-167.
37. Hartmann, G.; Münschenborn, W.; Schneider, C.; Simon, R.:  
Höherfeste Feinbleche und neue Blechkomponentern für den Automobilleichtbau; Konferenz Einzelbericht; Neuere Entwicklungen in der Blechumformung, Fellbach 07/08.05.1996; S. 47-119.
38. Diedrichs, H.:  
Raffen und Recken; In Bänder Bleche Rohre; Heft 3/95; S. 40-41
39. Diedrichs, H.:  
Genoppt oder glatt; In Konstruktionspraxis; Heft 9/95; S. 62.
40. Hellwig, U.; Görlich, T.; Nikolaus, H.:  
Anwendungstechnische Untersuchungen zur Beul- und Faltstrukturierung von dünnwandigen Stahlrohren-Machbarkeitsstudie und prospektive Marktanalyse; Forschungsbericht P 291; Studiengesellschaft für Stahlanwendung e.V.; Verlag und Vertriebsgesellschaft mbH; Düsseldorf, 1997.
41. Casajus, A.; Hering, L.; Rauer, J.:

## References

- Einsatz von Flachstahlprofilen in der Bauindustrie; Konferenz-Einzelbericht; Fachtagung; Walzprofilieren; Darmstadt, 06.09.2000.
42. Pauly, T.  
Edelstahl Rostfrei - Dekorative Oberflächen im Bauwesen; In Stahlmarkt; Heft 10/96; S. 60-66.
  43. N.N.: Wölbstruktur mit Perspektiven;  
In. Automobil- Produktion; Heft 6/98; S. 112
  44. Mirtsch, F.; Büttner, O.; Ellert, J.; Kunke, E.; Bräunlich, H.:  
Neuartige wölbstrukturierte Materialien - Eigenschaften und Einsatzpotentiale; Konferenz - Einzelbericht; Karosseriebau; Helt 14/1996; S. 57, 59-69.
  45. Giebel, M.; Reiner, T.:  
König der Dosen; In: Neue Verpackung; Heft 7/96; S. 14
  46. N. N.: Schwierige Bauteile sicher handhaben; In Fertigung; Heft 3/96; S. 42-44.
  47. Gordon, J. E.:  
The Science of Structures and Materials; The Scientific American Library, A Division of HPHLP, Scientific American Library; New York, 1988.
  48. Mustergewalzte Bleche; Firmenschrift Fa. Strukturmetall; Bretzfeld, BRD.
  49. DIN 8585-1:2003-09: Manufacturing processes forming under tensile conditions - Part 1: General; Classification, subdivision, terms and definitions
  50. Gebrauchsmuster 9405950, Strukturblech mit in einem Rechteckmuster angeordneten Prägungen; Gerhardi & Cie GmbH, 1994.
  51. Spur, G., Stöferle, Th.:  
Handbuch der Fertigungstechnik; Band 2/1; Carl Hanser Verlag; München, 1983.
  52. Spur, G.; Stöferle, Th.:  
Handbuch der Fertigungstechnik; Band 2/3; Carl Hanser Verlag; München, 1985.
  53. Website, address: <https://julongppgi.en.made-in-china.com/product/EBbQDeUMbkRN/China-Full-Hard-Metal-Sheet-Galvanized-Gi-Gl-Z40-60-Roofing-Sheet.html>. Accessed: 15.04.2016
  54. Fa. Achenbach; Internetpräsentation
  55. Mirtsch, F.:  
Verfahren zur Verformung dünnwandiger Bleche und Folien, Patent DE4311978 C1; 1993.
  56. Ostermann, F.:  
Anwendungstechnologie Aluminium; Springer Verlag; Berlin 1998.
  57. N. N.: More rigid, yet much lighter; In: Aluminium; Heft 3/98; S. 102 - 103, 106.
  58. Mirtsch, F.; Rötzel, W.:  
Measuring local heat transfer coefficients on profiled walls of heat exchangers; In: New Developments in Heat Exchangers; 167/177; Gordon and Breach Publishers; OPA Amsterdam B. V., 1996.

## References

59. Website, address: <https://ifworlddesignguide.com/entry/19687-hexal-langfeldleuchte>.  
Accessed: 19.09.2017
60. Website, address: [https://woelbstruktur.de/referenzen/bump\\_structured\\_washing\\_mashine\\_drum.php](https://woelbstruktur.de/referenzen/bump_structured_washing_mashine_drum.php). Accessed: 25.11.2016
61. Weidner, T.:  
Untersuchungen zu Verfahren und Werkzeugsystemen der wirkmedienbasierten Blechumformung; Dissertation; Universität Dortmund; Shaker Verlag; Aachen, 1999.
62. Magnusson, C.; Skare T.:  
Hydroblechumformung zur Herstellung von Katosserieteilen; Konferenz-Einzelbericht; Neuere Entwicklungen in der Blechumformung; Fellbach 23/24.05 2000; MAT INFO Werkstoff-Informationsges GmbH; Frankfurt, 2000.
63. Lange, K.:  
Umformtechnik, Band 3; 2 Auflage, Springer Verlag, Berlin, 1990.
64. DIN 8584-1:2003-09: Manufacturing processes forming under combination of tensile and compressive conditions – Part 1: General; Classification, subdivision, terms and definitions
65. Website, address: <https://www.schlosserei-vogel.com/carports-ulm.php>. Accessed: 15.02.2017
66. DIN 8580:2003-09: Manufacturing processes - Terms and definitions, division
67. Website, address: [https://www.iph-hannover.de/de/dienstleistungen/fertigungsverfahren/umformen/#:~:text=Unter%20dem%20Begriff%20%E2%80%9EUmformen%22%20wird,Umformen%20eine%20Hauptgruppe%20der%20Fertigungsverfahren](https://www.iph-hannover.de/de/dienstleistungen/fertigungsverfahren/umformen/#:~:text=Unter%20dem%20Begriff%20%E2%80%9EUmformen%22%20wird,Umformen%20eine%20Hauptgruppe%20der%20Fertigungsverfahren.). Accessed: 10.03.2017
68. DIN 8583-1:2003-09: Manufacturing processes forming under compressive conditions – Part 1: General; Classification, subdivision, terms and definitions
69. DIN 8586:2003-09: Manufacturing processes forming by bending - Classification, subdivision, terms and definitions
70. DIN 8587:2003-09: Manufacturing processes forming under sheering conditions - Classification, subdivision, terms and definitions
71. Ossenbrink R.:  
Presentation „Innovationen im Leichtbau. Weiterverarbeitungstechnologien für strukturierte Bleche“, website: <http://docplayer.org/52428992-Innovationen-im-leichtbau-weiterverarbeitungstechnologien-fuer-strukturierte-bleche-dr-ing-ralf-ossenbrink.html>.  
Accessed: 20.04.2017
72. Das sind Formen; Firmenschrift Fahde; Konstruktionspraxis (Sonderdruck); Heft 4/5
73. Bohmann, D.; Dahl, W.; Dilthey, U.; Hachmann, B.; Lüders, F.; Nicklas, D.; Paschen, M.; Sedlacek, G.:

## References

- Praxisreifmachung der Produktion, Verarbeitung und Anwendung von Höckerbleche  
Forschungsbericht P.241; Studiengesellschaft für Stahlwendung e.V.; Verlag und  
Vertriebsgesellschaft mbH; Düsseldorf 1998
74. Neubauer, A.; Robroek, L. M. J.; Schweitzer, K. H.:  
Hydrostatisches Streckumformen von Nebenformelementen für Strukturbleche aus  
Shahlfeinblech; In Bänder Bleche Rohre; Heft 5/98
75. Schiefenbusch, J., Witte, S., Kleiner, M. et al. (eds.):  
Das Höckerblech, ein universelles Bauelement, Umformtechnik, B. G. Teubner Stuttgart  
1992
76. Cordes, P.; Hüller, V.:  
Moderne Stahl-Leichtbaustrukturen für den Schienenfahrzeugbau; In: Blech Rohre Profile;  
Heft 12/95; S. 773-777
77. Chiesa L.: Animated hydroforming, animation, CC BY-SA 3.0  
<http://creativecommons.org/licenses/by-sa/3.0/2006>. Accessed: 24.02.2023
78. Website, address: <https://patents.google.com/patent/US2713314>. Accessed: 27.04.2018
79. Bartholomé, S.:  
Grundlegende Untersuchungen zu strukturierten Blechen in Stahlleichtbauträgern  
(Fundamental investigations on light weight steel girders with structured webs), Doctoral  
thesis, ISSN 1611-5023; Cottbus 2015
80. Malikov V.:  
Experimentelle und numerische Untersuchungen der Umformung von strukturierten  
Blechen, Doctoral thesis, Cottbus 2013
81. Olbrich, S.; Viehweger, B.; Schölzke, T.:  
Prozesssichere Herstellung von FQZ-Wabenstrukturen durch Hydroforming, Bänder Bleche  
Rohre, Jahrgang 53, S.66-67, 2012.
82. Henning, F.; Moeller, E.:  
Handbuch Leichtbau – Methoden, Werkstoffe, Fertigung. München: Hanser Verlag, 2011.
83. Schluß, L.:  
Fügen strukturierter Bleche. Widerstandpunkt und Metallschutzgas-Schweißen; Doctoral  
thesis; Band 11, ISBN 978-3-8440-5815-4, Shaker Verlag, 2017
84. Malikov, V.; Ossenbrink, R.; Viehweger, B.; Prof. Dr.-Ing. habil. Michailov, V.:  
Analytical and numerical calculation of the force and power for air bending of structured  
sheet metals. Key Engineering Materials Vol .473, S.602-609, Trans Tech Publications,  
2011.
85. Kazak, F., Schluß, L., Ossenbrink, R., Weiss, S., Prof. Dr.-Ing. habil. Michailov, V.:  
Particularities of testing structured sheet metals in 3-point bending tests, Materials and  
testing, Carl Hanser Verlag, München, 2016, 58 (2016)/6, S.495-500, DOI  
10.3139/120.110883, ISSN 0025-5300

## References

86. Mirtsch, M., Yadav, A.:  
Structured sheet metal - Part I Comparing processes, Stamping journal, 2006.
87. Mirtsch, F.:  
Bionic-Method of Efficient Light-Weight Production, Proceedings from Global Conference Sustainable Products, 29.9.2004 -1.10.2004, p. 97.
88. Website, address: <https://www.thefabricator.com/stampingjournal/article/metalsmaterials/structured-sheet-metal---part-i>. Accessed: 06.08.2017
89. Mirtsch, M., Yadav, A.:  
Structured sheet metal - Part II Comparing processes, Stamping journal, 2006.
90. Website, address: [http://www.woelbstruktur.de/info/baumetall\\_odessa.pdf](http://www.woelbstruktur.de/info/baumetall_odessa.pdf). Accessed: 28.09.2018
91. Bräunlich, H.:  
Innenhochdruck-Umformen von Al- und Mg- Legierungen, Workshop Leichtbau, Bautzen, 2005.
92. Rüter, M.:  
Wabenstrukturen, Leicht und gleichzeitig stabil. Website, address: <http://suite101.de/article/wabenstrukturen-a46666>. Accessed: 20.12.2017
93. Bmbf, Referat 423: Integrierter Umweltschutz in der Wirtschaft (Hrsg.): Leicht und ansprechend – stabil verpackt, Berlin, 2000.
94. Website, address: <https://www.esb-group.com/produkte-din-en/kaltgewalzter-stahl>. Accessed: 03.04.2019
95. Fritzsche S., Ossenbrink R., Prof. Dr.-Ing. habil. Michailov V.:  
Experimental characterization of structured sheet metal, Key Engineering Materials Vol.473, S.404-411, Trans Tech Publications, 2011.
96. DIN EN ISO 6892, Metallic materials - Tensile testing - Part 1, December 2009
97. Web site, address: <http://www.gom.com/de/messsysteme/systemuebersicht/aramis.html>. Accessed: 14.06.2017
98. DIN 50125, Testing of metallic materials, Tensile test specimens, Directions for their preparation, December 2016
99. Website, address: <https://www.3ds.com/products-services/simulia/products/abaqus/>. Accessed: 18.05.2018
100. EN 1993-1-3:2006: Eurocode 3: Design of steel structures – Part 1-3: Supplementary rules for cold-formed members and sheeting. CEN. Brussels 2006.
101. Abaqus Analysis User's Manual, Version 6.11-3, Dassault Systems, 2013.
102. EN 1993-1-5: Eurocode 3: Design of steel structures – Part 1-5: General rules – Plated structural elements. CEN. Brussels 2006.
103. Beg D., Kuhlmann U., Davaine L., Braun B.:

## References

- Design of plated structures Eurocode 3: Design of steel structures Part 1-5 – Design of plated structures. 1<sup>st</sup> Edition, ECCS, Berlin 2010
104. Fu F.:  
Design and Analysis of Complex Structures, Design and Analysis of Tall and Complex Structures, 2018
105. Kalkan E., Okur F.Y., Altunışık A.C.:  
Applications and usability of parametric modeling, Journal of Construction Engineering, Management & Innovation 2018 Volume 1, Issue 3, pp. 139-146, Trabzon, Turkey, 2018
106. Kästner J., Eckhart A.:  
When can a Computer Simulation act as Substitute for an Experiment? A Case-Study from Chemistry, Website, address:  
[https://eckhartarnold.de/papers/2013\\_Simulations\\_as\\_Virtual\\_Experiments/node4.html](https://eckhartarnold.de/papers/2013_Simulations_as_Virtual_Experiments/node4.html).  
Accessed: 21.04.2019
107. Shlychkova D., Pasternak H.:  
Numerical analysis of lightweight structured sandwich beams made of steel, Proceedings XVI International Scientific Conference VSU, pp.318-323, Sofia 2016
108. Shlychkova D., Pasternak H.:  
Numerical analysis and laboratory experiments of lightweight structured sandwich beams made of steel, Proceedings XVII International Scientific Conference VSU, pp.252-260, Sofia 2017
109. World Archaeology:  
History of Corrugated Iron, Website, address: <https://www.world-archaeology.com/features/history-of-corrugated-iron/>. Accessed: 30.08.2019

## 7 Appendixes

### Appendix A to Chapter 3: Laboratory experiments of C-sectioned beams (at the end of loading)

#### A.1 Beam 1

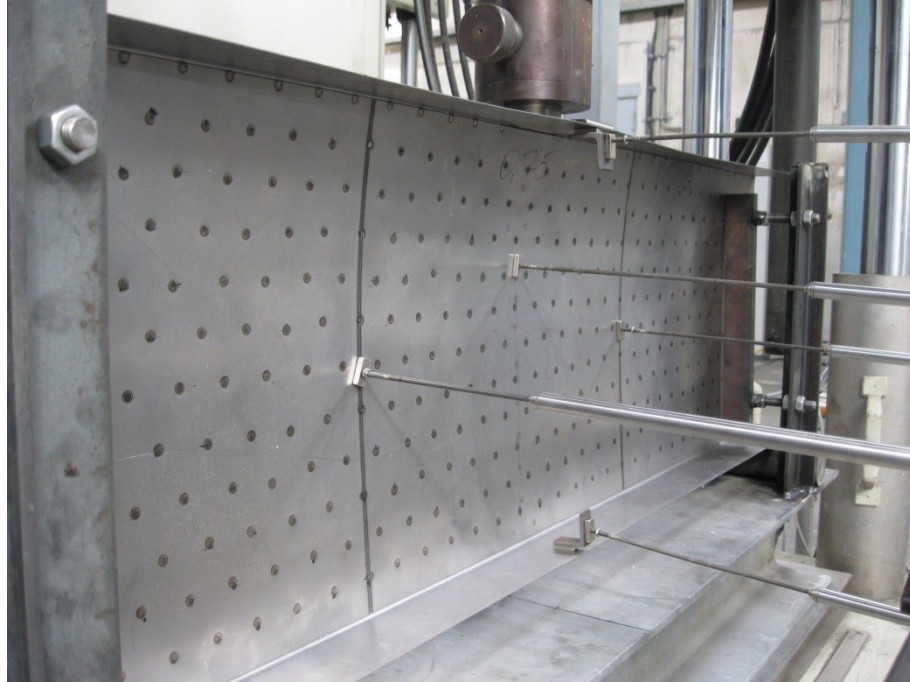


Figure 7.1. Beam 1 side view (flat 0.75 mm + flat 0.50 mm)

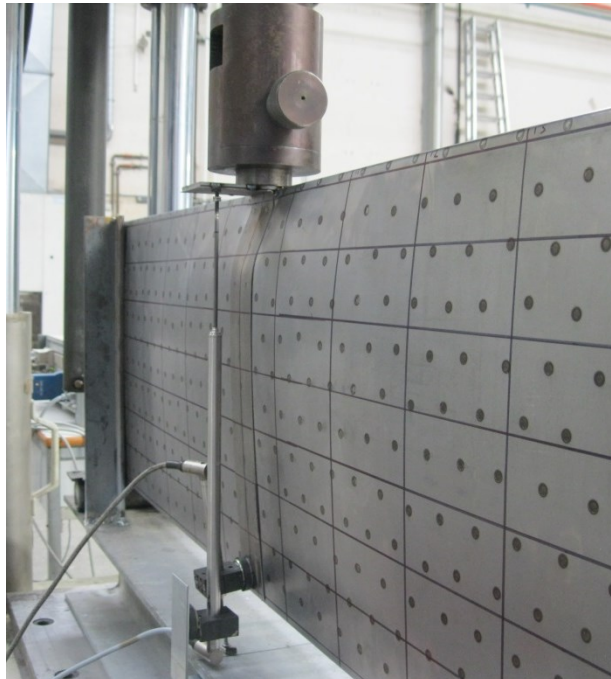


Figure 7.2. Beam 1 back view (flat 0.75 mm + flat 0.50 mm)

**A.2 Beam 2**

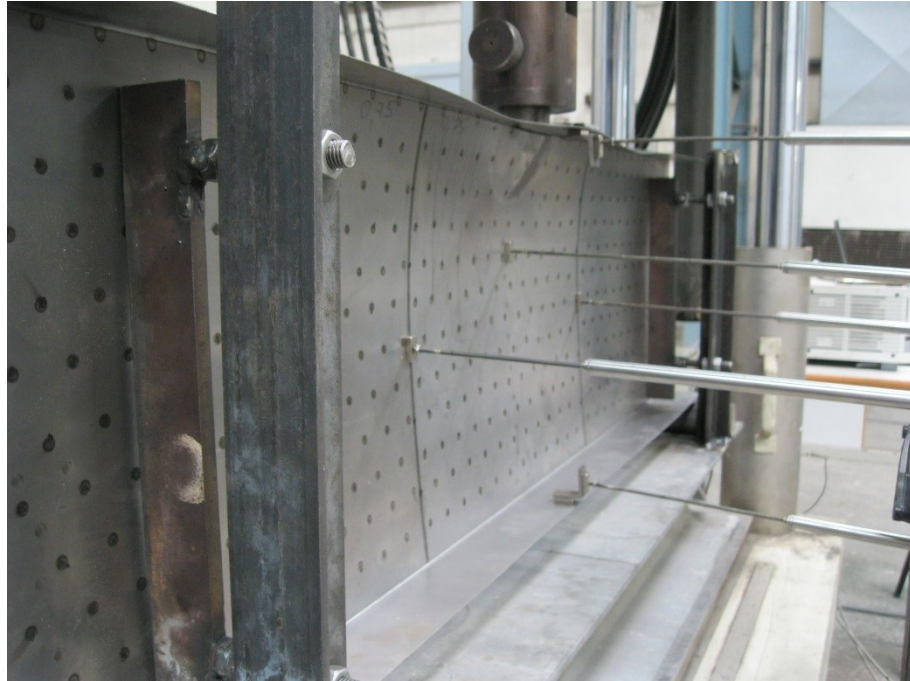


Figure 7.3. Beam 2 side view (flat 0.75 mm + flat 0.50 mm)

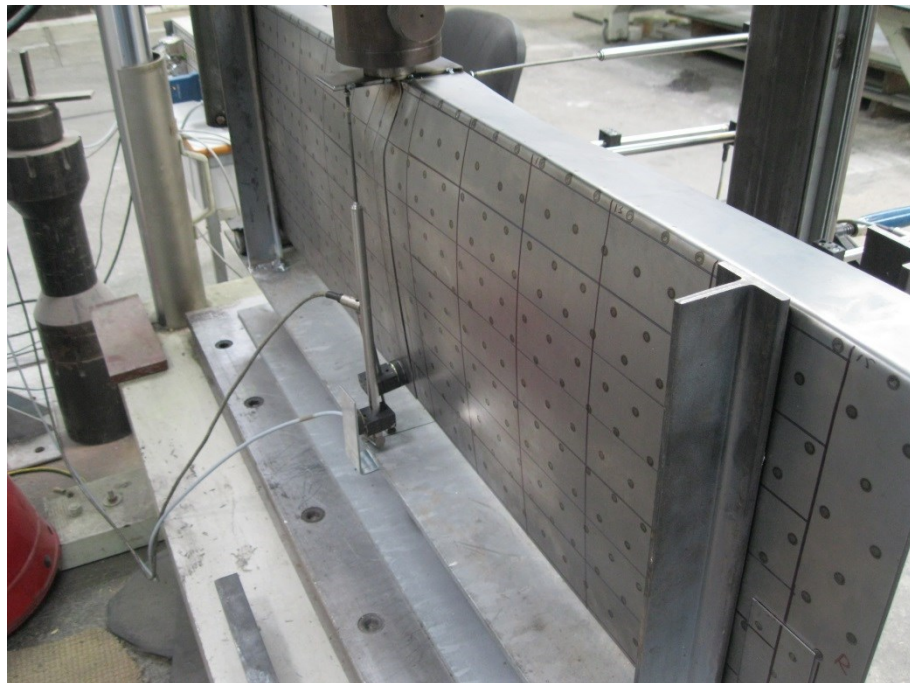


Figure 7.4. Beam 2 back view (flat 0.75 mm + flat 0.50 mm)



**A.3 Beam 3**

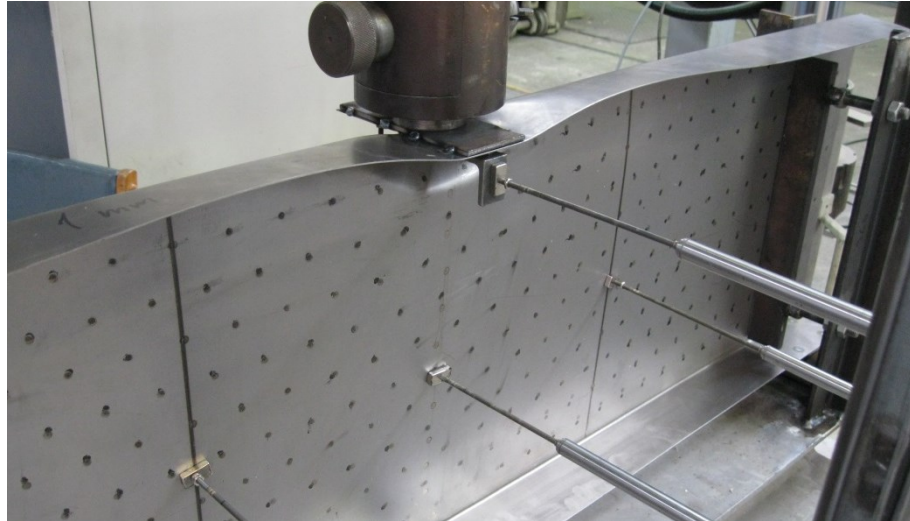


Figure 7.5. Beam 3 side view (flat 1.00 mm + flat 0.50 mm)



Figure 7.6. Beam 3 back view (flat 1.00 mm + flat 0.50 mm)

**A.4 Beam 4**

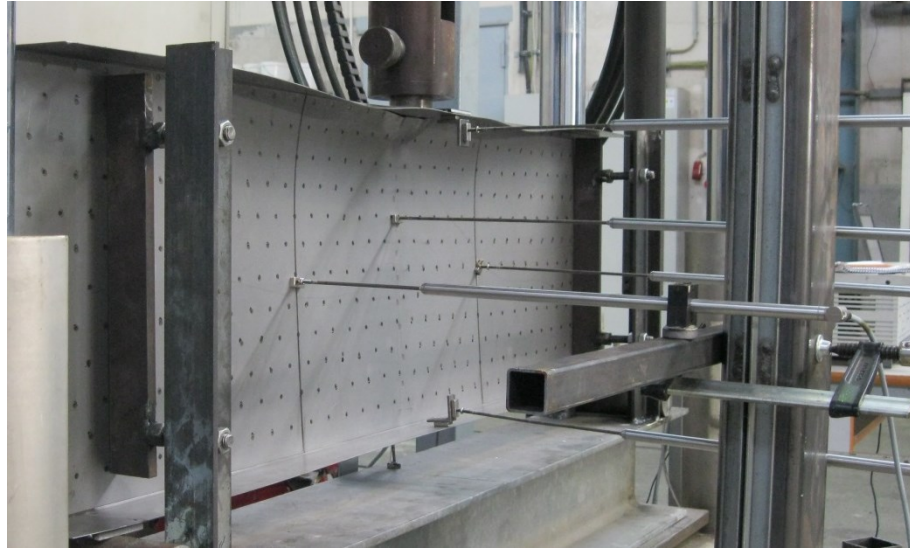


Figure 7.7. Beam 4 side view (flat 1.00 mm + flat 0.50 mm)

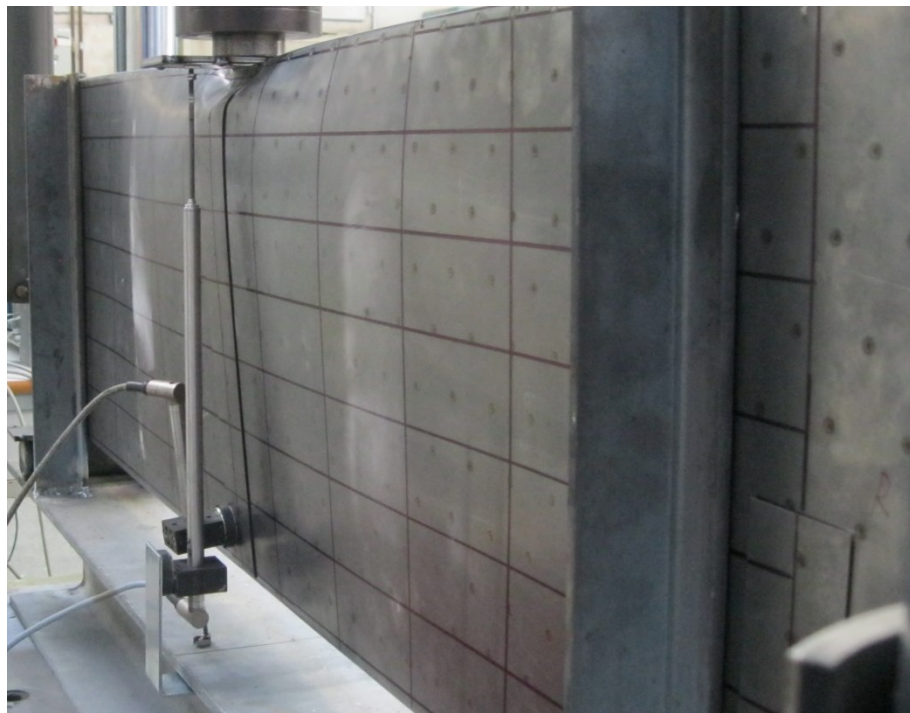


Figure 7.8. Beam 4 back view (flat 1.00 mm + flat 0.50 mm)

**A.5 Beam 5**

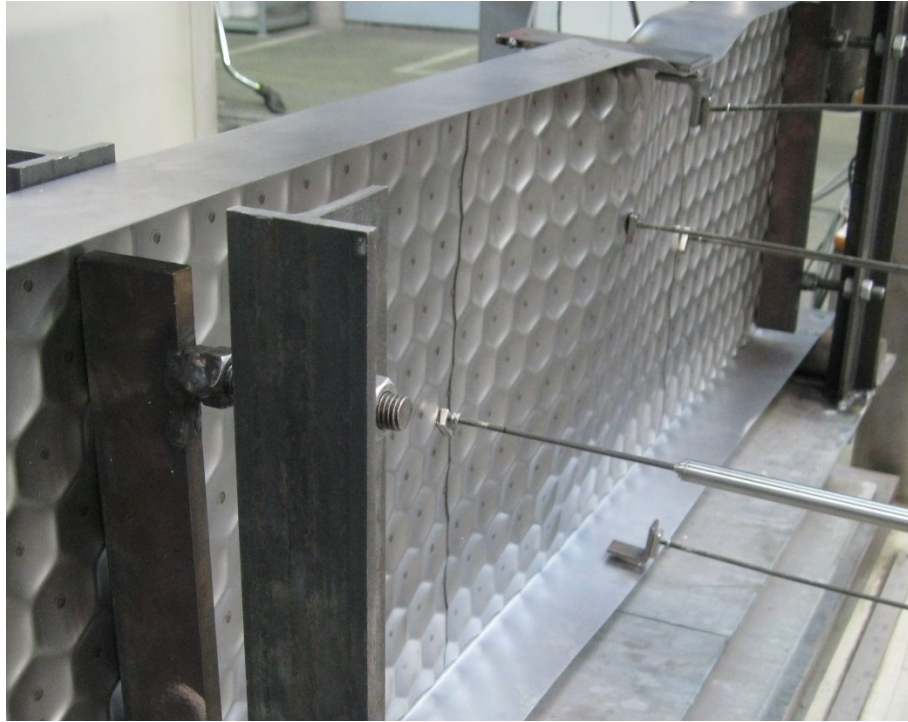


Figure 7.9. Beam 5 side view (flat 0.75 mm + structured 0.50 mm)

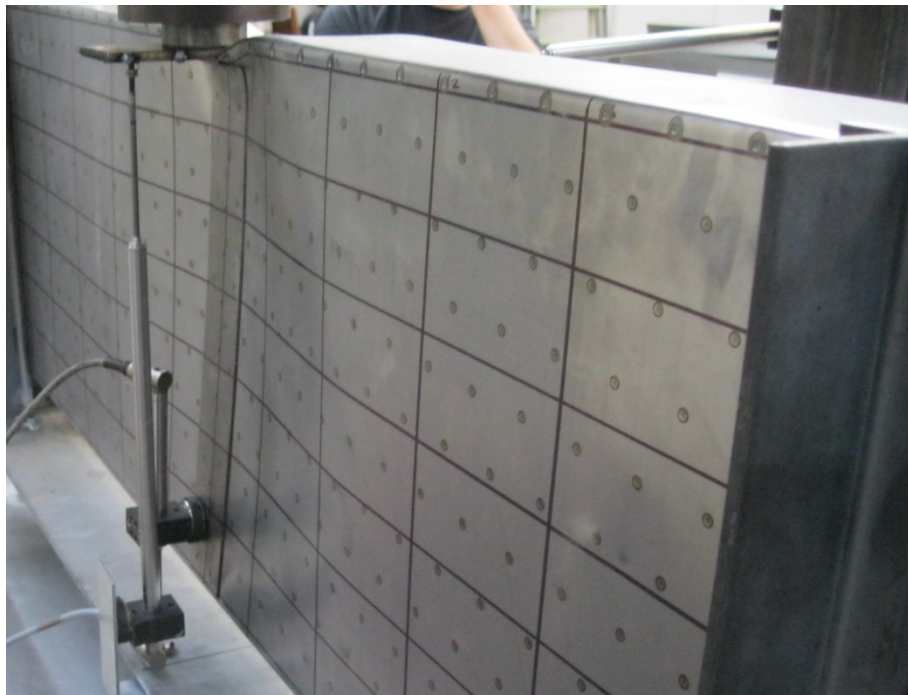


Figure 7.10. Beam 5 back view (flat 0.75 mm + structured 0.50 mm)

**A.6 Beam 6**

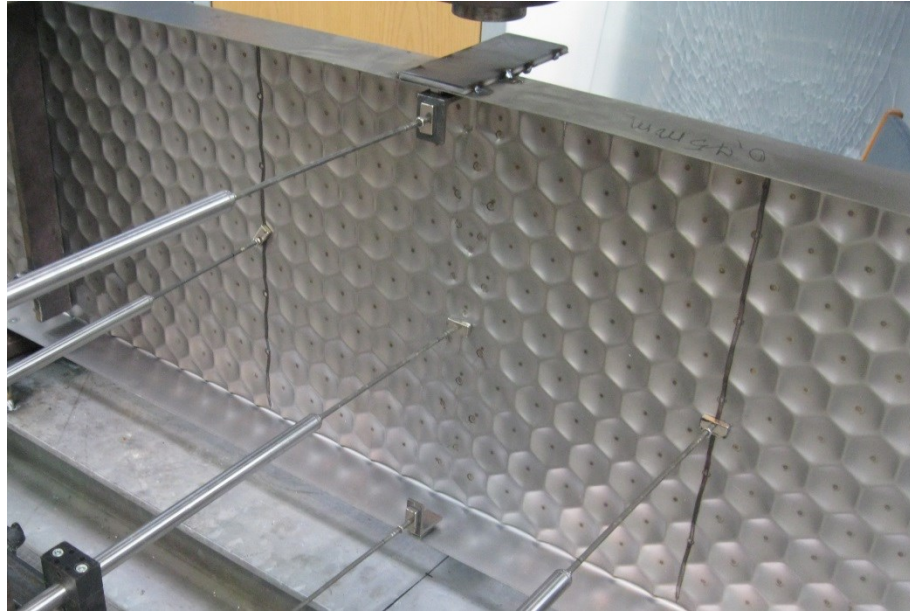


Figure 7.11. Beam 6 side view (flat 0.75 mm + structured 0.50 mm)

**A.7 Beam 7**

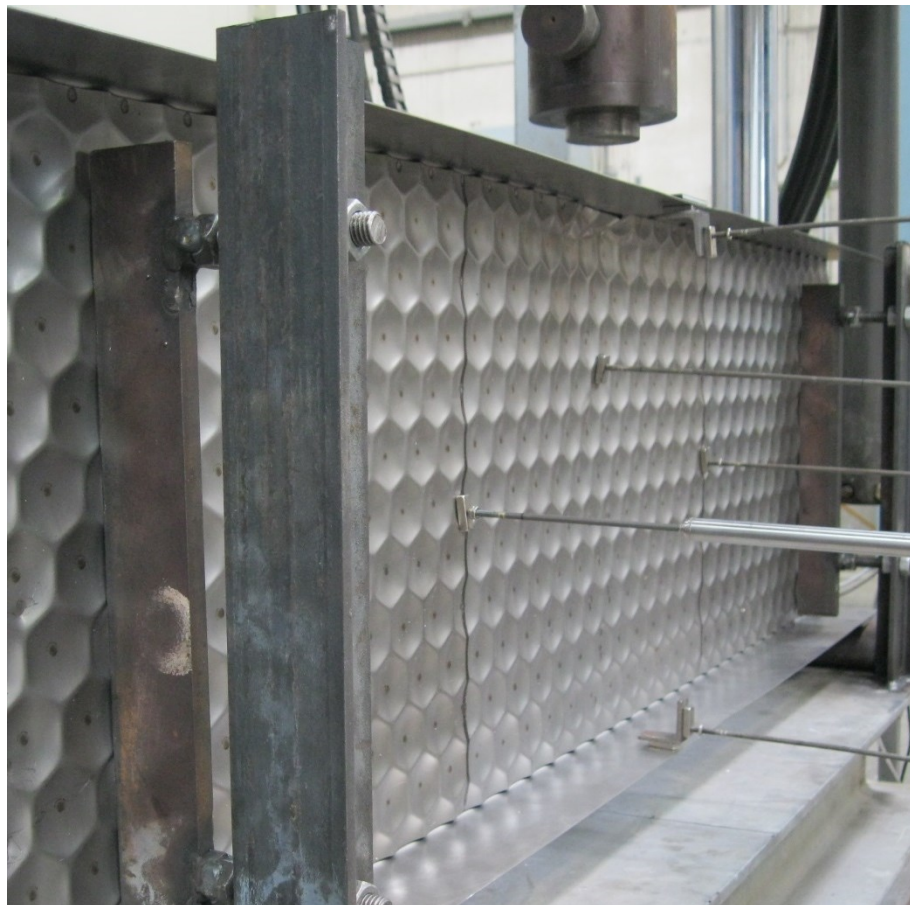


Figure 7.12. Beam 7 side view (flat 1.00 mm + structured 0.50 mm)



Figure 7.13. Beam 7 back view (flat 1.00 mm + structured 0.50 mm)

### A.8 Beam 8

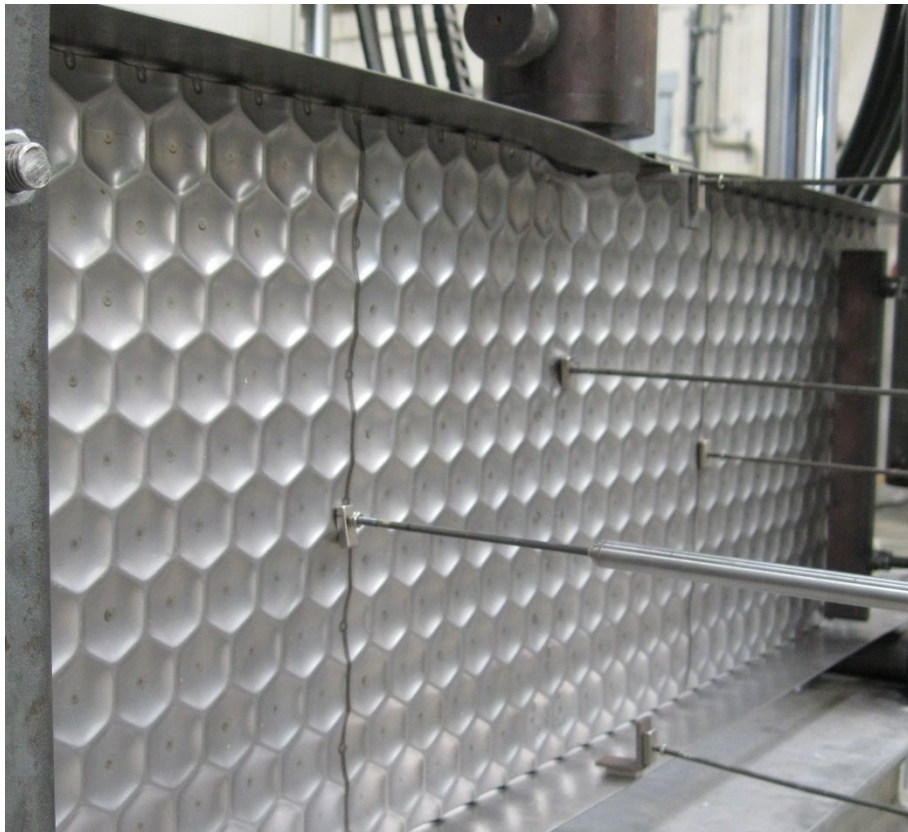


Figure 7.14. Beam 8 side view (flat 1.00 mm + structured 0.50 mm)



Figure 7.15. Beam 8 back view (flat 1.00 mm + structured 0.50 mm)

## Appendix B to Chapter 3: FEM simulations of C-sectioned beams (under maximal force)

### B.1 Beam type 1

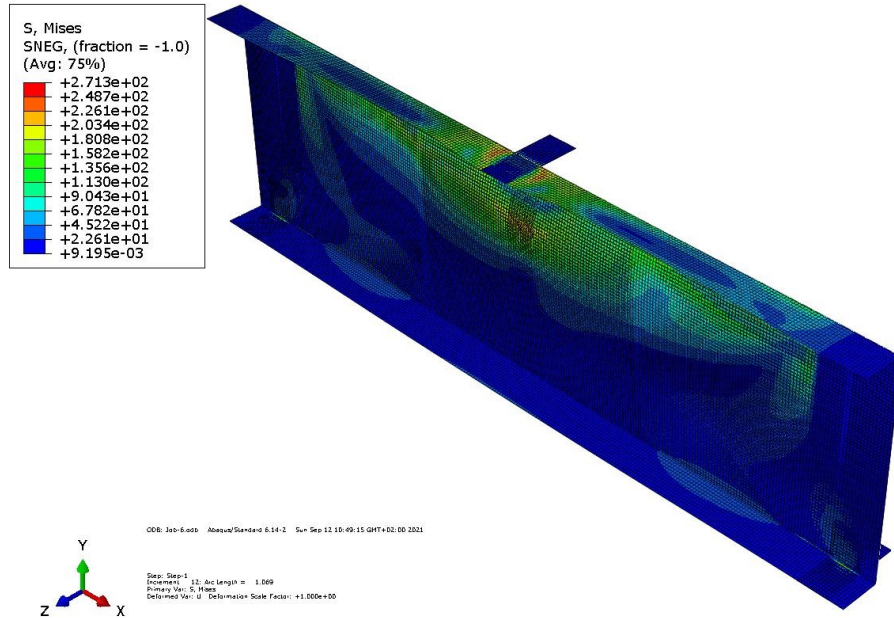


Figure 7.16. Beam type 1 (flat 0.75 mm+flat 0.50 mm), stress distribution in MPa

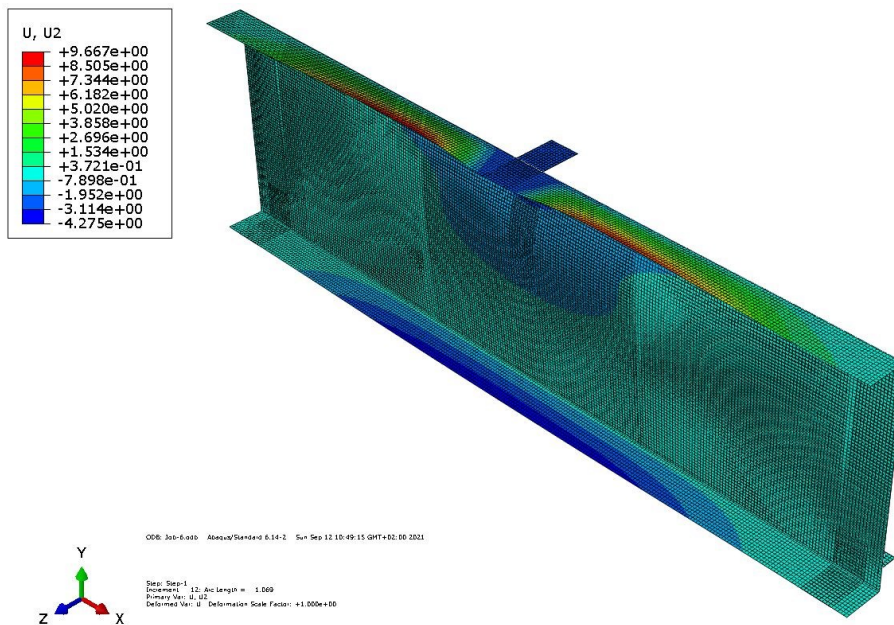


Figure 7.17. Beam type 1 (flat 0.75 mm+flat 0.50 mm), Y-distribution displacement in mm

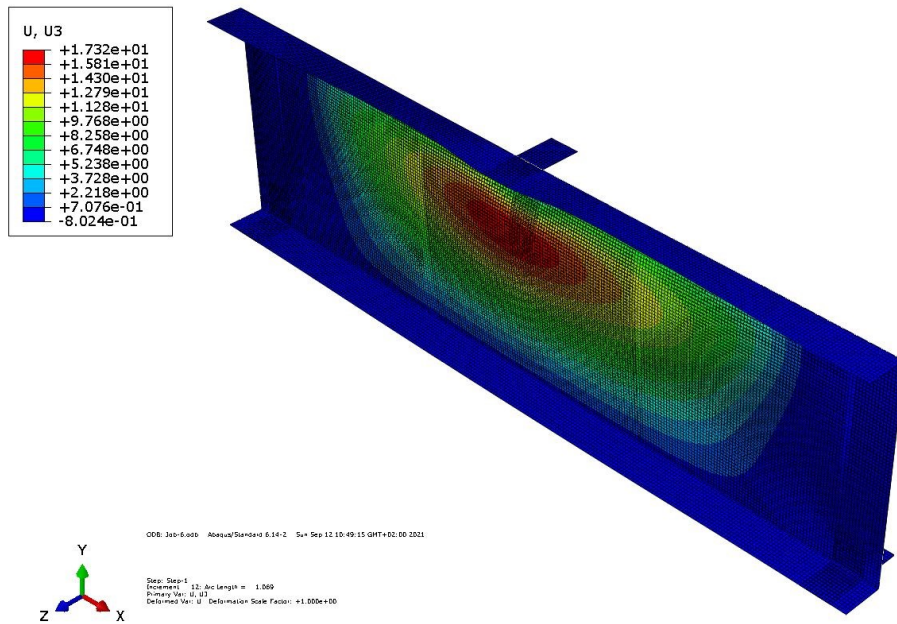


Figure 7.18. Beam type 1 (flat 0.75 mm+flat 0.50 mm), Z-distribution displacement in mm

## B.2 Beam type 2

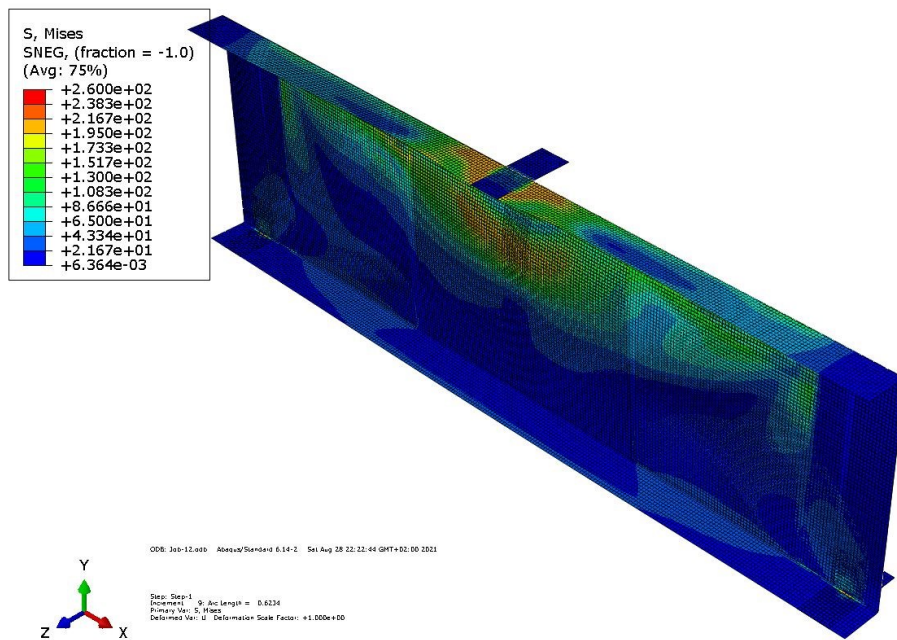


Figure 7.19. Beam type 2 (flat 1.00 mm+flat 0.50 mm), stress distribution in MPa



Appendix B to Chapter 3

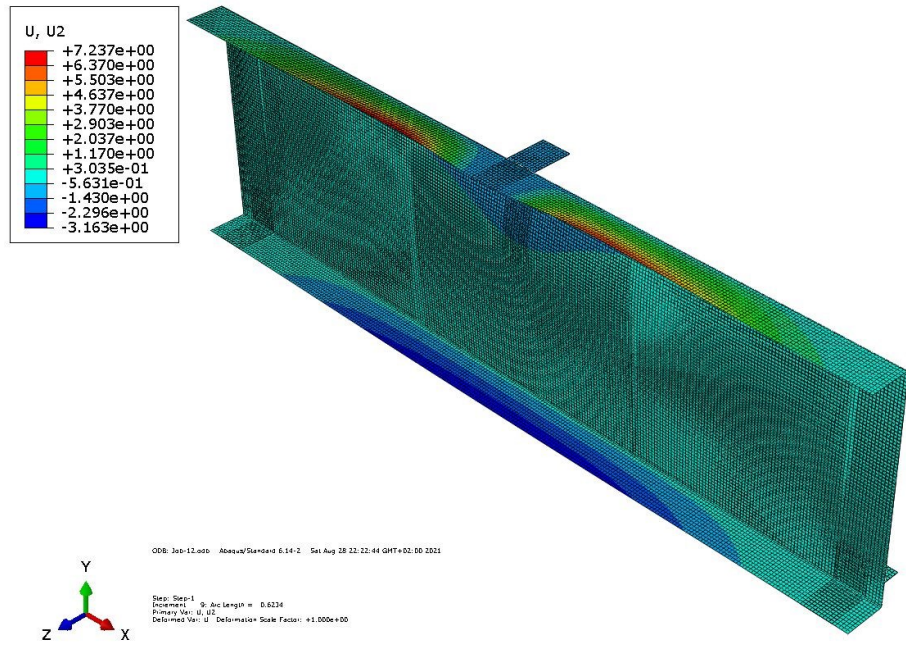


Figure 7.20. Beam type 2 (flat 1.00 mm+flat 0.50 mm), Y-distribution displacement in mm

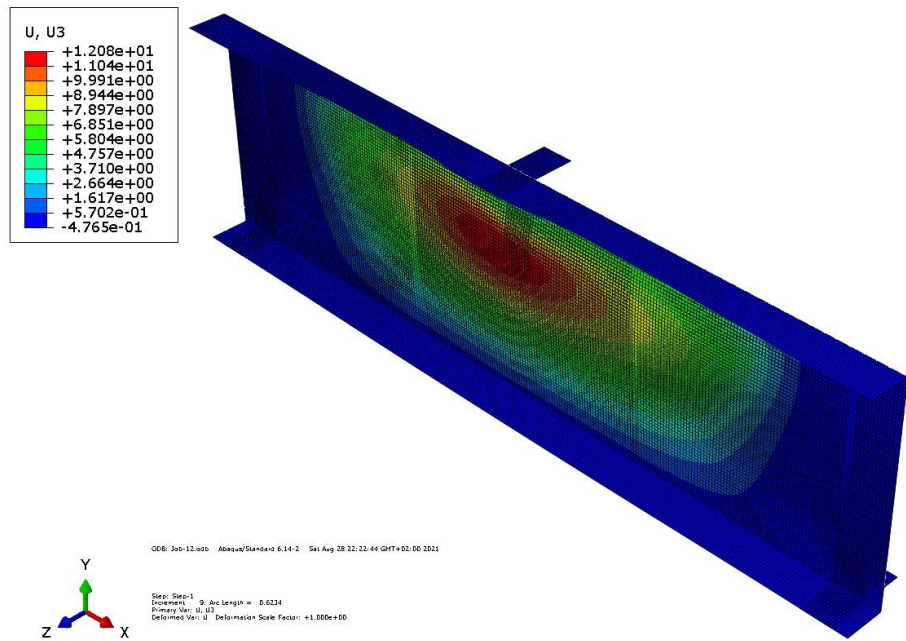


Figure 7.21. Beam type 2 (flat 1.00 mm+flat 0.50 mm), Z-distribution displacement in mm

B.3 Beam type 3

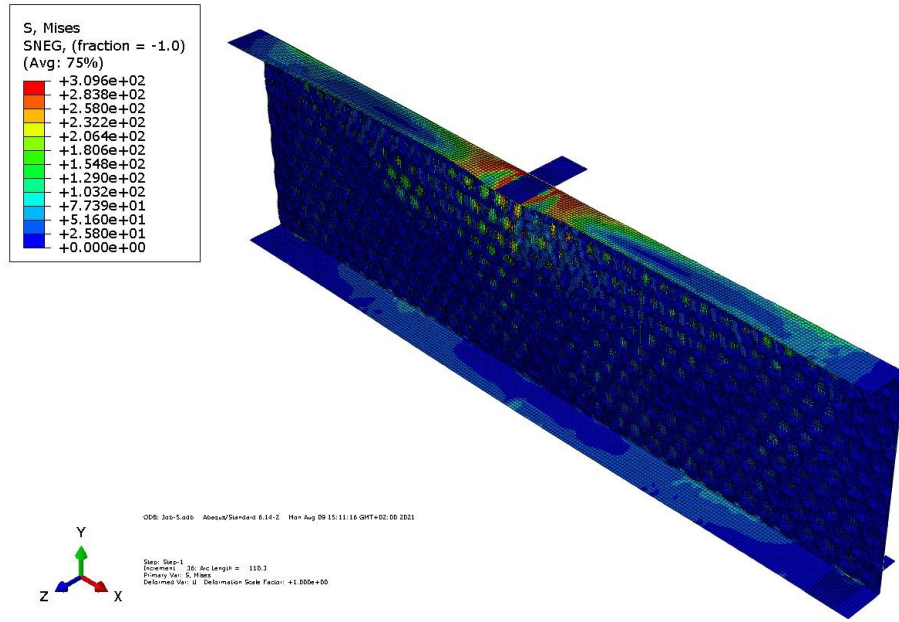


Figure 7.22. Beam type 3 (flat 0.75 mm+structured 0.50 mm), stress distribution in MPa

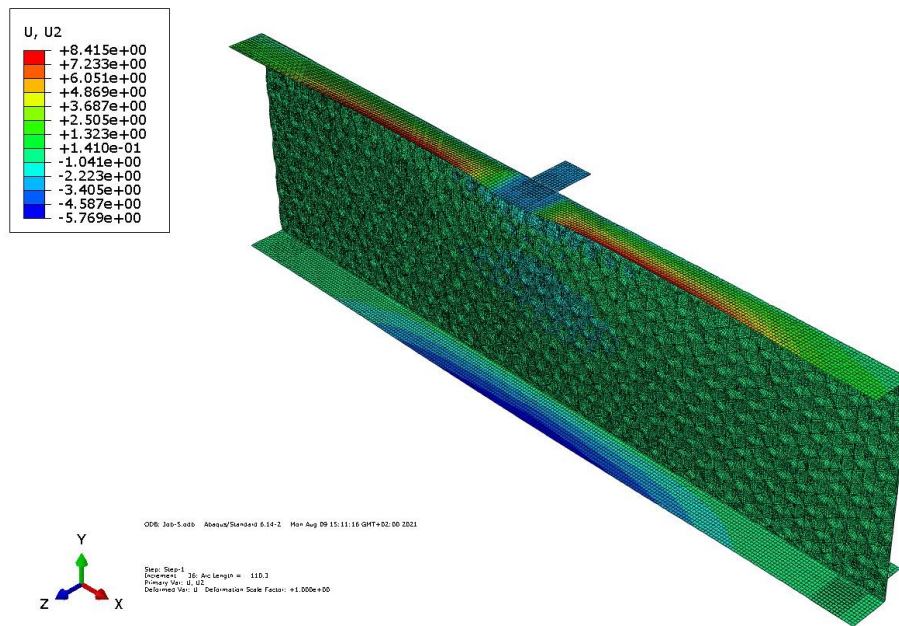


Figure 7.23. Beam type 3 (flat 0.75 mm+structured 0.50 mm), Y-distribution displacement in mm

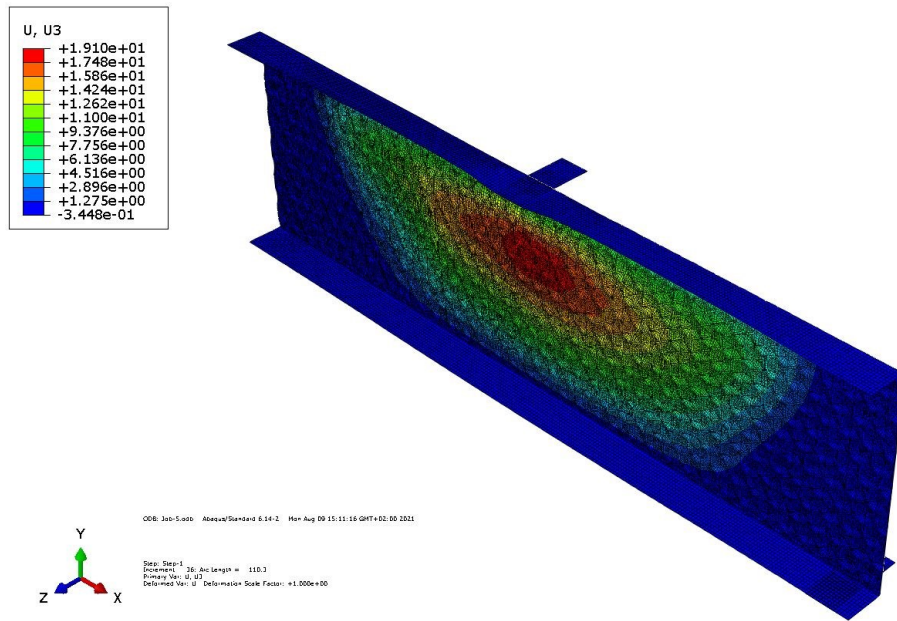


Figure 7.24. Beam type 3 (flat 0.75 mm+structured 0.50 mm), Z-distribution displacement in mm

### B.4 Beam type 4

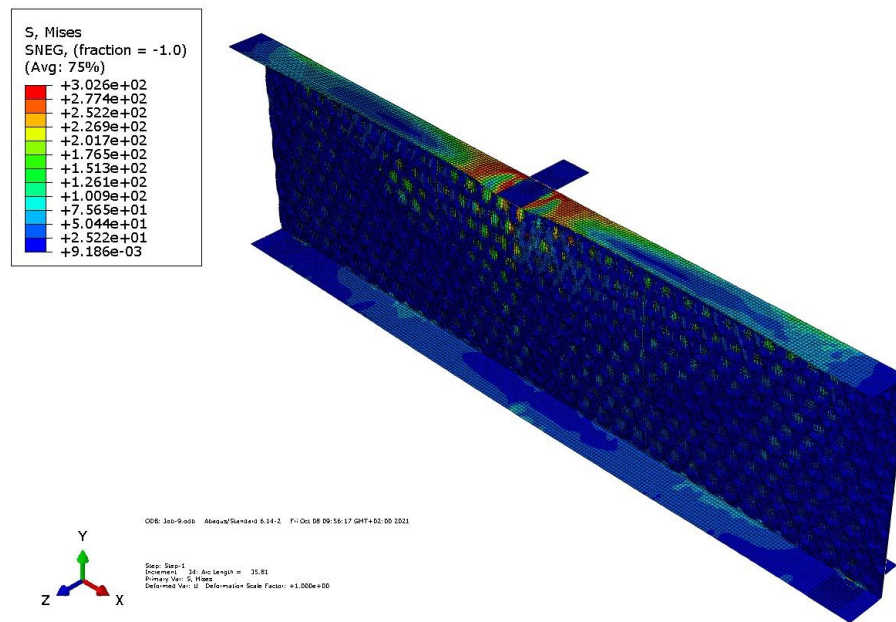


Figure 7.25. Beam type 4 (flat 1.00 mm+structured 0.50 mm), stress distribution in MPa

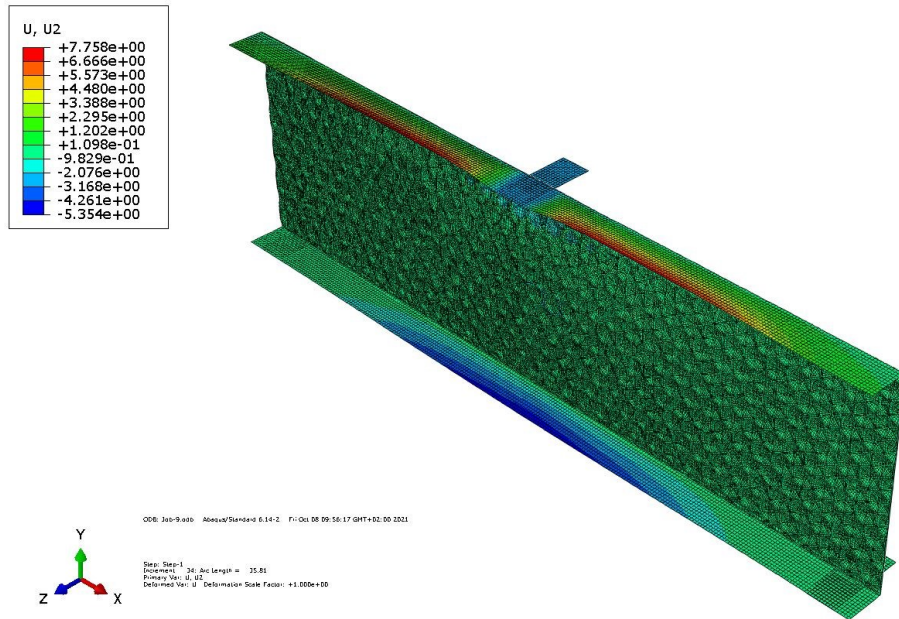


Figure 7.26. Beam type 4 (flat 1.00 mm+structured 0.50 mm), Y-distribution displacement in mm

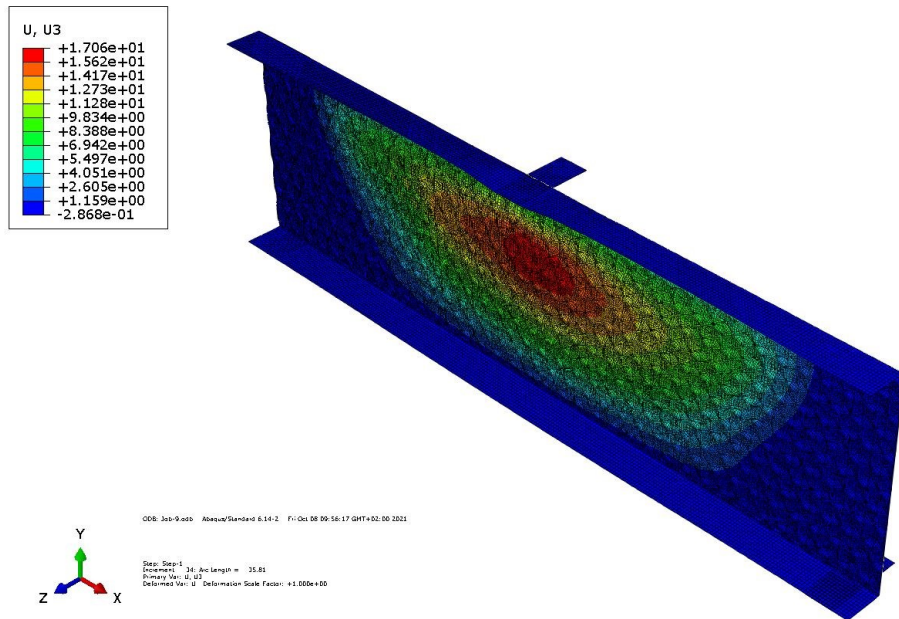


Figure 7.27. Beam type 4 (flat 1.00 mm+structured 0.50 mm), Z-distribution displacement in mm

## Appendix C to Chapter 4: Laboratory experiments of squared-sectioned beams (at the end of loading)

### C.1 Beam 1



Figure 7.28. Beam 1 side view (flat 1.25 mm)



Figure 7.29. Beam 1 front view (flat 1.25 mm)



Figure 7.30. Beam 1 back view (flat 1.25 mm)

C.2 Beam 2

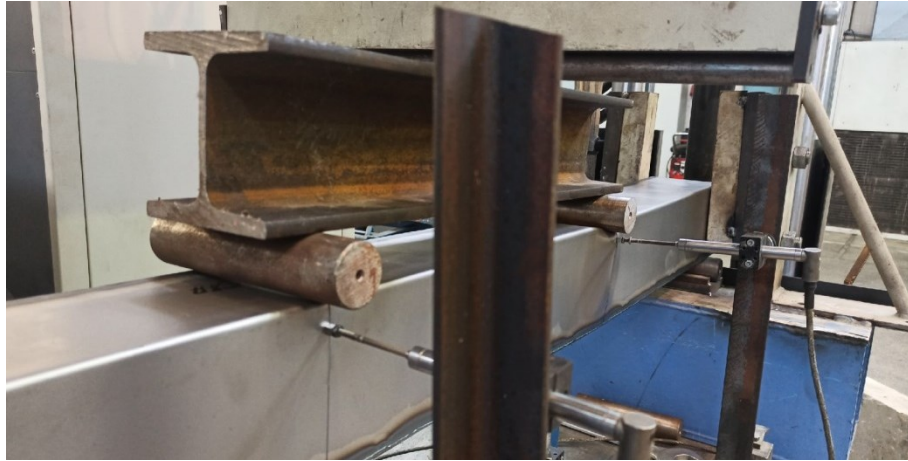


Figure 7.31. Beam 2 side view (flat 1.25 mm)

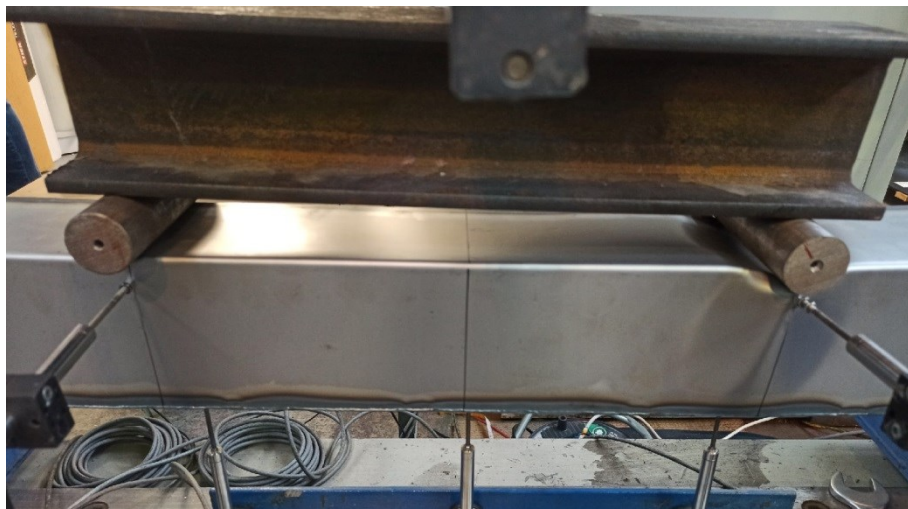


Figure 7.32. Beam 2 front view (flat 1.25 mm)



Figure 7.33. Beam 2 back view (flat 1.25 mm)

**C.3 Beam 3**



Figure 7.34. Beam 3 side view (flat 1.5 mm)



Figure 7.35. Beam 3 back view (flat 1.5 mm)

**C.4 Beam 4**

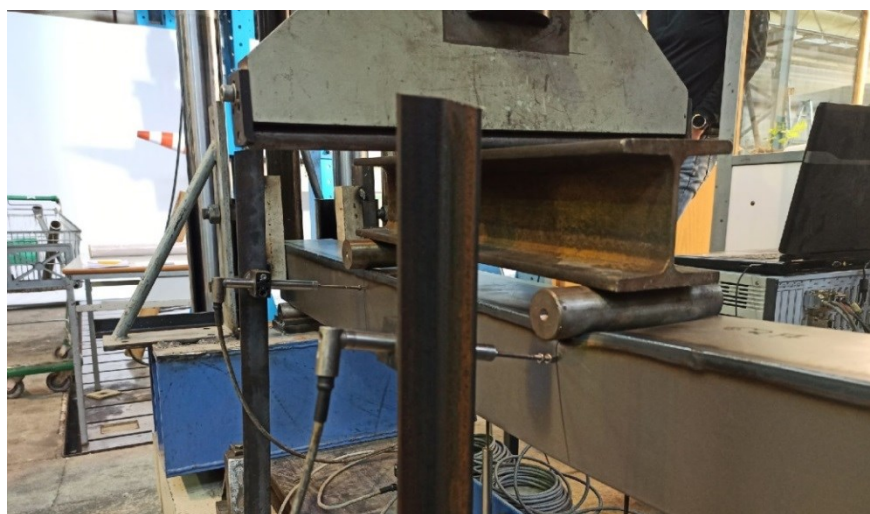


Figure 7.36. Beam 4 side view (flat 1.5 mm)



Figure 7.37. Beam 4 back view (flat 1.5 mm)

### C.5 Beam 5

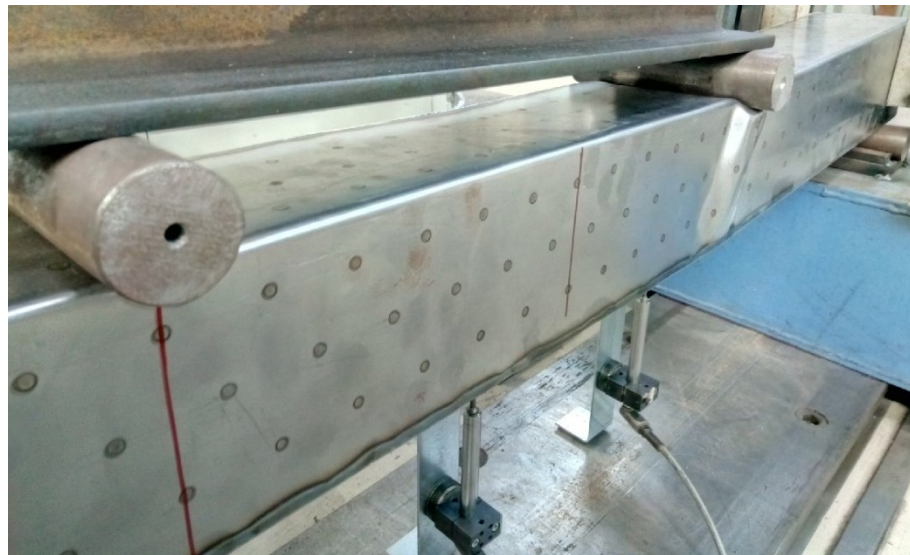


Figure 7.38. Beam 5 side view (flat 0.75 mm + structured 0.5 mm)



Figure 7.39. Beam 5 front view (flat 0.75 mm + structured 0.5 mm)





Figure 7.40. Beam 5 back view (flat 0.75 mm + structured 0.5 mm)

### C.6 Beam 6



Figure 7.41. Beam 6 side view (flat 0.75 mm + structured 0.5 mm)



Figure 7.42. Beam 6 back view (flat 0.75 mm + structured 0.5 mm)

**C.7 Beam 7**



Figure 7.43. Beam 7 side view (flat 1.00 mm + structured 0.5 mm)



Figure 7.44. Beam 7 back view (flat 1.00 mm + structured 0.5 mm)

**C.8 Beam 8**



Figure 7.45. Beam 7 front view (flat 1.00 mm + structured 0.5 mm)



Figure 7.46. Beam 8 back view (flat 1.00 mm + structured 0.5 mm)



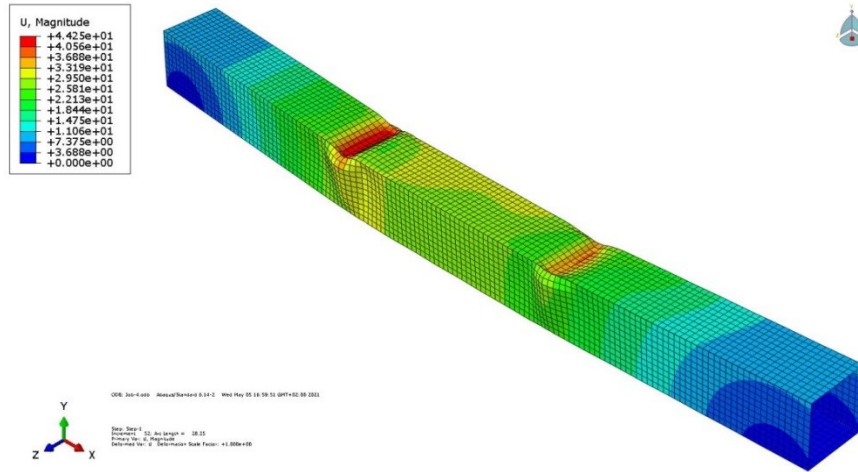


Figure 7.50. Beam type 1 (flat 1.25 mm), magnitude displacement in mm, at the end of loading

## D.2 Beam type 2

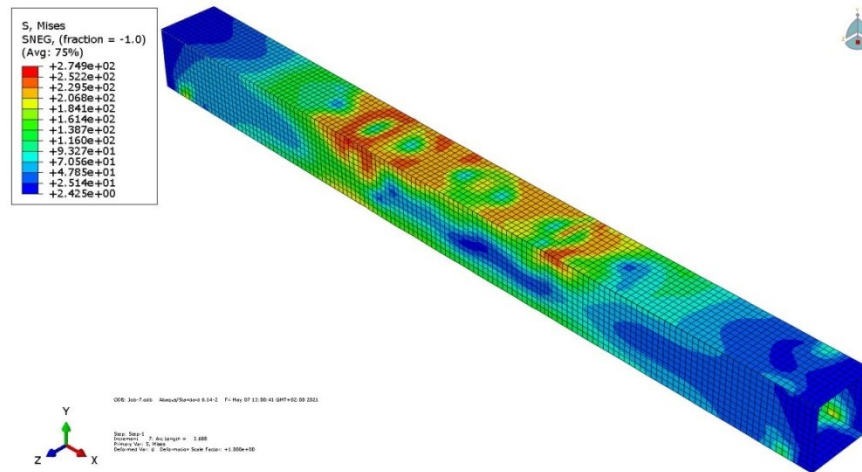


Figure 7.51. Beam type 2 (flat 1.5 mm), stress distribution in MPa

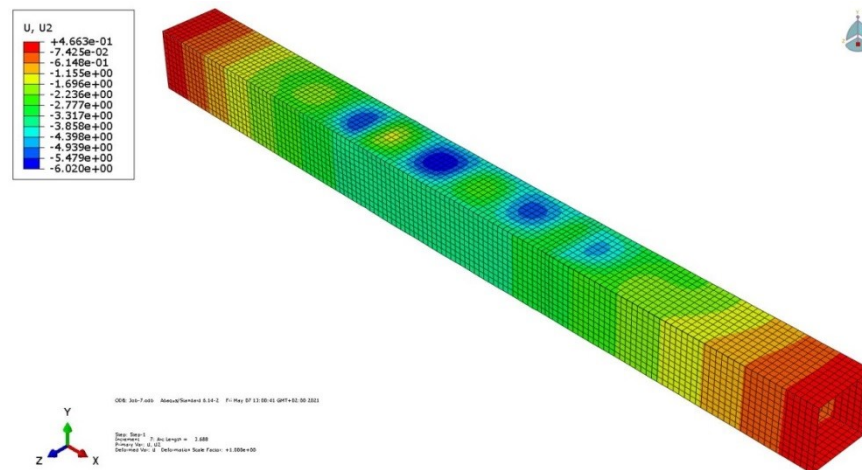


Figure 7.52. Beam type 2 (flat 1.5 mm), Y-distribution displacement in mm

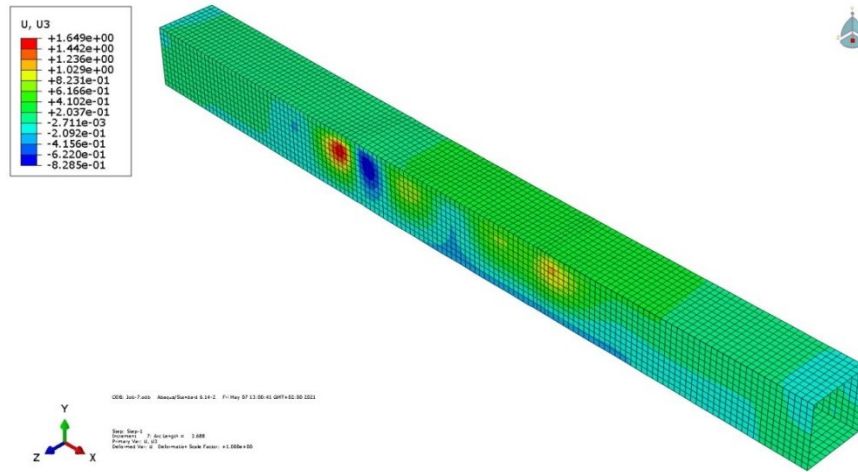


Figure 7.53. Beam type 2 (flat 1.5 mm), Z-distribution displacement in mm

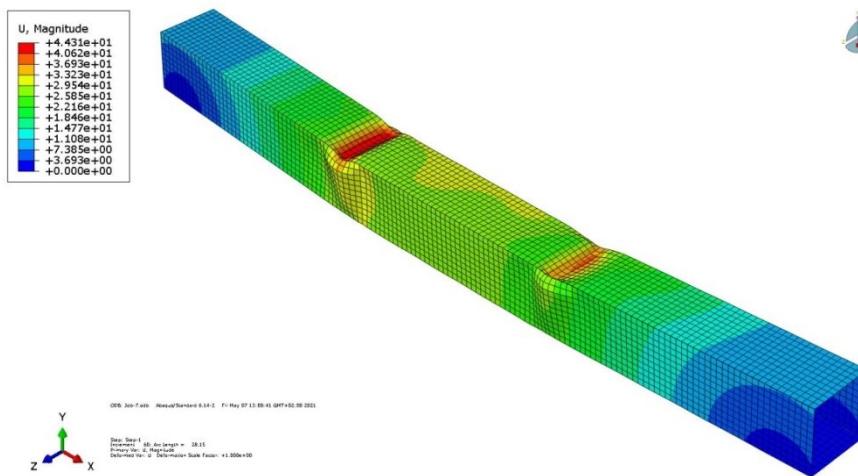


Figure 7.54. Beam type 2 (flat 1.5 mm), magnitude displacement in mm, at the end of loading

### D.3 Beam type 3

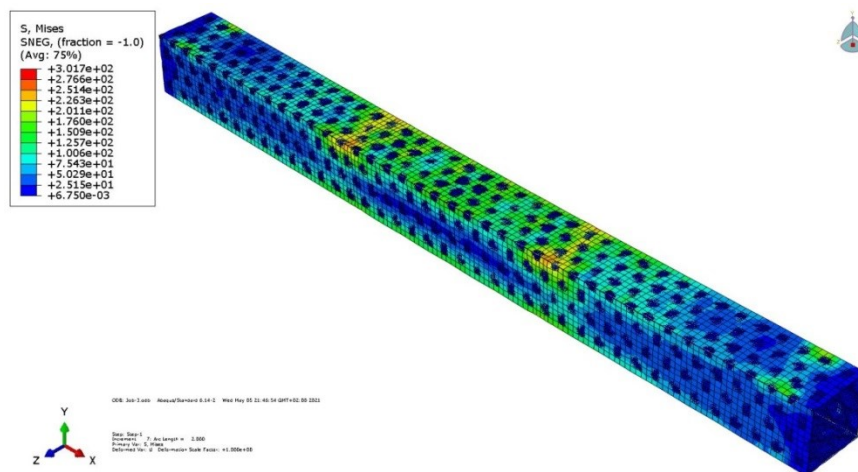


Figure 7.55. Beam type 3 (flat 0.75+structured 0.50 mm), stress distribution in MPa

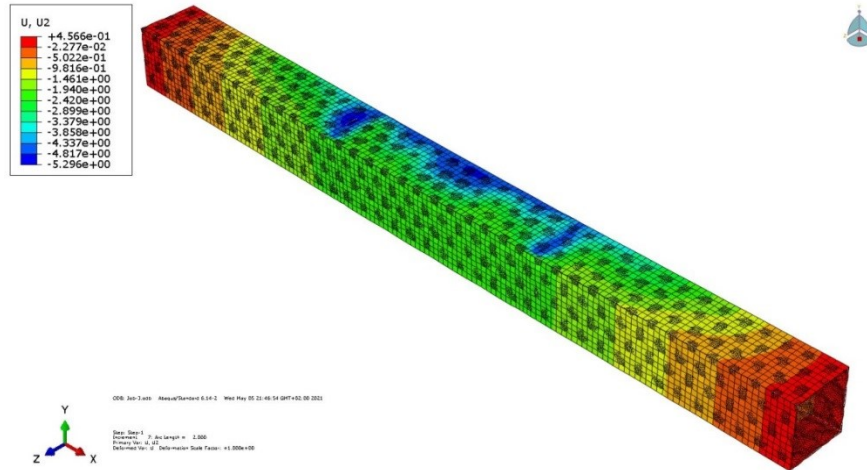


Figure 7.56. Beam type 3 (flat 0.75+structured 0.50 mm), Y-distribution displacement in mm

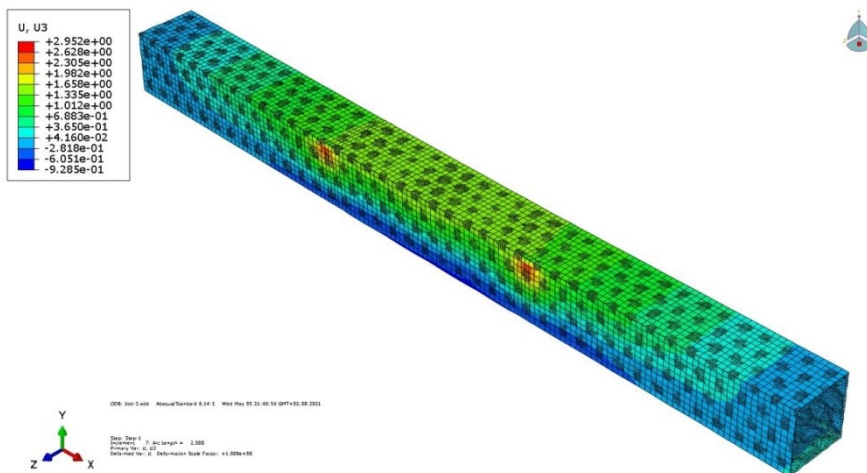


Figure 7.57. Beam type 3 (flat 0.75+structured 0.50 mm), Z-distribution displacement in mm

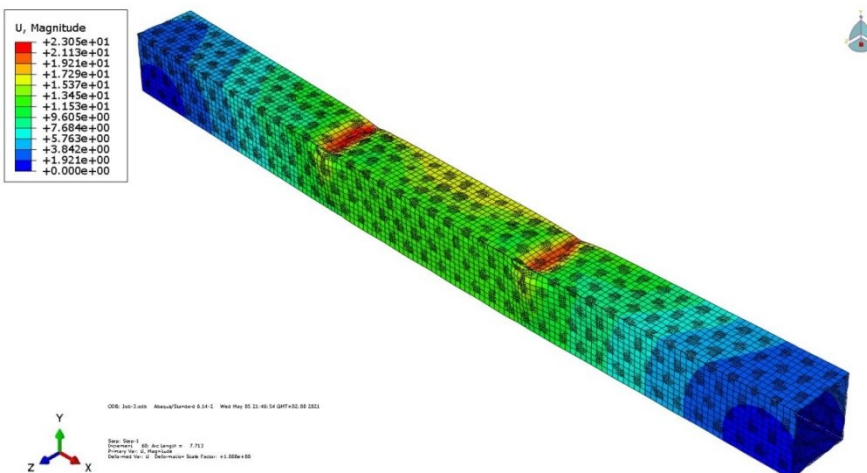


Figure 7.58. Beam type 3 (flat 0.75+structured 0.50 mm), magnitude displacement in mm, at the end of loading

D.4 Beam type 4

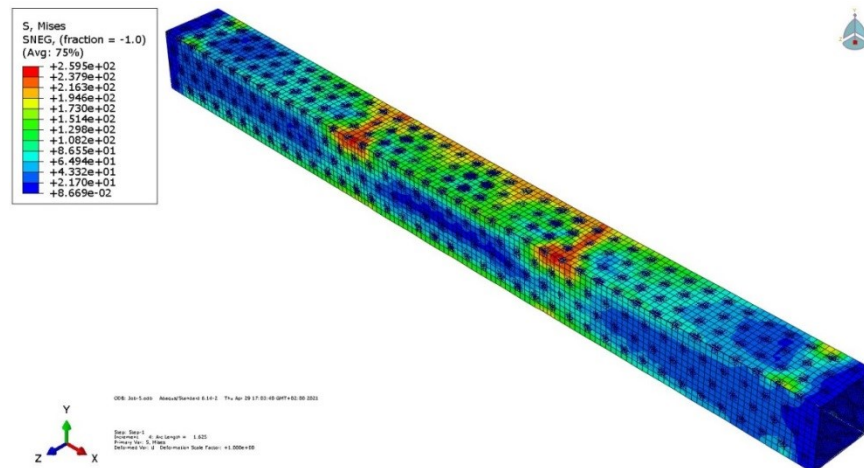


Figure 7.59. Beam type 4 (flat 1.00+structured 0.50 mm), stress distribution in MPa

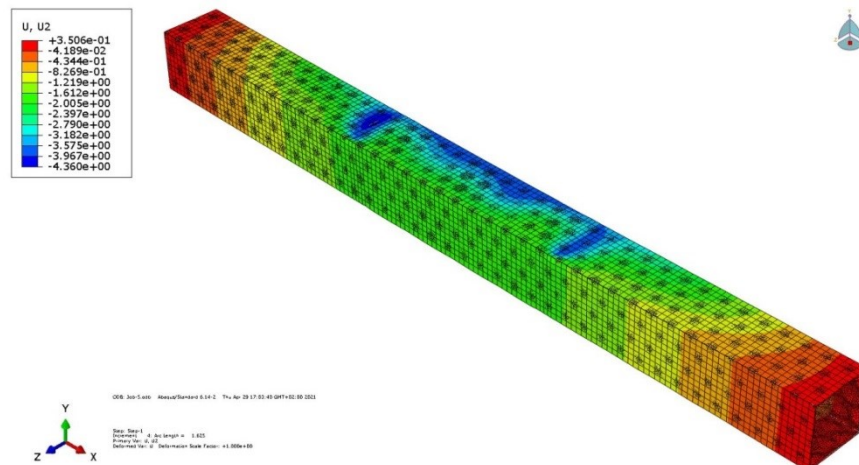


Figure 7.60. Beam type 4 (flat 1.00+structured 0.50 mm), Y-distribution displacement in mm

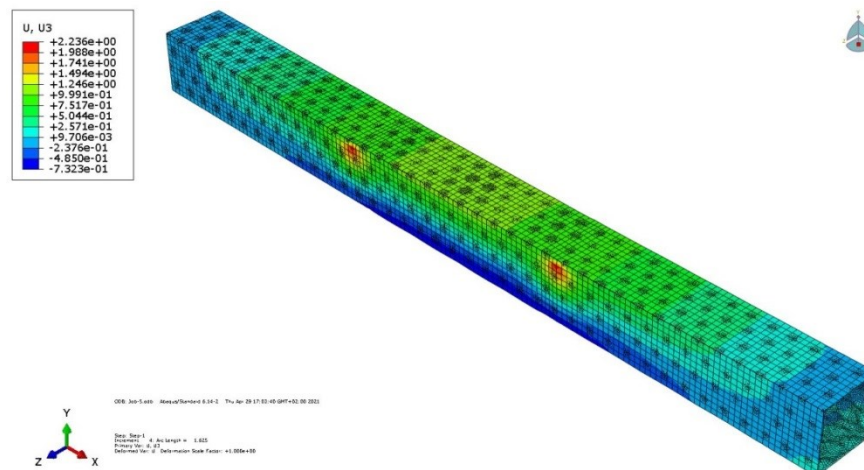


Figure 7.61. Beam type 4 (flat 1.00+structured 0.50 mm), Z-distribution displacement in mm



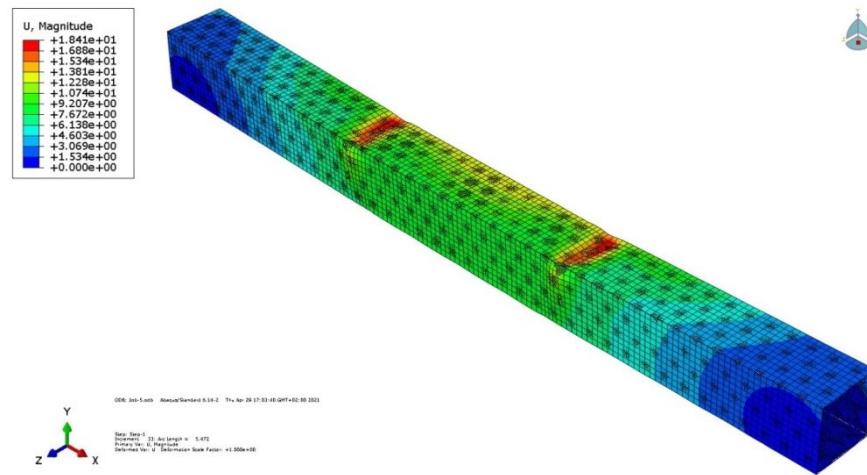


Figure 7.62. Beam type 4 (flat 1.00+structured 0.50 mm), magnitude displacement in mm, at the end of loading